19th World Congress of Soil Science

Symposium 2.1.1
Optimizing water use with soil physics

Soil Solutions for a Changing World,

Brisbane, Australia

1 – 6 August 2010

Table of Contents

Table of Contents (Cont.)

Table of Contents (Cont.)

Table of Contents (Cont.)

A variation of the Field Capacity (FC) definition and a FC database for Brazilian soils

Theophilo B. Ottoni Filho[A] and Marta V. Ottoni[B]

[A]Departamento de Recursos Hídricos e Meio Ambiente, Universidade Federal do Rio de Janeiro, Rio de Janeiro, RJ, Brazil, Email teottoni@poli.ufrj.br
[B]Companhia de Pesquisa de Recursos Minerais - CPRM, Rio de Janeiro, RJ, Brazil, Email mar025@terra.com.br.

Abstract
Field capacity (FC) is a widely applied parameter in Soil Science. It is related to frequent sequential infiltration and drainage in soils. This paper proposes a variation of the FC definition, based on 48-h drainage time, aiming not only at minimizing the inadequacies of its concept and determination, but also at maintaining its original, practical meaning. Data of 22 Brazilian soils showed that FC determined from standardized field procedures can primarily depend on basic soil data, especially volumetric water content data, such as θ(6 kPa) or θ(33 kPa).

Key Words
Drainage, pedotransfer function, Brazilian soils

Introduction
Field capacity (FC) is a soil parameter that is widely used in soil and water engineering. The original definition of FC by Veihmeyer and Hendrickson (1949) was slightly modified in the Glossary of Soil Science Terms (SSSA 1984) as: "FC is the amount of water remaining in soil two or three days after having been wetted and after free drainage is negligible". Despite the broad application of FC, its concept bears substantial uncertainty (Cassel and Nielsen 1986; Hillel 1998, chap. 16; Nachabe *et al*., 2003). Indeed, what a negligible free drainage rate is must be better stated. In addition, evapotranspiration is not specifically mentioned, profile wetting and initial soil moisture before water application are not precisely described, which may be relevant, particularly when hysteresis in soil water redistribution after infiltration (Hillel 1998, chap. 6) is significant. The presence of impeding or highly permeable layers and phreatic levels, as well as the influence of lateral flow in sloping landscapes, are also overlooked, especially if it is considered that the 'free drainage' in the above definition implies absence of these conditions. Indeed, all of these factors must be clarified before FC can be considered a reproducible, consistent, and intrinsic soil water variable.

The best standardized procedure to evaluate FC is by flooding a square or rectangular plot on a bare field (Cassel and Nielsen 1986); after irrigation, it is covered with a plastic sheet to avoid evaporation. The distribution of moisture in the upper part of the soil profile, which was fully moistened at the end of infiltration (quasi-saturated), measured 2 or 3 days after water application, defines the FC profile. This FC profile usually depends on the texture and structure of the individual soil layers (Salter and Williams 1965). Based on this dependence and on the operational difficulties of a field test, FC is commonly evaluated in a laboratory setting as the moisture of undisturbed soil samples at a specific matric potential. Cassel and Nielsen (1986) reported that a wide range of matric potentials (from -2.5 kPa to -50 kPa) has been used for this purpose, although suctions of 5 kPa, 6 kPa, 10 kPa, and 33 kPa are more common choices; however, there is no satisfactory general criterion for selection of the suction values for the determination of FC (Hillel 1998, chap. 16). Taking into account the dynamic nature of drainage, some authors (Nachabe *et al*., 2003) argue that the definition of FC must be based on an arbitrary choice for the "negligible" downward flux, instead of the drainage time of 2 or 3 days, or the suction at FC. Meyer and Gee (1999) considered that such selected small fluxes could be between 0.01 mm/d and 1.0 mm/d depending on the type of application. When FC is evaluated by the flux-based method, the drainage times may vary by an enormous range, even for an individual soil, from tens of hours to tens of days, depending on the flow rate chosen, as clearly demonstrated in Hillel (1998, chap. 16). Overall, despite being a widely applied soil parameter, the understanding of FC is neither unique nor exact.

In this paper, a variation of the definition of FC is proposed and empirically tested by the development and analysis of a FC database. The goal is to minimize the problems associated with the FC concept by creating a theoretical and practical framework for the proper and reproducible evaluation of the sequenced processes of infiltration (ponding) and internal drainage in the top soil layer. This will enable the standardization of experimental procedures, as well as the use of current mathematical tools, such as analytical and numerical

1 – 6 August 2010, Brisbane, Australia. Published on DVD.

modeling, and pedotransfer functions (Pachepsky and Rawls 2005) to determine FC profiles as required by engineers and land planners.

Variation of the FC Definition

"Field Capacity (FC) is the volumetric water content distribution in the upper part of a soil profile that, in the course of ponded infiltration (with ponding depth smaller than 10 cm), becomes fully wetted at the end of infiltration and remains exposed to the subsequent process of drainage without evapotranspiration or rain for 48 h". According to the above definition, measurement of FC is made only in the upper part of the profile, above the infiltration wetting front, which was monotonically drained from saturation or quasi-saturation so that the hysteresis effects were minimized (Hillel 1998, chap. 16). Rain and evapotranspiration effects were considered null during the 48 h of drainage. The duration of 48 h was chosen since it is a classical choice (Cassel and Nielsen 1986), and also because 2 days of drainage is a frequently used time period to infer crop damage by lack of soil aeration (Ochs *et al*., 1980; Hillel 1998, chap. 10). As a result, FC data can be utilized to evaluate soil profile aeration. Additionally, if a longer period were chosen, rain between irrigation and FC measurement would be more probable. We have not adopted a negligible constant downward flux due to difficulties in measuring small deep percolation flows in the field and due to the long test duration required for slow-draining profiles, sometimes over a week, which is particularly deleterious in wet climates because of the high frequency of rain.

FC Database

The FC database included soil data on FC, textural fractions (according to the USDA classification), bulk density (BD), organic matter content (OM), and volumetric water content at the suctions of 6, 33 and 1500kPa (respectively θ(6), θ(33), and θ(1500)). It comprises 22 soils (n=165 samples), most from the state of Rio de Janeiro, Brazil. The climate of the region is humid and tropical with rainy summers. Field work was in late fall and winter, when soil was relatively dry. In the FC test, a metal frame dike (1.0 m × 1.0 m × height = 0.25 m) (Embrapa 1979) was driven about 5 cm into the soil. The landscape slopes at the experimental sites varied from zero to approximately 20%. About 250 L of water was applied to most soils. Determination of antecedent soil moisture profiles near the experimental plots indicated that the used water volumes were frequently sufficient to saturate each of the soil profiles up to the 70-cm depth. Therefore, most soils were sampled in this depth range. At the end of infiltration, the wetted areas were covered with a plastic sheet and 48 h later, two undisturbed core samples were taken near the plot center, generally from the middle of each identified soil horizon. The soil property value reported in the database, including FC, was the arithmetic mean of the measurements made for each pair of samples at the corresponding depth and site.

The samples were sealed to prevent water loss and sent to the laboratory, where they were weighed for FC calculation. For detailed information on soils, laboratory and field procedures, sampled depths, and soil data see Fabian and Ottoni Filho (2000), Thurler (2000), Macedo *et al*. (2002), and Ottoni (2005).

Ranges of values of in situ FC in the database, according to textural classes, are shown in Table 1. For most samples, the suctions corresponding to FC were in the range from 6 kPa to 33 kPa, according to the comparisons made between the measured value of FC and the corresponding θ(6) and θ(33). The Pearson correlation coefficients (r) between FC and the soil properties are given in Table 2. The data set presents significant correlations between FC and soil properties. The most significant correlations were between moisture retention data (θ(6), θ(33), and θ(1500)), especially for θ(6), where r=0.93. This is an indication of the important influence of soil structure on FC, which was greater than the influence of texture. Silt was the least correlated textural content.

Table 1. Confidence intervals for FC (10^{-2} $m^3.m^{-3}$) in the database according to textural classes (n=165).

Subset 1		Subset 2			Subset 3		
Sand (s)	Loamy sand (ls)	Sandy loam (sl)	Loam (l)	Sandy clay loam (scl)	Clay loam (cl)	Sandy clay (sc)	Clay (c)
10.6±2.5 (n=8)	15.4±3.9 (n=10)	20.3±3.7 (n=38)	32.5±6.4 (n=4)	26.1±4.5 (n=56)	33.5±3.6 (n=8)	28.5±3.5 (n=15)	30.4±8.2 (n=26)

Table 2. Pearson correlation coefficients between field capacity and soil properties (n= 165).

Sand	Silt	Clay	θ(6)	θ(33)	θ(1500)	OM	BD
-0.720**	0.371**	0.628**	0.926**	0.795**[a]	0.825**[a]	0.223**	-0.213**

** Significative correlation at P= 5%, according to Pearson Test.
[a] Calculated for n= 149, since the work of Fabian and Ottoni Filho (2000) (n= 16) does not include information on θ(33) and θ(1500).

Based on the high correlations observed, we investigated how well FC could be calculated from basic soil properties; Table 3 presents 6 multilinear pedotransfer (PTF) models for FC (M1 to M6) and their root mean squared residues (RMSRs). The RMSRs are within the range commonly found in the literature for soil moisture PTFs (Nemes *et al*., 2003; Saxton and Rawls 2006). When θ(6) was added as an input variable (model M6), FC estimation improved significantly. However, for model M5, in which θ(6) was the sole predictor, RMSR (0.0281 m^3 m^{-3}) was only marginally larger than its correspondent, M6, a sophisticated model that had 6 predictors. This suggests that soil moisture is a useful input variable in the prediction of FC, which is generally the case with soil moisture evaluation by PTFs (Nemes *et al*., 2003; Schaap *et al*., 2004)

Table 3. Coefficients of multilinear PDFs for field capacity (m^3 m^{-3}). Models are enumerated in a decreasing order of RMSRs. Units of the input variables are: kg kg^{-1} (sand, silt, clay, OM); kg dm^{-3} (BD); m^3 m^{-3} (θ(6), θ(33)).

Model	Sand	Silt	Clay	OM	BD	θ (6)	θ (33)	Constant	RMSR
									m^3m^{-3}
M1	0.08478	0.4048	0.3792					0.03533	0.0514
M2	-0.0231	0.3912	0.3010		0.1077			-0.04645	0.0497
M3							0.6561	0.1043	0.0463
M4	0.1678	0.5967	0.4977	2.241	0.1190			-0.2877	0.0458
M5						0.8476		0.01181	0.0281
M6	0.03160	0.09379	0.03302	-0.3359	0.05547	0.8638		-0.1156	0.0270

Conclusion

FC has been defined here as the water content distribution in the soil profile as a function of sequential ponded infiltration and drainage without evapotranspiration or rain at 48 h after the end of infiltration. Therefore, the distribution FC(z) can be determined by hydraulic or numerical experiments that reproduce the above processes. Hysteresis effects are minimal in the above context. From standardized field procedures it was seen that FC can be accurately determined from basic soil properties. Without such standardization alternative laboratory, statistical or numerical methods for determining FC will remain ambiguous.

Acknowledgments

The authors wish to thank FINEP (CTHidro/GBH-02/2002) for the financial support. We are also grateful to Embrapa Solos for its technical support.

References

Cassel DK, Nielsen DR (1986) Field capacity and available water capacity. In 'Methods of soil analysis. Part 1, Physical and mineralogical methods'. (Ed. A Klute) pp. 901-926. (American Society of Agronomy and Soil Science Society of America: Madison, WI).

Embrapa (1979) 'Manual of soil analysis methods'. (in Portuguese). (Embrapa: Rio de Janeiro).

Fabian AJ, Ottoni Filho TB (2000) Determination of field capacity from in situ tests or regression equations. (in Portuguese). *Pesquisa Agropecuaria Brasileira* **35(5)**, 1029-1036.

Hillel D (1998) 'Environmental soil physics'. (Academic Press: Amsterdam).

Macedo JR, Meneguelli NA, Ottoni Filho TB, Lima JAS (2002) Estimation of field capacity and moisture retention based on regression analysis involving chemical and physical properties in Alfisols and Ultisols of the state of Rio de Janeiro. *Soil Science and Plant Analysis* **33(13-14)**, 2037-2055.

Meyer PD, Gee G (1999) Flux-based estimation of field capacity. *ASCE Journal of Geotechnical and Geoenvironmental Engineering* **125(7)**, 595-599.

Nachabe MH, Ahuja LR, Rokicki R (2003) Field capacity of water in soils: concepts, measurement, and approximation. In 'Encyclopedia of Water Science'. (Eds BA Steward, TA Howel), pp. 915-918. (Marcel-Deckker: New York)

Nemes A, Schaap MG, Wösten JHM (2003) Functional evaluation of pedotransfer functions derived from different scales of data collection. *Soil Science Society of America Journal* **67(4)**, 1093-1102.

Ochs WJ, Willardson LS, Camp Jr. CR, Donnan WW, Winger Jr. RJ, Johnston WR (1980) Drainage requirements and systems. In 'Design and operation of farm irrigation systems'. (Ed. ME Jensen), pp. 235-277. (American Society of Agricultural Engineering: St. Joseph).

Ottoni MV (2005) The physico-hydrical soil classification and the determination of in situ field capacity from infiltration tests. (in Portuguese). M.Sc. Thesis. (Federal University of Rio de Janeiro: Rio de Janeiro, RJ).

Pachepsky YA, Rawls WJ (2005) 'Development of pedotransfer functions in soil hydrology. Developments in Soil Science, V 30. m'. (Elsevier: Amsterdam).

Salter PJ, Williams JB (1965) The influence of texture on the moisture characteristics of soils. II. Available-water capacity and moisture release characteristics. *Journal of Soil Science* **16**, 310-317.

Saxton KE, Rawls WJ (2006) Soil water characteristic estimates by texture and organic matter for hydrologic solutions. *Soil Science Society of America Journal* **70**, 1569-1578.

Schaap MG, Nemes A, van Genuchten MTh. (2004) Comparison of models for indirect estimation of water retention and available water in surface soils. *Vadose Zone Journal* **3**, 1455-1463.

SSSA (1984) 'Glossary of soil science terms'. (Soil Science Society of America: Madison, WI)

Thurler AM (2000) Determination of field capacity and moisture retention in soils of the Tertiary of the Barreiras Formation, as a function of their granulometric characteristics and structural factors. (in Portuguese). Doctoral Thesis. (Rural Federal University of Rio de Janeiro: Seropedica, RJ).

Tomasella J, Hodnett MG, Rossato L (2000) Pedotransfer functions for the estimation of soil retention in Brazilian soils. *Soil Science Society of America Journal* **64**, 327-338.

Veihmeyer FJ, Hendrickson AH (1949) Methods of determining field capacity and wilting percentages of soils. *Soil Science* **68**, 75-94.

An evaluation of plant available water during reclamation of saline soils: Laboratory and field approaches

Nang ND, Grant CD and Murray RS
University of Adelaide, School of Agriculture, Food & Wine, Waite Campus

Abstract

The amount of water available to plants in the absence of all physical restrictions except high salinity is measured for a saline soil profile. Procedures and calculations are described and examples given for the initial unreclaimed soil, which shows that when osmotic stresses are taken into account (using the EC of a saturated paste extract) the water available to plants is about 33% less than that predicted when salt is ignored.

Key Words

Plant available water, PAW, integral water capacity, IWC, reclamation of saline soils

Introduction

Plant available water in saline soils is restricted primarily by osmotic pressures but also often by poor aeration, low hydraulic conductivity and high soil strength. Reclamation through leaching, introduction of divalent cations and salt-tolerant plants produces a number of structural states because as salt concentrations drop clays tend to swell and disperse. Eventually, however, conditions improve to the point where plants can grow and thereby contribute to the reclamation process. In the process, physical conditions can sometimes get worse before they get better because swelling and dispersion lead to poor aeration and reduced hydraulic conductivity, which can reduce the amount of water plants can extract. This project tracks the incremental changes in soil structure that take place during reclamation of saline land with a view to learning how to allocate resources to maximize plant available water at each stage. The integral water capacity (IWC) model of Groenevelt *et al*. (2001, 2004) is employed to calculate plant available water and this is checked against real plant response under field conditions. The project is in its early stages so this paper describes the approach and methods employed and gives some preliminary data to evaluate the amount of plant-available water in the initial, unreclaimed, saline state.

Methods

Laboratory evaluation of plant available water in saline state
Intact soil cores (50 mm diameter x 50 mm long) were collected from nine different depths to 180 cm in a saline profile at the University of Adelaide (Roseworthy campus). We first measured pH, EC, and solution-cations on 1:5 extracts of the loose soil to enable us to prepare isotonic solutions (in terms of sodium adsorption ratio, SAR, and total cation concentration, TCC) to measure saturated hydraulic conductivity, water retention and penetration resistance curves. Saturated hydraulic conductivity was measured using a constant head until the flux did not change after several days of hourly measurements. Water retention and penetrometer resistance were measured on the same soil cores at matric suctions 1, 5, 10, 50, 100 and 150 m. Water retention data were fitted to a variation of the model proposed by Groenevelt & Grant (2004) and the differential water capacity, $d\theta/dh$, calculated for use in determining the integral water capacity (Groenevelt *et al.* 2001).

Field evaluation of plant-available water in saline state
Two areas (each 3 x 3m) in the vicinity of the soil samples taken for laboratory analysis were isolated by excavating a trench on all four sides to a depth of 1.8m. Thick plastic sheeting was placed around the excavations and the soil back-filled to stop lateral movement of water inward or outward. Five neutron access tubes were installed across each area to allow volumetric water contents to be measured down to 1.8 m. Isotonic water was applied to the areas until the soil profiles were saturated and then the surfaces covered with thick

organic mulch and allowed to drain to a nominal field capacity. A neutron probe was calibrated for saline conditions and used to measure the volumetric water content of the soil profiles at the drained upper limit and as the soil profiles dried out. A salt-tolerant Kallar grass was established through the mulch and watered until its leaf area index, LAI, reached approximately 4.0 to minimize evaporation from the soil surface and to ensure that the only water losses were by transpiration. Irrigation was then stopped and the established plants were forced to extract water under increasingly dry conditions until they wilted and died (crop lower limit). The total amount of water extracted by the plants between the drained upper limit and the crop lower limit was taken as the real integral water capacity.

Results

Laboratory evaluation

The soil profile was neutral to highly-alkaline in pH, very saline and highly sodic (Table 1). As one might expect in such saline conditions, the saturated hydraulic conductivities (measured using isotonic solutions) were relatively large (ca 10^{-5} m s^{-1}) at least until the texture became more clayey below 1 m (Figure 1).

Table 1. Physical and chemical properties of the soil profile used in this study.

Depth (cm)	Texture	$pH_{1:5}$	EC* (dS m^{-1})	TCC** (mmol+/L)	SAR	K_s (± std error), 5 reps (m s^{-1})	
0 - 10	Loamy sand	7.42	5	60	2	6×10^{-5}	(3×10^{-5})
10 - 25	Sandy clay loam	8.24	4	45	6	3×10^{-5}	(8×10^{-6})
25 - 35	Light clay	8.30	4	39	7	4×10^{-5}	(6×10^{-6})
35 - 55	Light clay	8.47	3	38	9	3×10^{-5}	(4×10^{-6})
55 - 75	Light clay	8.91	3	34	15	2×10^{-5}	(7×10^{-6})
75 - 100	Light clay	9.51	3	41	41	2×10^{-5}	(3×10^{-6})
100 - 115	Medium clay	9.48	4	52	58	7×10^{-7}	(2×10^{-7})
115 - 150	Medium clay	9.34	5	65	64	2×10^{-7}	(6×10^{-8})
> 150	Heavy clay	8.86	8	96	94	8×10^{-9}	(1×10^{-9})

* 1:5 EC multiplied by 5 was very close to the sum of ICP-cation concentrations divided by 10.
** TCC total cation concentration, calculated as sum of ICP-cation concentrations: (2 x (Ca+Mg) + Na+ K).

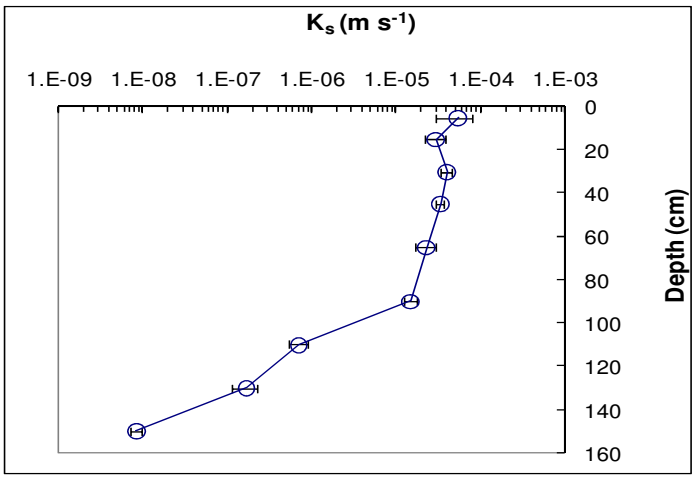

Figure 1. Profile of saturated hydraulic conductivity; horizontal bars indicate standard errors in K_s.

An example of the water retention curves produced in this work is shown in Figure 2 for the first soil horizon. The water retention curve was fitted to the model of Groenevelt et al. (2004):

$$\theta(h) = \theta_{wp} + k_1 \left\{ \exp\left(-\left(\frac{k_0}{150} \right) \right)^n - \exp\left(-\left(\frac{k_0}{h} \right)^n \right) \right\}, \quad [1]$$

where θ_{wp} is the water content at matric head h = 150 m, k_1, k_0 and n are adjustable fitting parameters.

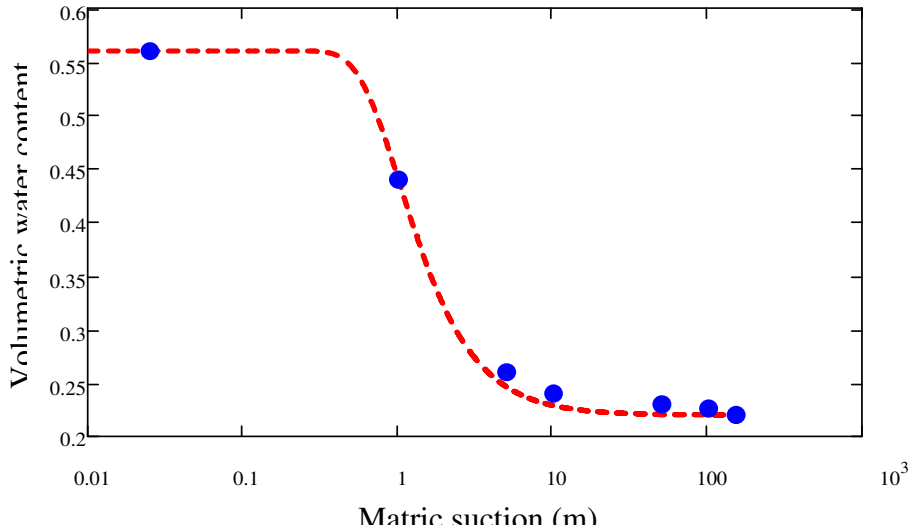

Figure 2. Water retention curve for the loamy sand in the top horizon (0 to 10 cm).

Eqn [1] was differentiated to produce the so-called 'water' capacity, C(h), which is actually the 'soil solution' capacity (green line in Figure 3):

$$C(h) = n\, k_0\, k_1\, h^{-(n+1)} \left\{ \exp\left(-\left(\frac{k_0}{h} \right)^n \right) \right\} . \qquad [2]$$

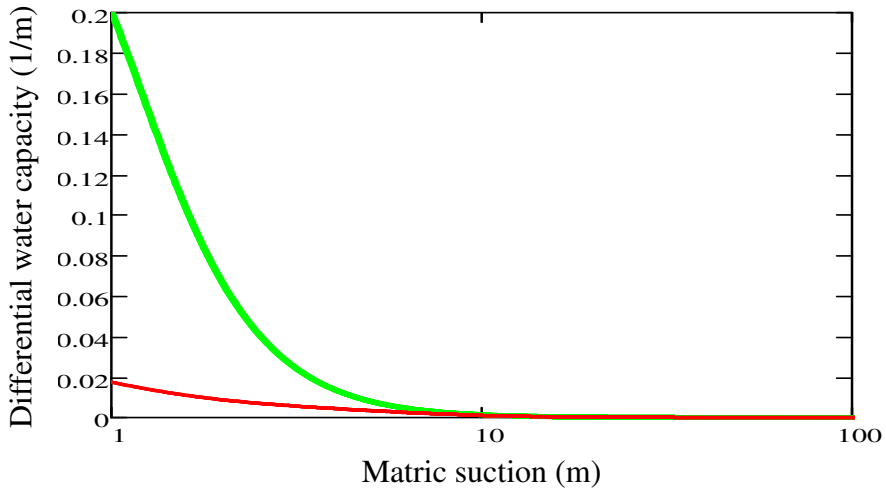

Figure 3. Differential water capacity, $C_{om}(h)$, for soil in horizon 1 unweighted (green) and weighted for soluble salts (red).

Eqn [2] was then weighted for osmotic limitations to produce an effective water capacity (red line in Figure 3). The IWC was then calculated as a function of the osmotic head (h_{os}, as measured in a saturated paste extract) as well as the matric head, h, according to the model of Groenevelt et al. (2004):

$$IWC(h_{os}) = \int_0^{\infty} C_{om}(h, h_{os})\, dh \ , \qquad [3]$$

where $h_{os} \sim 3.6\ EC_e$. In this way, if one has knowledge of the amount of salt in the saturated soil, the osmotic head can be calculated as well as the amount of water available to plants in the absence of other physical limitations. Integration of the two lines shown in Figure 3 produced values for IWC for the unweighted water capacity (classical value of plant available water) = 220 mm/m and for the weighted water capacity = 66 mm/m. The calculations for the other 8 horizons in this profile are shown in Table 2.

Table 2. Amount of plant available water in each horizon (and whole profile) when salt is ignored (PAW) and when salt is accounted for in the integral water capacity (IWC).

Depth (cm)	PAW (mm/m)	PAW total (mm)	IWC (mm/m)	IWC total (mm)
0 - 10	220	22	66	7
10 - 25	314	47	172	26
25 - 35	339	34	199	20
35 - 55	172	34	74	15
55 - 75	188	38	109	22
75 - 100	190	48	135	34
100 - 115	158	24	133	20
115 - 150	137	48	111	39
> 150	195	98	161	81
Total for profile		392		262

Field evaluation of plant-available water

Experimental work for the field component of this work is only just beginning and progress will be reported at the Congress.

Conclusions

The real amount of plant-available water in the un-reclaimed soil profile (i.e. IWC shown in Table 2) is at least 33% lower than the classical PAW that ignores osmotic stresses. In the reclamation process (yet to occur in this project), it is expected that the IWC will decrease in the first instance (because of swelling and dispersion processes) and then gradually increase toward the classical PAW as calcium replaces sodium, as the concentration of salt is decreased, and as salt-tolerant plants are introduced.

References

Groenevelt PH, Grant CD and Semetsa S 2001. A new procedure to determine soil water availability. *Australian Journal of Soil Research* **39**, 577-598.

Groenevelt PH and Grant CD 2004. A new model for the soil-water retention curve that solves the problem of residual water contents. *European Journal of Soil Science* **55**, 479-485.

Groenevelt PH, Grant CD and Murray RS 2004. On water availability in saline soils. *Australian Journal of Soil Research* **42**, 833-840.

Analytical Solution for Drainage from a Uniformly Wetted Deep Soil Profile

John H Knight[A] and **Freeman J Cook[B]**
[A]Queensland University of Technology, CSIRO Land and Water, john.knight@qut.edu.au john.knight@csiro.au
[B]CSIRO Land and Water 120 Meiers Rd Indooroopilly QLD 4068 Australia , eWater CRC, Irrigation Futures CRC, The University of Queensland, freeman.cook@csiro.au

Abstract
An analytical solution of the Richards equation for drainage of water from an initially uniformly wet homogeneous soil profile is discussed. This solution builds on an approach originally used for infiltration and later adapted to drainage. The mathematics for this solution are scattered and incomplete. Here we provide a complete unified solution. The results are presented for some soils from the HYDRUS-1D standard soil types. Results show progression of the draining front down through the soil with time and can be used to estimate the time for the soil to drain to a particular water content. Comparison of the analytical solution with HYDRUS-1D numerical solution shows the solution works well at small drainage times but estimates more drainage in the upper soil profile than HYDRUS-1D at larger times.

Key Words
Soil physics, Richards equation, modelling

Introduction

The drainage of water from a homogeneous soil is described by the Richards[’] equation

$$\frac{\partial \theta}{\partial t} = \frac{\partial}{\partial z}\left[D(\theta)\frac{\partial \theta}{\partial z} - K(\theta) \right] \qquad (1)$$

where z is depth below the soil surface, t is time, and θ is volumetric soil water content. The soil water diffusivity and unsaturated conductivity are $D(\theta)$ and $K(\theta)$ respectively, and are strongly dependent on soil water content. The $D(\theta)$ is assumed to be of the form (Broadbridge and White, 1988a):

$$D(\Theta) = K_s C(C-1))/\left[\alpha \Delta\theta (C-\Theta)^2 \right] \qquad (2)$$

where θ_s and θ_r are the saturated and residual soil water contents respectively and $\Delta\theta = \theta_s - \theta_r$ is their difference, $\Theta = (\theta - \theta_r)/\Delta\theta$ is the scaled water content, K_s is the saturated soil hydraulic conductivity, α is an inverse capillary length parameter of Philip (1985), and $C > 1$ is a dimensionless parameter. The hydraulic conductivity is assumed to have the functional form

$$K(\Theta) = K_s (C-1)\Theta^2/(C-\Theta). \qquad (3)$$

Broadbridge and White’s (1988a,b) model for soil water movement combines the functional form of the diffusivity from Fujita (1952) and Knight and Philip (1974) with the Burgers’ equation form of the conductivity used by Clothier *et al*. (1981). Saunders *et al*. (1988) also independently came up with a similar solution. The Broadbridge and White analytical solution uses a transformation found by Fokas and Yortsos (1982), and is a combination of the Storm (1951) solution used by Knight and Philip (1974) in the absence of gravitational effects and the Burgers’ equation solution given by Clothier et al. (1981). Warrick *et al*. (1990) adapted the Broadbridge and White solutions for soil water drainage, and Parkin *et al*. (1995) and Si and Kachanoski (2000) further explored their use. These drainage solutions use different boundary conditions to the Broadbridge and White solution and result in different functions in the solution. The mathematics of the analytical solution is scattered and incomplete in the published literature; this document presents a unified account of the theory. The solution for infiltration into a deep profile given by Broadbridge and White (1988a) and adapted for drainage in a deep soil by Warrick *et al*. (1990) and Parkin *et al*. (1995) had zero water flux at the soil surface;the initial and boundary conditions were; $\theta(z,0) = \theta_0$, $K(\theta) - D(\theta)\frac{\partial \theta}{\partial z} = 0$ at $z = 0$

$$\frac{\partial \theta}{\partial z} = 0, z \to \infty$$

The corresponding initial value for the scaled water content is $\Theta_0 = (\theta_0 - \theta_r)/\Delta\theta$. The transformations used by Broadbridge and White (1988) introduce a dimensionless time parameter $\tau = 4C(C-1)\alpha K_s t / \Delta\theta$, a new

dimensionless space-like parameter ς and a new independent variable $u(\varsigma,\tau)$ which satisfies a linear advection diffusion equation. It is important to note that the solutions $u(\varsigma,\tau)$ for the infiltration case studied by Broadbridge and White (1988) and the drainage case studied by Warrick et al. (1990) are different because of their different boundary conditions.

The Warrick *et al*. (1990) solution for $u(\varsigma,\tau)$ for drainage with zero surface flux is given by

$$u(\varsigma,\tau)=\exp\left(-\varsigma^2/\tau\right)\left[f\left(\varsigma/\sqrt{\tau}\right)+\tfrac{1}{2}f\left(\left[\tfrac{1}{2}B_0\tau-\varsigma\right]/\sqrt{\tau}\right)-\tfrac{1}{2}f\left(\left[\tfrac{1}{2}B_0\tau+\varsigma\right]/\sqrt{\tau}\right)\right] \quad (4)$$

with $f(x)\equiv\exp\left(x^2\right)\mathrm{erfc}(x)$, and the parameter B_0 given in terms of the initial condition by $B_0=\Theta_0/(C-\Theta_0)$. For the case of no surface flux the original space variable is given in terms of the solution $u(\varsigma,\tau)$ by $z(\varsigma,\tau)=\{\varsigma-\ln[u(\varsigma,\tau)]\}/(C\alpha)$ and the scaled water content is given by $\Theta(\varsigma,\tau)=C\left[1-\left(1-\frac{\partial u}{\partial\varsigma}(\varsigma,\tau)\Big/u(\varsigma,\tau)\right)^{-1}\right]$. The quantity $\frac{\partial u}{\partial\varsigma}(\varsigma,\tau)\Big/u(\varsigma,\tau)$ does not seem to be given explicitly in the published literature, and is

$$\frac{\frac{\partial u}{\partial\varsigma}(\varsigma,\tau)}{u(\varsigma,\tau)}=-B_0 f\left[\left(\frac{\frac{1}{2}B_0\tau-\varsigma}{\sqrt{\tau}}\right)+f\left(\frac{\frac{1}{2}B_0\tau+\varsigma}{\sqrt{\tau}}\right)\right]\left[2f\left(\frac{\varsigma}{\sqrt{\tau}}\right)+f\left(\frac{\frac{1}{2}B_0\tau-\varsigma}{\sqrt{\tau}}\right)-f\left(\frac{\frac{1}{2}B_0\tau+\varsigma}{\sqrt{\tau}}\right)\right]^{-1}. \quad (5)$$

The surface value of the scaled water content is then

$$\Theta(0,\tau)=C\left[1-\left(1-\frac{\partial u}{\partial\varsigma}(0,\tau)\Big/u(0,\tau)\right)^{-1}\right]=C\left[1-\left(1+B_0 f\left(\tfrac{1}{2}B_0\sqrt{\tau}\right)\right)^{-1}\right]. \quad (6)$$

When $\tau=0$, then eqn (6) becomes $\Theta(0,0)=C\left[1-(1+B_0)^{-1}\right]=\Theta_0$ as required.

Equations 4-6 provide a unified solution which is easily computed. We used the eqs 4-6 above to model drainage from a uniformly wet soil profile using soil properties taken from HYDRUS-1D soil catalogue and are presented in Table 1. The desorptivity was estimated from simulation of desorption of an initially saturated horizontal soil columns using HYDRUS-1D (Simunek *et al*. 1998) and C and α by fitting the water content, potential relationship to eqn (25) of Broadbridge and White (1988b). We also calculated results for the Brindabella silty clay loam (not shown) to check that we got the same results as Warrick *et al*. (1990). Eqs 4-6 were solved using MatLab.

Table 1. Soil properties derived from HYDRUS-1D catalogue.

Soil	θ_r ($m^3\ m^{-3}$)	θ_s ($m^3\ m^{-3}$)	C	K_s ($m\ s^{-1}$)	α (m^{-1})
Clay	0.068	0.38	1.0002	5.56×10^{-7}	6.92
Silt	0.078	0.46	1.0063	6.94×10^{-7}	5.15
Loam	0.078	0.43	1.0189	2.89×10^{-6}	7.11
Sand	0.045	0.43	1.0458	8.35×10^{-5}	17.94

Results and Discussion

The drainage of the soil from saturation with a free drainage (unit gradient) boundary condition was simulated in HYDRUS-1D for the soils in Table 1 and compare with drainage calculated with the analytical solution (Fig.1). The analytical solution appears to estimate more drainage near the surface especially at large times than does HYDRUS-1D. For times less than 10 days the analytical solution and HYDRUS-1D give similar ($r^2 >$ 0.88) estimates of the water content profile. The percentage difference in the water content at the surface between the analytical solution and HYDRUS-1D increase with time from negligible to approximately 28% by *t* = 50 days, except for the sand. This is most likely due to different functional relationships for *K* and *D* used in the analytical solution and HYDRUS-1D. This will be explored in the future.

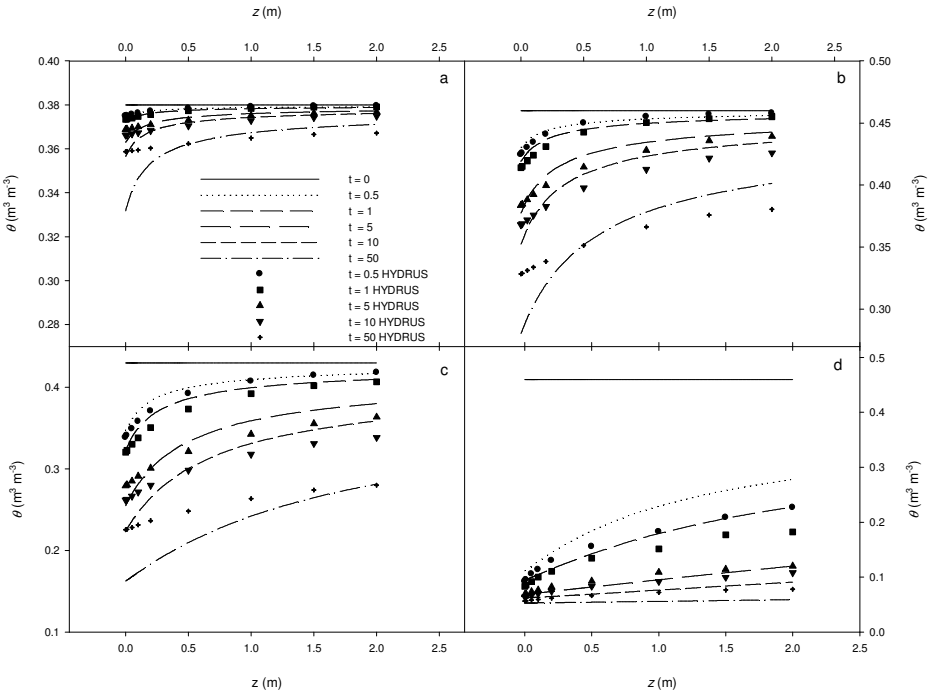

Figure 1. Comparison of the analytical solution with HYDRUS-1D for drainage of an initially saturated soil profile for a) clay, b) silt, c) loam and d) sand. The times indicated in the legend are days since drainage commenced.

The drainage from different initial uniform water content profiles was calculated with the analytical solution and HYDRUS-1D (Fig. 2). This indicates that the percentage difference between the analytical solution and the numerical solution at large times (t = 50 days) is approximately the same, as the initial water content decreases.

Conclusion

An analytical solution for drainage from uniformly wet soil profiles is shown to give similar water content profiles ($r^2 > 0.88$) at drainage times < 10 days to those simulated with a one-dimensional numerical solution of Richards' equation. This is especially so at the surface where the percentage difference in the water content between the two models for all but the sand soils increases with increasing time. At large times the analytical solutions water content near the surface is usually less than the numerical solution. The analytical solution may overestimate drainage at large times.

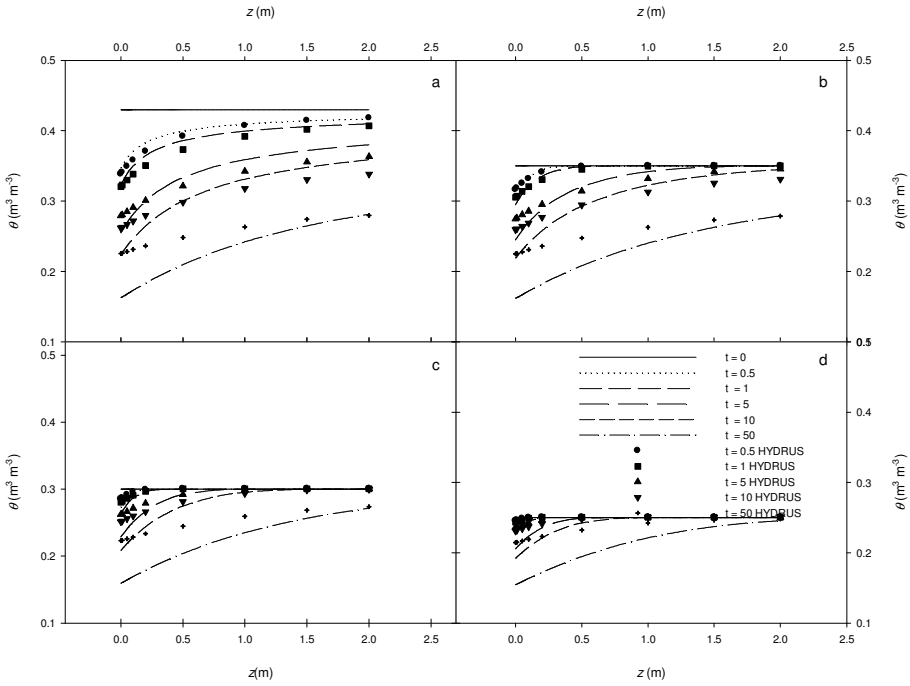

Figure 2. Comparison of the analytical solution with HYDRUS-1D for drainage of an initially saturated loam soil profile for a) $\theta = 0.43$, b) $\theta = 0.35$, c) $\theta = 0.30$ and d) $\theta = 0.25$. The times indicated in the legend are days since drainage commenced.

References

Broadbridge P, Knight JH, Rogers C (1988) Constant rate rainfall infiltration in a bounded profile: solutions of a nonlinear model. *Soil Science Society of America Journal* **52**, 1526-1533.

Broadbridge P, White I (1988) Constant rate rainfall infiltration: A versatile nonlinear model. 1. Analytical solution. *Water Resources Research* **24**, 145-154.y

Clothier BE, Knight JH, White I (1981) Burgers' equation: application to field constant-flux infiltration. *Soil Science* **132**, 255-261.

Fokas AS, Yortsos YC (1982) On the exactly solvable equation $S_t = \left[(\beta S + \gamma)^{-2} S_x\right]_x - \alpha(\beta S + \gamma)^{-2} S_x$ occurring in two-phase flow in porous media. *SIAM Journal Applied Mathematics* **42(2)**, 318-332.

Fujita H (1952) The exact pattern of a concentration-dependent diffusion in a semi-infinite medium. 2. *Textile Research Journal* **22**, 823-827.

Knight JH, Philip JR (1974) Exact solutions in nonlinear diffusion. *Journal of Engineering Mathematics* **8**, 219-227.

Lockington D, Parslow P, Parlange J-Y (1988) Integral estimates of the sorptivity. *Soil Science Society of America Journal* **52**, 903-908.

Parkin, GW, Warrick AW, Elrick DE, Kachanoski RG (1995) Analytical solution for one-dimensional drainage: Water stored in a fixed depth. *Water Resources Research* **31**, 1267-1271.

Sanders GC, Parlange J-Y, Hogarth, WL (1988) Air and water flow 1. Horizontal flow with an arbitary flux boundary condition. *Journal of Hydrology* **99**, 215-223.

Si BC, Kachanoski RG (2000) Unified solution for infiltration and drainage with hysteresis: Theory and field test. *Soil Science Society of America Journal* **64**, 30-36.

Simunek J, Sejna M, van Genuchten M Th (1998) The HYDRUS-1D software package for simulating the one-dimensional movement of water, heat, and multiple solutes in variably-saturated media. Version 2.0, IGWMC - TPS - 70, International Ground Water Modeling Center, Colorado School of Mines, Golden, Colorado, pp 202.

Storm ML (1951) Heat conduction in simple metals. *Journal of AppliedPhysics* **22**, 940-951.

Warrick AW, Lomen DO, Islas A (1990) An analytical solution to Richards' equation for a draining soil profile. *Water Resources Research* **26**, 253-258.

Application of GPR ground wave for mapping of spatiotemporal variations in the surface moisture content at a natural field site

B. Pallavi, H. Saito and M. Kato

United Graduate School of Tokyo University of Agriculture and Technology, Japan

Abstract
In the present study GPR ground wave (GW) was used to monitor the spatial distribution of surface moisture content at a natural Kanto loam site. To map the soil moisture variations, measurements were conducted on a regular interval of 2~3 days per week. Results revealed that ground wave data were sensitive to the upper surface soil conditions as well as seasonal variations. Significant increase in the moisture content values were observed a day after a precipitation event. However, moisture content increase was non-uniform over the entire area; the probable cause of the variations might be associated with soil hydraulic properties (e.g. hydraulic conductivity, water retention characteristics), and/or topography of the site. The GW sampling depth obtained by taking one quarter of wavelength (Pallavi, 2009) was found more reliable with the reference measurements. The GW sampling depth was found to be between 0.06 ~ 0.07 m at this site. The study shows that the GPR GW can be used as a principal tool for large scale spatiotemporal monitoring in non-invasive and rapid mode with high resolution and provides quality data with known sampling volume at a field scale.

Key Words
Ground penetrating radar (GPR), Ground wave (GW), GW sampling depth, moisture content, precipitation

Introduction

The near surface moisture content is a key parameter for soil/water conservation, irrigational and agricultural management. In general, surface moisture content is highly variable in space and still is difficult to characterize on a consistent and spatially comprehensive basis at a field scale. The measurement of spatial variation of moisture content at the field scale is thus important. The conventional method (TDRs, cores, neutron probes) provide the essential information, but are limited to a specific point location. Applications of GPR have shown promise for moisture content estimation at the field scale during last two decades (Grote *et al*., 2003; Huisman *et al.*, 2003). The ground wave (GW) of GPR provides a means to monitor large areas relatively fast, non-invasively, and cost-effectively with good resolution data quality. The most important character of the GPR method is that it estimates the moisture content in absence of shallow reflectors in the subsoil (Van Overmeeren *et al.*, 1997). However, the sampling depth of the GW is not well defined, and this uncertainty limits its application for large-scale monitoring. Therefore, the specific aim of the presented study was to monitor the seasonal variations in the spatial distribution of the moisture content.

Methods

Basics of ground wave of GPR

Ground penetrating radar is a geophysical technique that uses high frequency (MHz ~ GHz) electromagnetic energy to probe the subsurface. Energy is emitted from the GPR transmitter as a spherical wave, and some of this energy travels along the air-ground interface in the near subsurface toward the receiver. This energy creates a boundary wave that is referred to as the direct wave (air and ground wave). The first strong signal usually

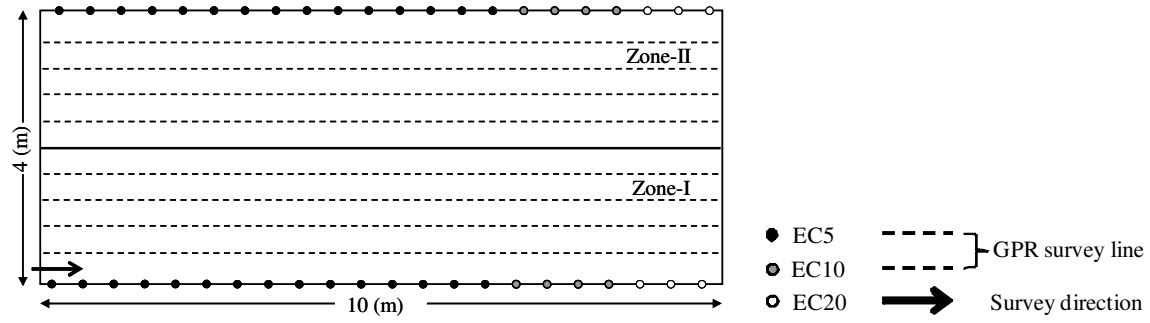

Figure 1. Schematic diagram of study site with GPR transects, sensor position and zone divisions (I: 0 ~ 2 m, vegetation, and II: 2-4 m, bare soil)

represents airwave (AW), which travels directly from the transmitter to the receiver through air at the speed of the electromagnetic wave in vacuum. GW is the part of the radiated energy that travels between the transmitter and receiver along the soil surface. The propagation velocity of GW (v_{gw}) depends on the dielectric constant of the soil K_{soil}, the moisture content θ, the soil texture etc. The velocity (v_{gw}) is calculated by dividing the antenna separation (S) by the GWTT (ground wave travel time: t_{gw}), e.g. $v_{gw} = (S/t_{gw})$. The dielectric constant K is then calculated by following equation, $K= (c/v_{gw})^2$ (Davis and Annan, 1989), where c is the speed of the EM wave in a vacuum (3×10^8 m s^{-1}). The volumetric water content is obtained from K using Topp's equation (Topp *et al.*, 1980). Two different GW depth models proposed by van Overmeeren *et al.* (1997), $[0.5(\lambda \times S)^{0.5}]$ and Pallavi *et al.* (2009) $[0.25 \times \lambda]$ are used for depth estimation. The wavelength λ is calculated by ($\lambda = v_{gw}/f$), where f is the central frequency of GPR and v_{gw} is the GW velocity.

Equipment and analysis

A pulseEKKO PRO 250 system (Sensors and Software, Canada) with 250 MHz central frequency antenna was used in this study. Radar signals were processed and analyzed by the EKKO view deluxe software. Simple processing was applied to the data, consisting of dewow filter to remove the background noise and AGC gain to distinguish the ground, refracted, and reflected waves at larger separations. Soil moisture sensors (ECHO sensors by Decagon Devices, Inc.) were also used for soil moisture and dielectric constant measurements.

Field site

An intensive study area of 10 m by 4 m in Field Science Centre of Tokyo University of Agriculture and Technology, Japan was used for measurements of moisture content variations of near surface soils pre- and post-precipitation. The schematic diagram of the study site is depicted in Figure 1. The whole area was divided into two zones, with and without vegetation, with 10 equidistant parallel transects for the GPR measurement. Along the boundary in x-direction, soil moisture sensors were also installed, where the black circles (EC5) represent the 5-cm-long sensors, gray circles (EC10) represent 10-cm-long sensors, and the open circles (EC20) represent 20-cm-long sensors, respectively. Vegetation was allowed to grow on the Zone-I, while Zone-II was cleaned weekly to maintain a bare soil surface during the research campaign.

Survey method

Measurements were conducted using both common-offset (CO) and common-midpoint (CMP) methods for moisture content mapping and velocity estimation. The CO profile provides the detailed information of the imaged area (e.g. surface-subsurface moisture content distribution, buried anomaly position, stratigraphical information etc.). However, in this study, our main concern was to monitor the behaviour of direct ground wave in relation to changes in surface soil moisture contents.

Results and discussions

CMP surveys were first conducted for velocity profile estimation. Measurements were performed along the central lines of the both zones (3rd and 8th line), with a step size of 0.10 m. In both surveys, ground waves were clearly recognized between antenna separations of 0.38 to 0.98 m. At larger separations, interference between shallow reflections and ground waves were observed. One of the CMP profiles (along transect 3) is given in Figure 2, where the AW and GW velocities were obtained by taking the inverse of linear slope of position-travel time plot. The estimated AW and GW velocity was 0.29, and 0.067 m ns^{-1} respectively.

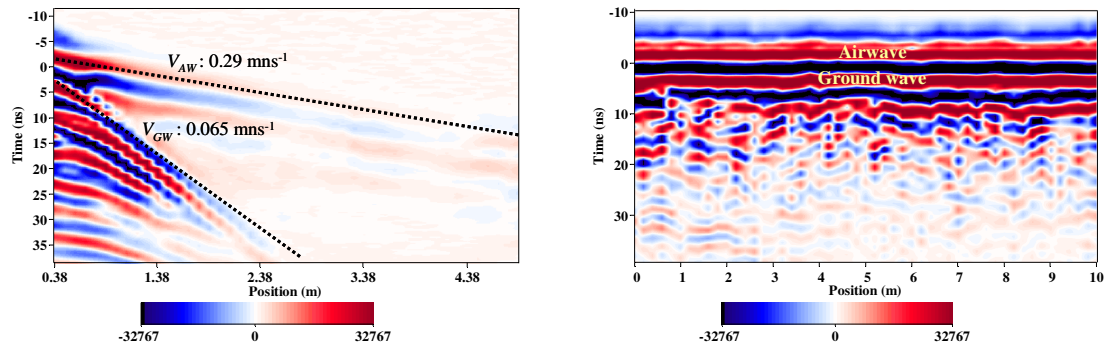

Figure 2. (a)CMP profile with AW and GW velocity and (b) unprocessed CO profile showing the AW and GW pick (same picking process for GW is used in all data analysis).

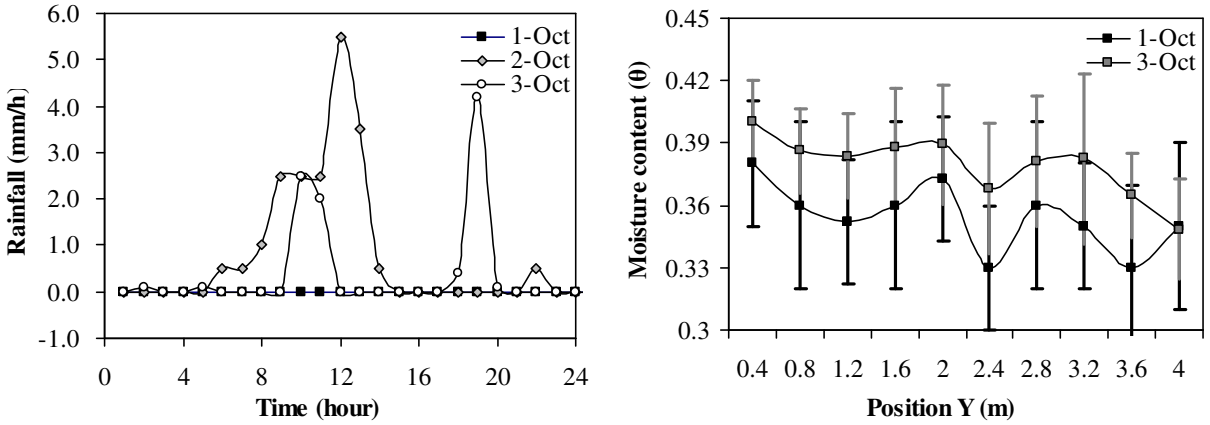

Figure 3. (a) Hourly rainfall intensity on the study site from Oct. 1st to 3rd, 2009 and (b) averaged moisture content along each survey lines on Oct. 1st and Oct. 3rd based on GW information.

The automatic velocity extraction from CMP profile also showed the GW velocity of 0.067 m ns^{-1} respectively. Similar response was observed in the second CMP survey (along transect 8), where the GW velocity by taking the inverse of linear slope was 0.061 m ns^{-1} and from the automatic velocity extraction was 0.067 m ns^{-1} respectively. CMP surveys were also used as a reference for true AW and GW picks from the CO profile and selection of an optimal antenna separation for the CO survey. After careful inspection of all CMP data and the results of semblance analysis, an antenna separation of 0.40 m was selected for CO survey. Data was collected 2-3 times a week during the monitoring experiment. The AW was selected as first maximum amplitude and GW as the second maximum value. A similar picking process was applied during all data acquisition campaigns. Soil heterogeneity, shallow reflections, and high and weak reflections zones were clearly observed from the profiles. In this paper, we focus only on two results that were collected pre- and post-precipitation; October 1st and October 3rd in 2009, respectively. The rainfall intensity during these data acquisitions is given in Figure 3a. During both campaigns, CO profiles were collected along each transect with a step size of 0.4 m, time window of 50 ns, sampling rate of 0.4 ns and eight stacks per trace. This survey resulted in ten CO profiles over the entire area in each campaign, five in bare soils and five in vegetated soils. Figure 2b shows one of the CO profiles collected during the first campaign.

Analysis of travel times of GW was performed to assess near-surface variations in space and time. The arrival times of the air and ground waves picked from the CO data were compensated for time-zero starting delays. The calibrated travel times were converted into velocities and velocity values were then converted into dielectric constants and finally Topp's equation (Topp, 1980) was used for moisture content estimation. Comparison of GPR and sensor data along Transect 1, GPR estimated moisture content values showed similar trend until 6.5 m where 5-cm-long sensors were installed, while the information based on 10-cm and 20-cm sensors (from 6.4 m to 10 m) underestimates the moisture content. The estimated depth of influence of GW based on two depth models for the GW velocities of 0.06, 0.065 and 0.07 mns^{-1} was; (a) van Overmeeren *et al.* (1997): 0.12 m to 0.14 m, and (b) Pallavi *et al.* (2009): 0.06 m to 0.07 m respectively. Model (b) was found more consistent with the obtained moisture content estimates. The similarities between 5-cm-long sensors and GPR data showed that GPR can provide spatially dense and potentially valuable information about the surface moisture content variations at rapid pace in non-invasive manner at our study site. In addition, inaccuracy in data picking for GWTT and difference in sampling volume, especially the depth of influence of GPR ground wave and the soil moisture sensors can not be ignored in this comparison.

Using the same approach, moisture content distributions were mapped one day after precipitation. An impact of precipitation was observed on the surface moisture content. Figure 3(b) shows the averaged moisture content along all survey lines during pre- (Oct.-1st) and post (Oct-3rd) precipitation campaigns. A significant increase in the moisture content was observed. Extending the investigated ground wave analysis into two-dimensional space, Figure 4 illustrates the spatial variation is the near surface moisture content over the entire study area. Figure 4a represents the data collected during the Oct.-1st, while Figure 4b represents the data obtained one day after precipitation (Oct. -3rd). The moisture content shows significant increase in the post precipitation campaign. Figure 4c shows the changes in the moisture content after precipitation. The moisture content change was not uniform over the study area. A probable cause might be related to the soil hydraulic properties and/or topography of the site. In summary, the present study signifies the potential of ground wave for spatial mapping of surface moisture content at the field scale.

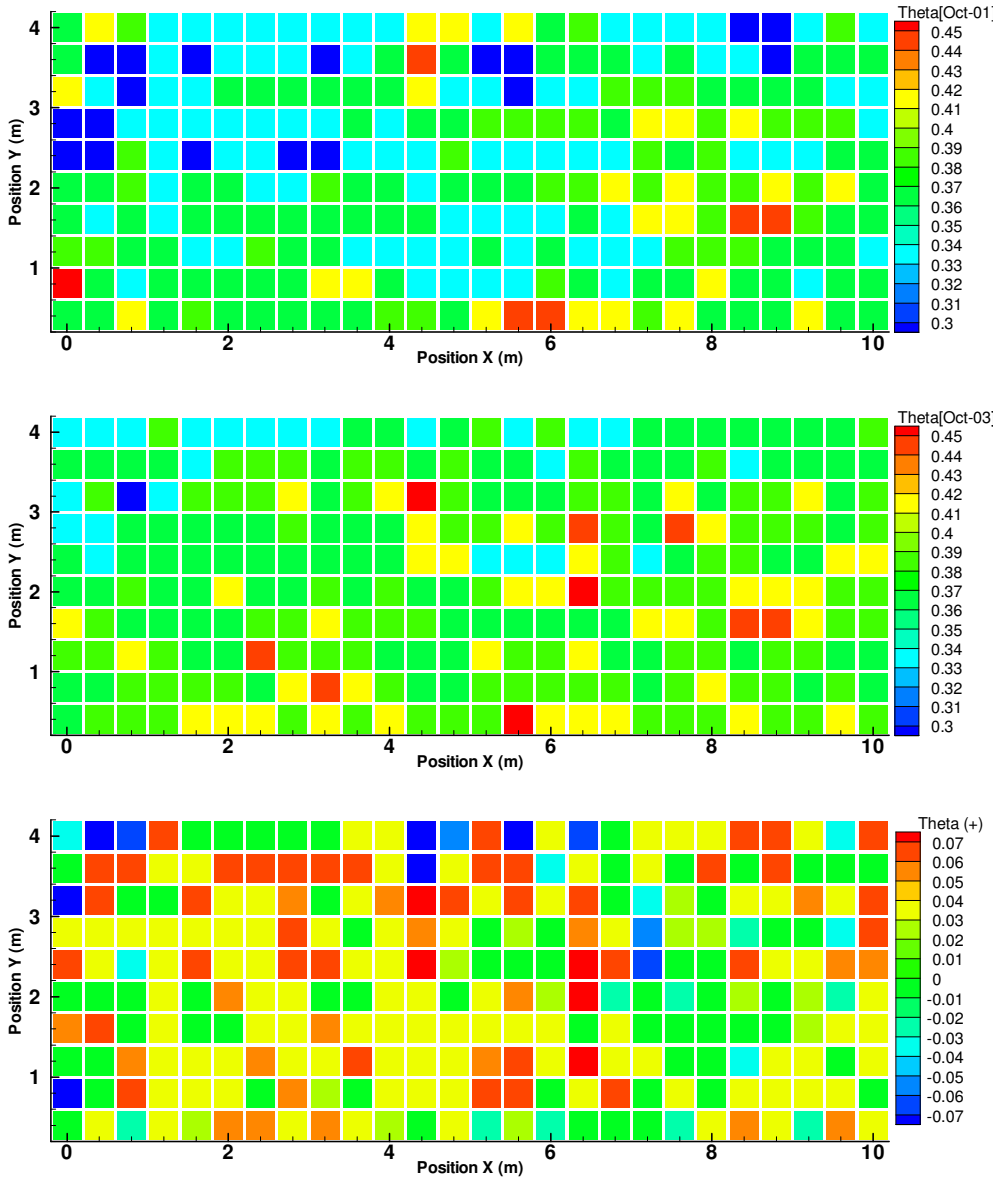

Figure 4. Spatial variations of moisture content (θ) maps obtained using GPR ground waves, (a) on fine sunny day (Oct.- 1st), (b) a day after precipitation (Oct.-3rd) in 2009, and (c) Change in moisture content after precipitation over the entire area.

Additionally, it was also verified that the GW depth can also be measured with GPR information only. Experimentally, it was observed that GW can image the seasonal variations of surface moisture content with high resolution and known sampling volume.

References

Davis JL, Annan AP (1989) Ground-penetrating radar for high resolution mapping of soil and rock stratigraphy. *Geophysical Prospect* **37**, 531-551.

Grote K, Hubbard S, Rubin Y (2003) Field-scale estimation of volumetric water content using GPR ground wave techniques. *Water Resources Research* **39**, 1321–1106.

Huisman JA, Hubbard SS, Redman JD, Annan AP (2003) Measuring soil water content with ground penetrating radar: A review. *Vadose Zone Journal* **2**, 476–491.

Pallavi B, Saito H, Kato M (2009) Estimating depth of influence of GPR ground wave in lysimeter experiment. *Journal of Arid Land Studies* **19(1)**, 121-124.

Van Overmeeren RA, Sariowan SV, Geherels JC (1997) Ground penetrating radar for determining volumetric soil water content; results of comparative measurements at two sites. *Journal of Hydrology* **197**, 316– 338.

Assessment of Soil-Amendment Mixtures for Subsurface Drip Irrigation Systems

Andreas Schwen and Willibald Loiskandl

Institute of Hydraulics and Rural Water Management, University of Natural Resources and Applied Life Sciences (BOKU), Vienna, Austria. Email andreas.schwen@boku.ac.at

Abstract
Subsurface drip irrigation (SDI) is the most water saving irrigation system. Inorganic soil amendments (IA) emplaced around the irrigation tubes can increase the water retention potential and might reduce the loss of water due to leaching. We analysed mixtures of sand for golf putting green construction and IA additions up to 10 mass percent by measuring their water retention in soil cores and modeling soil water storage and drainage under a reaslistic water application schedule. A simulation of the soil water dynamics was used to assess the effect of IA in terms of irrigation water conservation and drainage losses. Two different climatic situations, represented by climatic data of Brussels, Belgium (humid) and Cordoba, Spain (arid) were compared in the simulation. The irrigation schedules for each location with respect to the soil amendment were calculated employing a deficit-based protocol.
The addition of IA increased the available water capacity and resulted in a significant reduction of scheduled irrigation events and also a reduction of annual irrigation water requirements and water loss due to drainage for both climatic conditions. The observed water saving effect was larger for humid climatic conditions. Thus, the combination of subsurface drip irrigation with IA addition leads to additional water saving for irrigation on golf putting greens.

Key Words
Subsurface drip irrigation, inorganic soil amendment, simulation, deficit irrigation

Introduction
In times of increasing droughts and water shortages effective irrigation systems become more important. Regarding the losses by evaporation subsurface drip irrigation (SDI) is the most water saving irrigation system. Nevertheless, especially in sandy soils with low natural water holding capacity, the loss of water and nutrients due to leaching is still a serious disadvantage. Inorganic soil amendments (IA) emplaced around the irrigation tubes might increase the water retention potential.

In the present case study we assessed the potential of IA addition to reduce irrigation water requirements using SDI on golf putting greens. We compared the effect for humid and arid climatic conditions, represented by Brussels, Belgium and Cordoba, Spain, respectively. We used a numerical simulation of the soil water dynamics to evaluate the potential reduction of irrigation water requirements and the losses due to drainage.

Methods
Sand as proposed by the United States Golf Association (USGA) for golf putting green construction was mixed with an IA consisting of bentonite, silica gel, and volcanic tuff. Soil-amendment mixtures in a range between 0–10 mass percent were put in 200 cm^3 steel cores for analysis with three replicates. The saturated hydraulic conductivity K_s was measured using the falling head method. The water retention curves $\theta(h)$ were determined using a capillarimeter with pressure heads up to −150 cm. The parameters of the lognormal retention model of Kosugi (1994) were fitted to the data using RETC (US Salinity Laboratory; Fig. 1).
Daily climatic data for Brussels (Belgium) and Cordoba (Spain) were available from the United Nations Food and Agriculture Organization (FAO) for 1990 and 1986, respectively. AquaCrop 3.0 (FAO) was used to calculate an irrigation schedule for each location employing a deficit-based protocol (Allen *et al.* 1998). The Richards' equation (1931) was solved numerically using HYDRUS 2D/3D (Šimunek *et al.* 2006). Simulations were done for both locations with hydraulic properties of pure sand and 10 mass percent IA addition for one year. The 2D model geometry consisted of an upper rootzone layer (width: 100 cm, depth: 40 cm) and a lower gravel layer for drainage (depth: 15 cm). Two irrigation pipes with an diameter of 1 cm were implemented with a lateral distance of 50 cm in a depth of 30 cm. The upper boundary condition accounted for precipitation and evaporation. Turf grass transpiration was implemented as sink term according to Feddes *et al*. (2001). The lower boundary was set to a free drainage condition and the lateral boundaries were set to no-flux.

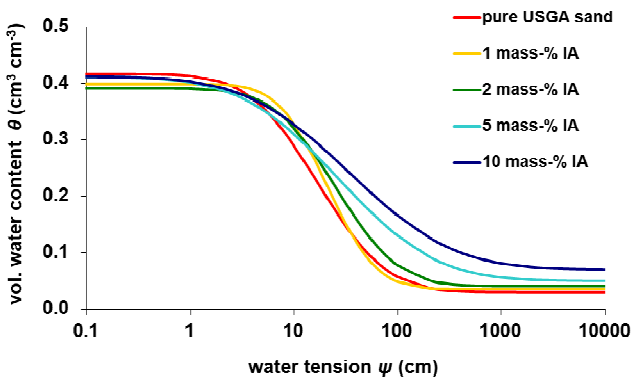

Figure 1. Water retention curves for USGA-conforming sand with different amounts of inorganic soil amendment (IA).

Results and Discussion

The addition of IA increased the available water capacitiy from 120 mm/m for pure sand up to 210 mm/m for 10 mass percent IA (Figure 1). The simulation revealed a significant reduction of scheduled irrigation events and also a reduction of annual irrigation water requirements and water loss due to drainage for humid and arid climatic conditions (Table 1, Figure 2). However, the observed water saving effect was larger for humid climatic conditions. This can be explained by a greater probability of precipitation events to replenish the available water capacity. These results are in agreement with McCoy and McCoy (2005). Nevertheless, the addition of 10 mass percent AI within a thickness of 40 cm might be very cost-intensive and need to be assessed in terms of its cost-benefit ratio in future investigations.

Table 1. Summary of the simulation results. The results base on climatic conditions as provided by the FAO (Brussels: 1990, Cordoba: 1986).

simulation result	Brussels	Cordoba
irrigation events for pure USGA-conform sand	68	225
irrigation events for sand + 10 mass-% amendment	61	177
reduction of irrigation events (%)	10.3	21.3
reduction of irrigation water requirement (%)	6.0	3.5
reduction of water loss due to deep drainage (%)	4.9	3.5

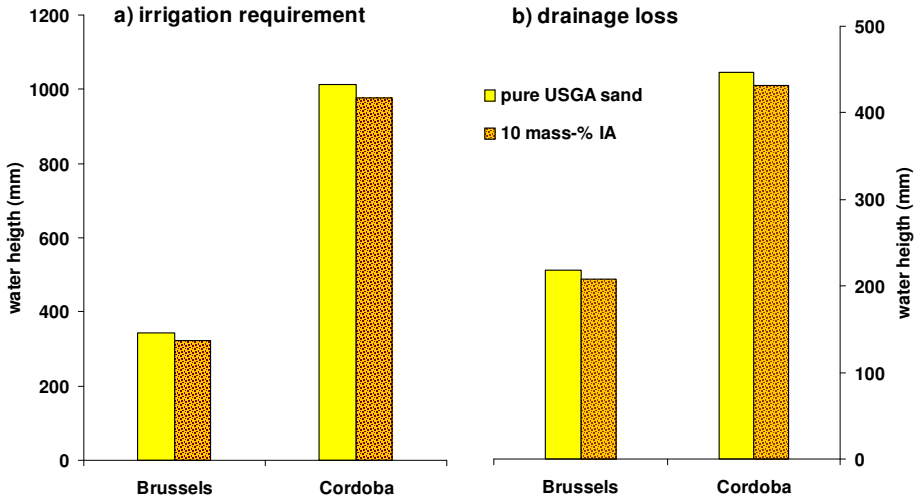

Figure 2. Results of the study. a) Calculated annual water requirement for irrigation. b) Water loss due to deep drainage. The results are on basis of the climatic data provided by the FAO (Brussels: 1990, Cordoba: 1986).

Conclusion and Perspective

The combination of subsurface drip irrigation with IA addition leads to additional water saving for irrigation on golf putting greens. The magnitude of water conservation depends on the climatic conditions and is higher for humid conditions than in arid areas.

References

Allen RG, Pereira LS, Raes D, Smith M (1998) 'Crop evapotranspiration – Guidelines for computing crop water requirements. *FAO Irrigation and drainage paper* **56'.** (Food and Agriculture Organization of the United Nations: Rome).

Feddes RA, Hoff H, Bruen M, Dawson T, de Rosnay P, Dirmeyer O, Jackson RB, Kabat P, Kleidon A, Lilly A, Pitman AJ (2001) Modeling root water uptake in hydrological and climate models. *Bulletin of the American Meteorological Society* **82**, 2797-2809.

Kosugi K (1994) Three-parameter lognormal distribution model for soil water retention. *Water Resources Research* **30(4)**, 891-901.

McCoy E, McCoy K (2005) Putting Green Rootzone Amendments and Irrigation Water Conservation. *USGA Turfgrass and Environmental Research Online* **4(8)**, 1-9.

Richards LA (1931) Capillary conduction of liquids through porous mediums. *Physics* **1:3**, 18-333.

Šimunek J, van Genuchten MT, Šejna M (2006) 'The HYDRUS Software Package for Simulating the Two-and Three-Dimensional Movement of Water, Heat, and Multiple Solutes in Variably-Saturated Media. Version 1.10', (PC-Progress: Prague).

Calculation of Canopy Resistance with a Recursive Evapotranspiration Model

Robert J. Lascano[A] and Steven R. Evett[B]

[A]Cropping Systems Research Laboratory, USDA-ARS, Lubbock, TX, USA, Email Robert.Lascano@ars.usda.gov
[B]Conservation and Production Laboratory, USDA-ARS, Bushland, TX, USA, Email Steve.Evett@ars.usda.gov

Abstract
The calculation of hourly and daily crop evapotranspiration (ET_c) from weather variables when using the combination method, e.g. Penman-Monteith, requires a corresponding hourly or daily value of canopy resistance (r_c). An iterative method first proposed by MI Budyko to calculate ET_c finds the surface canopy temperature (T_s) that satisfies the crop's energy balance. This method was used to calculate both hourly and daily values of r_c over a well-watered and established alfalfa crop for 26 days during the 1999-growing season in Bushland Texas. Hourly values of r_c were obtained using a graphical procedure from first, values of ET_c measured with a large weighing lysimeter; and second, from values of T_s measured with a radiometer. Results show that the daily seasonal average alfalfa r_c was 45 ± 12 s/m for both methods of calculating r_c. In the absence of a lysimeter installation to measure ET_c the measurement of T_s with a radiometer provides an alternative and practical means to calculate r_c provided that other required weather input variables are also measured over the crop canopy.

Key Words
Irrigation, crop water use

Introduction
The concept of a maximum rate of water evaporation, i.e. potential evapotranspiration (ET_p), was introduced by Thornthwaite (1944; 1948) and defined as the water loss from vegetation when a soil has at no time a deficiency of water. In general, methods to calculate ET_p are divided into empirical and theoretical; however, there is no clear distinction between the two approaches and available methods are usually a mixture of both physical considerations and empirical observations (Sibbons 1962). Theoretical methods relate the flux of water vapor from the evaporating surface to the process of turbulent diffusion, i.e. aerodynamic approach, and a second method considers the energy balance and calculates the amount of energy that is used in vaporizing water (e.g. Sutton 1953; Brutsaert 1982). A third method combines the aerodynamic and energy balance approaches eliminating the surface temperature from the relevant equations, i.e. *combination* method (Penman 1948). A similar and independent approach to calculate ET_p was given by Budyko (1951; 1956) who termed his technique the *complex* method. However, there is a major distinction between the *combination* and *complex* methods in that the assumption made by Penman (1948) regarding the linear relation between temperature and the humidity of the evaporating surface is not required by the method proposed by Budyko (1951; 1956). The Budyko method is *recursive* in that the temperature of the evaporating surface that satisfies the energy balance is found by iteration (Sellers 1964; Lascano and Van Bavel 2007; Lascano *et al.* 2009).

The application of using calculations of ET_p to estimate the amount of water used by a crop (ET_c, mm/h) was recognized by introducing a stomatal and a day-length factor (Penman 1953), which was equated to a bulk canopy resistance (r_c, s/m) term and considered in the so-called big leaf model (Monteith 1965). Methods to calculate r_c range from an explicit solution of $ET_a = f(ET_p)$ (Van Bavel and Ehrler 1968) to an empirical function of crop height and leaf area (Allen *et al*. 1989). In this paper we show how the method of Budyko (1951, 1956) hereafter, referred to as the Recursive Combination Method (RCM) and as given by Lascano and Van Bavel (2007) was used to calculate hourly and daily values of r_c for a well-watered alfalfa crop. For this purpose, two such methods on an alfalfa crop were explored and compared. First, r_c was calculated from hourly values of ET_c measured with a large weighing lysimeter and second, r_c was calculated from measured hourly values of canopy temperature (T_s, °C) measured with a radiometer.

Methods
Experimental field and weather data
In our calculations we used weather data from Bushland Texas, USA on a well-established and watered alfalfa crop. We selected 26 days, between 23 May and 12 September 1999, all after a day of irrigation and determined to be without equipment failure, rainfall, significant cloudiness and periods of high wind-speed. Weather data measured at Bushland Texas consisted of air (T_a, °C) and dewpoint (T_d, °C) temperature, net irradiance (R_n,

W/m^2), soil heat flux (G, W/m^2), and wind-speed (U_z, m/s). Weather variables were measured every 6 s and reported as 0.5-hour averages. Surface canopy temperature (T_s, °C) was measured with a calibrated radiometer (Everest Model 4000) and details on the lysimetric measurements of alfalfa ET_c are given by Evett *et al*. (2000). Additional information on instruments and methods used to measure weather variables, G, ET_c and T_s are described by Evett (2000) and further details are given by Lascano *et al*. (2009).

Calculations

Crop ET_c is calculated from the energy balance equation of the plant canopy surface:

$$ET_c = \left(\frac{R_n + H + G}{\lambda}\right)3600 \quad (1)$$

where λ is the latent heat of vaporization in J/kg and H is the sensible heat flux in W/m^2, and calculated as:

$$H = \frac{\rho_a C_p \left(T_a - T_s\right)}{r_a} \quad (2)$$

where ρ_a is the air density in kg/m^3, C_p is the specific air heat capacity in J/kg/°C, and r_a is the aerodynamic resistance in s/m calculated as given by Evett (2000):

$$r_a = \frac{ln\left[\frac{\left(z_w - d\right)}{z_{om}}\right] ln\left[\frac{\left(z_r - d\right)}{z_{ov}}\right]}{k^2 U_z} \quad (3)$$

where z_w is the height of the wind-speed measurement in m, z_r is the measurement height for humidity in m, z_{ov} is the vapor roughness length in m, d is zero-plane displacement height in m, and k is von Karman's constant. Values of d and z_{om} were calculated as a function of crop height (h_c, m), and T_s in Eq. (2) was found iteratively with an initial value of T_s = 10 °C written in Mathcad® (*v.* 14, PTC, Needham, MA, USA) syntax by:

$$T_s = root\left[\left[R_n + G + \frac{\left(T_a - T_s\right)\times\rho_a\times C_p}{r_a} - \frac{1.323\times\frac{\exp\left(17.269\times\frac{T_s}{T_s+237.0}\right) - e_a}{T_s+237.2}}{r_a + r_c}\times\lambda\right]\times\frac{r_a}{C_p\times\rho_a}, T_s\right] \quad (4)$$

where *root* is a Mathcad® built-in function to solve for the value of T_s and e_a is the ambient air density in kg/m^3.

The value of r_c in Eq. (4) was calculated from measured values of ET_c and T_s, using the graphical procedure of Lascano and Van Bavel (2007). For any given hour, the alfalfa energy balance was solved from the pertinent hourly weather input (T_a, T_d, U_z, R_n and G) using the RCM. For this purpose r_c was defined as a *range* variable in Mathcad®, i.e. 10 to 70 in 5 s/m increments. Thus for each value of r_c the solution of Eq. (4) gave ET_c and T_s as a function of r_c. Then for each hour the value of ET_c measured lysimetrically and T_s measured radiometrically were used to find the corresponding value of r_c. Calculations were done for hourly values when $R_n > 0$ W/m^2.

Results and Discussion

An example of an hourly calculation of alfalfa r_c for 4 July 1999 at 14:00 hour is given in Figure 1. The weather input for this hour was R_n = 690.2 W/m^2, G = 44.4 W/m^2, T_a = 27.7 °C, T_d = 16.5 °C, and U_z = 6.9 m/s, and h_c = 0.65 m. The measured ET_c with a lysimeter was 1.05 mm, intersecting the $ET_c = f(r_c)$ at 34.2 s/m (Figure 1a) and the measured T_s with a radiometer was 28.2 °C, intersecting the $T_s = f(r_c)$ at 35.6 s/m (Figure 1b). As examples, the diurnal course of r_c from hourly measurements of ET_c and T_s for 23 May and 1 August 1999 using the procedure shown in Figure 1 are shown in Figure 2. The daily average, standard deviation and range of r_c for the 26 days of 1999 obtained from lysimetric and radiometric measurements are summarized in Table 1.

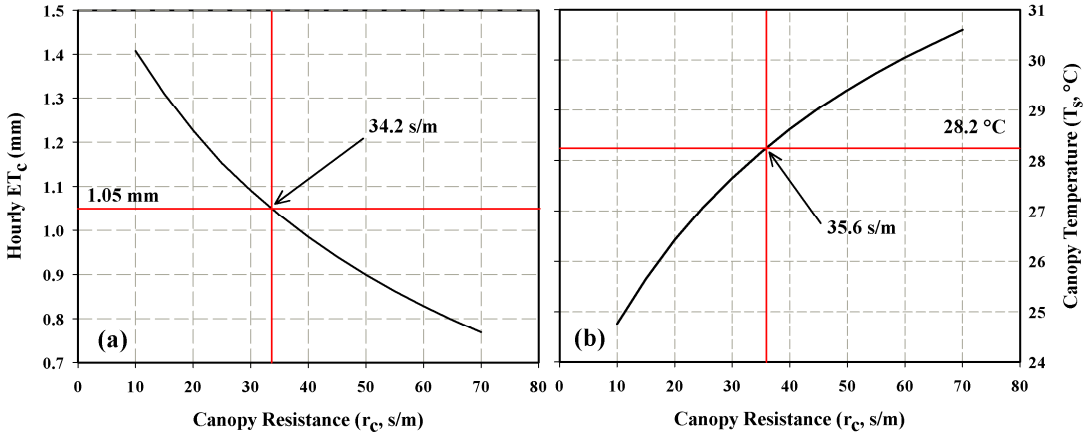

Figure 1. Graphical derivation of alfalfa canopy resistance (r_c) from (a) ET_c and (b) T_s on 4 July 1999 at 14:00 hour. The value of r_c = 34.2 s/m from the lysimeter measurement and r_c = 35.6 s/m from the radiometer measurement.

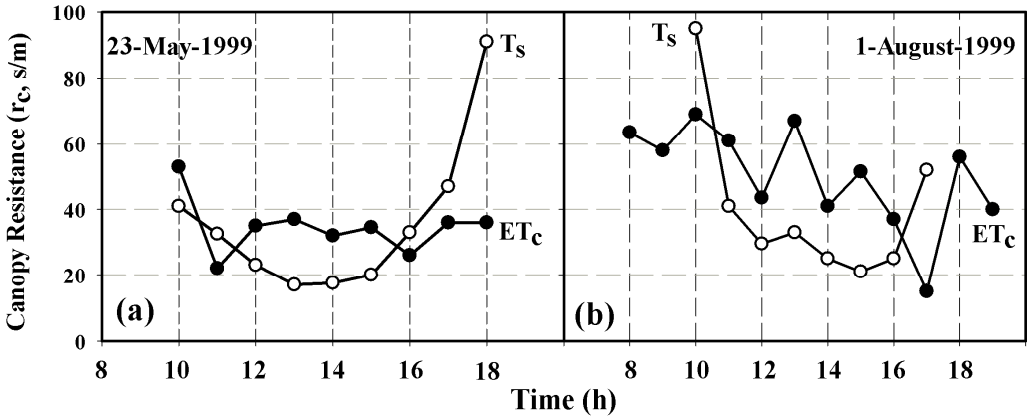

Figure 2. Diurnal values of r_c from ET_c (●) and from T_s (○) for (a) 23 May 1999 and (b) 1 August 1999 obtained using the graphical procedure shown in Figure 1.

Table 1. Daily average, standard deviation, minimum and maximum values of alfalfa r_c for 26 days 1999 in Bushland Texas, obtained from ET_c measured with a lysimeter and T_s measured with a radiometer.

	Daily canopy resistance (r_c, s/m)	
	Lysimeter (ET_c)	Radiometer (T_s)
Average	45.6	44.5
Standard Deviation	11.6	12.1
Minimum	27.0	26.3
Maximum	80.3	83.3

The graphical procedure to obtain hourly values of r_c is based on the RCM and uses an iterative solution to find T_s. This calculation does not require any more calculating effort than that used with the Penman-Monteith (PM) to find ET_c, which is based on the linearity assumption introduced by Penman (1948). However, as shown by Milly (1991) and Lascano and Van Bavel (2007) calculation of ET_c based on PM consistently underestimates evaporation, particularly under semiarid climates, where irrigation is normally used. However, a difficulty in using any model, either PM or RCM, to calculate ET_c is the selection of a r_c value that is correct.

An accurate measurement of crop ET_c can be obtained with lysimeters (Schneider *et al.* 1998); however, their construction is costly and requires continuous maintenance. An alternative is to measure the T_s of the crop with a calibrated radiometer, which can also be used to calculate r_c. Our results show that r_c can be calculated from either ET_c (Figure 1b) or T_s (Figure 1b) and that their diurnal trends are similar (Figure 2). The largest discrepancy (data not shown) occurs early in the morning and in the evening, i.e. at low values of R_n. Nevertheless, a statistical comparison of daily averages, standard deviation and range (Table 1) suggest no differences in the seasonal value of r_c for a well-watered alfalfa derived from either hourly values of ET_c or T_s. These results suggest that in the absence of lysimeters a radiometer can be used to calculate r_c with a RCM provided that weather inputs such as, T_a, T_d, R_n, G and U_z are also measured.

Conclusion

Two methods, both based on a RCM and using a graphical procedure of hourly values of ET_c measured with a lysimeter or T_s measured with a radiometer, can be used to derive values of r_c for a well-watered alfalfa crop. Values of seasonal r_c derived from both methods were similar, 45 ± 12 s/m, which give accurate values of daily ET_c (Lascano *et al*. 2009). In the absence of a lysimetric installation to measure ET_c the measurement of T_s along with required weather variables provides an alternative method to calculate r_c that is both practical and accurate.

References

Allen RG, Jensen ME, Wright JL, Burman RD (1989) Operational estimates of evapotranspiration. *Agronomy Journal* **81**, 650-662.

Budyko MI (1951) The effect of ameliorative measures on evaporation. Izvestiia of the Academy of Sciences S.S.S.R., *Ser Geograficheskaia*, No. **1**, 16-35. (In Russian and cited from Sibbons 1962 and Milly 1991).

Budyko MI (1956) 'The Heat Balance of the Earth's Surface.' (English translation, Stepanova, N.A. Office of Technical Services, PB 131692, U.S. Department of Commerce, Washington, D.C., 1958, 259 pp.).

Brutsaert W (1982) 'Evaporation into the Atmosphere.' (Kluwer Academic Publishers, Dordrecht, The Nertherlands, 299 pp.).

Evett SR (2000) Water and energy balances at soil-plant-atmosphere interfaces. In 'Soil Physics Companion'. (Ed. AW Warrick), Chapter **5**: 127-188. (CRC-Press, Boca Raton, FL, USA).

Evett SR, Howell TA, Todd RW, Schneider AD, Tolk JA (2000) Alfalfa reference ET measurement and prediction. In 'Proceedings of the 4th Decennial National Irrigation Symposium'. Nov 14-16, 2000, Phoenix, Arizona (Ed. RG Evans, BL Benham, TP Trooien) pp. 266-272.

Lascano RJ, Van Bavel CHM (2007) Explicit and recursive calculation of potential and actual evapotranspiration. *Agronomy Journal* **99**, 585-590.

Lascano RJ, Van Bavel CHM, Evett SR (2009) A field test of recursive calculation of crop evapotranspiration. *Agricultural and Forest Meteorology* (Submitted for publication).

Milly PCD (1991) A refinement of the combination equations for evaporation. *Surveys in Geophysics* **12**, 145-154.

Monteith JL (1965) Evaporation and environment. Proceedings 19th Symposium Society Experimental Biology, Swansea, 1964. The State and Movement of Water in Living Organisms, p. 205-234.

Penman HL (1948) Natural evaporation from open water, bare soil, and grass. *Proceedings Royal Society London* **A193**, 120-145.

Penman HL (1953) The physical bases of irrigation control. *Report 13th International Horticultural Congress: 1952* **2**, 913-924.

Schneider AD, Howell TA, Moustafa ATA, Evett SR, Abou-Zeid W (1998) A simplified weighing lysimeter for monolithic or reconstructed soils. *Applied Engineering in Agriculture* **9**, 227-232.

Sellers WD (1964) Potential evapotranspiration in arid regions. *Journal of Applied Meteorology* **3**, 98-104.

Sibbons JLH (1962) A contribution to the study of potential evapotranspiration. *Geografiska Annaler* **44**, 279-292.

Sutton G (1953) 'Micrometeorology.' (London and New York, McGraw-Hill, 302 pp.).

Thornthwaite CW (1944) Report of the committee on transpiration and evaporation, 1943-44. *Transactions, American Geophysical Union* **25**, 683-693.

Thornthwaite CW (1948) An approach toward a rational classification of climate. *Geographical Review* **38**, 55-94.

Van Bavel CHM, Ehler WL (1968) Water loss from a sorghum field and stomatal control. *Agronomy Journal* **60**, 84-86.

Contribution of stony phase in hydric properties of soils

Marion Tétégan[A, B], Isabelle Cousin[A], Alain Bouthier[B] and Bernard Nicoullaud[A]

[A]INRA, UR 0272 Science du Sol, Centre de recherche d'Orléans, 2163 Avenue de la Pomme de Pin, CS 40001 Ardon 45075 Orléans Cedex 2, France. Email Marion.Tetegan@orleans.inra.fr
[B] Arvalis – Institut du Végétal, Domaine expérimental du Magneraud 17700 Saint Pierre d'Amilly, France. Email a.bouthier@arvalisinstitutduvegetal.fr

Abstract
Stony soils cover about 30% of the surface soils of Western Europe, and 60% in Mediterranean areas. They consist of rock fragments whose diameters are larger than 2 mm (the rock fragment). These fragments may alter the physical, chemical and agricultural properties of soils. To better understand the role of stones in the water supply of crops, structure and hydric properties of coarse elements of stony soils were studied. Monitoring the moisture was done on coarse fragments from sedimentary rocks, and revealed that rock fragments can store as much water as the fine earth. Applying the concept of field capacity and wilting point to coarse fragments, a simple pedotransfer function was defined to estimate the contribution of the pebbles to the Available Water Content of a stony soil.

Key Words
Pebbles, pedotransfer function, bulk density, water content, field capacity, wilting point

Introduction
Stony soils contain coarse fragments, so called stones, which limits some tillage operations. Moreover, these soils are often thin, and therefore very vulnerable to the leaching of nitrates and pesticides. They cover about 30% of the surface soils of Western Europe and 60% in Mediterranean areas (Poesen and Lavee 1994). Though stony soils are widely spread and create problems to agriculture production, they have been little studied. As stones characterization is difficult, the stony phase is often neglected in the characterization of the properties of stony soils. However, the rock fragments could modify the physical, chemical and hydrodynamic properties of soils (Ravina and Magier 1984; Brakensiek and Rawls 1994; Poesen and Lavee 1994; Certini *et al*. 2004), and affect the behaviour and characteristics of agricultural soils. Indeed, the stony phase may participate in the water supply of crops (Coile 1953; Hanson and Blevins 1979; Gras 1994; Danatalos *et al*. 1995) and change the storage capacity of soil water (Coutadeur *et al*. 2000; Cousin *et al*. 2003). All these previous studies suggest some water transfers between the rock fragments and fine earth in soil. The objective of this work was to study the contribution of stony phase to some soils hydric properties using the structure and the water retention capacity of rock fragments from different types of stony soils.

Methods
Sampling
Stones were sampled in the cultivated horizon (0 - 30 cm) of different types of stony soils in the Central part of France. Only the pebble fraction (2 cm < stone diameter < 5 cm) was studied. Most of the stones were collected when the soil was at field capacity. The pebbles were sampled in soils developed over sedimentary rocks and were of the following types: gaize, chalk, chert, flint, and limestone.

Characterization of pebbles structure
The structure of each pebble was characterized by measurements on dried pebbles of bulk density and density of solid, and by calculation of the void ratio of the sample. The bulk density was determined by the oil method (Monnier *et al*. 1973) and the solid density by a gas pycnometer. The void ratio was calculated according to the following formula:

$$e = (Ds / Bd) - 1. \quad (1)$$

where e represents the void ratio, Ds represents the solid density and Bd represents the bulk density.

Characterization of pebbles hydric properties
The hydric properties were determined by measurements of gravimetric water content when the pebbles were at saturation or equilibrated at -100 hPa and -15000 hPa in pressure plates during 7 days.

Results

Characterization of pebbles structure

The porosity in pebbles was not equal to zero. In addition, the porosity, but also bulk density and void ratio varied according to the type of stone. Moreover, results showed that the bulk density of pebbles varied within a single type of stone, and especially for the limestones. The bulk density was the lowest for gaizes and the highest for flints and limestones (Figure 1).

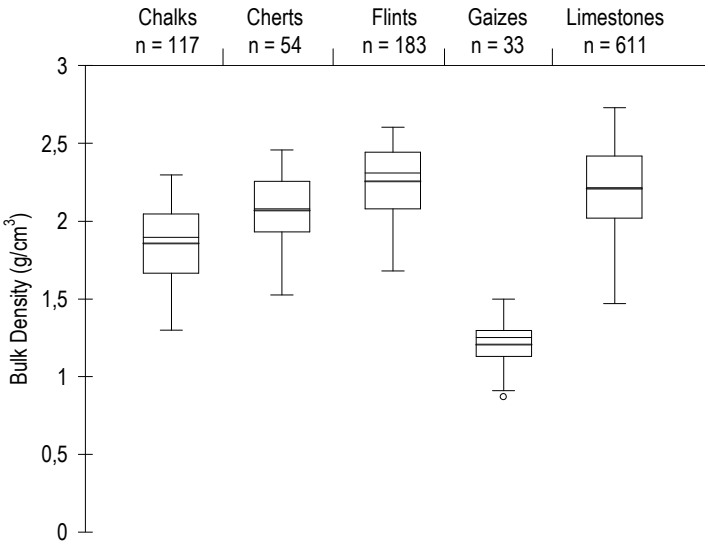

Figure 1: Box plot representing the ranges of bulk density by pebbles' type. n = sample number.

The same ordering was found for the measurements of solid density, but the reverse order was observed for the void ratio. Indeed, the void ratio increased in the following order limestones > flints > cherts > chalks > gaizes.

Characterization of pebbles hydric properties

Water content measurements showed that all types of studied pebbles can retain water, and the saturated water content can reach more than 60% for gaize. The determination of some points of the retention curve allowed us to show the following two results:

1/ Whatever the type of pebble, the water content at field capacity was very close to the water content at -100 hPa (Figure 2; Student test with r =0.99, P < 0.00001 and α = 0.05). For the different materials studied here, a simple relationship exists between the humidity of pebbles at -100 hPa and at field capacity.

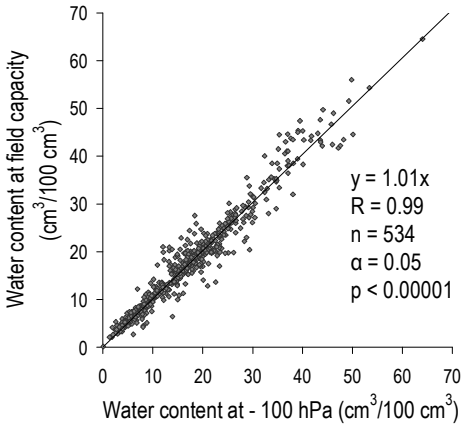

Figure 2: Relationship between water content at -100 hPa and at field capacity. R = correlation coefficient. n = sample number, all pebbles' type confused. α = threshold of significance. p = the probability that the hypothesis would be null.

2/ We also demonstrated that the water content at wilting point was, on average, equal either to half or three quarters of the water content at field capacity, depending on the pebble type. These relationships were validated statistically by a Student test.

From these two results, we derived a simple and useful pedotransfer function to calculate the Available Water Content (AWC) in pebbles contained in stony soils. The latter was calculated from the difference between the water content at -100 hPa and the water content at -15000 hPa:

$$AWC \sim \theta_{-100} - \theta_{-15000} \sim \zeta\, \theta_{fc} \quad (2)$$

where θ_{-100} represents the water content at -100 hPa, θ_{-15000} represents the water content at -15000 hPa, θ_{fc} represents the water content at field capacity and ζ is a parameter equal ½ or ¼ depending of the type of stone.

Conclusion

We demonstrated that pebbles have different porosity and water retention capacity depending of their type - limestones, flints, cherts, chalks, gaizes - but all could contribute to the hydric properties of stony soils. We also defined a simple pedotransfer function to estimate the contribution of the pebbles to the Available Water Content of a stony soil. The latter can be easily calculated from the water content at field capacity. This pedotransfer function has been validated over a large range of types of stones in sedimentary rocks and is robust. The next step would consist in determining pedotransfer functions in the fine earth to characterize its contribution to the Available Water Content. In the future, these pedotransfer functions will be used to map the Available Water Content of stony soils over large areas.

References

Brakensiek DL, Rawls WJ (1994) Soil containing rock fragments: effects on infiltration. *Catena* **23**, 99-110.

Certini G, Campbell CD, Edwards AC (2004) Rock fragments in soil support a different microbial community from the fine earth. *Soil Biology & Biochemistry* **36(7)**, 1119-1128.

Coile TS (1953) Moisture content of small stone in soils. *Soil Science* **75**, 203-207.

Cousin I, Nicoullaud B, Coutadeur C (2003) Influence of rock fragments on the water retention and water percolation in a calcareous soil. *Catena* **53(2)**, 97-114.

Coutadeur C, Cousin I, Nicoullaud B (2000) Influence de la phase caillouteuse sur la réserve en eau des sols. Cas des sols de Petite Beauce du Loiret. *Etude et Gestion des Sols* **7(3)**, 191-205.

Danalatos NG, Kosmas CS, Moustakas NC, Yassoglou N (1995) Rock fragments II. Their impact on soil physical properties and biomass production under Mediterranean conditions. *Soil Use and Management* **11**, 121-126.

Gras R. (1994) 'Sols caillouteux et production végétale'. (INRA Editions).

Hanson CT, Blevins RL (1979) Soil water in coarse fragments. *Soil Science Society American Journal* **43**, 819-820.

Monnier G, Stengel P, Fiès JC (1973) Une méthode de mesure de la densité apparente de petits agglomérats terreux. Application à l'analyse des systèmes de porosité du sol. *Annales Agronomiques* **24 (5)**, 533-545.

Poesen J, Lavee H (1994) Rock fragments in top soils: significance and processes. *Catena* **23**, 1-28.

Ravina I, Magier J (1984) Hydraulic conductivity and water retention of clay soils containing coarse fragments. *Soil Science Society American Journal* **48**, 736-740.

Deep drainage in a Vertosol under irrigated cotton

Anthony Ringrose-Voase[A] and Tony Nadelko[B]

[A]CSIRO Land and Water, GPO Box 1666, Canberra, ACT, Australia, Email anthony.ringrose-voase@csiro.au
[B]CSIRO Land and Water, Locked Bag 59, Narrabri, NSW, Australia, Email anthony.nadelko@csiro.au

Abstract
Deep drainage below the root zone of irrigated crops is both a waste of a scarce resource and a cause of potential environmental problems such as water logging and salinity. We measured deep drainage under furrow irrigated cotton on a Grey Vertosol using a variable tension lysimeter over two contrasting irrigation seasons. The amount of drainage was dependant on both the antecedent moisture conditions and the amount of early season rainfall. Bypass flow was detected in both seasons.

Key Words
Deep drainage, bypass flow, irrigation, water balance, Vertosol, cotton

Introduction

Over much of the history of the Australian cotton industry, it was believed that losses of water below the root zone – deep drainage – were insignificant because of the heavy clay soils on which cotton is grown. During the 1990s there was increasing concern that greater rates of deep drainage compared to native vegetation in both irrigated and dryland situations could raise watertables, mobilize salt stored in the landscape and cause waterlogging and salinity. Although salinity was not a problem for the cotton industry, it was sufficiently concerned to commission research on drainage, not just because of its potential to cause environmental problems but also because it represents a waste of an increasingly scarce resource. This research found deep drainage to be significant under furrow irrigated cotton, despite the low hydraulic conductivity of the Grey Vertosols on which it is grown, and in excess of what is required to prevent a build up of salinity.
Furrow irrigation is commonly used by the cotton industry in Australia since it can be implemented at relatively low cost over large areas. However, it can cause undesirable rates of drainage for several reasons. It is difficult to control the amount applied, which can lead to over application when the soil water deficit is small. During irrigation, free water is present at the soil surface with the potential of moving rapidly down macropores and bypassing the soil matrix. The project described in this paper aimed to directly measure deep drainage using lysimetry and investigate the mechanisms causing it.

Methods

Lysimeter location
We constructed an equilibrium drainage lysimeter at the Australian Cotton Research Institute near Narrabri in northern New South Wales (30° 11.53' South, 149° 36.31' East) in an experimental plot under a cotton-wheat rotation. Cotton crops are furrow irrigated, but wheat crops only receive supplementary irrigation if there is a risk of crop failure. Minimum tillage is used with stubble retention and permanent beds. Alternate furrows are used for traffic and irrigation. The plot is approximately 200 m long from head to tail ditch.
The soil is a Haplic, Self-mulching, Grey Vertosol (Isbell, 1996). Above 1.2 m depth the soil is 60% clay (<2 μm), 14% silt (2-20 μm) and 25% sand (20-2000 μm). Below 1.2 m, the clay content decreases to 50% by 2 m depth with corresponding increases in silt and sand to 20% and 30% respectively. Exchangeable sodium increases down the profile from <1% at the surface to 6.5% at 2 m.

Lysimeter design
Direct measurement of drainage is difficult because most instruments interfere with drainage by altering the hydraulic gradient which is the major driver of water movement. Brye *et al*. (1999) addressed this problem by designing an equilibrium tension drainage lysimeter (or variable tension drainage lysimeter). This consists of a collection tray to which a vacuum is applied that is equal to that in the surrounding soil to make the lysimeter "hydraulically invisible". The design was improved by Pegler *et al.* (2003) by introducing automated regulation of the vacuum. Our design was a modification of those by Brye *et al.* (1999) and Pegler *et al.* (2003). The lysimeter is situated under the root zone at 2.1 m depth, half way between the head and tail ditches. The lysimeter consists of an array of six collection trays (0.91 × 0.29 m area, 0.13 m high) covering a total area of 1.82 × 0.87 m. The trays are essentially stainless steel boxes, whose upper surface is made of porous, sintered

1 – 6 August 2010, Brisbane, Australia. Published on DVD.

stainless steel, 1 mm thick with a nominal pore size of 0.2 µm. Once saturated with water it can hold water up to a potential of -28 kPa. The floor of each tray slopes to a drain in one corner. Each tray also has an internal riser tube in the opposite corner for connection to a vacuum reservoir.
The trays were inserted by excavating horizontally from a cylindrical, concrete access shaft (4 m deep, 2 m diameter) located under neighbouring furrows. Hence the overlying soil is not disturbed. One benefit of having a lysimeter with no walls is that there is no interference with the natural shrink/swell behaviour of the soil. The ceiling of the cavity into which the trays were inserted was prepared by peeling away the soil using polyester resin to ensure a natural surface. A contact material was packed between the ceiling and the trays for hydraulic continuity. The material was manufactured from silica flour, graded to remove particles less than 15 µm. The drain from each tray was connected to a collection tank in the access shaft. Similarly the internal riser tube was connected to a vacuum reservoir kept at approximately -40 kPa.
Two vertical arrays of five tensiometers were installed though the wall of the access shaft at depths from 0.9 to 2.1 m. The vacuum inside the trays is regulated by a data logger via solenoids so that it equals the average potential measured by the two tensiometers at 2.1 m depth. The vacuum is adjusted every 15 minutes. At the same time the weight of drainage in the collection tanks and the soil water potentials measured by the tensiometers are recorded. The collection tanks can be isolated from the trays to allow emptying.
Four neutron probe access tubes are installed to 3 m depth around the lysimeter to allow measurement of soil water content at frequent intervals during the irrigation season.

Results

The lysimeter monitored both the 2006-07 and the 2008-09 irrigation seasons, although data monitoring was not automatic for the first of these. The amounts of drainage recorded after each irrigation are shown in Table 1. Cumulative drainage is shown in Figure 1. The total drainage for the seasons varied by a factor of 1.75 due to different conditions before and during the seasons. The subsoil was relatively wet at the start of the 2006-07 season. However, there was little rain before sowing, so the crop required irrigation shortly after sowing. In addition, in-season rainfall (September-April) was only 224 mm and the crop required a total of 8 irrigations. In contrast, the subsoil was relatively dry at the start of the 2008-09 season, but there was sufficient rain in the early part of the season that irrigation was not required until 22 December. There was more than twice the in-season rainfall, 498 mm, and only 6 irrigations were required.

Table 1. Drainage after each irrigation during the 2006/07 and 2008/09 irrigation seasons.

2006/07 season		2008/09season	
Irrigation date	**Drainage, mm**	**Irrigation date**	**Drainage, mm**
24 Oct	8.8		
22 Nov	22.0		
12 Dec	34.7	22 Dec	13.4
03 Jan	3.6	12 Jan	7.3
16 Jan	0.2	22 Jan	8.6
30 Jan	0.5	05 Feb	9.3
14 Feb	2.1	06 Mar	2.5
28 Feb	2.3	19 Mar	1.5
Total for season	**74.2**		**42.5**

2008-09 irrigation season

Figure 1 shows that the amount of drainage was greatest after the earlier irrigations and declined to very low values after the fifth and sixth irrigations. At the start of the season the subsoil below 0.75 m was relatively dry with a deficit of 88 mm between 0.75 and 1.95 m depth (Figure 2). There was 200 mm of rainfall before the first irrigation, which reduced the deficit to 49 mm. The first irrigation wet the soil above 0.75 m and, to some degree the soil below this. The crop was reasonably advanced by the first irrigation, and dried the soil above 0.75 m considerably after each irrigation. This helps explain why the 0.75-1.35 m layer was only slightly wetted up by each irrigation and, overall, dried from January onwards.
The 1.35-1.95 m layer was scarcely affected by each irrigation and reached a minimum deficit of 15 mm. It too dried from March onwards. This is also reflected in the matric potential at the bottom of the root zone (Figure 3) which reached a maximum of only -18 kPa. Despite the subsoil remaining reasonably dry, drainage still occurred throughout the season. The rate of drainage sharply increased about 6 hours after each irrigation front passed over the lysimeter, as shown in Figure 4 for the irrigation on 12 January 2009.

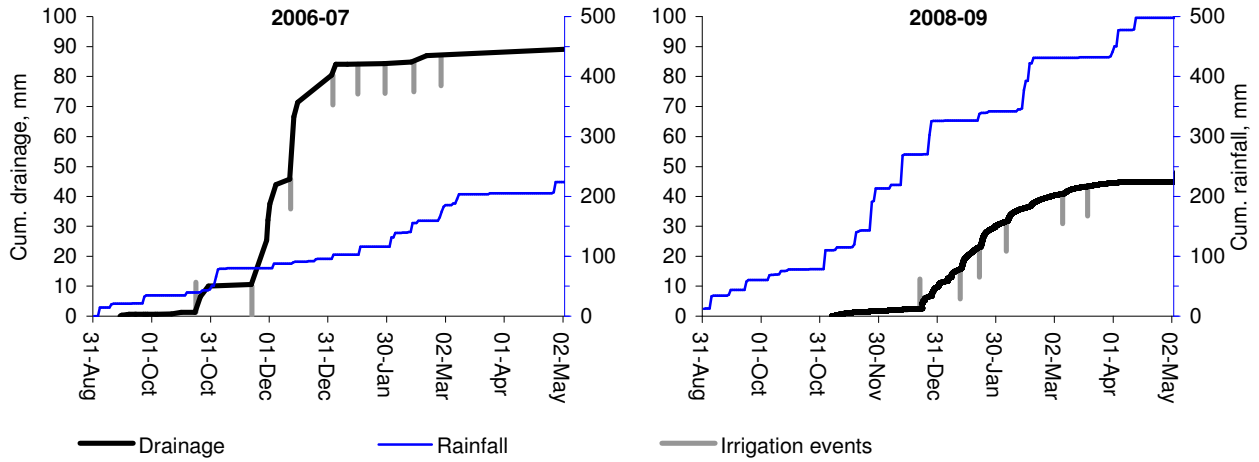

Figure 1. Cumulative drainage (left vertical axis) and cumulative rainfall (right vertical axis) during the 2006/07 and 2008/09 irrigation seasons. Dates of irrigation events are shown as vertical bars.

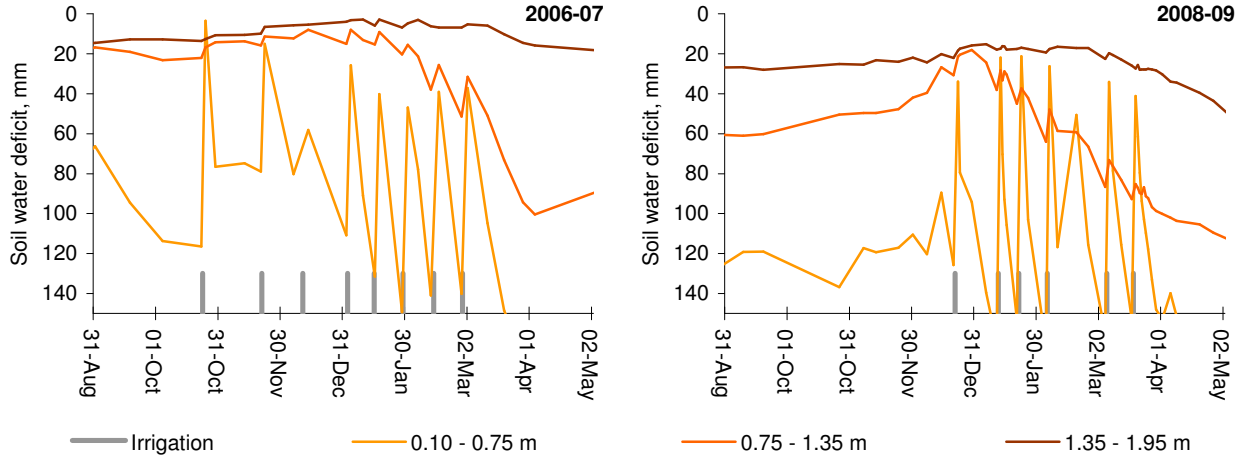

Figure 2. Soil water deficit of three layers during the 2006/07 and 2008/09 irrigation seasons calculated from measurements made by neutron moisture meter (means of 4 replicates). Dates of irrigation events are shown as vertical bars.

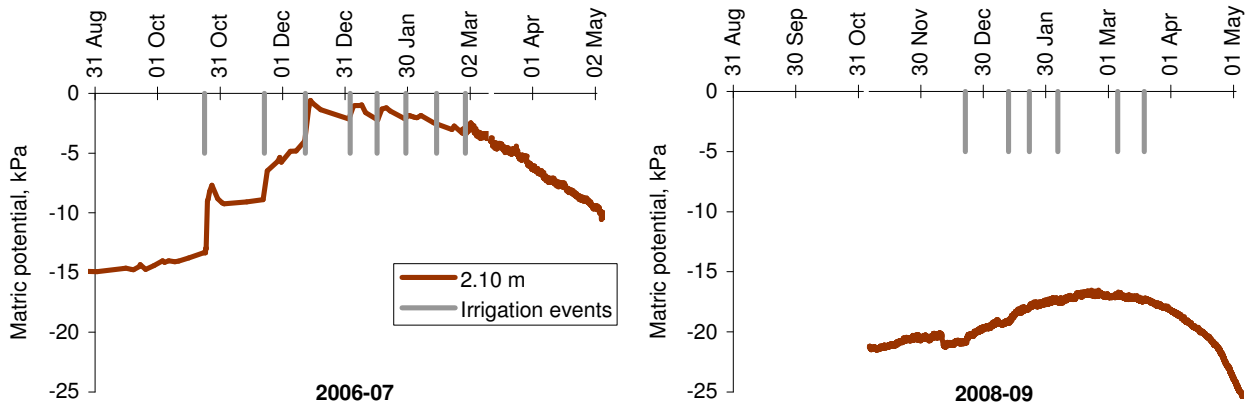

Figure 3. Matric potential of the soil at 2.1 m depth during the 2006-07 and 2008-09 irrigation seasons (means of 2 replicates).

The soil water potential of the soil below 1 m showed no response to this water movement. In fact the hydraulic gradient at 2.1 m during this event was upwards, with a downward gradient only occurring above 1.5 m (Figure 4). This suggests that most of the drainage occurring during the 2008-09 season was due to by-pass flow – that is flow through macropores that by-passes the soil matrix. Given that cracks only occur within the top metre or so, the likely route for by-pass flow was through slickensides that occur deep in this profile and which were observed during installation of the lysimeter. Interestingly, drainage occurred continuously between irrigations long after free water had disappeared from the soil surface, albeit at a decreasing rate. As the season progressed,

the gradually increasing deficit in the 0.75-1.35 m layer increased the amount of irrigation water that was 'captured' before it could become drainage, thereby reducing the drainage rate.

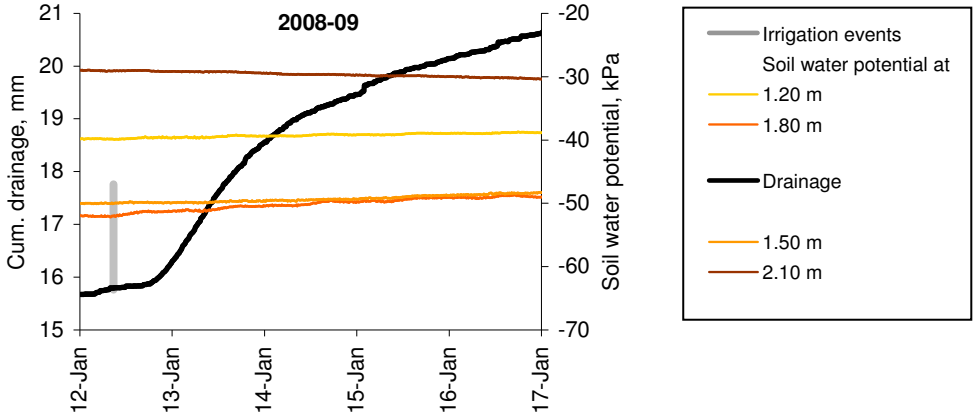

Figure 4. Detail of cumulative drainage after an individual irrigation event on 12 January 2009. Also shown is the soil water potential (matric + gravity) at 4 depths (means of 2 replicates). The time the irrigation front passed over the lysimeter is shown by a vertical bar.

2006-07 irrigation season

Drainage during the 2006-07 season was 1.75× greater than during the 2008-09 season. At the start of the season the soil water deficit from 0.75-1.95 m depth was 32 mm. There was little rain in the early part of the season, and by the third irrigation the deficit had been reduced to 13 mm (Figure 2). Figure 3 shows that this was accompanied by a rapid rise in matric potential at 2.1 m depth from -15 kPa to close to saturation.

The crop was relatively undeveloped up to the fourth irrigation, and created only small deficits between irrigations. This resulted in large quantities of drainage after the second and third irrigations. Drainage after the first irrigation was presumably mitigated as the profile wet up. As the season progressed, the rate of drainage decreased as the crop created increasingly large deficits between irrigations.

Conclusions

Antecedent conditions are very important in determining drainage during the cotton season. The deficit of the subsoil below 0.75 m depth plays an important role. In addition, the need for early season irrigation, before the crop is able to extract significant quantities of water, causes rapid wetting of the deep subsoil and high drainage rates. However, it appears that some drainage via by-pass flow is unavoidable due to the presence of free-standing water on the surface during furrow irrigation. It is possible that surface cracks increase by-pass flow by connecting the surface to slickensides in the deep subsoil. If so, then early season rainfall in 2008-09 could have caused the surface cracks to close and reduced the amount of water reaching the deep subsoil. In contrast, the early irrigations in 2006-07 could have reached the subsoil much faster due to surface cracks, and resulted in more bypass flow.

Acknowledgements

This work was funded by the Cotton Research and Development Corporation and the Cotton Catchment Communities Cooperative Research Centre. The authors thank Dr Nilantha Hulugalle and Industry and Investment NSW, for their cooperation in locating the lysimeter in their experimental field.

References

Brye KR, Norman JM, Bundy LG, Gower ST (1999) An equilibrium tension lysimeter for measuring drainage through soil. *Soil Science Society of America Journal* **63**, 536-543.

Isbell RF (1996) The Australian Soil Classification. (CSIRO Publishing: Melbourne).

Pegler D, Foley J, Silburn DM (2003) Design and construction of an equilibrium tension lysimeter for use in swelling clay soils. In 'International Soil Tillage Research Organisation 16th triennial conference. Brisbane, Queensland'. pp. 891-896. (University of Queensland: Brisbane).

Determination of irrigation depths using a numerical model and quantitative weather forecast

Haruyuki Fujimaki[A] and **Yu Sasaki[B]**

[A]Arid Land Research Center, Tottori University, Japan, Email fujimaki@alrc.tottori-u.ac.jp
[B]Graduate School of Life and Environmental Sciences, University of Tsukuba, Japan, Email yusasaki1103@yahoo.co.jp

Abstract
A method of determination of irrigation depth using a numerical model of crop response to irrigation and weather forecast was presented. To optimize each irrigation depth, a concept of virtual income, which is proportional to an increment in transpiration amount during an irrigation interval, is introduced. A numerical model that simulates water, solute, and heat transport and crop response is used in a numerical experiment. Results indicated that the optimized irrigation depth can be smaller than the value which attains maximum yield.

Key Words
Irrigation, weather forecast, transpiration, net return

Introduction

Soaring food price and intensified scarcity of water resources bring a new emphasis on efficient use of water in irrigation. The determination of irrigation depth has still widely relied on experience (i.e. fixed amount) or intuition of farmers even in industrialized countries. Such conventional irrigation may cause yield reduction or waste water. To precisely meet crop water requirements and respond to water/salinity stresses quickly, automatic irrigation systems using sensors have been developed. Such "water stat" systems, however, require high initial investment and have difficulty in adjusting irrigation depth to weather forecasts. For example, it is obviously wasteful to apply a full irrigation when rain is forecast on next day. "Water stat" systems may nevertheless do this if currently monitored value reaches its threshold value. Expensive monitoring using sensors can be altered by numerical simulation of water, solute, and heat transport in soil and crop response to them. High-spec personal computers are getting affordable even for farmers in developing countries. Not only monitoring current status, a numerical model can predict near future conditions. Numerical prediction requires knowledge of atmospheric boundary condition: quantitative weather forecast. Today, freely accessible quantitative weather forecasts, whose accuracy is improving, have been provided on the web (e.g. wetherunderground.com). These progresses have enabled the optimization of irrigation depths using quantitative weather forecast as input data for numerical models such that net return is maximized. This paper presents a procedure for the determination of irrigation depths using quantitative weather forecast. We also demonstrate its effectiveness with a numerical experiment.

Methods

Maximization of virtual net return

Like other inputs such as labour or fertilizer, the purpose of irrigation is not necessarily to obtain the highest yields, nor even water use efficiency, but to maximize the net returns. Timing of irrigation is generally restricted to social factors such as rotation or availability of labour. In contrast, irrigators have more discretion with regard to the amount of irrigation. Thus, we focus on the optimization of the amount.

If we can calculate net return until the next irrigation, the irrigation depth can be optimized such that net return is maximized. Although in reality income is realized when harvest is sold, we assume that a farmer can obtain virtual income, which is proportional to an increment of dry matter attained during an interval. Also, water must be priced high enough to give irrigators incentive to save water. Net return, N_r (\$ a^{-1}), during a period is then defined as:

$$N_r = P_c \varepsilon \tau - P_w W - C_{ot} \quad (1)$$

where P_c is the price of crop (\$ /kgDM), ε is water use efficiency of the crop, τ is cumulative transpiration (1 cm $=10^7$ kg/ha), P_w is the price of water (\$ /kg), W: irrigation depth (kg/ha), and C_{ot} is the other costs (\$ ha^{-1}). The amount of valuable part (fruit, grain etc.) of the crop is assumed to be proportional to dry matter production, which is well known to be approximately proportional to cumulative transpiration. Under given conditions, N_r is thus a function of W. The problem is thus a simple one-dimensional search.

To estimate transpiration amount, τ, which dynamically responds to matric and osmotic potential in soil and therefore, irrigation, a sophisticated model of the response of crop to irrigation is required. Numerical models developed in the realm of soil physics can be such ones.

Procedure
First, using the records of climatic condition, numerical simulation is performed to estimate the current status. Then, download quantitative weather forecast as input data and repeat simulations changing irrigation depth until maximum anticipated N_r is obtained. Then perform irrigation. On the early morning of the next irrigation day, current status is estimated by simulation using the actual records of irrigation depth and climatic condition from the last irrigation until the moment. This cycle continues until the last irrigation.

Numerical model
Algorithm and user interface described above was incorporated into a numerical model, WASH_1D, which solves governing equations for one-dimensional movement of water, solute and heat in soils with the finite difference method. The one-dimensional maximization was implemented with the golden section method with searching range 0 to 10cm. Governing equation of water flow is Richards equation including water vapor movement. Solute and heat transport are described with the convection-dispersion equation. It can be applied to layered soil, and consider thermal vapor diffusion and hysteresis.

Root water uptake and crop growth sub-models
A widely used macrospopic root water uptake (RWU) model (Feddes and Raats 2004) was used in calculating root water uptake and transpiration rate, T(cm/s) . The crop growth model describes the growth of the each plant part as a function of cumulative transpiration amount. In WASH_1D, root activity distribution, β(/cm), is given as

$$\beta = (b + 1)d_{rt}^{-b-1}(d_{rt} - z)^b \quad (2)$$

where b is plant-specific parameter, d_{rt} is the depth of lower boundary of the root zone(cm), and z is the depth(cm). The d_{rt} is described as a function of cumulative transpiration amount, ΣT(cm):

$$d_{rt} = a_{drt}[1 - \exp(b_{drt}\Sigma T)] + c_{drt} \quad (3)$$

where a_{drt}, b_{drt} , and c_{drt} are plant-specific parameters.
Leaf area index, I, which affects both radiation and wind, is also handled as a function of ΣT.

$$I = a_{LAI}[1 - \exp(b_{LAI}\Sigma T)] \quad (4)$$

where a_{LAI}, and b_{LAI} are plant-specific parameters.
The potential transpiration rate, T_p, which is used in the RWU model, is given by multiplying potential evapotranspiration, E_p(cm/s), from Penman equation by crop coefficient, K_c:

$$T_p = E_p K_c \quad (5)$$

The K_c is also assumed to be a function of ΣT.

$$K_c = a_{kc}[1 - \exp(b_{kc}\Sigma T)] + c_{kc} \quad (6)$$

where a_{kc}, b_{kc} , and c_{kc} are plant-specific parameters.
The evaporation rate is calculated with the bulk transfer equation (Daamen and Simmonds 1996; Noborio *et al.* 1996; Yakirevich *et al.* 1997):

$$E = \frac{\rho^*_{vs} h_{rs} - \rho^*_{va} h_{ra}}{r_a} \quad (7)$$

where ρ_v^* is the saturated water vapor density (g cm^{-3}), h_r is the relative humidity, r_a is the aerodynamic resistance (s /cm), and where the subscripts s and a denote the soil surface and air at the reference height, respectively. Since ρ_{vs}^* is a function of surface temperature, heat movement also must be analysed. The main energy input, solar radiation, is absorbed and reflected by leaves. Such attenuation is commonly described as (e.g. Campbell 1985)

$$R_s = R_{s0}\exp(-a_{rs} I) \quad (8)$$

where R_{s0} is R_s(W m^{-2}) above canopy and a_{rs} is plant-specific parameter. As crops grow, r_a is increased as leaves restrict water vapor transport. Such an additional resistance is expressed as a function of leaf area index, I:

$$r_a = r_{a0}(1 + a_{ra} I) \quad (9)$$

where r_{a0} is r_a from bare soil surface, and a_{ra} is plant-specific parameter.
Numerical experiment of the proposed procedure

A numerical experiment was performed from August 7 to October 26, 2009. We assumed the experiment using upland rice, Toyohatamochi, in Tsukuba, Japan. Irrigation interval was two days. The records of climatic condition were downloaded from the website of Japan Meteorological Agency (www.kishou.go.jp/) and quantitative weather forecasts were downloaded from the website of Yahoo! JAPAN (www.yahoo.co.jp).

Soil properties of Tottori sand were used in the simulation. Lower boundary was set at the depth of 40cm. Initial cumulative transpiration amount and initial pressure head were set at 1.4cm and -5cm, respectively. Pressure head at the bottom and temperature at the lower boundary were assumed to be constant at -30cm and 23 ^{o}C, respectively. Supposed parameter values in the net return equation are listed in Table 1. Irrigation was started 9:00 of August 9 at an intensity of 5 cm/h.

Table 1. Assumed parameter values in the net return equation.

Parameter	Value	Unit
P_c	0.33	\$ /kg
P_w	0.0001	\$ /kg
E	0.001	
C_{ot}	0	\$

Numerical experiment of an automatic irrigation system
Experimental period and condition were same as the experiment of the proposed procedure. The records of climatic condition from August 7 to October 26 were downloaded, and numerical simulation was performed to estimate the change of status and when irrigation was occurred. The automatic irrigation system was set to apply irrigated 5cm water when volumetric water content at the depth of 5cm was lower than 0.02.

Results

Table 2 shows the cumulative irrigation depth, transpiration amount and net income of the proposed procedure and automatic irrigation system. Automatic irrigation system irrigated more water than the proposed procedure and cumulative transpiration amount of automatic irrigation system was more than that of the proposed procedure. However, net return of automatic irrigation system was less than that of the other because of the greater irrigation cost.

Table 2. Cumulative irrigation depth, transpiration amount and net income of the proposed procedure and automatic irrigation system.

	Irrigation depth (cm)	Transpiration amount (cm)	Net return (\$/a)
The proposed procedure	34.6	39.9	9.7
Automatic irrigation system	63.9	45.2	8.5

Figure 1 shows the temporal change of soil water content at the depth of 5 cm for the proposed procedure and automatic irrigation system. On September 29, automatic irrigation system applied 2 cm while the proposed procedure applied far less because of the climatic condition on next two days and volumetric water content of automatic irrigation system was higher than that of the proposed procedure after the irrigation. Figure 2 displays the temporal change of net return of the proposed procedure and automatic irrigation system. When rainy or non-rainy days continued, difference in net return was small.

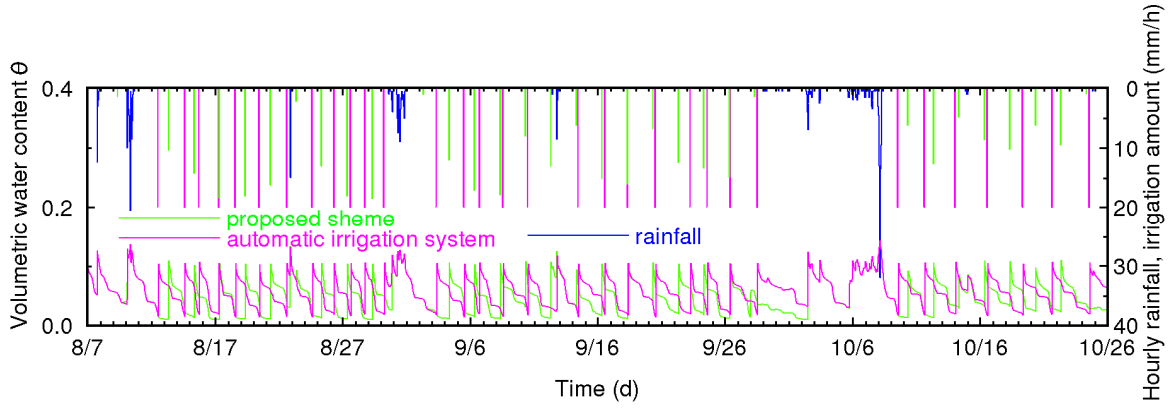

Figure 1. Temporal change of soil water content at a depth of 5cm of the proposed procedure and automatic irrigation system.

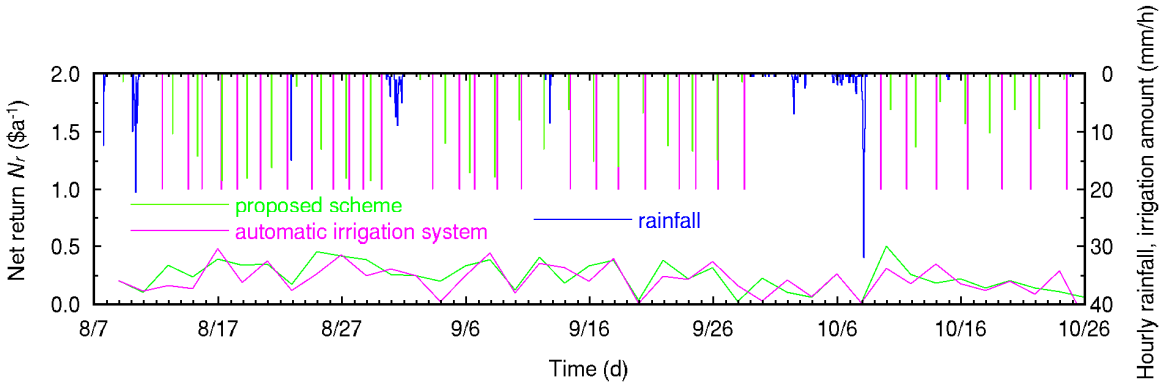

Figure 2. Temporal change of net return of the proposed procedure and automatic irrigation system.

Figure 3 shows net return and cumulative transpiration over 48h hours from 0:00 on September 28 as a function of irrigation depth, W. Plots interpolated with spline curves were the trajectory of optimization, and points are realized values determined by the actual climatic condition. Predicted N_r and ΣT increased with W, with diminishing gradients, and N_r reached to the peak at $W = 0.15$ cm, beyond which the N_r decreased with W. Note that maximum cumulative transpiration (i.e. yield) is achieved at larger irrigation depth. According to the actual value, irrigation depth of automatic irrigation system was larger than that of the proposed procedure while the difference in transpiration amount between the two was small. As a result, net income of the proposed procedure was higher than that of the other. In addition, the differences in both net return and cumulative transpiration between optimization and actual values were small during the period.

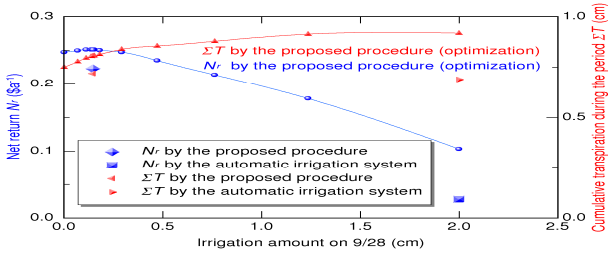

Figure 3. Net return and cumulative transpiration from September 28 to 29 as a function of irrigation depth.

Conclusion

In this study, a method of determination of irrigation depth using a numerical model of crop response to irrigation and weather forecast was outlined. The numerical experiment showed encouraging results. Still, some of the employed plant specific parameter values were hypothetical. We are performing an experiment to determine these parameter values and test the effectiveness of this method by comparing with an automatic irrigation system.

References

Campbell GS (1985) 'Soil Physics with Basic'. (Elsevier: New York).

Daamen CC, Simmonds L (1996) Measurement of evaporation from bare soil and its estimation using surface resistance. *Water Resour. Res.* **32,** 1393-1402.

Feddes RA, Raats PAC (2004) Parameterizing the soil–water–plant root system In 'Unsaturated-zone modeling: Progress, Challenges, and Applications'. Wageningen UR Frontis Ser., Vol. 6. (Ed RA Feddes) pp. 95–141. (Kluwer Academic: Dordrecht, The Netherlands).

Noborio K, McInnes KJ, Heilman JL (1996) Two-dimensional model for water, heat, and solute transport in furrow-irrigated soil. I. *Theory. Soil Sci. Soc. Am. J.* **60,** 1001–1009.

Yakirevich A, Berliner P, Sorek S (1997) A model for numerical simulation of evaporation from bare saline soil. *Water. Resour. Res.* **33,** 1021-1033.

Development of preferential flow below a soil moisture threshold

Marcus Hardie[A, B, E], Richard Doyle[A], William Cotching[C, E], Shaun Lisson[D]

[A]Tasmanian Institute of Agricultural Research, University of Tasmania, Private Bag 98, Hobart, TAS 7001, Australia. Email marcus.hardie@utas.edu.au
[B]School of Agricultural Science, University of Tasmania, Private Bag 54, Hobart, Tas 7001, Australia
[C]Tasmanian Institute of Agricultural Research, University of Tasmania, PO Box 3523 Burnie, Tasmania. 7320, Australia
[D]CSIRO Sustainable Ecosystems University of Tasmania, PB 98, Hobart, Tasmania 7001, Australia
[E]Secondment from Department of Primary Industries, Parks Water and Environment (DPIPWE)

Abstract
Application of 25 mm dye tracer to a 'dry' texture contrast soil (Sodosol) soil resulted in infiltration to a depth of between 85 cm and 114 cm via a combination of preferential flow processes. However when the same soil was 'wet' the dye tracer infiltrated uniformly to a depth of between 24 cm and 40 cm. Long term soil moisture monitoring demonstrated that a soil moisture threshold existed at approximately 300 mm total stored soil moisture (0-90 cm) which corresponded to approximately 30 % of plant available water content (PAWC). When rainfall occurred on soil with an antecedent soil moisture below the 300 mm threshold, infiltration was dominated by preferential flow processes, however when antecedent soil moisture was above the 300 mm threshold, infiltration resulted from equilibrium flow as predicted by the Richards equation. Knowledge that preferential flow occurs below a soil moisture threshold, enables agricultural managers to reduce loss of agrochemicals below the root zone by restricting application to times when soil moisture is above the threshold.

Key Words
Antecedent soil moisture, capacitance probe

Introduction
Preferential flow refers to processes in which infiltrating water by-passes the soil matrix, resulting in more rapid and deeper movement of water and solutes than would otherwise be expected (Simunek and van Genuchten, 2007). Numerous studies have demonstrated that preferential flow is both common and widespread (Flury *et al.,* 1994), resulting in the potential off-site movement of fertiliser and agrichemicals. The presence of preferential flow also invalidates assumptions of the Richards equation used in single porosity models to predict infiltration into variable saturated soils (Jarvis, 2007). Through dye tracer studies and long term soil moisture monitoring, the effect of antecedent soil moisture on preferential flow was investigated.

Methods
Dye staining
A 25 mm solution containing 4 g/litre Brilliant Blue FCF (C.I. Food Blue 42090) dye tracer was applied to a texture contrast soil (Sodosol) the soil via either a Morin rotating-disk rainfall simulator or hand held sprayer. Dye stained areas were excavated approximately 30 hours after dye application. Images of dye stained soil were captured using a Cannon 400D EOS digital camera, under a large white tent to exclude shadows. Images were corrected for radial and keystone distortion in Photoshop CS3 software. Dye stained regions were separated from unstained soil and converted to binary format in Image J software to enable analysis of the proportion of dye stained soil with depth.

Moisture treatments
Dye was applied to the soil surface in wet and dry conditions. The dry treatment was established by ambient drying under a rainout shelter during a prolonged period without rainfall. The wet treatment was established by applying 20 - 30 mm irrigation with pop-up sprinklers four times a week, for a period of 45 days.

Soil moisture measurement
Soil moisture was monitored using a continuously logging capacitance probe (EnviroSCAN Solo - Sentek Environmental Technologies, Kent Town, South Australia). The EnviroSCAN probe was mounted inside a 5.6mm diameter PVC plastic access tube which was rammed into the soil, ensuring a tight fit between the soil and the access tube. Soil moisture was monitored at 10 cm, 20 cm, 30 cm, 50 cm, 70 cm, 90 cm and 130 cm depths at 60 minute intervals between 19/9/07 and 30/5/08 and intervals between 1 and 10 minutes between 26/6/08 and 10/7/09.

The effect of antecedent moisture on the occurrence of preferential and equilibrium flow was determined from changes in soil moisture following 44 rainfall events between 24/9/2007 and 16/8/2009. Soil moisture response to rainfall (>5 mm) was classified into five infiltration types.

(i) PF-A: Preferential flow, evidenced by by-pass flow in which soil moisture response (>0.2 %) does not follow a logical sequence with depth.
(ii) PF-B: Preferential flow, evidenced by infiltration rates in excess of 200 mm/hr.
(iii) EQ: Equilibrium flow, in which infiltrating rainfall caused soil moisture sensors to respond in depth order and at infiltration rates <200 mm / hr.
(iv) NR: No response, (>0.2 %) change in soil moisture following > 5 mm rainfall.
(v) UR: Unknown response, in which soil moisture response to rainfall was unable to be classified as resulting from preferential or equilibrium flow.

Results

In the dry treatment, preferential flow processes resulted in dye infiltration to depths between 85 cm and 119 cm. Preferential flow included finger flow in the A1 horizon resulting from hydrophobicity, funnel flow in the A2 horizon and sand infills, ponding and spilling of thin rivulets down the side of the clay columns, and filling from the bottom up in shrinkage cracks and void spaces in the lower B horizons (Figure 1a-c). In the wet treatment, the dye tracer infiltrated to depths between 24 – 40 cm. Dye staining indicates that while the wetting front developed perturbations, true finger flow did not develop in the wet treatment (Hardie *et al., Submitted*) (Figure 1d-f).

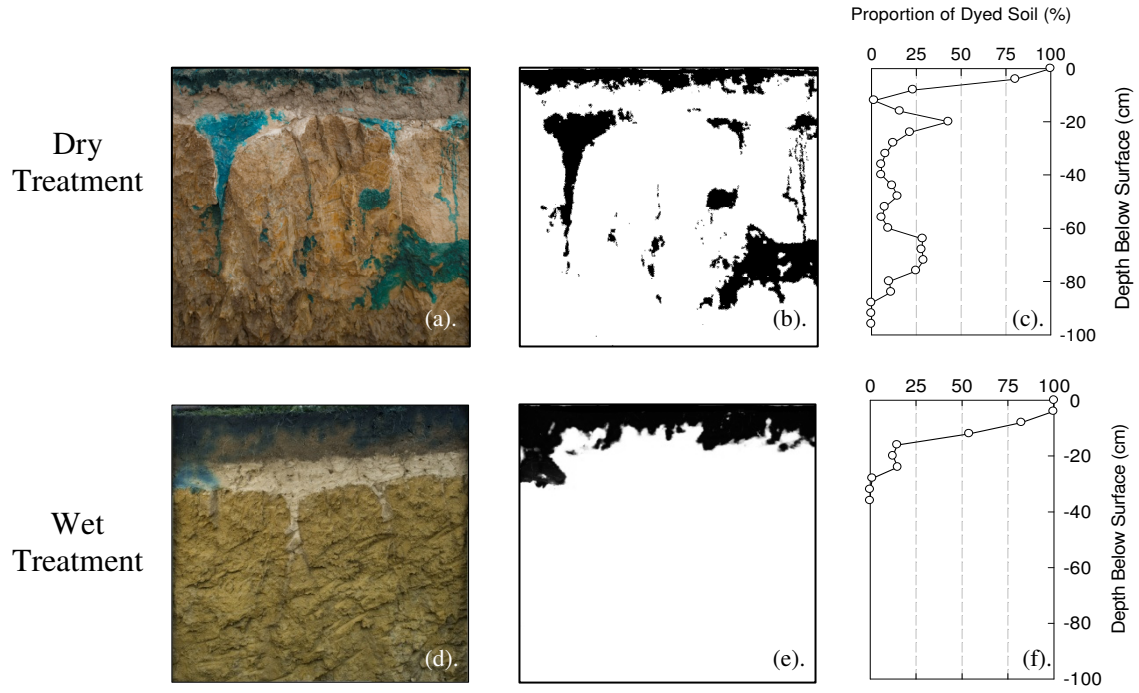

Figure 1. Example of the effect of antecedent soil moisture on dye tracer infiltration –dry treatment (a) image, (b) binary image (c) proportion of dye stained soil with depth. Wet treatment (d) image, (e) binary image (f) proportion of dye stained soil with depth.

The mean antecedent soil moisture (0-90 cm) of the two preferential flow classes (PF-A, PF-B) was significantly ($P<0.05$) lower than the antecedent soil moisture of the equilibrium (EQ) flow class (Figure 2b). Results presented in Figure 2 indicate that when total soil moisture (0-90 cm) was below approximately 300 mm, infiltration, occurred via preferential flow (figure 1a). However when antecedent soil moisture was above 300 mm, rainfall infiltrated as uniform flow, which was largely restricted to the A horizon (Figure 1d). Based on seasonal changes in soil moisture the 300 mm soil moisture threshold corresponded to approximately 30 % of plant available water capacity (PAWC).

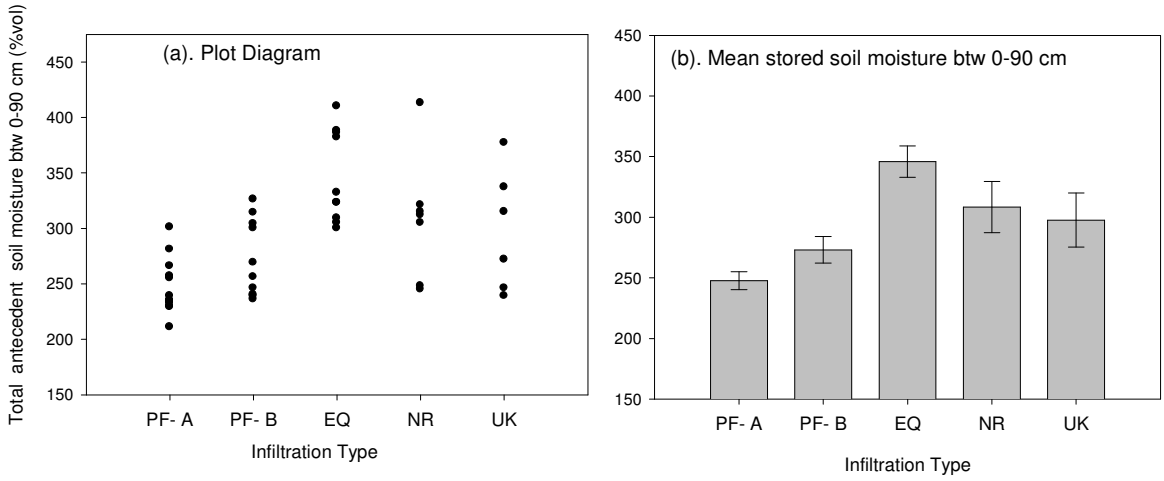

Figure 2. Effect of cumulative antecedent soil moisture between 0 cm and 90 cm on infiltration type (a) plot graph, (b) bar chart with – error bars represent ±1 SE.

Discussion & Conclusion

Infiltration into the texture contrast soil at antecedent soil moisture contents below 300 mm total soil moisture (0 -90 cm) were dominated by preferential flow processes, which resulted in the rapid infiltration to approximately 1.0 meter depth. When the antecedent soil moisture was greater than 300 mm (0-90 cm), infiltration occurred as equilibrium flow. By restricting application of pesticides and fertiliser to times when soil moisture is above the 300 mm soil moisture threshold, agricultural managers can reduce the risk of shallow groundwater contamination via preferential flow. Results also imply that use of tipping bucket models or Richards equation based single porosity models which do not account for preferential flow are likely to be invalid when applied to soils below the threshold soil moisture content.

References

Flury M, Fluhler H, Jury WA, Leuenberger J (1994) Susceptibility of soils to preferential flow of water: A field study. *Water Resources Research* **30**, 1945-1954.

Hardie M, Cotching WE, Doyle R, Holz G, Lisson S (*in Press*) Effect of antecedent soil moisture on preferential flow in a texture contrast soil. *Journal of Hydrology*.

Jarvis NJ (2007) A review of non-equilibrium water flow and solute transport in soil macropores: Principles, controlling factors and consequences for water quality. *European Journal of Soil Science* **58**, 523-546.

Simunek J, van Genuchten MT (2007) Chapter 22: Contaminant Transport in the Unsaturated Zone: Theory and Modelling. In 'The Handbook of Groundwater Engineering. - 2nd edition'. (Ed. JW Delleur), pp. 22.21 - 22.38. (CRC Press: Boca Raton).

Differences in topsoil properties of a sandy loam soil under different tillage treatments

Kamila Špongrová[A], Svatopluk Matula[A], Cedric Kechavarzi[B] and Marc Dresser[C]

[A]Faculty of Agrobiology, Food and Natural Resources, Czech University of Life Sciences Prague, Kamýcká 129, 165 21 Praha 6, Czech Republic, Email spongrova@af.czu.cz, matula@af.czu.cz
[B]School of Applied Sciences, Cranfield University, Cranfield MK43 0AL, United Kingdom, Email c.kechavarzi@cranfield.ac.uk
[C]Landcare Research, Private Bag 3127, Hamilton 3240, New Zealand, Email DresserM@landcareresearch.co.nz

Abstract
Soil tillage is one of the key soil management practices in agricultural land use. Hydraulic conductivity of the surface layer modifies water infiltration into the soil profile and possible runoff formation. The treatment of the surface layer affects the soil pore system (distribution and connectivity of macroscopic cracks, voids, holes, etc.). The aim of this study was to evaluate an effect of different tillage treatments on soil hydrophysical properties in the top layer of a sandy loam soil. The tillage treatments were as follows: conventional plough, shallow plough, minimum tillage, direct drill and no-treatment. The effect of wheel traffic was also evaluated by measuring the infiltration rates in the wheel marks. An automated tension infiltrometer (Špongrová *et al.,* 2009) was employed to measure the infiltration rates. The following soil characteristics were calculated: hydraulic conductivity function $K(h)$, hydraulic conductivity at saturation K_s, numbers of macro- and mesopores per m^2 of soil. The ANOVA results show that the plot with no-treatment and minimum tillage had higher $K(h)$ values near saturation than the tilled soils which did not differ significantly from each other. The wheel traffic led to soil compaction and a significant reduction in the hydraulic conductivity close to saturation.

Key Words
Soil properties, hydraulic conductivity, tillage, wheel traffic

Introduction
Tension infiltrometry is a useful *in situ* technique commonly used to estimate the hydraulic conductivity of the soil matrix near saturation without the influence of preferential flow usually affecting measurements of hydraulic conductivity in saturated conditions. This allows one to characterise the infiltration capacity of hydraulically active and fast water-conducting macro- and mesopores *in situ* (Bodhinayake *et al.,* 2004), which is essential for understanding the influence of soil and water management practices on water infiltration and solute and contaminant transport as well as temporal changes and spatial variability of surface hydraulic properties.

Methods

Field experiments
Infiltration tests were carried out in the field on Cranfield University farm between 27th July and 12th August 2006 on a sandy loam soil (Cottenham series). The texture of the soil was 63% sand, 23% silt and 15.0% clay. Five different tillage treatments were tested: conventional tillage (CT, depth 25 cm), shallow plough (SP, depth 12.5 cm), minimum tillage (MT, depth 12.5 cm), direct drill (DD, 7.5 cm) and no-treatment (NT, untreated soil, no plants sieved). The soil ploughing and cultivation were carried out on 24 April 2006, and drilling on 4 May 2006. In three of the treatments (CT, MT, and NT) infiltration tests were also carried out in the wheel-marks created by wheel-traffic after the tillage. The weather conditions during the period between the soil cultivation and the experimental period were relatively warm and dry. Monthly averaged maximum temperatures ranged between 12.8°C (April) and 26.6°C (July); total amounts of precipitation (rain) ranged between 16 mm (June) and 99.2 mm (August); May was also relatively rainy with 87.8 mm of precipitation. Three fully automated tension infiltrometers connected to a single Mariotte bottle (Špongrová *et al.,* 2009) were used to determine the infiltration rates for soil near saturation for each treatment. The soil surface was smoothed and levelled before the infiltrometers were placed onto the plots. The sandy loam soil was relatively easy to smooth and level using a knife, and good hydraulic contact was achieved without the need for any contact material creating an additional layer. The replicates were placed approximately 1 m apart. Infiltration measurements were performed for 8 water pressure heads in the following order: -13, -11, -9, -7, 5, -3, -2 and -1 cm. The tensions were set to change automatically every 60 minutes. The datalogger sampling interval for the water level measurements in the reservoirs was set to 3 minutes. When the measurement was finished, three undisturbed soil samples (100 cm^3, sampling depth 0-6 cm) were taken from below each infiltration surface. The soil during the sampling was

1 – 6 August 2010, Brisbane, Australia. Published on DVD.

almost saturated, however, no visible change in the soil structure or soil compaction due to the weight of the infiltrometer was observed. The samples were weighed and left to saturate on wet filter paper immersed in water. Initial and final volumetric moisture content as well as moisture content at saturation and dry bulk density were determined by oven-drying the undisturbed soil samples at 105°C for 48 hours.

Data analysis

Šimůnek and van Genuchten (1996, 1997), and Šimůnek *et al.* (1998) proposed an inverse numerical method to estimate the parameters of the hydraulic conductivity function from transient infiltration data from disc infiltrometers. The soil hydraulic functions are commonly described by the expressions defined by Mualem (1976) and van Genuchten (1980). HYDRUS-2D model (Šimůnek *et al*., 1999) was used for the numerical solution of the Richards' equation and to estimate the hydraulic parameters (θ_r, θ_s, α, n and K_s) by minimising the sum of squared deviations between observed and simulated cumulative infiltration. The values of θ_s were determined in the laboratory by saturation and oven-drying of three undisturbed soil samples, while θ_r, α, n and K_s were used as fitting parameters in the inverse modelling procedure. To evaluate the amount of meso- and macropores present in the soil for each tillage treatment, number of conductive pores per unit area N_h characteristic was used. The expression reported by Reynolds *et al.* (1995) was used to estimate the N_h value needed to observe the particular value of *K(h)*. The same criteria as in Moret and Arrúe (2007) were used to define macro- and mesopores. Pores that drain at pressure heads close to saturation with a lower pressure head limit of -4 cm were defined as macropores; and pores draining at lowerer pressure heads with an upper limit of -4 cm (in this study pressure heads between -4 and -13 cm) were defined as mesopores.

Statistical analysis

Analysis of variance (significance level 0.05) was performed to determine whether the different tillage treatments and wheel traffic had a significant effect on *K(h)* or not. In order to obtain normally distributed data, Log_{10} (logarithm to the base of 10) transformed *K(h)* data were used for the analysis.

Results and discussion

The infiltration experiments were carried out approximately three months after the soil cultivation, the sandy loam soil had already consolidated and no large differences in dry bulk densities between tilled and untilled plots were observed. The mean of the initial and final moisture content as well as that of the soil moisture content at saturation and the dry bulk density are summarised in Table 1 for each of the treatments. The HYDRUS-2D results, the fitting parameters θ_r, K_s, α and n, together with the coefficient of determination R^2, averaged over the three replicates, are presented in the left part of Table 2.

The values of *K(h)* for CT, ranged between 0.0010 cm min^{-1} at tension -12 cm and 0.5125 cm min^{-1} at saturation. The ranges of *K(h)* for other tillage treatments were as follows: 0.0010 to 0.6473 cm min^{-1} for SP, 0.0025 to 0.5345 cm min^{-1} for MT, 0.0011 to 0.5162 cm min^{-1} for DD, and 0.0012 to 0.5404 cm min^{-1} for NT. Figure 1 shows the mean Log *K(h)* values calculated for each tension using the hydraulic functions obtained by numerical inversion for the different tillage treatments. The results show the soil with MT had a significantly higher hydraulic conductivity than all the other treatments (CT, SP, DD, NT) at almost all tensions except at saturation. In addition, the differences were, in general, larger at higher tensions.

Table 1. Mean initial ($\theta_{initial}$), final (θ_{final}), and water content at saturation (θ_s), and dry bulk densities (ρ_d) for each tillage treatment.

Tillage treatment	$\theta_{initial}$ ($cm^3\ cm^{-3}$)	θ_{final} ($cm^3\ cm^{-3}$)	θ_s ($cm^3\ cm^{-3}$)	ρ_d ($g\ cm^{-3}$)
CP	0.100	0.293	0.348	1.39
SP	0.081	0.283	0.323	1.39
MT	0.098	0.260	0.332	1.41
NT	0.089	0.281	0.350	1.43
DD	0.099	0.331	0.380	1.45
MT wheel mark	0.126	0.276	0.363	1.48
CP wheel mark	0.110	0.303	0.356	1.50
NT wheel mark	0.089	0.281	0.350	1.50

Table 2. HYDRUS-2D model parameters for each tillage treatment; scaling parameter of the van Genuchten's equation α, curve shape parameter of van Genuchten's equation *n*, hydraulic conductivity K_s at saturation, residual soil water content θ_r, and coefficient of determination for measured and modelled infiltration rates R^2 (left part). The right part of the table contains information about numbers of macropores and mesopores per unit area calculated for each tillage treatment.

Tillage treatment	α (cm^{-1})	*n* (-)	K_s (cm min^{-1})	θ_r (cm^3 cm^{-3})	R^2	Numbers of macropores per m^2	Numbers of mesopores per m^2
CP	0.169	1.464	0.419	0.050	0.998	122	542
SP	0.175	1.549	0.460	0.062	0.998	153	711
MT	0.147	1.392	0.467	0.050	0.999	177	824
NT	0.189	1.519	0.499	0.050	0.998	161	842
DD	0.192	1.462	0.501	0.050	0.998	150	586
MT wheel mark	0.121	1.473	0.259	0.050	0.999	91	488
CP wheel mark	0.110	1.681	0.234	0.050	0.999	70	649
NT wheel mark	0.186	1.440	0.240	0.050	0.998	66	377

Conversely, the tilled soils did not differ significantly from each other and formed a homogeneous group together with plots with DD and NT. Furthermore, the highest *K(h)* values were measured on the plot with MT, and the corresponding Log *K(h)* values were significantly larger than those of the NT treatment for tensions higher than 2.5 cm.

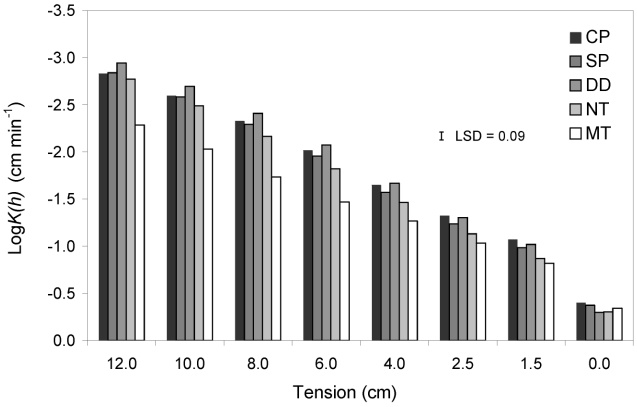

Figure 1. Log *K(h)* values calculated for each applied tension (-13, -11, -9, -7, -5, -3, -2, and -1 cm) using the hydraulic functions obtained by numerical inversion in HYDRUS-2D for the different tillage treatments.

Number of conductive pores per unit area N_h was increasing with increasing *K(h)* values. The N_h values varied for all tillage treatments and throughout the whole range of tension between 664 and 1004 pores m^{-2} (right part of Table 2). There was about four times more mesopores than macropores for CT, SP, and MT; for DD and NT, the number of mesopores was even larger. The data suggest that the CT operation carried out in this study changed the soil structure generated naturally under NT systems, leading to a reduction in mesopore class sizes and the creation of new macropore volumes which resulted in lower hydraulic conductivity at higher tensions. These results are in agreement with those of Cortadeur *et al.* (2002), who compared tilled and untilled soils and reported the reducing effect of ploughing on the near-saturated hydraulic conductivity, with *K(h)* values in the ploughed soil being one third of those measured on the untilled soil. However, as reported by Pelegrin (1990) and Ferreras *et al.* (2000), when K_s was measured *in situ*, the values for tilled soils were significantly higher than those measured on untilled soils. However, studies of the influence of tillage on infiltration rates are not always conclusive; Cameira *et al.* (2003) and Ankeny *et al.* (1990) reported little difference in *K(h)* when comparing untilled and tilled soils. When characterising the effect of wheel traffic, the following ranges of *K(h)* were measured on wheel-marks: 0.0004 to 0.2651 cm min^{-1} for CT, 0.0019 to 0.3692 cm min^{-1} for MT, and 0.0004 to 0.2636 cm min^{-1} for NT. Except for the CT, the reduction in Log*K(h)* on plots with MT and NT was significant at all tensions ($P < 0.001$). The largest reduction in *K(h)* was observed at lower tensions (2.5 cm, 1.5 cm, and 0 cm) and was most significant for K_s with a reduction varying between 50% and 60%. For the CP, there was a 43% reduction in macropores per unit area, while the number of mesopores increased by 20%. For the plots with MT and NT, the macropores were reduced by 49% and 59%, and the mesopores by 41% and

55%, respectively. This shows that wheel-traffic leads to the loss of hydraulically active macropores. The soil compaction created by the wheel traffic is also shown by the values of the soil dry bulk density (Table 1), which are significantly higher in the wheel-marks for all three tillage treatments (t-test, significance level 0.05). Ankeny *et al.* (1990) showed that wheel-traffic is one of the main source of soil compaction in agricultural fields. The effect of wheel traffic on *K(h)* was also reported by Courtadeur *et al.* (2002) who measured a 60% reduction in hydraulic conductivity at saturation in the wheel-mark of a tilled soil.

Conclusion

Soil tillage operations carried out on the tested sandy loam soil led to a reduction of mesopores and had no beneficial effect on the near-saturated hydraulic conductivity of the soil. In addition, wheel traffic resulted in large reductions in near-saturated hydraulic conductivity through compaction and the loss of macropores.

Acknowledgement

This research was supported by the National Agency of Agricultural Research, Project No. 1G58095, and by the Ministry of Education, Youth and Sports of the Czech Republic, Project No. 6046070901.

References

Ankeny MD, Kaspar TC, Horton R (1990) Characterization of tillage and traffic effects on unconfined infiltration measurement. *Soil Science Society of America Journal* **54**, 810-837.

Bodhinayake W, Si BC, Xiao C (2004) New method for determining water conducting macro- and mesoporosity from tension infiltrometers. *Soil Science Society of America Journal* **68**, 760-769.

Cameira MR, Fernando RM, Pereira LS (2003) Soil macropore dynamics affected by tillage and irrigation for a silty loam alluvial soil in southern Portugal. *Soil & Tillage Research* **70**, 131-140.

Coutadeur C, Coquet Y, Roger-Estrade J (2002) Variation of hydraulic conductivity in a tilled soil. *European Journal of Soil Science* **53**, 619-628.

Ferreras LA, Costa JL, Garcia FO, Pecorari C (2000) Effect of no-tillage on some soil physical properties of a structural degraded Petrocalcic Paleudoll of the southern "Pampa" of Argentina. *Soil & Tillage Research* **54**, 31-39.

Moret D, Arrúe JL (2007) Characterizing soil water-conducting macro and mesoporosity as influenced by tillage using tension infiltrometry. *Soil Science Society of America Journal* **71**, 500-506.

Mualem Y (1976) A new model for predicting the hydraulic conductivity of unsaturated porous media. *Water Resources Research* **12**, 513-522. Cited in: van Genucten M-Th (1980) A closed-form equation for predicting the hydraulic conductivity of unsaturated soils. *Soil Science Society of America Journal* **44**, 892-898.

Pelegrin F, Moreno F, Martin-Aranda J, Camps M (1990) The influence of tillage methods on soil physical properties and water balance for a typical crop rotation in SW Spain. *Soil & Tillage Research* **16**, 345-358.

Reynolds WD, Gregorich EG, Curnoe WE (1995) Characterization of water transmission properties in tilled and untilled soils using tension infiltrometer. *Soil & Tillage Research* **33**, 117-131.

Šimůnek J, Angulo-Jaramillo R, Shaap MG, Vandervaere JP, van Genuchten MT (1998) Using an inverse method to estimate the hydraulic properties of crusted soils from tension-disc infiltrometer data. *Geoderma* **86**, 61-81.

Šimůnek J, Šejna M, van Genuchten M-Th (1999) The HYDRUS-2D software package for simulating the two-dimensional movement of water, heat, and multiple solutes in variably-saturated media. Version 2.0. U.S. Salinity laboratory, Agricultural Research Service, USDA, Riverside, California.

Šimůnek J, van Genuchten M-Th (1996) Estimating unsaturated soil hydraulic properties from tension disc infiltrometer data by numerical inversion. *Water Resources Research* **32**, 2683-2696.

Šimůnek J, van Genuchten M-Th (1997) Parameter estimation of soil hydraulic properties from multiple tension disc infiltrometer data. *Soil Science* **162**, 383-398.

Špongrová K, Kechavarzi C, Dresser M, Matula S, Godwin RJ (2009) Development of an automated tension infiltrometer for field use. *Vadose Zone Journal* **8**, 810-817.

van Genuchten M-Th (1980) A closed-form equation for predicting the hydraulic conductivity of unsaturated soils. *Soil Science Society of America Journal* **44**, 892-898.

Drip irrigation as a sustainable practice under saline shallow ground water condtions

Blaine R. Hanson[A], Don M. May[B], Jan W. Hopmans[C,*], and Jirka Simunek[D]

[A]Dept. of Land, Air and Water Resources, University of California, Davis, CA 95616; brhanson@ucdavis.edu
[B]University of California Cooperative Extension, Fresno County, Fresno, CA; dmay@ucdavis.edu
[C]Dept. of Land, Air and Water Resources, University of California, Davis, CA 95616;jwhopmans@ucdavis.edu
[D]Dept. Environmental Sciences, University of California, Riverside CA 92521; Jiri.Simunek@ucr.edu
*Corresponding and presenting author

Abstract
Many areas along the west side of the San Joaquin Valley of California are affected by saline soil due to shallow, saline ground water conditions. Artificial subsurface drainage is not an option for addressing the salinity problem because of the lack of drainage water disposal facilities. Thus, the salinity/drainage problem of the valley must be addressed through improved irrigation practices such as converting to drip irrigation. The effect of drip irrigation on soil salinity, soil water content, and water table depth was evaluated from both experimental and model results. While a water balance showed little or no field-wide leaching, soil salinity data clearly showed localized leaching around the drip lines.

Key Words
Irrigation water management, leaching fraction, water use

Introduction
About 1 million ha of irrigated land are affected by saline, shallow ground water conditions along the west side of the San Joaquin Valley, California. Upward flow of the shallow groundwater has resulted in excessive levels of root-zone soil salinity. The traditional approach to coping with shallow ground water problems is to install subsurface drainage systems for water table control and improved leaching, but the proper operation of these drainage systems requires disposal of the subsurface drainage water. No economically, technically, and environmentally feasible drain water disposal method exists for the San Joaquin Valley, and thus, the drainage problem must be addressed through options such as better management of irrigation water to reduce drainage below the root zone. Schoups *et al.* (2005) concluded the following:

- for irrigated agriculture to remain sustainable, a soil salt balance must be maintained that allows for productive cropping systems,
- continued irrigation without changing management practices is not sustainable.

One option for improving irrigation water management is to convert from furrow or sprinkler irrigation to drip irrigation. Drip irrigation can apply water both precisely and uniformly compared with furrow and sprinkler irrigation resulting in the potential to reduce subsurface drainage, control soil salinity, and increase yield.

Subsurface drip irrigation of processing tomatoes was evaluated to determine its effect on crop yield and quality, soil salinity, water table depth, and profitability in salt-affected, fine-textured soil underlain by saline, shallow groundwater. Because tomatoes are a high cash value crop, a better potential for increased profitability with drip irrigation exists compared to cotton. However, tomatoes are much more sensitive to soil salinity, which could result in reduced crop yields in salt-affected soil. This study presents a sensitivity analysis of drip irrigation for different quality irrigation water with a shallow groundwater, using both experimental and modeling results.

Materials and Methods
Field Experiments
Experiments in three commercial fields involved comparing subsurface drip irrigation of processing tomatoes with sprinkle irrigation under saline, shallow ground water conditions. Drip irrigations occurred every two to three days. At one field, water table depths were about 2 m, while at the other two fields, water table depths generally ranged between 0.5 m and 1 m. The electrical conductivity (EC) of the irrigation water ranged between 0.30 to 0.35 dS/m and between 1.06 to 1.2 dS/m , whereas the EC of the shallow ground water ranged

from 4.7 dS/m to 16.4 dS /m, depending on the particular field and time of year. Soil type was clay loam at the three sites.

Computer Simulations
Soil water and soil water salinity distributions around the drip line were modeled using an adapted version of the computer simulation model HYDRUS-2D (Šimůnek *et al.* 1999). This software package can simulate the transient two-dimensional or axi-symmetrical three-dimensional movement of water and nutrients in soils. This model has been previously used in studies of water and chemical movement under drip irrigation (Gardenas *et al.* 2005; Hanson *et al.* 2006). Subsurface drip irrigation was simulated using system design characteristics typical of the drip systems used for processing tomatoes.

Simulations were conducted for water table depths of 0.5 and 1.0 m, irrigation water salinities of 0.3, 1.0, and 2.0 dS/m, and applied water amounts of 80, 100, 115% of the potential evapotranspiration. For the 0.3 dS/m irrigation water, additional simulations for a water application of 60% were also conducted. Two irrigations per week were applied for the 1.0 m water table depth and daily irrigations were used for the 0.5 m depth. The EC of the shallow ground water was assumed to equal 10.0 dS/m and 8.0 dS/m for the 0.5 and 1.0 m water table depths, respectively, based on measured levels at the field sites.

Results and Discussion
Field Experiments
Soil salinity around drip lines was found to depend on the depth to the ground water, salinity of the shallow ground water, salinity of the irrigation water, and amount of applied water. For water table depths of 2 m, soil salinity (expressed as the EC of a saturated extract) was smaller than the threshold salinity and was distributed relatively uniformly around the drip line (Figure 1A). For water table depths of less than 1 m, soil salinity varied considerably around drip lines with the smallest levels near the drip line and high values near the periphery of the wetted volume (Figure 1B). Higher values of soil salinity occurred near the drip line for the field using the higher EC irrigation water (Figure 1C).

The key to the profitability and sustainability of drip irrigation of tomatoes in the valley's salt affected soils is salinity control. Salinity control requires leaching or flushing of salts from the root zone by applying irrigation water in excess of the soil moisture depletion. The leaching fraction, defined as the percent of applied water that percolates below the root zone, is used to quantify the amount of leaching. It was concluded that because of salinization issues, sustainable agriculture may not be possible in these salt affected soils of the valley, based on a regional salt balance assessment which showed salt imports into the valley to exceed salt exports (Schoups *et al.* 2005).

The field-wide leaching fraction historically has been calculated as the difference between the seasonal amount of applied water and the seasonal crop evapotranspiration. Data from our experiments showed that based on the historical approach, little or no field-wide leaching occurred, which appears to raise questions about the sustainability of drip irrigation. The field-wide leaching fraction is the ratio of the seasonal crop evapotranspiration (determined with a computer evapotranspiration model and measurements of canopy growth and reference crop evapotranspiration) to the seasonal applied water.

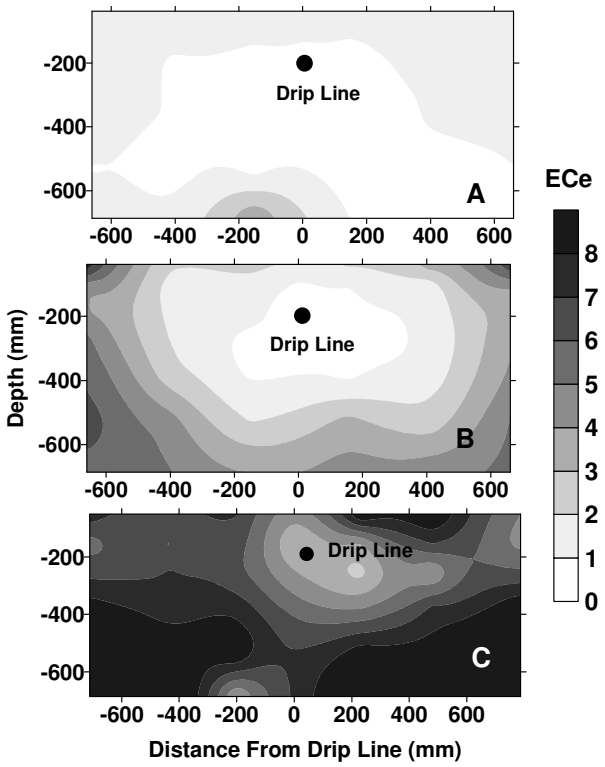

Figure 1. Patterns of soil salinity around drip lines for (A) an average water table depth = 2 m, EC of the irrigation water = 0.3 dS/m, and ground water EC = 8 to 11 dS/m; (B) water table depth between 0.61 and 1 m, EC of the irrigation water =0.3 dS/m, and ground water EC = 5 to 7 dS/m; and (C) water table depth between 0.61 and 1 m, EC of the irrigation water = 1.1 dS/m, and ground water EC = 9 to 16 dS/m. The black dots are the drip line locations. Values are EC of saturated extracts (dS/m).

Yet, considerable leaching occurred around the drip lines (defined as localized leaching), as seen in Figure 1. Localized leaching increased with increasing amounts of applied water. Thus, the historical approach to estimating leaching fractions may be inappropriate for drip irrigation. However, it is difficult to estimate the localized leaching fraction under drip irrigation because leaching fraction, soil salinity, soil moisture content, and root density all vary with distance and depth around drip lines. Thus, HYDRUS-2D was used to estimate leaching fractions under drip irrigation.

Computer Simulations

The simulations showed that reclamation of the soil near the drip line was rapid with salt patterns around the drip line similar to those shown in Figures 1B and 1C. As time progressed, the volume of reclaimed soil increased with most of the reclamation occurring below the drip line and salt accumulating above the drip line (data not shown). However, the simulation data show that considerable leaching occurred around the drip line for water applications of 60 and 80 percent, considered to be deficit irrigation conditions with no field-wide leaching (Hanson *et al.* 2008).

Based on the water balance approach, no field-wide leaching occurred for water applications equal to or less than 100% of the potential crop evapotranspiration. However, the actual leaching fraction, called the localized leaching fraction, ranged from 7.7% (60% water application) to 30.9% (115% water application), and was 24.5% for the 100% water application. The localized leaching fraction is defined as the ratio of the cumulative amount of flow out of the bottom of the modeling domain to the amount of irrigation water applied. As the salinity of the irrigation water increased, the localized leaching fractions increased for a given amount of applied water because of reduced root water uptake. Thus, even for applications considered to be deficit irrigation conditions, considerable localized leaching occurred around the drip lines. This behavior reflects the wetting patterns that occur under drip irrigation. This localized leaching is highly concentrated near the drip line, an area where root densities are likely to be the highest. These data, coupled with the measured soil salinity data, indicate that the historical approaches to measuring leaching fractions are inappropriate for drip irrigation.

References

Gärdenäs A, Hopmans JW, Hanson BR, Šimůnek J (2005) Two-dimensional modeling of Nitrate Leaching for Different Fertigation Strategies under Micro-Irrigation. *Agricultural Water Management* **74**, 219-242.

Hanson BR, Šimůnek J, Hopmans J (2006) Numerical Modeling of Urea-Ammonium-Nitrate Fertigation under Microirrigation. *Agricultural Water Management* **86**, 102-113.

Hanson BR, Hopmans JW, Simunek J (2008) Leaching with subsurface drip irrigation under saline, shallow groundwater conditions. *Vadose Zone J*. **7(2)**, 810–818. doi: 10.2136/vzj2007.0053.

Schoups G, Hopmans JW, Young CA, Vrugt JA, Wallender WW, Tanji KK, Panday S (2005) Sustainability of irrigated agriculture in the San Joaquin Valley, California. *Proceedings of the National Academy of Sciences of the United States of America* **102**(43), 15352-15356.

Šimůnek J, Šejna M, van Genuchten MTh (1999) The HYDRUS-2D software package for simulating two-dimensional movement of water, heat, and multiple solutes in variably saturated media. Version 2.0, *IGWMD-TPS-53*, International Ground Water Modeling Center, Colorado School of Mines, Golden, Colorado. 251 pp.

Effect of land use on the soil physical properties and water budget in a small water shed in NE Thailand

Siwaporn Siltecho[A, F], Claude Hammecker[B], Vichai Sriboonlue[C, E], Jean Luc Maeght[D] and Vidhaya Trelo-ges[A, E]

[A]Faculty of Agriculture, Khon Kaen University, Thailand, E mail aom_siwaporn@yahoo.com
[B]Institute of Research for Development (IRD), UR 176, Land Development Department, Thailand, E mail claude.hammecker@gmail.com
[C]Faculty of Engineering, Khon Kaen University, Thailand
[D]Institute of Research for Development (IRD), Water Management Institute-National Agriculture and Forestry Research Institute, UR Solutions, BP 06, Vientiane, Lao P.D.R.
[E]Ground Water Research Center, Khon Kaen University, Thailand
[F]Land Development Department, Ministry of Agriculture, Thailand

Abstract
Land clearing has severely affected the uplands in the Northeast of Thailand, where the original forest has been converted into agricultural land, with most probably important modifications of the soil properties. The aim of this study was to assess the effects of land use changes on both the soil physical properties and on the soil water budget in a small watershed. The experiment was conducted in 2008, in a mini watershed located near the village of Ban Non Tun (16°19'43.90" N, 102 ° 45'07.91" E), in the Khon Kaen Province, Thailand. The experiment was set up in several plots with different land uses: a young rubber tree (RT) plantation, ruzi grass (RG), and natural forest (F). Under the RT and under the RG the presence of a clayey layer at a depth varying from 90 to 150 cm, with low permeability, hindered the water infiltration and led to the occurrence of a perched water table during rainy season. The drainage was around 40% of the total rainfall in RT and RG respectively. The surface runoff was 10.73, 2.76 and 4.80% of total rainfall and the average evapotranspiration in the dry season was 1.80, 1.57 and 2.04 mm d^{-1} for the RT, RG and F respectivity.

Key Words
Hydraulic property

Introduction
In the northeast of Thailand where undulating topography dominates the landscape, the soil is mainly sandy and of low fertility. During these last decades the original *dipterocarpus* forest located in the uplands of the landscape has been cleared into agricultural land dedicated to cash crops. The conversion from forest to agricultural land had several noticeable impacts especially on the soil and water quality. Some studies (Chen *et al.,* 2009) found that land cover changes affect the distribution of soil moisture and hydraulic properties. However, this process has not been addressed in terms of precise quantification in this area. The temporal change of land use and management can thoroughly affect soil hydraulic properties and the soil water cycle. Therefore the aim of this study is to quantify the consequences of land use changes on the soil physical properties and soil water budget in a small watershed.

Materials and Methods
Experimental sites
The study site has been set up in a mini watershed located near Ban Non Toon, Khon Kaen Province, Thailand (16°19'43.90" N, 102 ° 45'07.91" E). In this undulating landscape, the higher parts of the mini watershed reach 210 m AMSL and 185 m AMSL in the lower parts, with a general average slope of 3.5%. Most of the area is planted with rubber trees (RT) and ruzi grass (RG) along the slopes and paddy fields in the valley line. Some patches of original forest (F) are still present in the watershed. Previously the land was planted with jute, cassava and ruzi grass. The climate of the site is considered as tropical savanna climate, with an annual rainfall of 1,309 and 1,957 mm in 2007 and 2008 respectively, and an average annual temperature of 29 °C.

Hydraulic properties of soil and water budget
The saturated hydraulic conductivity was measured in situ with a disc infiltrometer (Perroux and White 1988) in three different situations of land use: rubber tree plantation, ruzi grass pasture and forest. The water retention curves were derived from Wind evaporation method (Wind 1968) and with van Genuchten model (van Genuchten 1980).

$$Se = \frac{\theta - \theta r}{\theta s - \theta r} = (1+(-\alpha h_p)^n)^{-m} \qquad (1)$$

where θ_r and θ_s represent the residual and saturated water content, h is the matrix pressure head, α, n and m empirical parameters (m=1-1/n).
In order to monitor the water flux in this experimental watershed and in the different situations, a series of experimental devices was installed in the field namely: (i) a network of piezometers to measure the groundwater flow, (ii) several stations with tensiometers and neutron probes to monitor the water flow in the vadoze zone, (iii) in each situation the surface runoff was measured with a PVC cylinder (diameter 60 cm) slightly driven into the soil with a superficial outlet connected to a plastic tank and (iv) a micro-meteorology station. Considering the different terms of the water budget equation evapotranspiration was calculated as below:

$$P - R - D - \Delta S_{soil} = ET \qquad (2)$$

where P is precipitation was estimated from tipping bucket rain gauge, R is surface runoff, D is deep drainage calculated from tensiometric data and ΔS is change in soil water storage.

Results and Discussion

Soil properties

Some physical and chemical properties of soil are shown in Table 1. The texture of RT soil and RG soil is sandy at the top whereas the subsoil is sandy in its upper part, but becomes clay soil in depth. This clayey layer represents the interface between the soil profile and the bed rock composed of sandstone. Under the forest, the soil texture is sandy from the top to the bottom, even if the clay content also increases with depth. The soil pH of RT, RG and F soil is very acidic in the sandy layer but moderately acidic in the clayey layer except at 90 cm depth in forest soil where it is very acidic. The organic matter status is extremely low in all situations, but systematically shows a slight increase in the top soil.

Table 1. Physical and chemical properties of rubber tree (RT), ruzi grass (RG) and forest (F) soil.

Depth (cm)	Sand	Silt (%)	Clay	Texture	pH (1:1) H_2O	OM (%)
RT soil						
10	91.4	5.6	3.0	S	5.1	0.6
50	87.0	8.5	4.5	LS	5.3	0.1
90	57.7	14.3	28.0	SCL	5.5	0.4
RG soil						
10	89.0	7.5	3.5	S	5.4	0.5
40	87.2	10.6	2.2	S	5.4	0.1
90	57.6	12.1	30.3	SCL	5.7	0.2
F soil						
10	84.6	11.1	4.3	LS	5.4	0.5
40	87.8	8.7	3.5	LS	5.2	0.1
90	72.9	10.9	16.2	SL	4.9	0.3

The bulk density of RT and RG soil showed a regular increase with depth (Figure 1a), whereas for F soils it decreased slightly at 40 cm though the general trend from surface to depth is also an increase. Conversely, the value of saturated hydraulic conductivity (K_s) decreased with depth under RT soil (figure 1b). On the RG soil, the value of K_s was noticeably higher at 40 cm than at 10 cm soil depth, but similarly to RT soil the value of Ks is extremely low at 90 cm depth. On the other hand the saturated hydraulic conductivity was much more homogeneous along the soil profile under forest as the clayey layer was not as clearly identified as in the other situations. Saturated hydraulic conductivity shows higher variation on the superficial sandy soil than in the lower clayey soil. The comparison of three land uses showed that the hydraulic conductivity at top soil RT soil and RG soil was significantly higher than in F soil. This may be due to differences in soil compaction, as illustrated by bulk density, but it is mainly the slight difference in clays content that may explain particular properties. Similarly deeper, around 90 cm, the saturated hydraulic conductivity of F soil was much higher than for the soil of the two other situations, due to the difference in clay content.

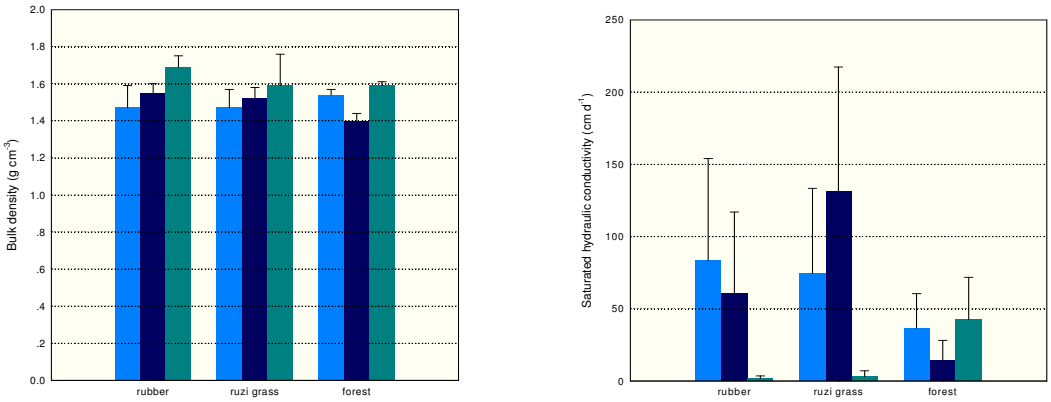

(a) (b)

Figure 1. Bulk density (a) and saturated hydraulic conductivity (b) of rubber tree, ruzi grass and forest soil (Cyan color is 10 cm depth, Blue color is 40 or 50 cm depth and Dk Cyan color is 90 cm depth).

Water retention parameter was show in Table 2. The value of residual water content θ_r of RT soil and RG soil was higher in the clayey layer than in the sandy layer. Inversely the value of saturated water content θ_s was higher in the sandy layer than in the clayey layer, indicating more available water in the sandy layer than in the clayey layer. In the F soil, the value of θ_r and θ_s slightly decreased with depth. The water retention parameter α in sandy layer is quite similar for most soils but is lower in clay layer. These values tend to decrease slightly from top soil to sub soil with narrow range of variation, accordingly to the clay content. The value of parameter *n* decreased with depth in all situations.

Table 2. Soil water retention parameter of rubber tree (RT), ruzi grass (RG) and forest (F) soil.

Depth (cm)	θr (cm^3 cm^{-3})	θs (cm^3 cm^{-3})	α (cm^{-1})	n
RT soil				
10	0.07±0.04	0.37±0.009	0.02±0.002	3.09±0.31
50	0.03±0.01	0.36±0.01	0.01±0.0004	2.82±0.25
90	0.12±0.02	0.28±0.01	0.01±0.005	1.92±0.17
RG soil				
10	0.06±0.001	0.39±0.001	0.02±0.002	4.16±0.33
40	0.07±0.02	0.40±0.01	0.02±0.0003	2.57±0.14
90	0.012	0.31±0.018	0.002±0.0001	2.70±0.23
F soil				
10	0.07±0.014	0.32±0.01	0.02±0.0004	2.68±0.45
40	0.06±0.0002	0.32±0.01	0.01±0.001	2.55±0.19
90	0.05±0.07	0.28±0.01	0.02±0.002	1.91±0.72

Soil water budget

The study of the soil water budget under RT and RG was carried out from January to December 2008, except for F, where the tensiometric data was unavailable from January to June 2008. Therefore drainage could only be calculated for half a year in this situation. The annual rainfall in 2008 was exceptionally high with 1,958 mm. In the RT soil, three different topographic situations have been considered: up-, mid-, and downslope. The evolution of surface runoff has been represented in Figure 2. In RT soil, at the beginning of the rainy season upslope and midslope situations have higher runoff than the downslope but at the end of rainy season cumulative runoff becomes higher downslope. Possibly due to lateral perched water flow downslope. In RG and F the surface runoff is noticeably less, and increases mainly at the end of the rainy season when soils are thoroughly saturated.

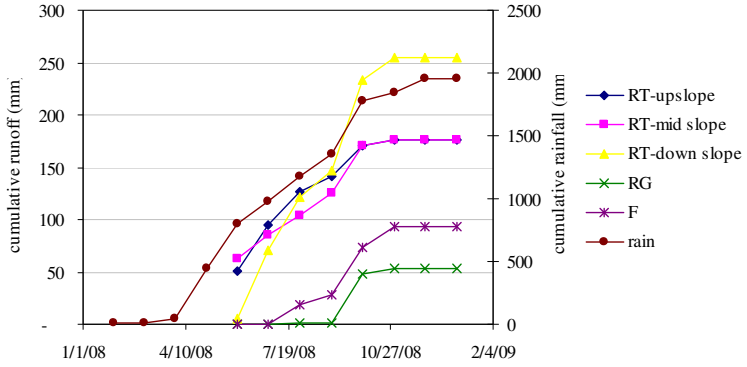

Figure 2. The evolution of surface runoff under three land uses.

In RT and RG, the sandy layer, with its high permeability, had an high drainage capacity, but the low permeability of clay layer limited downward percolation. Consequently a perched water table developed during rainy season. The drainage was higher in RG soil than RT soil (Table 3). From July to December 2008, the drainage in F soil was 459 mm, and in the same period it was 776, 1175 for RT at and RG Evapotranspiration (ET) calculated from the soil water balance equation was similar to Penman's potential evapotranspiration calculated with the meteorological data (1000.13mm). In the RT situation the topography played an important role in the water balance, as shown in Table 3: in mid slope position, drainage was less but ET was highest. The drainage represented around 40% of the total rainfall for RT and RG, whereas it represented only 23% of the total rainfall in the forest. The surface runoff was 10.73, 2.76 and 4.80% of total rainfall and the average ET of RT, RG and F in dry season was 1.80, 1.57 and 2.04 mm d^{-1} respectively .

Table 3. The cumulative drainage water and evapotranspiration in the three land uses

Land use	Drainage	ET
	(mm)	
Rubber soil	776	1012
- upslope	852	1002
- midslope	586	1227
- downslope	890	808
Ruzi grass soil	1175	870
Forest soil	459*	418*

* calculated from July-December 2008

Conclusions

The soil differentiation in the different land use situations, especially the clay distribution, conditioned specific soil hydraulic properties and water balances. The contrasted saturated hydraulic conductivity in RT and RG between sandy layer and clayey layer, contributed to the occurrence of a perched water table during rainy season when rainfall was high and potential evaporation was low. The shallow water table persisted for 2–3 months, with downward and lateral flux causing drainage losses. On the other hand in more the homogeneous soil of the forest, the water storage was higher, the runoff and the drainage less, and finally the ET higher.

Reference

Chen X, Zhang Z, Chen X, Shi P (2009) The impact of land use and land cover changes on soil moisture and hydraulic conductivity along the karst hillslopes of southwest China. Environmental Earth and Science http://www.springerlink.com/content/b77806842737j815/

Perroux KM, White I (1988) Design for disc permeameters and soil dispersion. *Soil Science Society of America Journal* **48**, 50-55.

van Genuchten MT (1980) A closed form equation for predicting the hydraulic conductivity of unsaturated soils. *Soil Science Society of America Journal* **44**, 892-898.

Wind GP (1968) Capillary conductivity data estimated by a simple method. In 'Water in the unsaturated zone. Vol. 1'. (Eds P.E. Rijtema and H. Wassink), pp. 181–191. (UNESCO).

Effect of leaching on hydrophobicity and infiltration into a texture contrast soil

Marcus Hardie[A, B, E], William Cotching[C, E], Richard Doyle[A], Shaun Lisson[D]

[A]Tasmanian Institute of Agricultural Research, University of Tasmania, Private Bag 98, Hobart, TAS 7001, Australia. Email marcus.hardie@utas.edu.au
[B]School of Agricultural Science, University of Tasmania, Private Bag 54, Hobart, Tas 7001, Australia
[C]Tasmanian Institute of Agricultural Research, University of Tasmania, PO Box 3523, Burnie, Tas 7320, Australia
[D]CSIRO Sustainable Ecosystems University of Tasmania, PB 98, Hobart, Tas 7001, Australia
[E]Secondment from Department of Primary Industries, Parks Water and Environment (DPIPWE)

Abstract
Water repellence in a texture contrast soil was found to be more strongly related to rainfall/leaching history, than the soil moisture content at the time of analysis. Field samples collected after prolonged rainfall had significantly lower water drop penetration time (WDPT) than samples collected after a prolonged period with minimal rainfall. A sequential leaching experiment also demonstrated that compounds causing water repellence could be leached from the soil, and that water repellence did not return following drying. Infiltration experiments demonstrated that leaching of water repellent substances was sufficient to prevent the development of finger flow even when soils were air dried, however fingering was observed in both leached and non-leached soil when air flow at the base of the Helle-Shaw tank was prevented. The work has important implications for timing of application of many agrochemicals to these soils.

Key Words
Water repellence, duplex, finger flow, infiltration, preferential flow

Introduction
Water repellence is thought to affect approximately 5 million hectares in Australia (Blackwell, 2000). Water repellence has been associated with increased erosion, poor seedling establishment, uneven crop growth, reduced irrigation efficiency and accelerated leaching of solutes including pesticides and fertiliser (Blackwell, 2000; Ritsema and Dekker, 2000). In water repellent soil, development of soil water fingers or 'fingering' results from instability in the wetting front when either the infiltration rate of a soil is less than the saturated hydraulic conductivity, or the depth of ponding is below the water entry potential (Wang *et al.,* 1998). Numerous studies have demonstrated that water repellence is inversely related to soil water content and that a critical water content exists below which fingering develops (Ritsema *et al.* 1998). Doerr and Thomas (2003) however found that for at least some soils that the relationship between soil moisture and water repellence is hysteretic, and that water repellence is not re-established after seasonal rainfall, unless input of new hydrophobic substances occurred. This paper details findings resulting from seasonal rainfall and leaching of a water repellent texture-contrast soil.

Methods
Effect of moisture content and leaching on water repellence
Samples were collected from the A horizon (0-10 cm) of a texture contrast soil, at the end of summer in April 2008, following 12 mm rainfall in the 30 days prior to sampling (non-leached), and July 2009 following 103 mm rainfall in the 30 days prior to sampling (leached). The relationship between antecedent soil moisture and water drop penetration time (WDPT) was determined by wetting a 1 kg sample of air dried non-leached soil to saturation. Subsamples were then dried at 40°C for durations ranging from 6 to 140 hours to produce a range of soil moisture contents. Samples were cooled to room temperature and the WDPT determined according to Caron *et al.*(2008). The relationship between leaching history and water repellence was investigated by sequentially leaching a 1200 cm^3 air dried, non-leached soil. Following leaching, soil was dried at 40°C for 24 hours, and the WDPT and water entry potential (WEP) determined, following similar procedure to Wang *et al.*(2000).

Finger flow – Helle Shaw tank
The effects of soil moisture and air entrapment on infiltration was investigated by applying water to leached and non-leached soil packed into a 2 cm wide glass walled tank (Helle-Shaw cell) (Wang *et al.,* 2003). Infiltration was conducted with and without air entrapment into soils with differing moisture content and leaching history. The head of water was maintained between 0.5 and 0.8 mm by controlling the rate of flow from the drippers or setting the air tube to the depth of ponding. Water flow down the sides of the glass panes was prevented by

coating the glass with either Teflon (moist soil) or thinly smeared Vaseline (dry soil). Visualisation of infiltration into wet soil was aided by application of 20 g/L Brilliant Blue FCF (C.I. Food Blue 42090) and recorded by still camera every 1 to 5 minutes depending on rate of infiltration.

Results

Prolonged rainfall significantly reduced water repellence (WDPT). Non-leached samples collected in April 08 had significantly higher WDPT than leached samples collected in July 09 (Table 1).

Table 1. Effect of leaching history on water repellence.

Site	Non Leached (April 08)			Leached (July 09)		
	Grav. Soil Moisture %	WDPT (mins)	Repellence Class[+]	Grav. Soil Moisture %	WDPT (mins)	Repellence Class[+]
B	0.91	5	High	0.42	0.18	Weak
C	1.13	15-20	Severe	0.40	0.63	Weak

[+] Classification based on Dekker *et al.* (2000).

The relationship between soil moisture and WDPT was poor ($r^2 = 0.56$, df 16) (Figure 1b), however artificial leaching significantly ($p<0.05$) reduced water repellence measured as both WDPT and WEP (Figure 1a). The WDPT decreased significantly from 170 minutes to 7.8 minutes following the first leaching event. Further leaching events did not significantly reduce WDPT, however the water entry potential (WEP) decreased significantly ($p<0.05$) with each leaching event (except second and third events) (Figure 1a). The relationship between WDPT and *WEP* was best described by a logarithmic function ($r^2 = 0.94$, $p <0.001$, df 7). Difference between the WDPT and *WEP* response suggests that initial leaching had greater effect on the time required for water repellence to breakdown, than the water entry pressure required to overcome water repellence and initiate infiltration.

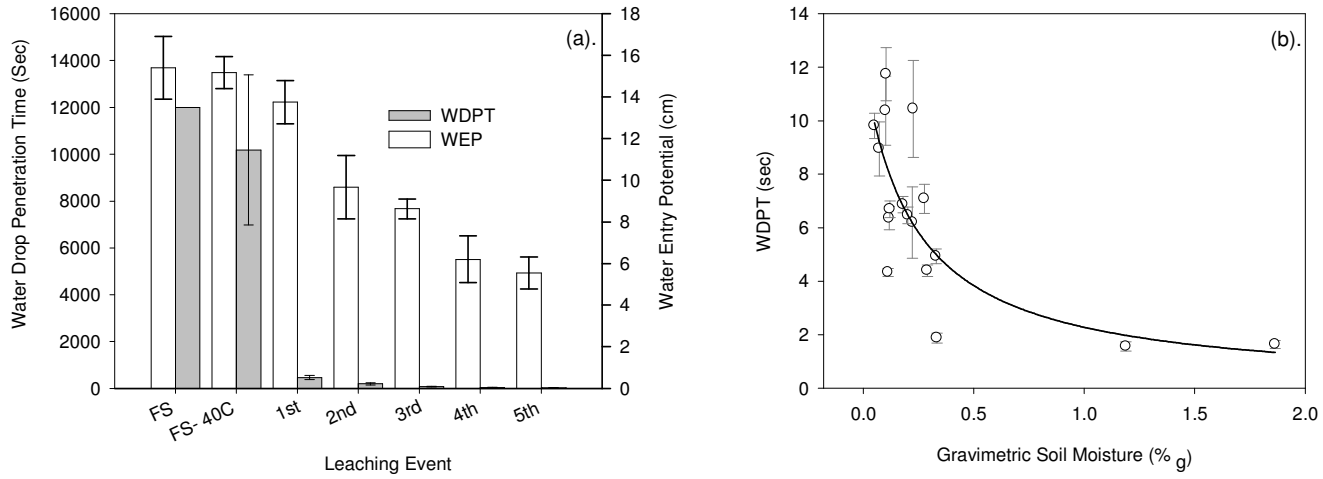

Figure 1 (a). Effect of leaching on water drop penetration time (WDPT), and water entry potential (WEP), FS = Field sample, FS-40°C = field sample dried to 40°C (b). Relationship between WDPT and WEP. Error bars represent ±1 standard deviation.

Finger flow and uneven wetting fronts, developed in dry non-leached soil (Figure 2b) and wet, leached soil with air entrapment (Figure 2d). Uniform flow occurred in leached soil with no air entrapment regardless of soil moisture (Figures 2 a & c). Results indicate that the reduction in water repellence followed prolonged rainfall (Table 1) prevented development of finger flow in soils with no air entrapment (Figures 2 a & c). However finger flow was induced in leached soil as a result of air entrapment at the base of the soil horizon. Finger flow propagation rate in dry, non-leached soil was 355 mm/hr (Figure 2b), which was similar to the infiltration rate for uniform flow in leached, dry soil at 385 mm/hr and wet soil at 410 mm/hr (figures 2 a &c respectively). Finger propagation with air entrapment in leached soil (Figure 2d) was considerably slower than the other infiltration events at 45 mm/hr.

Discussion & Conclusion

Water repellence was found to be dependent on rainfall/leaching history. Leaching resulting from rainfall and the laboratory experiment significantly reduced water repellence, resulting in uniform infiltration. Results from this study confirm previous findings by Doerr and Thomas (2003) of a hysteretic relationship between soil moisture and water repellence in some soils, and that input of hydrophobic substances is necessary to re-establish water repellence after leaching. These findings cast doubt on the modelling approaches based on Ritsema *et al.* (1993) in which finger flow develops below a static critical water threshold. In the absence of rainfall, it is recommended agricultural managers apply irrigation or wait for rainfall to leach hydrophobic substances from soils prior to application of pesticides or fertiliser, in order to reduce the risk of shallow groundwater contamination via finger flow.

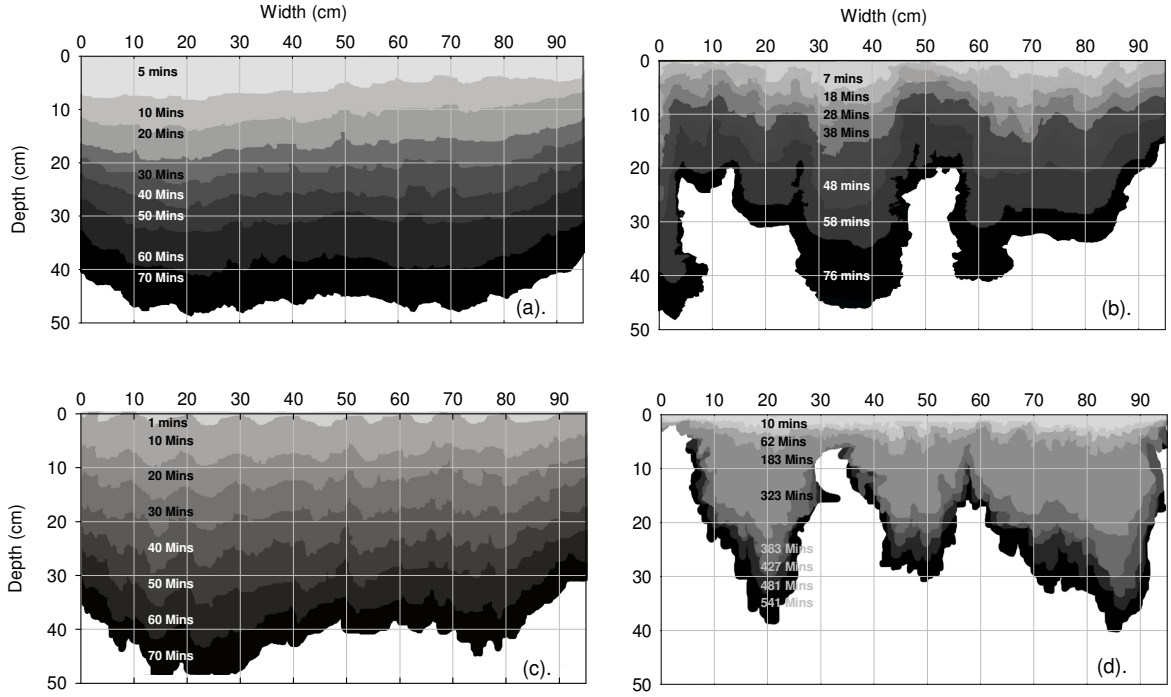

Figure 2. Helle-Shaw tank experiment. Infiltration into (a) leached, dry soil collected July 09, no air entrapment (b) non-leached, dry soil collected April 08, no air entrapment (c) leached, wet soil collected July 09, no air entrapment (d) leached, wet soil collected July 09, with air entrapment.

References

Blackwell PS (2000) Management of water repellency in Australia, and risks associated with preferential flow, pesticide concentration and leaching. *Journal of Hydrology* **231-232**, 384-395.

Caron J, Elrick DE, Michel JC, Naasz R (2008) Chapter 68: Physical properties of organic soils and growing media: water and air storage and flow dynamics. In 'Soil Sampling and Methods of Analysis'. (Eds MR Carter, EG Gregorich) pp. 885-912. (Canadian Society of Soil Science, CRC Press: Boca Raton).

Dekker LW, Ritsema CJ, Oostindie K (2000) Wettability and wetting rate of Sphagnum peat and turf on dune sand affected by surfactant treatments. In 'Proceedings of the 11th International Peat Congress'. Edmonton, Canada. (Eds L Rochefort, JY Daigle) pp. 566-574.

Doerr SH, Thomas AD (2003) Soil moisture: a controlling factor in water repellency? In 'Soil water Repellency: Occurrence, Consequences, and Amelioration'. (Eds. CJ Ritsema, LW Dekker), pp. 137-149 Wageningen, Netherlands).

Ritsema CJ, Dekker LW (2000) Preferential flow in water repellent sandy soils: principles and modeling implications. *Journal of Hydrology* **231-232**, 308-319.

Ritsema CJ, Dekker LW, Hendrickx JMH, Hamminga W (1993) Preferential flow mechanism in a water repellent sandy soil. *Water Resources Research* **29**, 2183-2193.

Ritsema CJ, Nieber JL, Dekker LW, Steenhuis TS (1998) Stable or unstable wetting fronts in water repellent soils - Effect of antecedent soil moisture content. *Soil and Tillage Research* **47**, 111-123.

Wang Z, Feyen J, Ritsema CJ (1998) Susceptibility and predictability of conditions for preferential flow. *Water Resources Research* **34**, 2169-2182.

Wang Z, Tuli A, Jury WA (2003) Unstable Flow during Redistribution in Homogeneous Soil. *Vadose Zone Journal* **2**, 52-60.
Wang Z, Wu L, Wu QJ (2000) Water-entry value as an alternative indicator of soil water-repellency and wettability. *Journal of Hydrology* **231-232**, 76-83.

Electrical conductivity and nitrate concentrations in an Andisol field using time domain reflectometry

Teruhito Miyamoto[A], Koji Kameyama[A] and Yoshiyuki Shinogi[A]

[A]Department of Agricultural Land and Water Resources, National Institute for Rural Engineering, National Agricultural and Food Research Organization, Tsukuba, Ibaraki, Japan, Email teruhito@affrc.go.jp

Abstract
Andisols exhibit unique dielectric properties which may affect estimation of electrical conductivity by time domain reflectometry (TDR). We investigated the potential to continuously monitor electrical conductivity (σ_w) and nitrate concentrations of soil solution using TDR in an Andisol field from December of 2007 through August of 2008. Before the field experiment, we investigated the relationship between σ_w, bulk soil electrical conductivity (σ_b), and volumetric water content (θ) for an Andisol and assessed the use of the Hilhorst model to describe the relationship. The obtained σ_w - σ_b - θ relationship was fitted well by the Hilhorst model with the dielectric permittivity of soil at $\sigma_b = 0$, $\varepsilon_0 = 10$. In the field experiment, σ_w values estimated using TDR with the Hilhorst model were in agreement with those obtained from solution samplers. In addition, a linear regression between σ_w and nitrate concentrations showed positive correlation. The combination of this regression with the σ_w estimated from TDR measurement and Hilhorst model will provide a useful tool for monitoring soil nitrate concentrations in Andisol fields under transient conditions.

Key Words
Time domain reflectometry (TDR), Andisol, nitrate concentrations, soil solution, electrical conductivity.

Introduction
Contamination of groundwater by excess fertiliser is a common problem in upland field areas in Japan. To establish sustainable agricultural practices, it is important to estimate the displacement of water and solutes that will occur at a depth below the plant root zone during a given time period. Time domain reflectometry (TDR) has become an established and reliable means to determine volumetric water content (θ) and bulk soil electrical conductivity (σ_b) (e.g. Noborio 2001). As TDR can measure both θ and σ_b in the same soil volume rapidly, it has been used to monitor solutes. Some researchers have applied TDR to estimate nitrate concentrations (Nissen *et al.* 1998; Das *et al.* 1999; De Neve *et al.* 2000). Although Andisols exhibit unique dielectric properties which may affect the estimation of electrical conductivity by TDR, available works evaluating the use of TDR for studying solute transport are still limited (Vogeler *et al.* 1996; Muñoz-Carpena *et al.* 2005). Moreover, little information is available on comparing soil solution electrical conductivity (σ_w) based on TDR measurement with that obtained by conventional methods, soil coring or solution samplers under field transient state conditions. The main objective of this study was to test the applicability of TDR measurements for assessing the temporal dynamics of nitrate concentrations in Andisol fields. To this end, we evaluated a new model to describe the σ_w - σ_b - θ relationship for Andisol. We also conducted a field experiment to compare σ_w based on TDR measurement with that obtained by conventional methods. In addition, we obtained a regression for predicting nitrate concentrations from the σ_w values.

Methods
The σ_w - σ_b - θ relationship model developed by Hilhorst
Hilhorst (2000) developed a novel method for estimating σ_w directly from the measurements of the dielectric permittivity of soil, ε_a, and the bulk electric conductivity of soil, σ_b.

$$\sigma_w = \frac{\varepsilon_p \sigma_b}{\varepsilon_a - \varepsilon_0} \quad (1)$$

ε_p is the dielectric permittivity of soil solution ($\cong 81$), and ε_0 is the dielectric permittivity of soil at $\sigma_b = 0$. For a capacitance sensor, values between 1.9 and 7.6 have been reported for ε_0 (Hilhorst 2000).

Calibration experiment
Soil samples were obtained at the surface and at a depth of 0.6 m from the experimental field. The samples were washed by three pore volumes of distilled water. They were then air-dried, passed through a 2-mm sieve and packed as uniformly as possible into an acrylic cylinder (62.8 mm in diameter and 130 mm high) up to a height

of 110 mm high. ε_a and σ_b were measured using a TDR cable tester (Tektronix 1502B). For all measurements, we used the same three-rod TDR probe (3 mm in diameter and 100 mm long with a 15 mm in space between the centre and outside rods). The TDR probe was inserted vertically into the soil columns. Waveform analysis was conducted using the WinTDR waveform analysis software (Or *et al.* 1997), which enables automated TDR control, data acquisition, and waveform analysis. Water contents were measured by weighing the soil samples gravimetrically using an electronic balance. σ_w was obtained by centrifuging the soil samples at 6000 rpm for 30 min and measuring the electrical conductivity of the supernatant with a conductivity metre.

Field experiment
A field experiment was conducted from 17 December, 2007 to 31 August, 2008 at the National Institute of Rural Engineering in Tsukuba, Japan. The type of soil at this site is Andisol (Typic hydrudand). The soil's physical and chemical properties are listed in Table 1. The soil profile was divided into two layers, a surface layer and a subsurface layer at a depth of 0.4 m. The experimental field was 10 × 10 m in size. The experimental field was fertilised with 200 kg N/ha, 87 kg P/ha and 166 kg K/ha as chemical fertiliser on 25 December, 2007. The ground surface was kept unplanted during the field experiment.

Three-rod TDR probes (5 mm in diameter and 300 mm long with a 25 mm in space between the centre and outside rods) were horizontally installed into pit faces at three locations, at three depths (0.2 m, 0.4 m and 0.6 m). The TDR probes were connected to a cable tester (Tektronix 1502B) through a multiplexer (SDMX50, Campbell Scientific). A copper-constantin thermocouple was installed at a central pit at three depths to compensate for soil temperature when measuring σ_b. Two porous cups were buried at three depths same as the TDR between each pit to collect soil solution samples. ε_a, σ_b and soil temperature data were recorded every hour throughout the field experimental period. The soil solution was sampled one to three times a month during the field experiment.

Table 1. Physical and chemical properties of soils taken from the experimental site.

	Bulk density (g/cm^3)	*Ks* (mm/h)	pH[*1]	T-C (%)	T-N (%)	CEC[*2] ($cmol\ kg^{-1}$)
Topsoil	0.71	126	6.2	4.3	0.4	22.2
Subsoil	0.63	108	6.3	2.0	0.4	17.4

*1 soil:solution = 5g:25mL
*2 Wada (1986)

Results

Calibration experiment
The TDR-measured σ_b is plotted against σ_w as measured by a conductivity meter on the extracted solution (Figure 1). The results show that a linear relationship exists between σ_b and σ_w in the range of 0.5 to about 3.0 dS/m at each θ. In addition, the data for topsoil and subsoil are similarly. These results may indicate that the σ_w - σ_b - θ relationships are not sensitive to the bulk density. Results from fitting the experimental data to the Hilhorst model are also given in Figure 1. The calculated σ_w - σ_b - θ relationships agree well with the experimental data. In the Hilhorst model, ε_0 is the only parameter calculated from the relationship between σ_b and ε_a. The value of ε_0 was 10 in this study. Ochiai and Noborio (2003) used $\varepsilon_0 = 9$ for σ_w calculations from TDR-measured σ_b and ε_a in an Andisol field. The ε_0 values for the Andisols in Japan are likely to fall around 10.

Field experiment
The σ_w value estimated using TDR with the Hilhorst model was similar to that obtained from solution samples with porous cups (Figure 2). A distinct breakthrough 0.2 m deep was observed in both measured and estimated σ_w values. However, solute transport was detected earlier with TDR than with the porous cups. At a depth of 0.4 m, TDR estimates exhibited similar magnitude and pattern as those for solution samples with porous cups. A gradually increasing σ_w at a depth of 0.6 m from mid-April to mid-May was detected with both TDR and porous cups. In contrast, the σ_w estimated by TDR did not correspond well with the σ_w measured by porous cups after mid-May. The scatter plots show the potential of using σ_w combined with site-specific regressions for predicting the soil nitrate concentrations, which are relatively well correlated to changes in σ_w (Figure 3). The regressions are similar to those reported in previous works. In particular, the regression is close to that obtained from a field calibration experiment by Das *et al.* (1999).

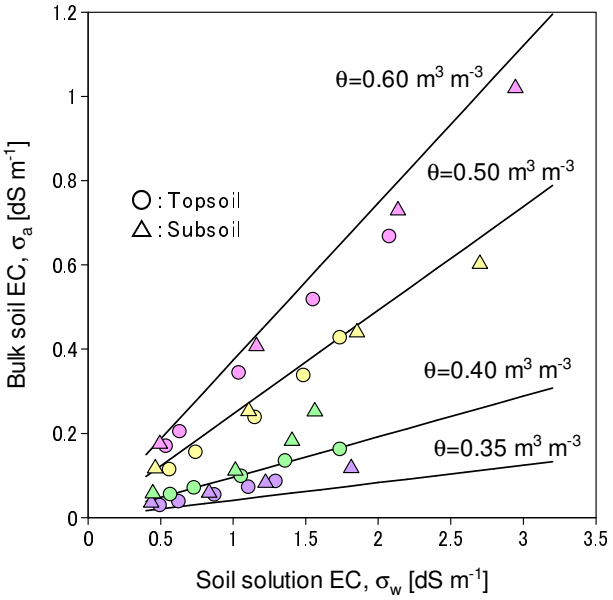

Figure 1. TDR-measured bulk soil electrical conductivity vs. electrical conductivity of the soil solution measured with a conductivity meter for different water contents of an Andisol. Solid lines are prediction of the Hilhorst model using $\varepsilon_{0=10}$.

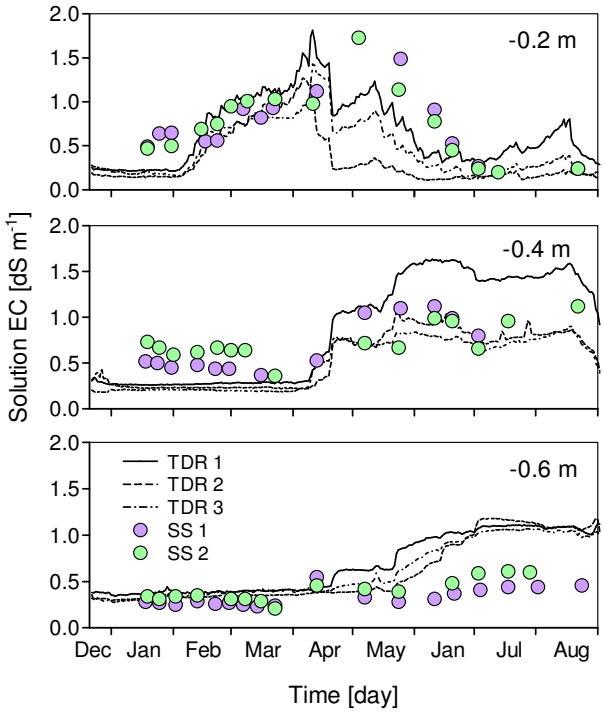

Figure 2. Electrical conductivity of soil solution (σ_w) at 25 °C calculated from TDR measurements compared with values obtained from soil solution extracted with porous cups (SS 1 and SS 2).

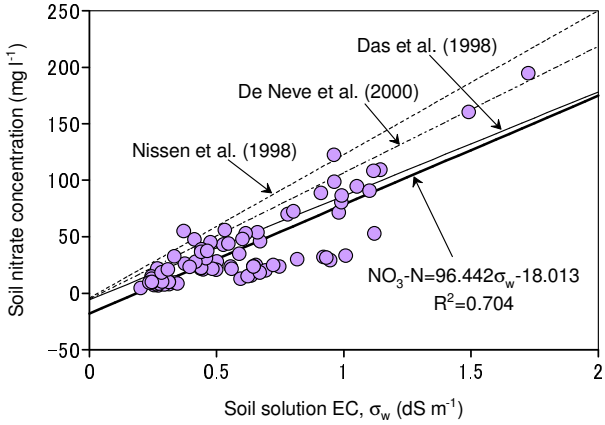

Figure 3. Scatter plots of soil nitrate concentrations as a function of soil solution electrical conductivity. Linear regressions obtained in previous studies are also shown.

Conclusion

Andisols differ from the other soils in their dielectric properties, affecting the estimation of electrical conductivity by TDR. Therefore, we investigated the σ_w - σ_b - θ relationship for Andisols and assessed the use of the Hilhorst model to describe the relationship. The obtained σ_w - σ_b - θ relationship agreed well with the Hilhorst model with ε_0 = 10. In a field experiment, σ_w values estimated using TDR with the Hilhorst model were in agreement with those obtained from solution samplers. In addition, a linear regression between σ_w and nitrate concentrations showed positive correlation. The combination of this regression with the σ_w estimated from TDR measurement and the Hilhorst model will provide a useful tool for monitoring soil nitrate concentrations in Andisol fields under transient conditions.

References

Das BS, Wrath JM, Inskeep WP (1999) Nitrate concentrations in the root zone estimated using time domain reflectometry. *Soil Science Society of America Journal* **63**, 1561-1570.

De Neve S, Van de Steene J, Hartmann R, Hofman G (2000) Using time domain reflectometry for monitoring mineralization of nitrogen from soil organic matter. *European Journal of Soil Science* **51**, 295-304.

Hirholst MA (2000) A pore water conductivity sensor. *Soil Science Society of America Journal* **64**, 1922-1925.

Muñoz-Carpena, R, Regalado CM, Ritter A, Alvarez-Benedí J, Socorro AR (2005) TDR estimation of electrical conductivity and saline solute concentration in a volcanic soil. *Geoderma* **124**, 399-413.

Nissen H. H., Moldrup P, Henriksen K (1998) Time domain reflectometry measurements of nitrate transport in manure-amended soil. *Soil Science Society of America Journal* **62**, 99-109.

Noborio K (2001) Measurement of soil water content and electrical conductivity by time domain reflectometry: a review. *Computers and Electronics in Agriculture* **31**, 213–237.

Ochiai H, Noborio K (2003) Effects of the excrement and urine of domestic animals applied to a grass field on groundwater quality. *Transactions of the Japanese Society of Irrigation, Drainage and Reclamation Engineering* **228**, 1-8. (in Japanese with English abstract)

Or D, Fisher B, Hubscher RA, Wraith JM (1997) 'WinTDR98 Users Guide'. (Utah State University, Environmental Soil Physics Group: Logan. Utah) http://www.usu.edu/soilphysics/wintdr/index.cfm

Vogeler I, Clothier BE, Green SR, Scotter DR, Tillman RW (1996) Characterizing water and solute movement by time domain reflectometry and disk permeametry. *Soil Science Society of America Journal* **60**, 5-12.

Wada K (1986) 'Ando Soils in Japan.' (Kyushu University Press: Fukuoka).

Estimating hysteretic soil-water retention curves in hydrophobic soil by a mini tensiometer-TDR coil probe

Anurudda K. Karunarathna[A], Tshering Chhoden[A], Ken Kawamoto[A], Toshiko Komatsu[A], Per Moldrup[B], Lis Wollesen de Jonge[C]

[A]Graduate School of Science and Engineering, Saitama University, Japan, Emails: tshering_chho@yahoo.com, anujica@yahoo.com, kawamoto@mail.saitama-u.ac.jp, komatsu@mail.saitama-u.ac.jp
[B]Department of Biotechnology, Chemistry, and Environmental Engineering, Aalborg University, Denmark, Email: pm@bio.aau.dk
[C]Department of Agroecology and Environment, Aarhus University, DK-8830 Tjele, Denmark, Email: Lis.W.de.Jonge@agrsci.dk

Abstract
The precise and continuous measurement of hydraulic properties of hydrophobic soils is of vital importance for the understanding of soil-water interaction in hydrophobic soils. The water repellency (WR) persistence of a volcanic ash soil that was preheated for different temperatures between 20°C and 200°C was measured by the water drop penetration time test. Although the heat treatment lowered the soil organic carbon (SOC) content of soil, the persistence of water repellency was increased in soil samples heated between 60°C and 175°C. To study the hysteretic soil-water retention behaviour of the preheated soils during wetting and subsequent drying processes, a mini tensiometer-TDR coil probe was developed. The sensor was capable of measuring the soil-waster content (θ) and the soil-water potential (ψ) simultaneously in a small pocket of soil. The soil-water retention measurements by wetting and subsequent drying processes implied that; the water entry in term of soil-water potential is positive in water repellent soils.

Key Words
Soil-water repellency, soil-water retention, mini tensiometer-TDR coil probe

Introduction
Soil-water repellency (WR) accounts for influencing many of the key soil hydrological processes such as reduce infiltration and increase of overland flow (DeBano 1971), preferential flow (Wallis and Horne 1992), and reduction of soil-water availability (Bond 1972) in hydrophobic soils. The occurrence of WR reduces the affinity of soils to water such that they can resist wetting for a certain period of time ranging from a few seconds to hours or days (Doerr and Thomas 2000). Although the soil-water content (θ) and soil organic carbon (SOC) are the key factors controlling the soil WR, the occurrence and magnitude of WR are believed to be effected by several other soil and environmental conditions (Doerr *et al.* 2000). Moreover, it has shown that the spatial distribution of soil WR is not uniform even at smaller scales (Hubbert *et al.* 2006). However, most of regular soil-water measuring devices are incapable of simultaneous measurements of θ and ψ in such small resolution (Vaz *et al.* 2002). And, development of measuring device that can measure the θ and ψ at same spatial location within approximately the same bulk soil is of vital importance for the understanding of the soil-water interaction in water repellent soils. Thus, the objectives of this study were (i) to estimate the WR persistence of a volcanic ash soil prior to and after heat pre-treatment, (ii) to develop a mini tensiometer-TDR coil probe that can measure θ and ψ simultaneously at the approximately the same soil volume, and (iii) to investigate the effect of WR on soil-water characteristics during repeated wetting and drying processes, by using an experimental apparatus equipped with mini tensiometer-TDR coil probe.

Methods
Soil materials and physicochemical properties
Soil samples were collected from 0.00-0.05m depth layers of an excavated soil profile in a forested hill-site at Fukushima prefecture in north-eastern Japan (see Kawamoto *et al.* (2007) for further site description). The soil was a volcanic ash soil (Andisol) which was covered by various plant species dominated by red pine trees (*Pinus densiflora*). Soil samples were first hand sieved through a 2-mm mesh screen at the field water contents (0.45 m^3 m^{-3}) prior to all laboratory analysis. The soil texture was clay loam with 17.8% clay, 27.4% silt and 54.8% sand.

Heat pre-treatment and water repellency characterization
Soil samples initially at field moisture were placed on open metal dishes and heated at different temperatures either in an oven (20, 60, 105 and 125°C) or muffle furnace (150, 175, 190 and 200°C) for 24 hours. After

cooling down to room temperature in oven/muffle furnace, the samples were kept in a room at 20°C and 75% relative humidity for 48 hours for equilibration. The SOC content of air-dried and preheated samples was determined using an automatic C-N analyzer (CHN corder MT-5, Yannaco, Kyoto). Water repellency persistence of preheated samples was determined by the water droplet penetration time (WDPT) test, and preheated soils were categorized into different classes according to Bisdom *et al.* (1993).

Tension table with combined mini tensiometer-TDR coil probe

To determine the soil-water characteristic curves for preheated soils with different WR persistence, an experimental set up was arranged as shown in Fig. 1. The setup was composed of a plastic column, a Marriott tank, and a mini tensiometer-TDR coil probe. The mini tensiometer-TDR coil probe was made by guiding a 50Ω copper wire (0.3 mm diameter) along the outside wall of a Perspex pipe. The coil was coated and fixed to pipe by a Polyethylene resin, and surrounded by four 0.3 mm diameter copper wires that soldered to the earth wire of the coaxial cable. The porous cup tensiometer was fixed next to the TDR coil, at the tip of the Perspex tube. The mini tensiometer-TDR coil probe was fixed to a 50 mm diameter plastic ring by side through a rubber stopper, and coaxial cable was connected to a metallic cable tester (Tektronix 1502C) and a personal computer, respectively. The open end of the Perspex tube was connected, through a flexible tube, to a digital pressure transducer that connected to a data logger.

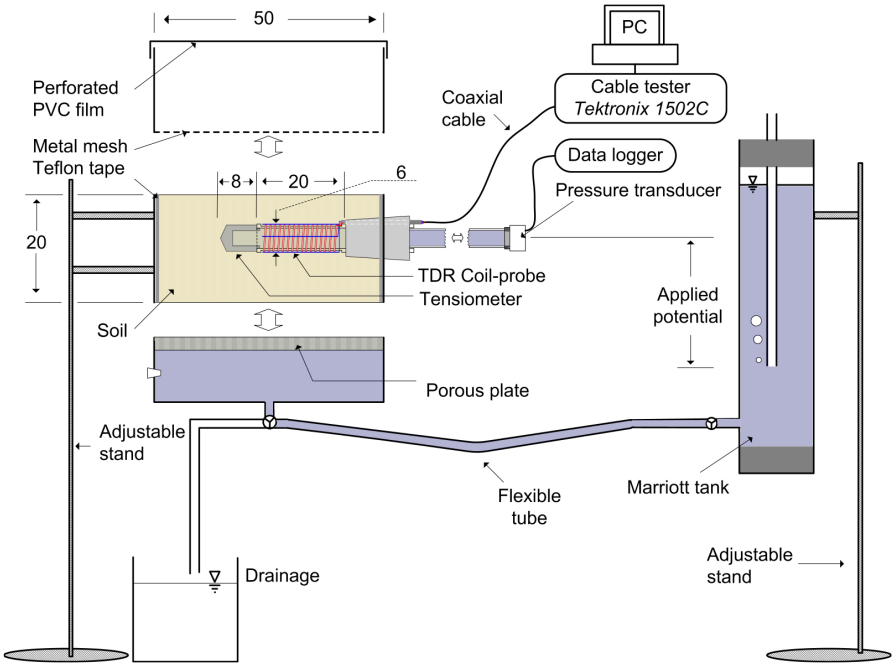

Figure 1. Schematic diagram of the tension table with mini tensiometer-TDR coil probe (all dimensions are in millimetres).

Measurement of soil-water characteristics of water repellent soils

First, the lower part of assemble was saturated, and kept continually under saturation by adjusting the Marriot tank. The ring with TDR-tensionmeter assemble was mounted on lower ring, and fixed by adhesive tapes. The preheated and equilibrated soil sample at air-dry moisture was then uniformly packed in the middle ring, with the same dry bulk density as field (0.56 Mg m^{-3}). Soil surface was covered by another Perspex ring with a metal mesh fixed at the bottom and a perforated PVC film on top. The hydraulic characteristics of soil representing different WR classes were determined by a series of repeated wetting and drying processes.

Results and Discussion

Effect of heat pre-treatment on soil water repellency

The heat treatment lowered the SOC content of soil, and changed the WR persistence of soil (Fig. 2). The soil sample which was dried at 20°C was strongly water repellent (WDPT, 60-600s), however heating at temperatures between 105 and 175°C increased the persistence of WR to extremely water repellent state (WDPT, > 3600s). In contrast, water repellency was disappeared when heated at and above 175°C.

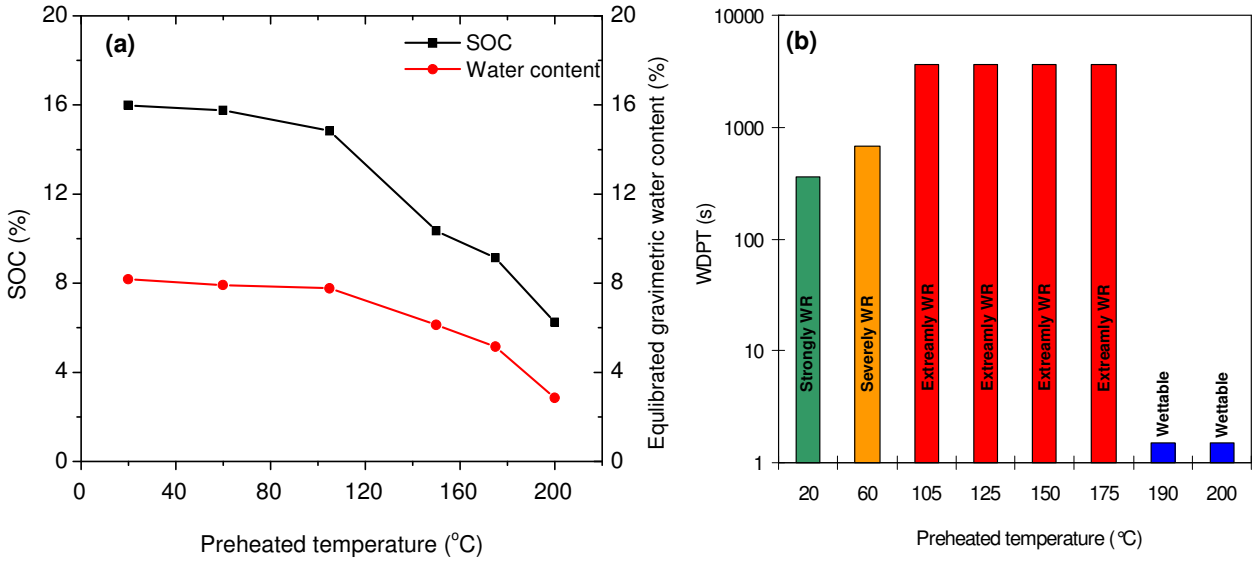

Figure 2. The impact of heating temperature on (a) the SOC content and equilibrated soil-water content, and (b) the WDPT and WR classes (Bisdom *et al.* 1993) of the 0.0-0.05m depth layer of Fukushima volcanic ash soil.

Simultaneous measurement of θ and ψ during wetting-drying cycles

A typical result of a simultaneous measurement of θ and ψ during the wetting process of extremely WR soil (preheated at 105°C) is shown in Fig. 03. It is noted that the extremely and severely WR soils were difficult to be wetted, therefore, the wetting process was started with positive water pressure (e.g. 5 cm of water head as indicated in Fig. 3). Thereafter, wetting process was controlled by switching between water supply and cut-off conditions to obtain the equilibrium state of θ and ψ. Once the equilibrium was reached, wetting process was resumed. The controlled wetting process was continued until the soil becomes fully saturated showing stable water content approximately equal to saturated water content. The water content (θ) and applied water pressure were frequently measured (1 to 3 min. intervals) and recorded at each step of change.

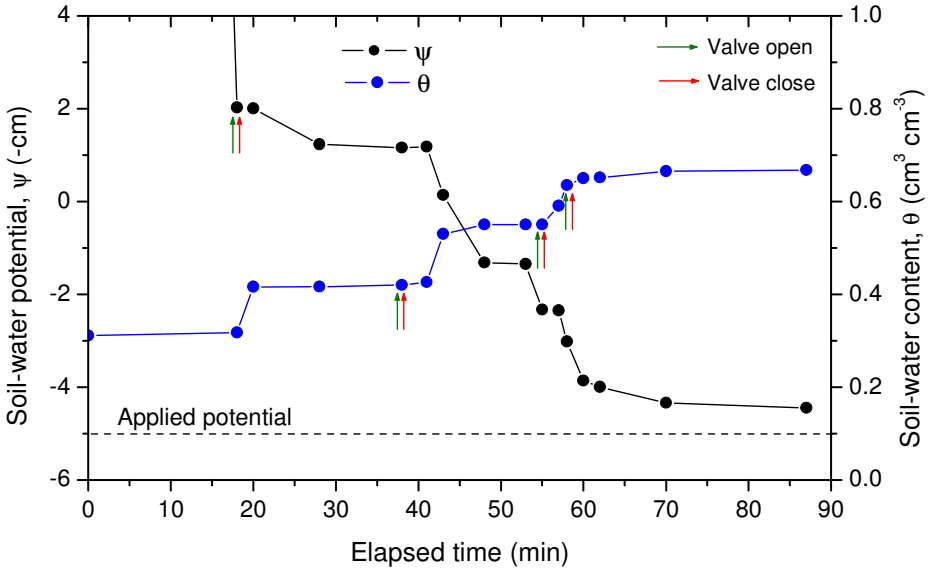

Figure 3. Change in soil-water content and soil-water potential during controlled wetting process of the extremely water repellent soil.

Soil-water retention characteristics of water repellent soil

The soil-water content at each step of equilibrium is plotted against the corresponding soil-water potential to obtain the soil-water retention curve. The Fig. 04 shows the soil water characteristic curves obtained from the relationship described in Fig. 03, together with drying curve.

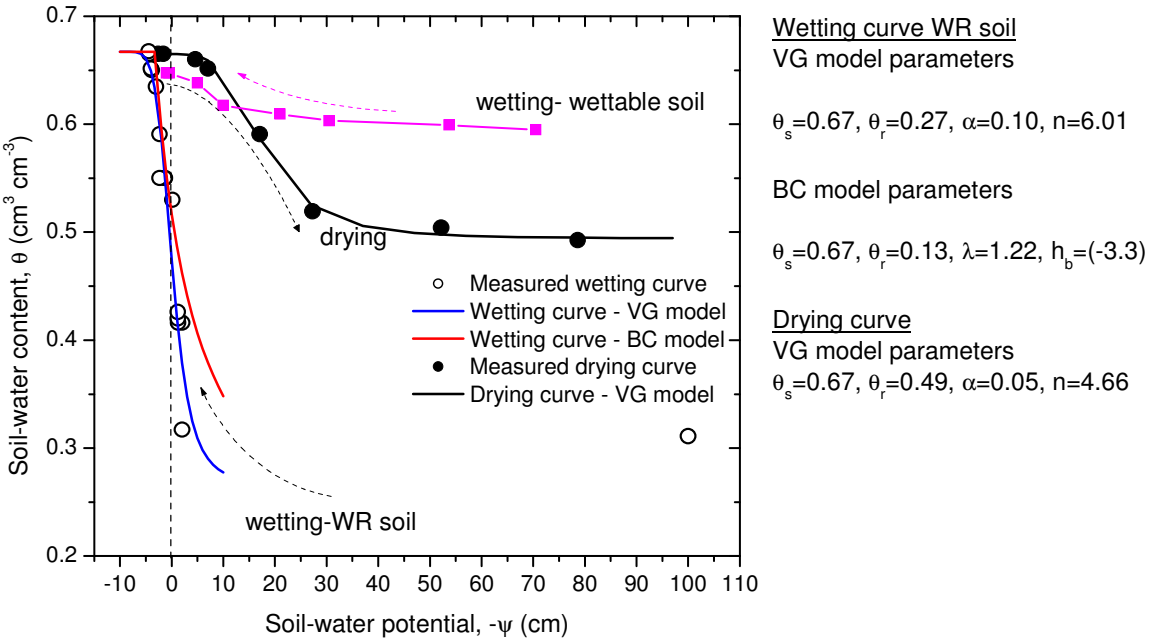

Figure 4. The wetting curve and the main drying curve of the extremely water repellent soil.

Conclusion

The water repellency persistence of a volcanic ash soil was measured after preheating at different temperatures between 20°C and 200°C. The preheated soil showed elevated water repellency when drying between 60 and 175°C; however the soil became completely wettable heating beyond 175°C. The soil-water characteristics of preheated soils were assessed by a newly developed mini tensiometer-TDR coil probe which allowed simultaneous measurement of both the soil-water content and soil-water potential for same soil volume. The water-entry into water repellent soil occurred under positive soil-water potential, and the mini tensiometer-TDR coil probe were capable of measuring change of θ and ψ even during the rapid infiltration at positive water potentials.

References

Bisdom EBA, Dekker LW, Schoute JFT (1993) Water repellency of sieve fractions from sandy soils and relationships with organic material and soil structure. *Geoderma* **56**, 105-118.

Bond RD (1972) Germination and yield of barley when grown in water-repellent sand. *Agron. J.* **64**, 402-403.

DeBano LF (1971) The effect of hydrophobic substances on water movement in soil during infiltration. *Proc. Soil Sci. Soc. Am.* **35**, 40-343.

Doerr SH, Shakesby RA, Dekker LW, Ritsema CJ (2006) Occurrence, prediction and hydrological effects of water repellency amongst major soil and land-use types in a humid temperate climate. *Eur. J. Soil Sci.*, **57**, 741-754.

Doerr SH, Shakesby RA, Walsh RPD (1998) Spatial variability of soil hydrophobicity in fire-prone eucalyptus and pine forests, Portugal. *Soil Science* **163**, 313-324.

Doerr SH, Thomas AD (2000) The role of soil moisture in controlling water repellency: new evidence from forest soils in Portugal. *J. Hydrol.* **231-232,** 134-147.

Hubbert KR, Preisler HK, Wohlgemuth PM, Graham RC, Narog MG (2006) Prescribed burning effects on soil physical properties and soil water repellency in a steep chaparral watershed, southern California, USA. *Geoderma* **130**, 284-298.

Kawamoto K, Moldrup P, Komatsu T, de Jonge LW, Oda M (2007) Water repellency of aggregate-size fractions of a volcanic ash soil. *Soil Sci. Soc. Am. J.* **71,** 1658-1666.

Vaz CMP, Hopmans JW, Macedo A, Bassoi LH, Wildenschild D (2002) Soil Water Retention Measurements Using a Combined Tensiometer-Coiled Time Domain Reflectometry Probe. Soil Sci. Soc. Am. J. 66, 1752-1759.

Wallis MG, Horne DJ (1992) Soil water repellency. *Adv. Soil Sci.* **20**, 91-146.

Estimating unsaturated hydraulic conductivity from air permeability

M. R. Neyshabouri [A], S. A. R Rafiee Alavi[B], H. Rezaei[C] and A.H. Nazemi[D]

[A]Faculty of Agriculture, University of Tabriz, Soil Science Department, Tabriz, Iran, Email neyshmr@hotmail.com
[B]Faculty of Agriculture, University of Tabriz, Soil Science Department, Tabriz, Iran, Email sarrasc@gmail.com
[C]Faculty of Agriculture, University of Urmia, Irrigation and Drainage Department, Urmia, Iran, Email h.rezaei@urmial.ac.ir
[D]Faculty of Agriculture, University of Tabriz, Department of Water Engineering, Tabriz, Iran, Email ahnazemi@yahoo.com

Abstract
Reliable functions relating unsaturated hydraulic conductivity (K(θ)) to air permeability (K_α) may greatly facilitate K(θ) prediction. In the current research K(θ) and K_α were measured by pressure plate outflow and variable head methods, respectively, in the range of 0 to -10 mH_2O matric potential (ψ_m). A non-linear regression model as log K(θ) = a+b logK_a with the correlation coefficient(*R*) ranging from 0.856 to 0.942(significant at P<0.01) were established for the 22 soils grouped into five textural classes. The slope (*b*) and intercept (*a*) varied within narrow ranges of -2.504 to -3.65 and -23.4 to -28.73, respectively. For the comparison purpose K(θ) were also predicted from *RETC* using experimental *SMC* data and van Genuchten and Brooks-Corey models. The reliability of the K(θ) prediction from K_α based on root mean square deviation (*RMSD*), geometric mean error ratio (GMER), and geometric standard deviation of error ratio (GSDER) criteria became considerable smaller than those predicted from the two models implying that rapid and simple prediction of K(θ) from K_a is quite promising.

Key Words
Air permeability, Brooks-Corey, hydraulic conductivity, van Genuchten model

Introduction
When water or air passes through a soil at particular water content, water takes liquid filled pores and air takes gas filled pores. Evidently the increase in soil water content raises water permeability expressed as K(θ) and lowers air permeability (K_α) and thus it is speculated that a close relation or function between the two must exist. Direct measurement of K_α is easier and much rapid than K(θ) and in contrast to water, establishing air flow through a soil seldom may change or alter the pore geometry, which often occurs during K_s or K(θ) measurements. There are several studies that have attempted to relate K_s to K_α. Schjoning (1986) presented an exponential relation predicting K_s from K(θ) at -1 mH_2O in 405 examined soil cores. Blackwell *et al.* (1990) concluded that the volume and depth of samples did not alter the nature of the equation derived between K_s and K_α . Poulsen *et al*. (1999) developed a K_s model based on total and air filled porosity at -1 mH_2O matric potential. Loll and Schjoning (1999) carried out similar study with emphasis on the application of predicted K_s in infiltration modeling. In spite of the cited studies carried out for estimating K_s from K_α, predicting K(θ) from K_α as far as the authors know has not yet been investigated. The aim of this research was to study about the possibility of fast and reliable prediction of K(θ) from K_α.

Methods
Twenty-two soil series with nine various textural classes were selected from Karaj, Varamin and Urmia plains in Iran. Bulk and particle densities, soil texture and saturated hydraulic conductivity were measured by routine laboratory methods and using both disturbed and core samples taken from 0-10 cm depth. Volumetric water content of each core sample at 0.25, 0.35, 0.70 mH_2O moisture suctions were determined by water hanging column and at 1, 2, 3, 5 and 10 mH_2O by pressure plate apparatus.
Air permeability (K_α) was determined by the falling head method (Taylor and Ashcroft 1972) in each soil core after its equilibration at various matric potentials (Ψ_m)using hanging columns or pressure plate apparatus. The Eq. [1] was used for the K_a computation.

$$K_\alpha = -2.303 \frac{V\eta\delta_s(\log P_2 - \log P)_1}{AP_\alpha \Delta t} \quad (1)$$

where V is the chamber volume, η is viscosity, δ_s is soil core length, P_1 and P_2 are the initial and final air pressures in the chamber, A is the area(m^2), P_a is the atmospheric air pressure (kPa), and Δt is the time that air flows through the soil core. With the appropriate dimensions (Taylor and Ashcroft 1972) applied to the variables in Eq. [1], K_a of each core at various Ψ_m (or water contents) were computed in Darcy. 1 Darcy represents the number of m^3 of air with 1 Nsm^{-3} viscosity passing in one second through a unit cross section area

of the soil core under the pressure gradient of $1Nm^{-2}$ per meter. Unsaturated hydraulic conductivity K(θ) of the soil cores were computed from Eq.[2] by using the experimental data from the pressure plate outflow method (Ghildyal and Tripathi 2001) at 5 or 7 various suctions.

$$K(\theta) = 4\beta Q_0 \rho_w g L^2 / \pi^2 V \Delta P \quad (2)$$

where β is the slope of the regression line plotted as $\log[Q_0-Q_t)$ against time (t), Q_0 is total outflow volume(m^3) at the pressure increment (ΔP), Q is the volume(m^3) of water released at various times(t) over the ΔP, ρ_w is the density of water (Mg m^{-3}), *g* is the acceleration due to gravity (m s^{-2}) and *L* is the length of the core in the flow direction (m). With applying appropriate dimension to the variables (Q_0, V, ΔP and β) and to the constants (ρ_w, g and L) as described by Ghildyal and Tripathi (2001), K(θ) was computed in/ms for the average Ψ_m at each successive pairs of pressures P_1 and P_2. Measured K(θ) were regressed against K_α for each individual soil core, for the soils within each texture class and for the whole 22 examined soils, and the regression equations were developed. The values of K(θ) at various Ψ_m (or water contents) were also estimated from van Genuchten-Mualem and Brooks-Corey-Mualem models (van Genuchten 1980) using experimental SMC data and RETC software (van Genuchten *et al.* 1991). The following statistical criteria (Wagner *et al.* 2001) were employed for the comparison of the K(θ) predicted from air permeability and from the two mentioned models.

$$RMSD = [\frac{1}{n}\sum_{i=1}^{N}(X_{m,i} - X_{p,i})^2]^{1/2} \quad (3)$$

$$\varepsilon_i = \frac{X_{p,i}}{X_{m,i}} \quad (4)$$

$$GMER = \exp[\frac{1}{n}\sum_{i=1}^{n}\ln(\varepsilon_i)] \quad (5)$$

$$GSDER = \exp\left[\frac{1}{n-1}\sum_{i=1}^{n}[\ln(\varepsilon_i) - \ln(GMER)]^2\right]^{1/2} \quad (6)$$

$X_{m,i}$ and $X_{p,i}$ refer to the measured and predicted K(θ) at specified suctions or water contents, respectively, and ε_i denotes their ratio.

Table 1. The regression coefficients (*a* and *b*), and correlation coefficient R between log K(θ) and log K_α for 22 examined soils.

Soil No.	Soil texture class	Db(kg/m^3)	A	B	R	n
1	Sandy loam^{+}	1460	-30.48	-3.909	0.982**	15
2	Silty loam^{+}	1390	-21.04	-2.121	0.914**	21
3	Loam^{+}	1360	-25.67	-2.953	0.961**	21
4	Loam^{+}	1390	-24.00	-2.632	0.951**	21
5	Silty Clay Loam^{++}	1270	-20.72	-2.102	0.920**	21
6	Silty clay^{++}	1230	-38.96	-5.503	0.967**	21
7	Loam^{+}	1470	-32.72	-4.280	0.921**	21
8	Sand^{+}	1490	-29.92	-4.148	0.880**	21
9	Clay loam^{++}	1550	-25.75	-3.221	0.977**	21
10	Sandy loam^{+}	1520	-28.85	-3.731	0.889**	21
11	Sandy clay loam^{++}	1620	-26.43	-3.072	0.997**	15
12	Sandy clay loam^{++}	1630	-22.86	-2.388	0.985**	15
13	Silty clay^{++}	1510	-22.13	-2.283	0.963**	15
14	Silty clay^{++}	1550	-21.86	-2.252	0.970**	15
15	Sandy clay loam^{++}	1390	-26.80	-3.305	0.961**	15
16	Loam^{+}	1280	-23.34	-2.442	0.924**	15
17	Silty loam^{+}	1440	-25.08	-2.787	0.988**	15
18	Loam^{+}	1540	-19.65	-1.661	0.989**	15
19	Loam^{+}	1480	-28.23	-3.515	0.976**	15
20	Silty loam^{+}	1500	-20.97	-1.961	0.964**	15
21	Silty clay^{++}	1460	-25.07	-2.999	0.972**	15
22	Loam^{+}	1460	-33.63	-5.188	0.732**	11
Mean	-	1454	-26.09	-3.111	0.944	-
C.V	-	7.22	18.57	32.82	-	-

$^{+}$Constant and $^{++}$Falling pressure methods for measuring K_s

Results

The regression and correlation coefficients (*a, b* and *R*) relating log K(θ) to log K_α for individual soils is depicted by (Table 1). Negative slopes (*b*) demonstrate that with increasing K_α (decrease in water filled pores) K(θ) diminishes. The logarithmic nature of the regression implies that the rate of decrease in K(θ) is much more rapid than the rate of increase in K_α. This is expected because of exponential or power dependence of K(θ) to θ (Hillel 1998). Except for the soils 8, 10 and 22, for the other soils (Table 1) *R* values exceeded 0.92 being significant at 1% probability level which implies that on the average basis about 88% (R^2=0.88) of the variation in K(θ) in the 0.25 to 10 mH_2O moisture suction range is attributed to the variation in K_α. Large shrinkage in the core samples of soil number 22 particularly at low Ψ_m led to erratic K_α measurements and decreased its *R* to 0.733 even though it is still statistically significant (P< 0.01).

The plot of K(θ) against K_a (log K(θ) = a+b log K_α) for the five groups of soils falling in the same textural classes is depicted by Figure 1.

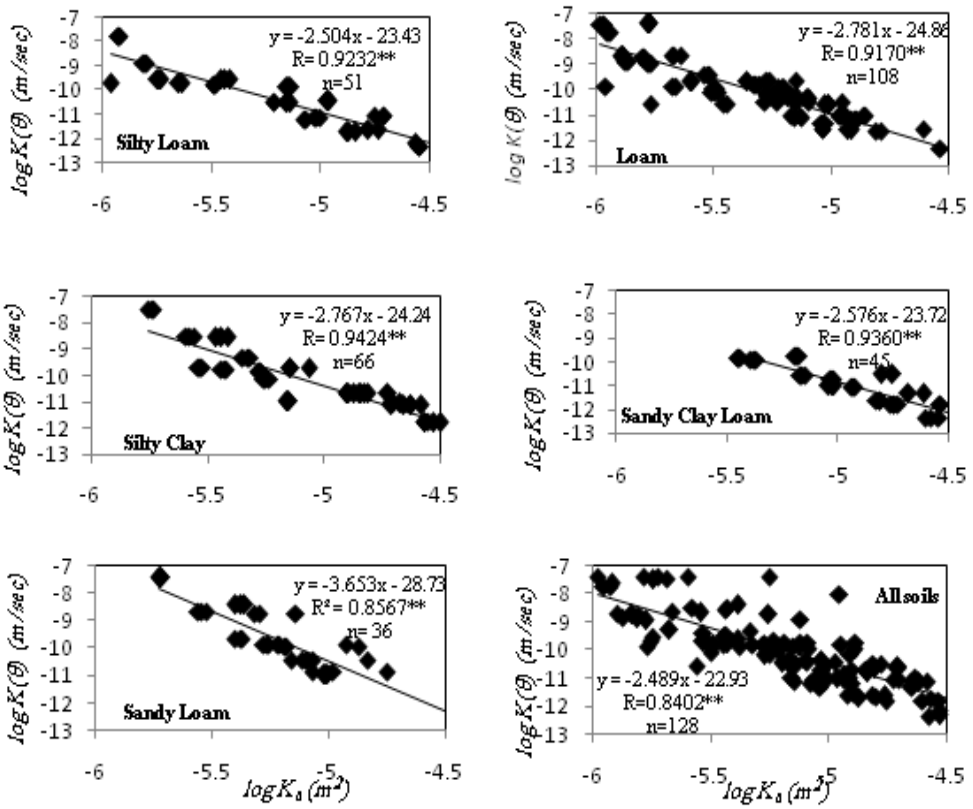

Figure 1. Regression equation and coefficient of correlation (*R*) between water K(θ) and air (K_α) permeability for the five textural class (ordinate axis is in log scale).

There is no particular trend in the variation of *R* or *a* and *b* of the regression equations with soil textural class. Grouping the examined soils according to their texture, however, improved correlation coefficient (*R*); it ranged from 0.856 to 0.942. The ranges of *a* and *b* values also became narrower. Their variations did not exceed 7.5% and 4%, respectively, implying that the developed regression equations for the texture classes in Figure1 may be reliably applied to other soil falling into the appropriate texture class.

Table 2. Comparison of the prediction reliability of K(θ) from measured K_α and from van Genucthen and Brooks-Corey models (van Genuchten 1980).

Prediction method	Average of RMSD	$1-\frac{1}{n}\sum_{i=1}^{n} CMERi$	Average of GSDER
van Genuchten-Mualem	1.053	-0.022	1.207
Brooks-Corey-Mualem	0.996	0.200	1.259
Regression method (from K_a)	0.651	0.012	1.060

The averages of three reliability criteria computed for the predicted K(θ) from K_α using the regression equations in Figure 1 and from van Genuchten and Brooks-Corey models (van Genuchten 1980) is summarized in Table 2.

Average *RMSD* of 0.651 is much lower for the regression method implying that K(θ) has been predicted with greater reliability than the two methods. The second comparison criterion for the K(θ) prediction is *GMER*. When the value of the expression "$1-\frac{1}{n}\sum_{i=1}^{22} GMER_i$" is equal to zero it corresponds to an exact match between the measured and predicted K(θ). When greater than zero it implies over-prediction and when less than zero under prediction of K(θ) relative to the measured values. Table 2 again reveals that K(θ),s predicted from K_α are more reliable than those predicted by van Genuchten and Brooks-Corey models that currently are employed in many studies. Negative value for "$1-\frac{1}{n}\sum_{i=1}^{22} GMER_i$" implies that van Genuchten model for 22 soils produced slightly under prediction where as Brooks-Corey slightly over prediction of K(θ). Average of *GSDER*, for 22 soils again is smallest for the K(θ) predicted from K_α.

Conclusion

For the 22 examined soils results revealed an existence of strong and significant (P<0.01) correlation between K_α and K(θ) in the range of 0 to -10 mH_2O matric potential. If the relationship for the large number of soils could be generalized, it appears a very effective way for K(θ) prediction. Reliability of the estimates turned to be better than the well known models such as van Genuchten or Brooks-Corey. Possibility of determining the regression equation coefficients relating K(θ) to K_α from the easily measured soil attributes needs further investigation.

Acknowledgment

The authors wish to thanks Tabriz University for its support during the course of M.Sc thesis work by Sayed Alireza Rafiee Alavi

References

Blackwell PS, Ringrose -Voase AJ, Jayawardan NS, Olsson KA, Mc Kenzie DC, Mason WK (1990) The use of air- filled porosity and saturated hydraulic conductivity of clay soils. *Journal of Soil Sci*. **41**, 215- 228.

Ghildyal BP,Tripathi RP (2001) 'Soil physics'. New Age International (P) Limited, Publishers. New Dehli. pp. 311-344.

Hillel D (1998) 'Environmental Soil Physics'. (Academic Press, Inc.: London).

Loll P, Schjonning PRH (1999) Predicting saturated hydraulic conductivity from air permeability: Application in stochastic water infiltration modelling. *Water Resources Research* **35**, 2387- 2400.

Poulsen TG, Molderap P, Yamaguch T, Jacobsen Ole H (1999) Predicting saturated and unsaturated hydraulic conductivity in undisturbed soils from soil water characteristics. *Soil Science* **164**, 877-887.

Schjonning P (1986) Soil permeability by air and water as influenced by soil type and incorporation of straw (in Danish with English summary). *Tidsskrift for Plaintival* **90**, 227-240.

Taylor SA, Ashcroft GL (1972) 'Physical Edaphology'. (WH Freeman and Company: San Fransisco).

van Genuchten MT (1980) A closed- form equation for predicting the hydraulic conductivity of unsaturated soils. *Soil Science Society of American Journal* **44**, 892-898.

van Genuchten MT, Leij FJ, Yates SR, Williams JR (1991) 'The RETC code for quantifying the hydraulic functions of unsaturated soils'. (Office of Research and Development: Washington, DC).

Wagner B, Tarnawski VR, Hennings V, Muller U, Wessolek G, Plagge R (2001) Evaluation of pedotransfer function for unsaturated soil conductivity using an independent data set. *Geoderma* **102**, 275-297.

Estimation of crop losses associated with soil water repellency in horticultural crops

M.F. McMillan[A], D.J. Bell[B], S.J. Kostka[A] and N.J. Gadd[C]

[A]Aquatrols Corporation of America, Paulsboro, NJ 08066, USA
[B]David J Bell & Associates Pty Ltd, Arcadia 3631 Victoria, Australia
[C]Aquatrols Corporation of America, Gray, GA 31032, USA

Abstract
Soil water repellency (SWR) reduces soil affinity to water and affects an array of hydrological and geomorphological processes including infiltration, overland flow, accelerated soil erosion, uneven wetting, the development of preferential flow, and accelerated leaching of agrichemicals (Doerr *et al.* 2000) – all influencing irrigation efficiency, water conservation, and agricultural productivity (Blackwell 2000; Cooley *et al.* 2007; Robinson 1999).

Globally, the sustainability of crop and biomass production is being impacted by water scarcity and deteriorating water quality, however few studies exist that have assessed the potential influence of SWR on crop productivity. Previous studies have estimated losses in potatoes, lupin, and barley (Blackwell 2000; Cooley *et al.* 2007; Robinson 1999). The objective of this study was to utilize surfactant treatments to modify soil hydrological properties under precision irrigation as a means of estimating potential crop losses to SWR in three high value horticultural crops - grapes (*Vitis vinifera* L.), apples (*Malus domestica* Borkh.) and oranges (*Citrus sinensis*). Results indicate that the use of a novel surfactant maximizes water use efficiency and significantly increases yields.

Key Words
Yield loss, irrigation efficiency, hydrophobicity

Methods
Three trials were conducted on each apples and grapes and one on oranges in Victoria, Australia on clay loam, loam soils, or sandy loam soils, respectively. Apple varieties included 'Pink Lady' and 'Gala' Grape trials included table grapes ('Black Muscat') or wine grapes ('Shiraz'). Orange variety studied was the 'Navel'. The test design was a randomized complete block with each treatment replicated 4-6 times. Plot size varied by crop. SWR was mitigated by applying surfactant [a blend of alkylpolyglycoside (APG) and ethylene oxide/propylene oxide (EO/PO) block copolymer surfactants (Kostka and Bially 2005)] at initial rates of 0 or 5 L/ha in the spring, then at 0 or 2.5 L/ha respectively monthly for up to five months. Plots were irrigated either by drip irrigation, micro-jet sprinklers or mini sprinklers and received the same irrigation volumes and management practices. Soil volumetric water content (VWC) was monitored at a depth of 10 cm using a Theta probe (Delta-T Devices, Cambridge, UK). At harvest, fruit weights were measured and used for crop yield estimations.

Results and Discussion
In each test location, VWC was significantly lower ($p = 0.05$) in control soils than in the surfactant treatments on each measurement date regardless of soil type or irrigation method (Figure 1). Surfactant treatment resulted in higher VWC in the upper region of the soil profile. Soil VWC was not systematically monitored deeper in the rootzone at each location however where measured, a deeper wetting front and higher VWC at 20-25 cm were encountered (data not presented).

1 – 6 August 2010, Brisbane, Australia. Published on DVD.

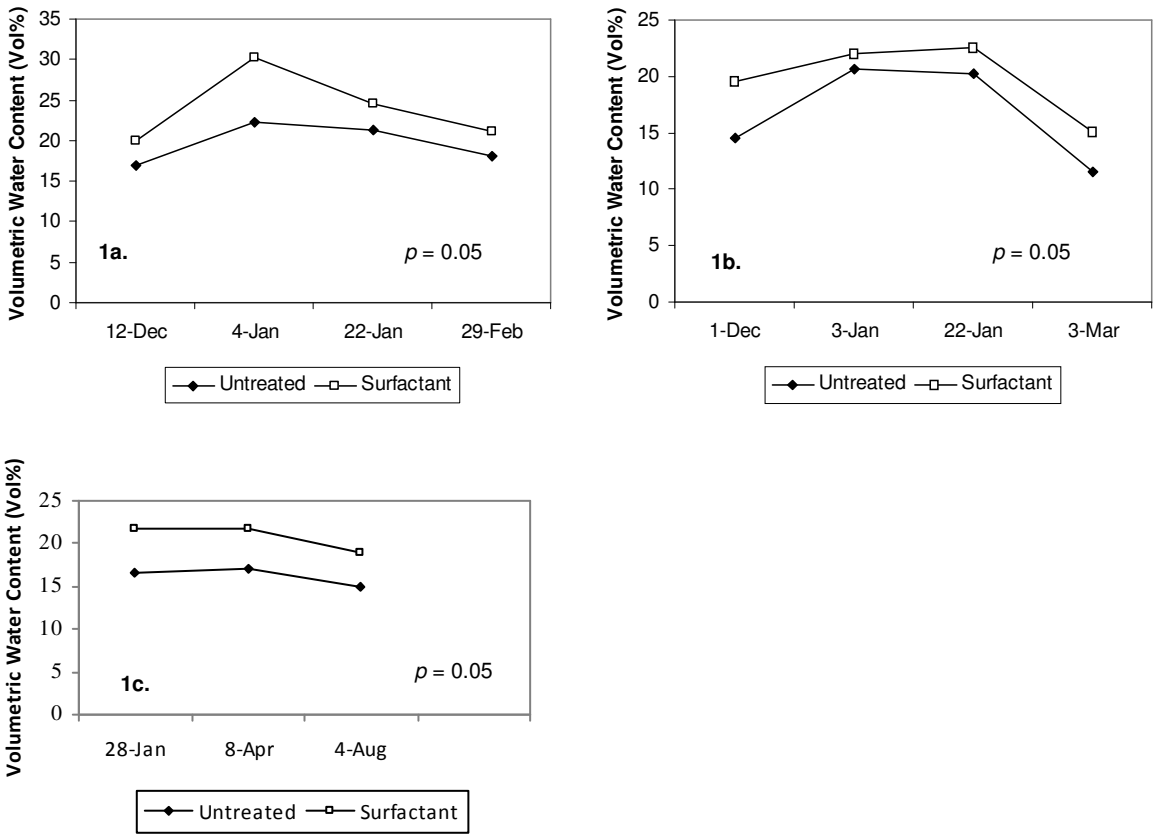

Figure 1. Soil volumetric water content in selected untreated and surfactant-treated soils under precision irrigation: a) loam soil in a vineyard and b) clay loam soil in an apple orchard and c) sandy loam soil in a citrus grove.

Yields in each of the untreated controls were significantly lower ($p = 0.05$) than in the surfactant treatment (Table 1, Table 2 and Table 3). Total yield differences of 2.4–2.6 Mg/ha (14-45% increase) were observed between the two treatments in grapes (Table 1). In apples, yield differences between treatments ranged between 3.9-6.1 Mg/ha (19-49% increase). While in oranges the yield difference was 7 Mg/ha (24% increase). Total yield differences across all trials and crops is 4.3 Mg/ha (27% increase) were observed between the control and surfactant treatments. Due to thinning, there were no differences in fruit or bunch number in apples or grapes, respectively, however, fruit size and bunch weights were significantly lower in the untreated controls (data not presented).

Table 1. Yield effects in untreated control and surfactant treatments in precision irrigated grapes (*Vitis vinifera* L.) on different soil types in Victoria, AU.

			Yield (Mg/ha)	
Location	Soil Type	Variety	Control	Surfactant
G-1	Clay Loam	Shiraz	5.6 b[a]	8.1 a
G-2	Loam	Shiraz	16.6 b	19.0 a
G-3	Loam	Muscat	15.9 b	18.5 a

[a]Numbers in rows followed by the same letter are not significantly different. LSD (0.05).

Table 2. Yield effects in untreated control and surfactant treatments in precision irrigated apples (*Malus domestica* Borkh.)on different soil types in Victoria, AU.

			Yield (Mg/ha)	
Location	Soil Type	Variety	Control	Surfactant
A-1	Clay Loam	Pink Lady	29.3 b[a]	34.9 a
A-2	Clay Loam	Gala	7.9 b	11.8 a
A-3	Clay Loam	Pink Lady	30.2 b	36.3 a

[a]Numbers in rows followed by the same letter are not significantly different. LSD (0.05).

Table 3. Yield effects in untreated control and surfactant treatments in irrigated citrus (*Citrus sinensis*) on different soil types in Victoria, AU.

			Yield (Mg/ha)	
Location	Soil Type	Variety	Control	Surfactant
1	Clay Loam	Navel Oranges	28.8 b[a]	35.8 a

[a]Numbers in rows followed by the same letter are not significantly different. LSD (0.05).

Conclusion

The results from these studies provide evidence that SWR deleteriously impacts soil hydrological status resulting in reduced productivity, yield, and quality in high value horticultural crops. Irrigation practices and rates were identical in both the control and surfactant treatments. While irrigation volumes were identical, water use efficiency was higher in the surfactant treatments and resulted in significant yield increases. At a cost of $100 AUS per hectare and an application rate of 10-12L/ha over the season, the net return was on average $4500 AUS, $3500 AUS and $5000 AUS for apples, grapes and oranges, respectively.

In light of the severity of drought conditions experienced by growers in the Murray-Darling River Basin and projections that due to climate change such precipitation deficit conditions are becoming the norm, simple innovative management strategies such as the incorporation of surface active agents in irrigation programs can have profound effects on soil hydrological status, crop yield, and water use efficiency.

Additional research is underway to determine if the surfactant treatment solely influenced hydrological status or if other plant stress defense mechanisms were impacted. Assessment of fruit quality and chemistry is the subject of ongoing research, particularly in wine grapes.

References

Blackwell PS (1997) Development of furrow sowing for improved cropping of water repellent sands in Western Australia. Proc. 14th ISTRO Conf, July 27th – 1st August Pulawy, Poland, pp 83-86.

Cooley ET, Lowery B, Kelling KA, Wilner S (2007) Water dynamics in drip and overhead irrigated potato hills and development of dry zones. *Hydol. Process.* **21**, 2390-2399.

Doerr SH, Shakesby RA, Walsh RPD (2000) Soil water repellency, its causes, characteristics, and hydro-geomorphological significance. *Earth Sci. Rev.* **51**, 33-65.

Kostka SJ, Bially PT (2005) The hydrophilicity of water repellent soil. U.S. Patent No. 6,851,219.

Robinson D (1999) A comparison of soil-water distribution under ridge and bed cultivated potatoes. *Agric. Water Manage.* **42**, 189-204.

Evaluating the scale dependency of measured hydraulic conductivity using double-ring infiltrometers and numerical simulation

Li Ren and Jianbin Lai

Department of Soil and Water Sciences, China Agricultural University, and Key Laboratory of Plant-Soil Interactions, MOE, Beijing, China, Email renl@mx.cei.gov.cn

Abstract
Saturated hydraulic conductivity measurements are important for understanding and modeling hydrological processes at the field scale. Few systematic studies have been conducted on how the size of double-ring infiltrometers affects the measured hydraulic conductivity. To determine this size effect, we measured saturated hydraulic conductivity at seven sites using four different sizes of double-ring infiltrometers. Inner ring diameters d_i were 20, 40, 80, and 120 cm. Detailed numerical investigations were also conducted to explain how the inner-ring size of a double-ring infiltrometer influences the measured hydraulic conductivity in a heterogeneous soil. Field and simulation results both demonstrated that the variability of measured hydraulic conductivity was greater for smaller inner rings (e.g. $d_i < 40$ cm), and it gradually decreases as the ring size increases. Our study indicates that where soil spatial variability is high, infiltrometers having a large inner ring (in general $d_i > 80$ cm) are essential for reliable measurement.

Key Words
Soil, saturated hydraulic conductivity, measured scale, double-ring infiltrometer, field experiments, numerical simulation

Introduction
Studies investigating the size dependency of ring infiltrometer measurements have mainly focused on lateral flow, and little attention has been devoted to size dependency caused by soil heterogeneity. Hydraulic conductivity measured in a heterogeneous soil is strongly linked to the representativeness of the measured volume. This representativeness involves both the representative elementary volume (REV), and the correlation scale of the hydraulic conductivity (Ciollaro and Romano, 1995). The objectives of this study were (i) to evaluate the effect of measurement size on the soil hydraulic conductivity, and (ii) to find the smallest diameter double-ring infiltrometer needed to cover a representative area for reliable soil hydraulic conductivity measurements in the semi-arid region of China.

Methods
Philip (1957) showed that cumulative infiltration I under water-ponded conditions is approximated at time t by:

$$I = S\,t^{0.5} + \mathrm{A}\,t \qquad (1)$$

where I is cumulative infiltration (L), S is sorptivity(L/T$^{0.5}$), and A is a constant (L/T). As time progresses, the first term becomes negligible and the importance of A, which represents the main part of the gravitational influence, increases (Koorevaar, *et al*., 1983). The A term can be taken as the saturated hydraulic conductivity of the wetted zone (K_w) after a long period of infiltration (Bouwer, 1986). This equation was applied to the data collected in the present study. By fitting Eq. (1) to the cumulative infiltration data, we obtained the saturated hydraulic conductivity K_w of the wetted zone for each infiltration test.

Field experiments
The field experiment was conducted in a long-term tillage plot within the Minqin oasis in the lower reaches of the Shiyang River (38°54′N, 103°03′E) in Gansu province, northwest China. Seven sites within the 100 × 100 m experimental plot were randomly selected, and the experimental sites are about 30 ~ 40 m away from each other. At each site, one measurement was taken with each of the four double-ring infiltrometers (see Figures 1-3), each in close proximity to the others.

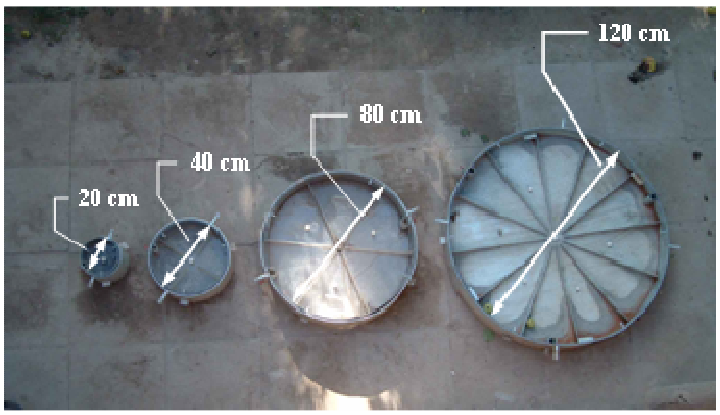

Figure 1. Photograph of the four sets of double-ring infiltrometers of different diameters (only inner-rings with nested-rings are shown here, the diameters of corresponding outer-rings, from left to right, are 70, 70, 100, and 140 cm, respectively).

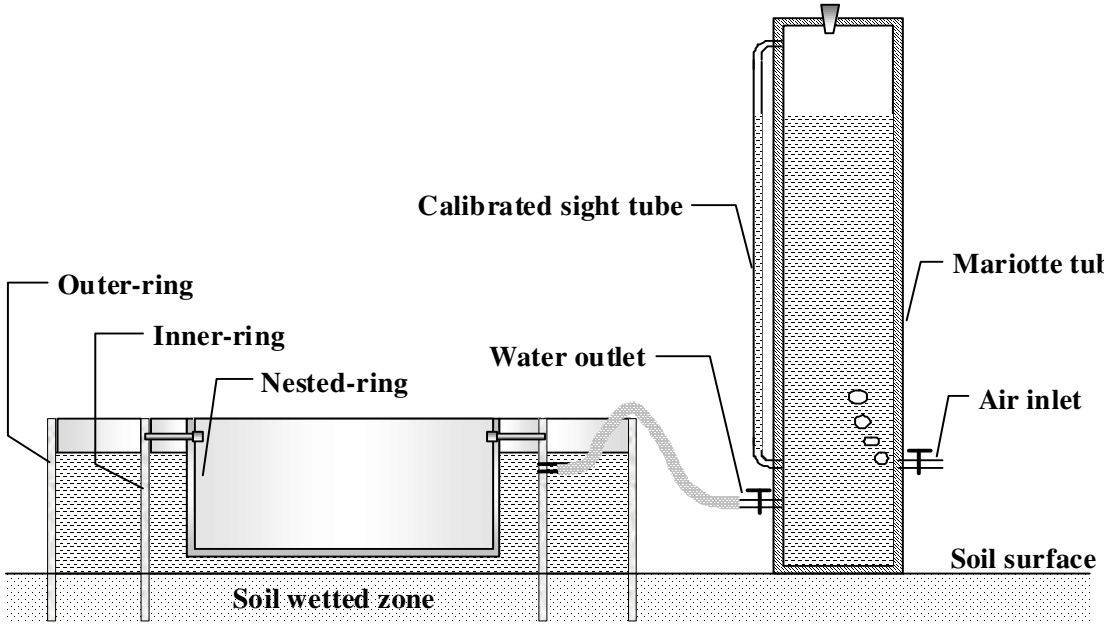

Figure 2. Cross-section sketch of the double-ring infiltrometer. (The nested ring, a cylinder with a base that was nested and fixed in the inner-ring by four pins, was held several centimeters above the soil surface, so it did not affect the infiltration process. The nested-ring had two functions: (i) it mainly reduces the upper free water area in the inner-ring, resulting in improved measurement accuracy; and (ii) it minimizes surface evaporative losses, especially for a long-term infiltration.)

Figure 3. Photograph of field experiment setup, double-ring infiltrometer (d_i = 40 cm, d_o = 70 cm).

Numerical Experiments

A series of numerical experiments was conducted to investigate how the inner-ring size of a double-ring infiltrometer influences the accuracy of the measured saturated hydraulic conductivity in heterogeneous soil. The two-dimensional model HYDRUS-2D (Šimůnek *et al*., 1999) was used to simulate infiltration under a double-ring infiltrometer.

Conclusions

It is generally known that soil saturated hydraulic conductivity (K_s), which is one of the parameters to describe the ability of water movement in soil, is similar for the same soil texture. When infiltrometers (Double-ring infiltrometer, Guelph infiltrometer, *et al*.) are used to determine saturated hydraulic conductivity, it is commonly assumed that the soil is homogeneous within the measured area. However, hydraulic conductivity can vary significantly within a short distance due to soil spatial variability and heterogeneity. This suggests that double-ring infiltrometers, widely used for determining the saturated hydraulic conductivity, may give scale-dependent results.

We have measured soil saturated hydraulic conductivity at seven sites using four different sizes of double-ring infiltrometers to identify the size dependency. In the study, the inner ring diameters, d_i, were 20, 40, 80, and 120 cm, and the soil textures at seven sites were similar. The results showed that the mean hydraulic conductivity does not change significantly over the full range of inner ring diameters, but the range and standard deviation of the measurements decrease appreciably with increasing d_i. As the ring size increases, the representativeness of the area covered by the infiltrometer also increases, so the measured hydraulic conductivity becomes more representative and stable.

How does the inner-ring size of a double-ring infiltrometer influence the measured hydraulic conductivity in various heterogeneous soil? It is necessary to investigate this size effect in more soil conditions. HYDRUS-2D was well performing in simulating the soil water infiltration process, detailed numerical investigations have been conducted for this purpose. In the study, six correlation lengths (L = 0 cm, 10 cm, 20 cm, 50 cm, 100 cm, and 200 cm) and six standard deviation values (SD = 0, 0.1, 0.25, 0.5, 0.75, and 1.0) of random field of $\log(K_s)$ were used for the various realizations of hydraulic conductivity fields. Ten realizations have been performed for each combination of (L, SD) treatment and infiltrometer diameter (10-, 20-, 40-, 80-, 120-, and 200-cm). Because only a single realization is needed when SD = 0, this gave a total of 1806 realizations, and it seems to conduct 10 replicates of field experiments for each infiltrometer at 31 different locations.

The study showed that the variability of measured hydraulic conductivity is greater for smaller inner rings (e.g. $d_i < 40$ cm), and it gradually decreases as the ring size increases. Where soil spatial variability is high, infiltrometers having a large inner ring (in general $d_i > 80$ cm) are essential for reliable measurement, large-diameter infiltrometers produce more stable values than small diameter ones, so they represent an efficient method for improving measurement representativeness.

Acknowledgments
This research was funded by Grant No.50339030 key research project and Grant No. 50479012 research project from National Natural Science Foundation of China. It was also sponsored by the Program for Changjiang Scholars and Innovative Research Team in University (IRT0412), Ministry of Education, China. We are very grateful to Dr. Toby Ewing for providing us insightful suggestions and helping us go over the manuscript. We also would like to express our heartfelt thanks to Dr. Jirka Šimůnek who helped us upgrade the HYDRUS-2D model.

References
Bouwer H (1986) Intake rate: Cylinder infiltrometer. In 'Methods of soil analysis, Part 1. 2nd ed. Agron. Monogr. 9'. (ed A Klute) pp. 825-844. (ASA and SSSA, Madison, WI.)

Koorevaar P, Menelik G, Dirksen C (1983) Elements of soil physics. Fifth impression, (Elsevier Science. Amsterdam, Netherlands).

Philip J R (1957) The theory of infiltration: 1. The infiltration equation and its solution. *Soil Sci.* **83,** 345-357.

Šimůnek J, Šejna M, van Genuchten M Th. (1999) HYDRUS-2D software for simulating water flow and solute transport in two-dimensional variably saturated media. Version 2.0. International Ground Water Modeling Center, Colorado School of Mines, Golden, CO.

Evaluation of conservation tillage by means of physical soil quality indicators

Jan Vermang[A], Hannah Desauw, Wim M. Cornelis and Donald Gabriels

Faculty of Bioscience Engineering, Ghent University, Ghent, Belgium, Email Jan.Vermang@Ugent.be

Abstract
Water erosion is a widespread phenomenon in Belgium. In order to abate erosion problems, conservation tillage is proposed as an alternative tillage technique. In this study, a set of indicators are calculated in order to compare physical soil quality under conventional tillage and conservation tillage by deep and shallow non-inversion tillage. Two fields located in the loess belt in Flanders, Belgium and Northern-France were sampled. The field in Flanders was tilled under wet conditions, largely influencing the measured penetration resistance, infiltration rate, macroporosity and air capacity, thus resulting in a poor soil quality. The field in France was tilled under better circumstances, resulting in less compaction and a better infiltration rate. No significant differences between conventional and conservation tillage could be found for these parameters. The higher soil organic matter (SOM) at the surface of the non-inversion tillage plots rendered the aggregates a higher aggregate stability.

Key Words
Physical soil quality, soil quality indicator, conservation tillage, compaction, hydraulic properties

Introduction
Water erosion is a widespread phenomenon in Belgium. Because of its texture and its hilly topography, the loess belt in central Belgium is especially prone to erosion (Verstraeten *et al.,* 2003). This situation is aggravated by the highly mechanised agriculture of row crops (sugar beets, potatoes, maize) leaving large areas of soil vulnerable to water erosion. Conservation tillage is proposed as an alternative tillage technique to diminish erosion problems. Recent research indicates that non-inversion tillage is also a promising technique to maintain soil quality.

Methods
Study area
Different tillage techniques were compared on two fields located in the loess belt in Flanders (Belgium) and Northern-France. A texture analysis can be found in Table 1. The field in Flanders is located in the village of Heestert and has been under non-inversion tillage since 2003. Long term non-inversion tillage was applied in Radinghem in Northern-France (since 1997). Maize, which is an erosion-sensitive crop, was cultivated on both fields in a maize–wheat rotation. The fields were divided into strips, each strip being tilled by an alternative tillage technique. In Heestert, tillage techniques under investigation were: conventional tillage (mouldboard plough), two types of deep non-inversion tillage (erosion plough and subsoiler) and shallow non-inversion tillage (tine cultivator). In Radinghem, conventional tillage by mouldboard plough was compared to shallow non-inversion tillage by a tine cultivator.

Table 1. Texture analysis of the experimental fields.

Location	Clay (0-2 µm) $g\ kg^{-1}$	Silt (2-50 µm) $g\ kg^{-1}$	Sand (50-2000 µm) $g\ kg^{-1}$	SOC $g\ kg^{-1}$	$CaCO_3$ $g\ kg^{-1}$
Heestert	120	512	368	20	6
Radinghem	174	725	99	196	110

Soil sampling
Per cultivation method, 5 plots of 36 m² (6 m × 6 m), each spaced 15 metres apart, were selected. All plots were located at least 15 m from the border of the strip in order to minimize edge effects. On all plots, disturbed soil samples were taken from 0-10 cm soil layer to determine aggregate stability, soil water content and texture. From the soil layers 0-10, 10-20, 20-30, 30-40, 40-50, 50-60 cm, disturbed soil samples were taken for the determination of soil organic matter (SOM) and soil water content. From the plots of Heestert, undisturbed samples were taken for three out of five plots at depths of 5, 15, 25, 40 and 60 cm to determine the soil-water retention curve (SWRC) and bulk density. Penetration resistance was measured by means of a penetrologger (Eijkelkamp Agrisearch Equipment, Giesbeek, The Netherlands) on every plot in 10 replicates. Field saturated hydraulic conductivity K_{fs} was determined in 2 replicates on every plot by means of a pressure disc infiltrometer

1 – 6 August 2010, Brisbane, Australia. Published on DVD.

(Soil Moisture Equipment, Santa Barbara, CA). K_{fs} was calculated by a double head approach using the equation proposed by Reynolds and Elrick (1990).

Laboratory analysis

SOM was analysed according to the method of Walkley and Black (1934). Soil texture was determined using the combined sieve and pipette method (De Leenheer, 1959). The three methods of Le Bissonnais (1996) were used for the determination of aggregate stability. In a first method, a heavy rain storm is simulated by fast wetting of the aggregates. The second method consists of a slow wetting of the aggregates on a sand box at a matric potential of -0.3 kPa. The third method tests the wet mechanical cohesion of the aggregates independently of slaking by stirring the aggregates in ethanol. SWRC was determined as described by Cornelis *et al.* (2005). Several soil quality parameters were calculated from the SWRC (Reynolds *et al.* 2007). The macroporosity (MacPOR) defines the amount of macropores present in the soil and can be calculated as:

$$MacPOR = \theta_s - \theta_m \quad (1)$$

with θ_s ($m^3\ m^{-3}$) the saturated volumetric water content and θ_m ($m^3\ m^{-3}$) the matrix porosity, being the porosity of the soil matrix excluding the macropores. θ_m was calculated at pressure heads of -1 and -6 kPa, corresponding to pore sizes of 0.3 and 0.05 mm. Pores larger than 0.05 mm are considered here as macropores, corresponding to transmission pores facilitating air movement and drainage of excess water. Air capacity (AC) is an indicator for soil aeration and is calculated as:

$$AC = \theta_s - \theta_{FC} \quad (2)$$

with θ_{FC} ($m^3\ m^{-3}$) the field capacity, which is the volumetric water content at a pressure head of -10 kPa. The soil's capacity to provide water available to plant roots is defined as the plant available water content (PAWC) and is calculated as:

$$PAWC = \theta_{FC} - \theta_{PWP} \quad (3)$$

with θ_{PWP} ($m^3\ m^{-3}$) the permanent wilting point, calculated at a pressure head of -1500 kPa. The soil's capacity to store water relative to the total pore volume is given by the relative water capacity (RWC) which is the proportion of θ_{FC} to θ_s.

Results and discussion

Penetration resistance

On the plots of Heestert, no clear plough layer could be detected (Figure 1). Although the different tillage techniques were able to decompact the soil to the same extent at the surface, the mouldboard plough could clearly loosen the soil more at deeper soil layers (15 – 35 cm). The subsoiler was not able to loosen the soil throughout the whole profile. The cause of the high penetration resistance is the harvest in wet conditions of the preceding crop. Non-inversion tillage proved not to be able to loosen the soil to the same extent as the mouldboard plough. The slightly better results of the shallow non-inversion tillage can be explained by the build up of a better soil structure at shallow depth.

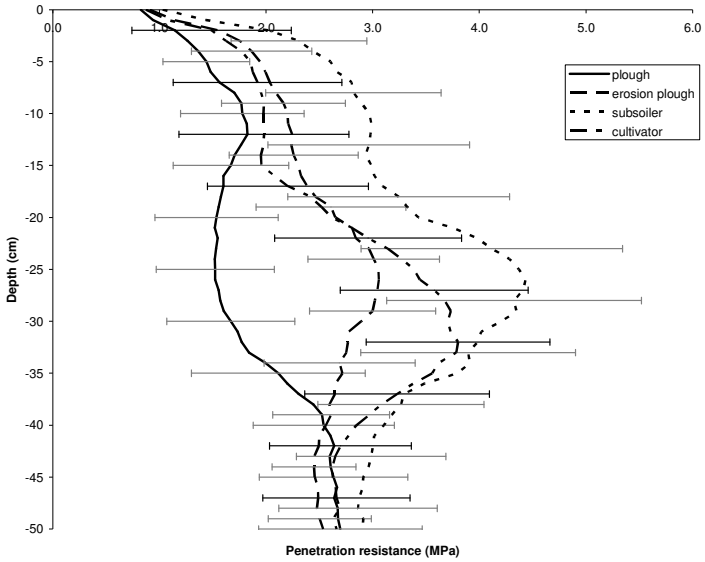

Figure 1. Penetration resistance profiles for the different tillage techniques applied in Heestert. Error bars represent standard deviations.

On the plots at Radinghem, similar results were obtained, though to a lesser extent. Mouldboard plough was able to loosen the soil the most throughout the tillage layer, the cultivator rendering a higher (though not significant) penetration resistance at depths between 10 – 35 cm.

Organic matter content

As a consequence of several years of non inverting the soil, a stratification in organic matter content can be observed (Figure 2). Organic matter content stays fairly constant with depth in the tillage layer for mouldboard plough, while organic matter decreases steadily with depth for non-inversion tillage. While SOM is higher in the first 10 cm of the profile for non-inversion tillage, the SOM is lower in the layer of 20-30 cm. At a depth of 30-40 cm, similar levels of SOM are reached. This stratification is a direct effect of keeping the organic matter at the surface in non-inversion tillage. The strongest stratification was observed for shallow non-inversion tillage. In Radinghem, the same stratification of organic matter content for the shallow non-inversion tillage can be found (data not shown).

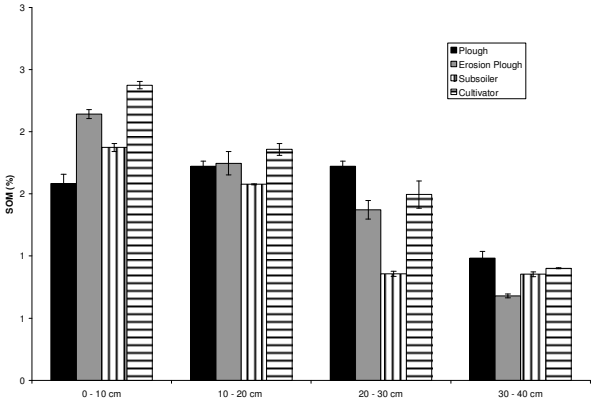

Figure 2. Organic matter content for the different tillage techniques applied in Heestert. Error bars represent standard deviations.

Aggregate stability

The fast wetting method produced very low values for Mean Weight Diameter (MWD) (see Table 2). As both soils contain considerable amounts of clay (see Table 1), slaking occurs to a large extent and most aggregates are destroyed. Both on the plots of Heestert and Radinghem, the aggregates from non-inversion tillage proved to withstand the fast wetting slightly more, though the difference is not significant. Slaking is prevented in the second method by prewetting the aggregates. This is reflected in the higher values of MWD. This method is preferred for unstable soils as a better discrimination can be expected (Le Bissonnais, 1996). The aggregates under non-inversion tillage proved to be significantly more stable with this method. The higher SOM content at the surface may have strengthened the aggregates for the non-inversion tillage applications. The mechanical cohesion for aggregates of Heestert proved to be similar except for the subsoiler. In Radinghem, aggregates of the plot cultivated with the cultivator proved to be less stable than those at Heestert, but still significantly more stable than those for conventional tillage.

Table 2. Mean Weight Diameter (mm) after fast wetting (MWD_{fast}), after prewetting at -0.3 kPa (MWD_{slow}) and after stirring (MWD_{stir}) measured by the three methods of Le Bissonnais (1996). Standard deviations are given between brackets. Same letter indicates no significant difference between plots at P = 0.05.

Location	Management	MWD_{fast} (mm)			MWD_{slow} (mm)			MWD_{stir} (mm)		
Heestert	Plough	0.29	(0.03)	a	2.85	(0.31)	a	0.54	(0.10)	a
	Erosion Plough	0.36	(0.04)	a	3.20	(0.14)	b	0.53	(0.02)	a
	Subsoiler	0.35	(0.06)	a	3.14	(0.16)	b	0.45	(0.07)	b
	Cultivator	0.43	(0.06)	a	3.08	(0.29)	ab	0.57	(0.09)	a
Radinghem	Plough	0.30	(0.61)	a	2.65	(0.21)	a	1.43	(0.16)	a
	Cultivator	0.44	(0.08)	a	2.92	(0.22)	b	1.06	(0.28)	b

Hydraulic conductivity and soil quality indicators obtained from the SWRC

Hydraulic conductivity for the plots of Heestert was strongly influenced by the compacted subsoil. As deep non-inversion tillage suffered more from compaction, these plots had the lowest K_{fs}. The plough and the cultivator had similar K_{fs}. Also in Radinghem, the mouldboard plough and the cultivator had similar K_{fs}, as was expected as this field didn't suffer compaction.

From the SWRC, several soil quality indicators could be deduced (see Table 3). Nevertheless, for none of the calculated indicators could a significant difference between the different plots be observed. There was also no significant difference with soil layers at -15 and -25 cm. The plot tilled with the mouldboard plough showed slightly less macropores and a slightly higher air capacity. Nevertheless, all plots showed a value of the AC lower than 0.15, which is recommended for clay loam soils, according to Reynolds *et al.* (2007). As a result, aeration deficits in the root zone may occur. The low values for macroporosity and AC can be explained by the compacted soil. PAWC proved to be higher than the recommended value of 0.20 and increased at increasing soil depth. Recommended values for RWC fall between 0.6 and 0.7 in order to keep the optimal balance between soil water capacity and soil air capacity. All plots showed values higher than 0.7, indicating a possible problem with soil aeration.

Table 3. Soil quality indicators deduced from the SWRC of samples taken at a depth of 5 cm from the plots of Heestert.

Soil quality indicator	Plough	Erosion plough	Subsoiler	Cultivator
MacPor (m^3 m^{-3}) (-0.1kPa)	0.01	0.02	0.02	0.02
MacPor (m^3 m^{-3}) (-0.6kPa)	0.06	0.09	0.08	0.08
AC (m^3 m^{-3})	0.09	0.12	0.12	0.11
PAWC (m^3 m^{-3})	0.22	0.21	0.25	0.26
RWC	0.77	0.7	0.73	0.75

Conclusion

Making use of a set of soil quality indicators, the physical soil quality of two selected soils could be described. In order to get a deeper insight into the soil's processes, the interaction between the different indicators was investigated. The soil's history proved to play a major role in the measured values. As such, information on preceding crop and soil state (especially soil water content) at harvest and tillage operation should always be taken into account.

The field plots in Heestert were heavily influenced by the wet conditions at harvest and seeding. As non-inversion tillage proved not able to loosen the soil to the same extent as the mouldboard plow, compacted soil layers and a lower infiltration rate could be observed. Nevertheless, this was not reflected in differences in macroporosity, AC and PAWC. As the field plots of Radinghem were tilled under optimal soil water conditions, no significant differences in penetration resistance and infiltration rate were observed. The higher SOM at the surface of the non-inversion tillage plots resulted in aggregates with a higher stability.

References

Cornelis WM, Khlosi M, Hartmann R, Van Meirvenne M, De Vos B (2005) Comparison of unimodal analytical expressions for the soil-water retention curve. *Soil Science Society of America Journal* **69**, 1902-1911.

De Leenheer L (1959) Werkwijzen van de analysen aan het Centrum voor Grondonderzoek. Rijkslandbouwhogeschool Gent, Ghent, pp. 60-61.

Le Bissonnais Y (1996) Aggregate stability and assessment of soil crustability and erodibility: I. Theory and methodology. *European Journal of Soil Science* **47**, 425-437.

Reynolds WD, Elrick DE (1990) Ponded infiltration from a single ring: I. analysis of steady flow. *Soil Science Society of America Journal* **54**, 1233-1241.

Reynolds WD, Drury CF, Yang XM, Fox CA, Tan CS, Zhang TQ (2007) Land management effects on the near-surface physical quality of a clay loam soil. *Soil and Tillage Research* **96**, 316-330.

Verstraeten G, Poesen J, Govers G, Gillijns K, Van Rompaey A, Van Oost K (2003) Integrating science, policy and and farmers to reduce soil loss and sediment delivery in Flanders, Belgium. *Environmental Science and Policy* **6**, 95-103.

Walkley A, Black IA (1934) An examination of the Degtjareff method for determining soil organic matter, and a proposed modification of the chromic acid titration method. *Soil Science* **34**, 29-38.

Field-scale bromide transport as a function of rainfall amount, intensity and application time delay

Ole Wendroth and Vicente Vasquez

Department of Plant and Soil Sciences, University of Kentucky, Lexington, KY 40546.

Abstract
Leaching of surface-applied agri-chemicals depends on a variety of factors, especially rainfall amount and intensity, but also the time delay between surface application and subsequent rainfall. It is difficult to study the impacts of these factors in a randomized plot design, especially if leaching of a tracer is quantified based on soil core samples. The objective of this study was to vary important factors periodically in space along a transect. The spatial distribution of leaching depth and its covariance behavior should reveal association to transport-causing factors. Rainfall amount had the strongest effect on leaching depth. Only highest and lowest rainfall intensity treatments showed an obvious inverse effect The longer the time delay between surface application of the tracer and subsequent rainfall, the shallower the leaching depth. The design of this experiment manifests a promising way to quantify how different influences affect leaching, based on spatial association and frequency-domain covariance analysis.

Key Words
Bromide transport, rainfall amount

Introduction

Rainfall events following application of fertilizers and agrochemicals to the land surface can cause rapid leaching of solutes to deep soil layers and pollute ground water. The transport rate and the flow phenomena causing leaching strongly depend on the amount and intensity of a rainfall (Flury *et al.* 1994; Bronswijk *et al.* 1995). Moreover, the time lag after a chemical application to the subsequently occurring rainfall can strongly influence the transport rate of a solute (Ghuman *et al.* 1975). The objective of this study was to quantify bromide transport at the field scale for different rainfall amount, intensity, application time delay and initial soil water content, while amount, intensity and time delay of rainfall were varying at four levels to derive strategies for avoiding rapid leaching of solutes. Another goal of this study was to identify a sampling scheme with a non-random periodically repetitive spatial distribution of treatment intensities along a transect that allows to quantify solute transport at the field scale.

Materials and Methods

The experiment was carried out on a Maury silt loam soil at the Spindletop Research farm of the Agricultural Experiment Station, University of Kentucky, Lexington, KY. The field site was divided into 32 plots, each being 2 m long and 4 m wide. These plots were located next to each other along a 64-m transect. One half of the field (32 plots) was pre-irrigated with water to cause slightly larger initial soil water content than in the other half.

A KBr tracer was applied in October 2008 in a spatial design and time schedule that allowed subsequent rainfall to be applied in groups of four plots with a sprinkler irrigation system. The plots were spatially arranged in a periodic distribution of different treatment intensities at various wavelengths as shown in Figure 1. The two levels of precipitation amount were applied in blocks of eight plots. Four precipitation intensities were established in groups of four plots. Application time delay varied from plot to plot, regularly repeated eight times along the transect. The regularly repeating distribution of treatments in space manifests an experimental design allowing to decompose variability components through Fourier transformation and spectral analysis (Bazza *et al.* 1988; Shumway 1988). The spatial covariance analysis of bromide leaching and the underlying processes should reveal the impact of rainfall amount, intensity and application time delay on transport through crosscorrelation and cospectra (Shumway 1988; Wendroth and Nielsen 2002; Nielsen and Wendroth 2003).

Soil water pressure head was measured at 48 locations (Figure 2). At each of these locations, six tensiometers were installed at 10, 30, 50, 70, 90, and 110 cm depth. The measurements revealed the spatial distribution of soil water pressure head and hydraulic gradients before and during the leaching experiment. Soil cores were taken after the experiment to measure unsaturated soil hydraulic properties, i.e., the soil water retention curve and the

1 – 6 August 2010, Brisbane, Australia. Published on DVD.

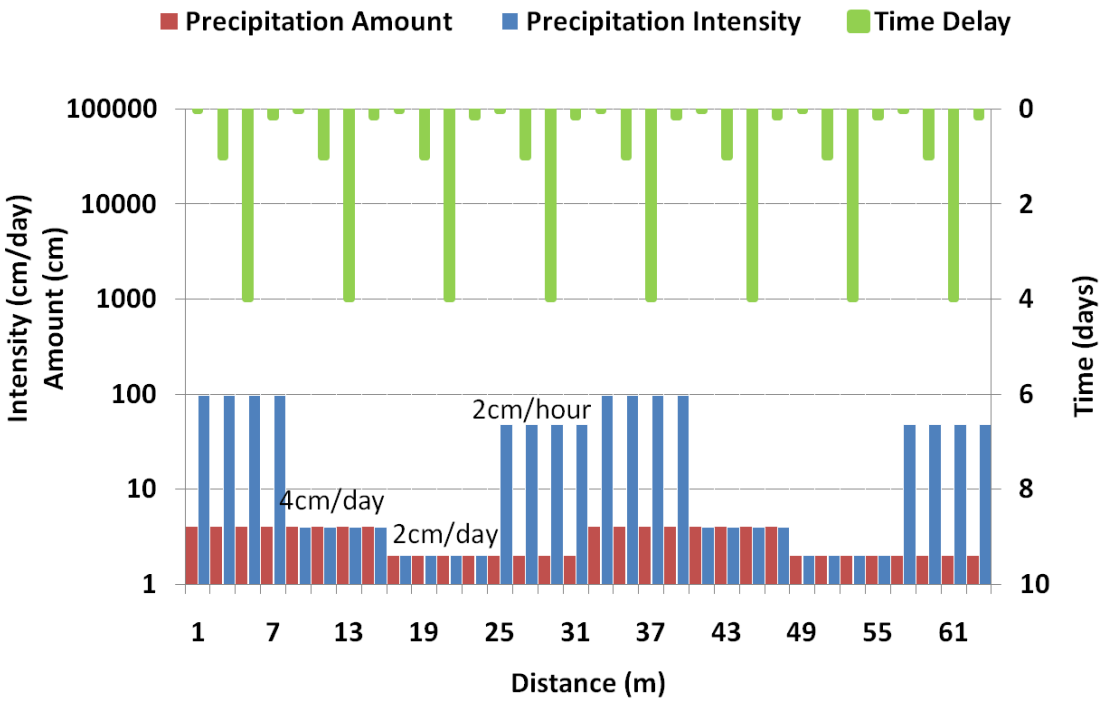

Figure 1. Experimental design and spatial arrangement of plots receiving rainfall at different total amount, intensity, and delay after solute application.

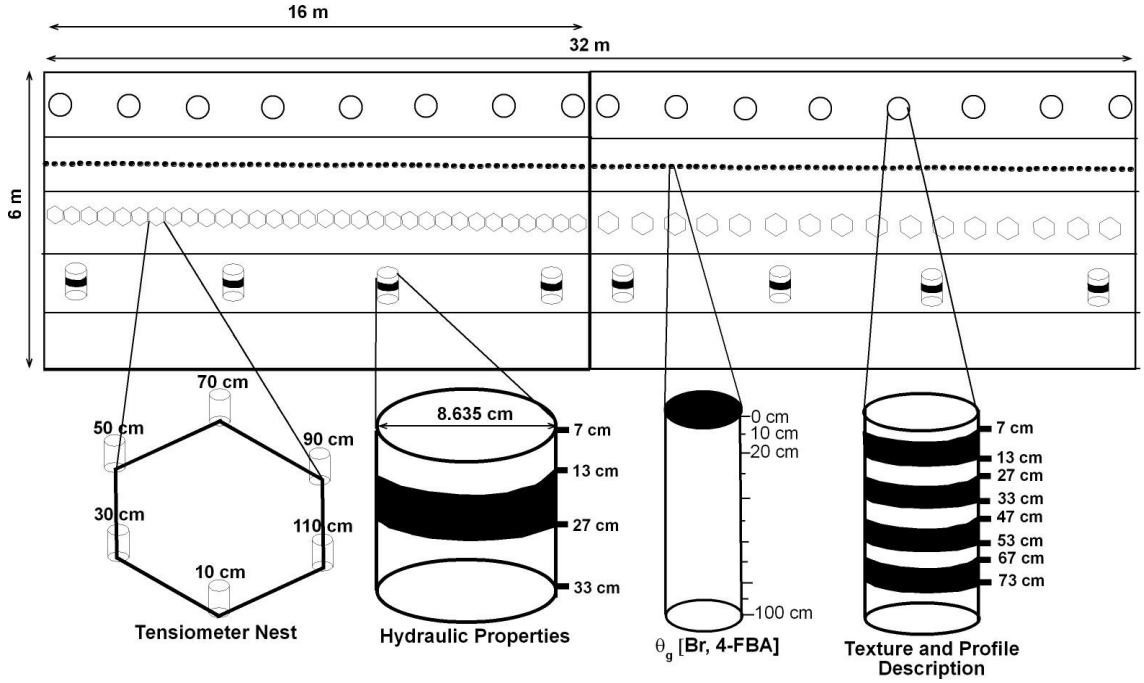

Figure 2. Layout of spatial soil sampling design for soil water pressure head, solute concentration and tracer concentration.

hydraulic conductivity – pressure head relationship. After the tracer application and subsequent irrigation events, a soil core was taken between 0 and 100 cm depth at spatial intervals of 50 cm along the transect resulting in four cores per plot (Figure 2). Each 100-cm soil core was separated in 10-cm depth increments and those samples obtained from each depth interval analyzed for soil water content and bromide concentration. Bromide was only measured for the upper five depth intervals, i.e., to a depth of 50 cm.

Based on the bromide concentration depth profiles, for each of the 128 sampling locations, the bromide leaching depth was characterized with the center of mass COM, defined by

$$\mathrm{COM} = \frac{1}{M}\sum_{i=1}^{n} m_i r_i$$

where M was the total bromide mass recovery at a given location over $i = 1 \ldots n$ depth compartments, m_i was the bromide mass in a specific depth compartment i, and r_i was the center of depth in the specific soil layer. Bromide concentration data, COM and the spatial distribution of rainfall amount, intensity and application time delay were statistically analyzed with respect to auto and crosscovariance, i.e., auto- and crosscorrelation, semi- and cross-semivariance, power spectrum, cross- and quad spectrum and coherency.

Results

Results are focused here on the center of Bromide mass distribution along the transect under the cyclically repeating pattern of treatments. Increasing the amount of precipitation generally increased the leaching of depth bromide as expected (Figure 3). However, for the same rainfall amount, leaching was the more effective the lower the rainfall intensity. In other words, a high intensity rainfall may not cause as much leaching as the same amount of rainfall occurring at a slower rate which would therefore last longer.

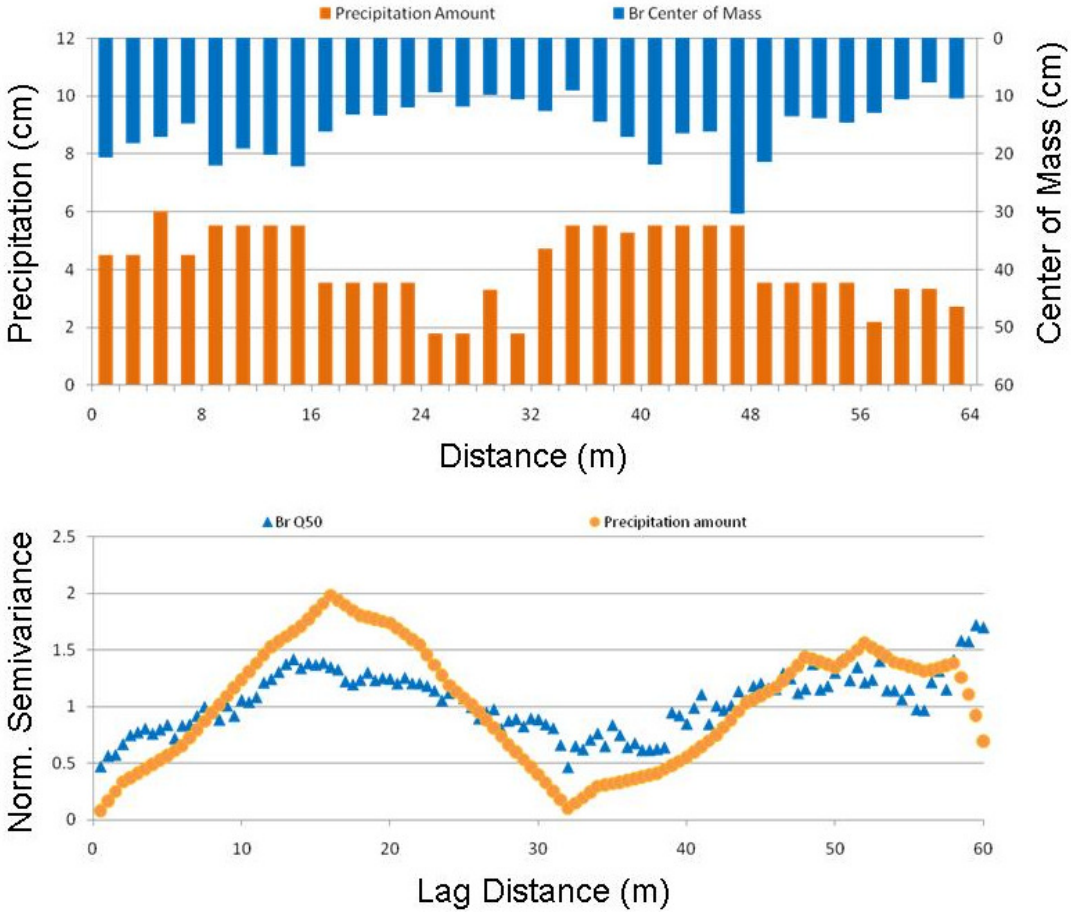

Figure 3. Spatial distribution of precipitation amount and center of mass of Bromide along the 64-m-transect (top) and normalized semivariograms for both variables (bottom).

Cospectral analysis revealed a strong covariance and spatial association between Bromide center of mass and all three factors investigated here (Figure 4). The time delay effect on Bromide leaching depth was manifested in cross- and quadspectra at frequencies corresponding to wavelengths of 32 and 8 m, respectively. The long wave variation was caused by amount and intensity of rainfall. The signal at 8 m wavelength indicates an invers relationship between application time delay and center of mass (Figure 4). This implies, that the longer the delay between Bromide surface application and subsequent rainfall, the less effective is the leaching. In other words, the sooner a rainfall occurs after a surface application of a chemical, the larger is the leaching depth.

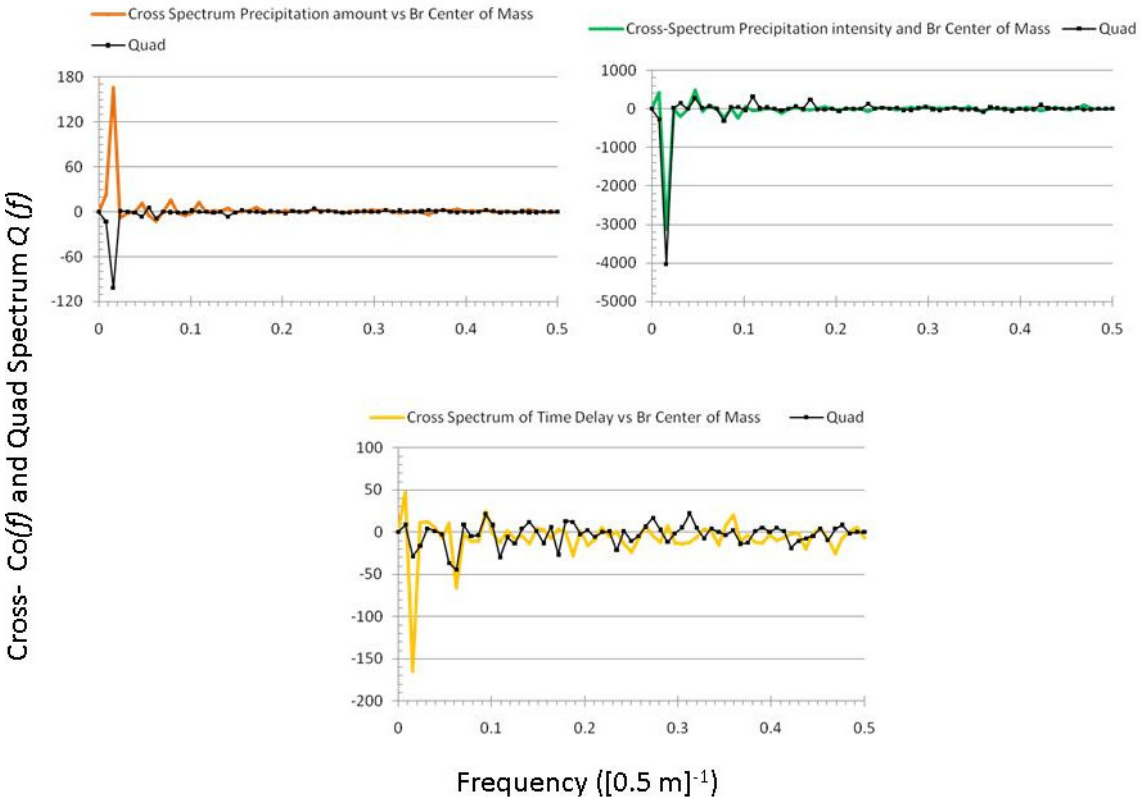

Figure 4. Cross-and quadspectra for the spatial distribution and cyclic variation of Bromide center of mass versus precipitation amount (upper left panel), precipitation intensity (upper right panel) and time delay (lower panel).

References

Bazza M, Shumway RH, Nielsen DR (1988) Two-dimensional spectral analyses of soil surface temperature. *Hilgardia* **56,** 1-28.

Bronswijk JJB, Hamminga W, Oostindie K (1995) Field-scale solute transport in a heavy clay soil. *Water Resour. Res.* **31**, 517-526.

Flury M, Flühler H, Jury WA, Leuenberger J (1994) Susceptibility of soils to preferential flow of water: a field study. *Water Resour. Res.* **30,** 1945-1954.

Ghuman BS, Verma SM, Prihar SS (1975) Effect of application rate, initial soil wetness, and redistribution time on salt displacement by water. *Soil Sci. Soc. Am. J.* **39,** 7-10.

Nielsen DR, Wendroth O (2003) 'Spatial and Temporal Statistics - Sampling Field Soils and Their Vegetation'. (Catena: Reiskirchen, Germany).

Shumway RH (1988) 'Applied Statistical Time Series Analysis'. (Prentice Hall: Englewood Cliffs, NJ).

Wendroth O, Nielsen DR (2002) Time and space series. In 'Methods of Soil Analysis' 3rd ed. Chapter 1, Soil sampling and statistical procedures (Eds GC Topp, JH Dane) pp. 119-137. (ASA-CSSA-SSSA monograph: Madison, WI, USA).

Green, blue and grey waters: Minimising the footprint using soil physics

Brent Clothier, Steve Green and Markus Deurer

Production Footprints, Plant & Food Research, PB 11-600, Palmerston North, New Zealand 4442
brent.clothier@plantandfood.co.nz

Abstract
Virtual water is the water embodied in products. It comprises the green water of rain transpired by the plant, the blue water added as irrigation, and the grey water contaminated by agrichemicals. Biophysical knowledge of green-water use by plants, when complemented with soil physics modelling of both blue and green water flow in soils, permits development of irrigation practices and policies to protect the natural capital stocks of our opportunity-rich blue-water resources that are used for irrigation. Modelling of leaching processes is leading to practices for limiting grey water. These tools and techniques will lead to eco-efficient practices to reduce the virtual water content of the food, fibre and fuel products we grow, while maintaining other ecosystem services that are water dependent.

Key Words
Water footprint, virtual water, irrigation, climate change, ecosystem services, food

Introduction

The *Guardian Weekly* noted in 2002 that "water is now known as 'blue gold' … and 'blue gold' is this century's most urgent environmental issue". Even more recently, *The Economist* (18 September, 2008) asserted, in an article on water for farming entitled "Running dry", that "… the world is facing not so much a food crisis as a water crisis'.

Many of the world's regions are currently experiencing water stress, as measured by the fraction of water withdrawals to that available. The IPCC Special Report on Emissions Scenarios of 2000 considered future climate change impacts. Scenario A1B is a moderate scenario in terms of the global rise in temperature. In Figure 1 below are shown the projections by the IPCC in 2007 for the change in annual water runoff, which is a metric of water availability, in terms of percentages for 2090-2099, relative to 1980-1999. The world's key agricultural regions of California, Mexico, Chile, Argentina, the Mediterranean, South Africa and Australia are destined to suffer even greater water stresses than are presently being felt. Water will assuredly become scarcer and more valuable, such that its management will call for better scientific knowledge about the functioning of agricultural soils.

The Economist (18 September, 2008) found that some 70% of the world's water consumption is used in farming and that there is a pressing need to make it go further, by developing knowledge and tools to monitor water-use efficiency. It concluded that indeed "… farming tends to offer the best potential for thrift".

Water for irrigation to overcome droughts and nutrients applied in fertilisers for enhanced plant growth, are key inputs for most modern and intensifying production systems. Some 40% of the world's food comes from 20% of our lands - thanks to irrigation. One third of the world's population relies on food whose production comes directly from the use of nitrogenous fertilisers. Measurement and modelling of water use by pastures and crops will provide the basis for the development of thrifty options, and shrinking the virtual water content of agricultural products.

1 – 6 August 2010, Brisbane, Australia. Published on DVD.

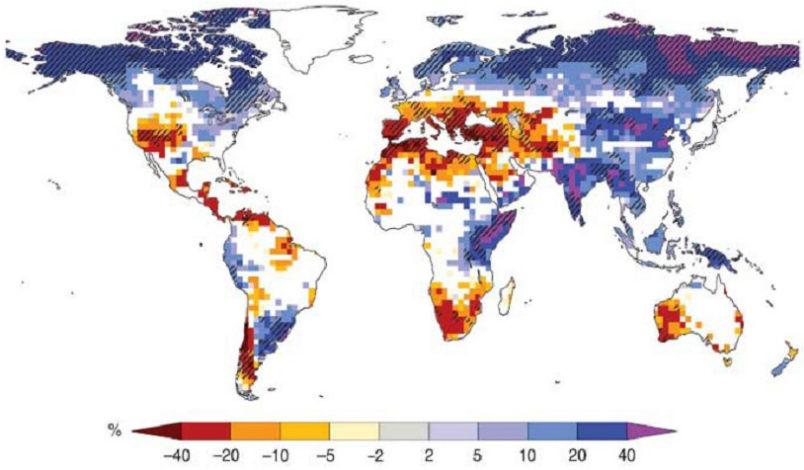

Figure 2. The Intergovernmental Panel on Climate Change (IPCC) projection for the global change in water availability at the end of the 21st century under their moderate scenario A1B.

Virtual Water

Virtual water, first defined by Allan (1998), is the volume of water used to make a product, and is the sum of the water use in the various steps of the production chain. Virtual water comprises three components of different colours: the green, blue and grey waters.

Green water is the water transpired by the plant that comes from rain water stored in soil. Blue water is the water in our surface and groundwater reservoirs. In irrigated agriculture, blue water is abstracted to maintain transpiration. It is imperative that it is used with a high level of efficiency. Soil is a storage reservoir for the green water that falls from the sky, or that which has been added through irrigation from blue-water reservoirs. Grey water is the water that becomes polluted during production, say in agriculture because of the leaching of nutrients and pesticides. Grey-water volume can be quantified by calculating the blue water that would be required to dilute the receiving water body to an acceptable quality standard.

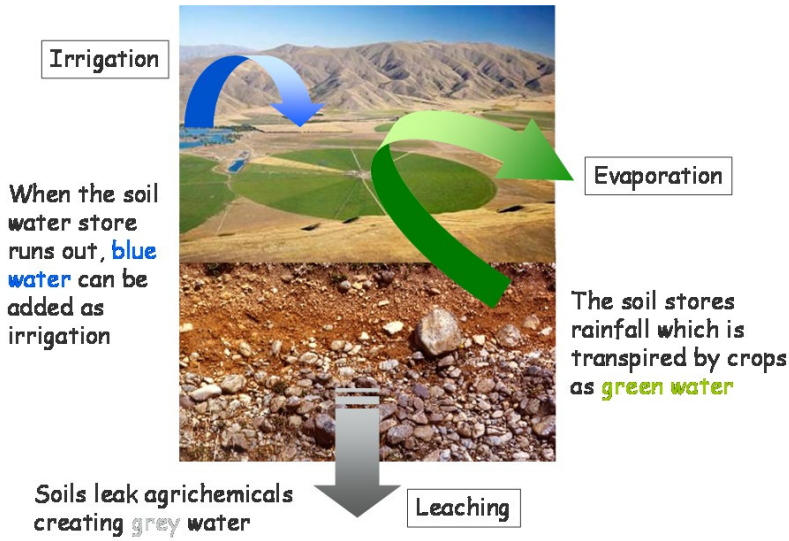

Figure 2. The three colours of water: green water being evapotranspired rainwater from soil, blue water used for irrigation and grey water contaminated by agrichemicals.

Shrinking the water footprint of agriculture can be achieved using practices that reduce the virtual water content of the food, fibre and fuel products. For a country, reducing the water footprint can reduce the total human appropriation of the nation's natural capital stocks of water used for the provisioning service provided by irrigation. This will ensure that requisite amounts of national waters are preserved for environmental flows to maintain the supporting, regulating and cultural services provided by water.

Maximising utility: Green water use

Soil physical and plant biophysical knowledge can be used to develop practices to maximise the utility of green

water. Canopy management can, especially with horticultural crops, reduce levels of green-water use through transpiration by limiting vegetative vigour. In Figure 3 the pattern of green-water transpiration is measured directly by sapflow within the stem of a grapevine using the heat-pulse technique (Green *et al.* 2008). Also shown there is the prediction of vine water-use using a biophysical model of transpiration. Green water use by the vine rises in spring after bud burst, and then it is limited in summer by hedging of the vines, plus leaf plucking and the use of deficit irrigation to limit vegetative vigour.

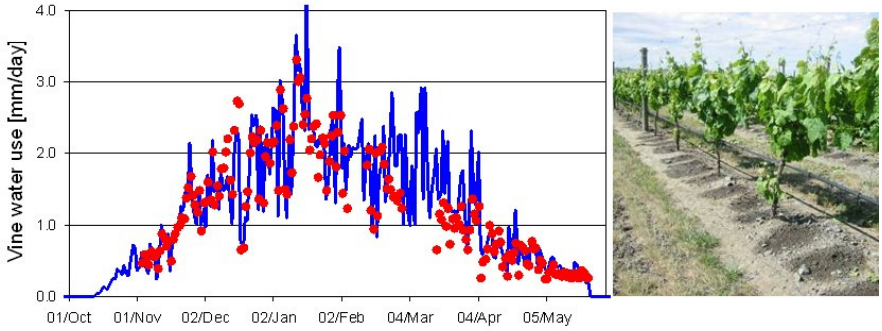

Figure 3. Measured daily grapevine transpiration using sapflow devices (red dots) in relation to a biophysical model of plant transpiration (blue line) based on ambient weather, soil physics and the changing leaf area of the vine.

Minimising irrigation: Blue water abstraction

Irrigation, blue water use, is only required when the green water store in the soil runs short. The soil's ability to store green water is determined by the physical characteristics of the soil. Soils that can store more green water will have a higher natural capital value and thus should be favoured, and protected for primary production. Soil physicists have long studied the ability of soil to store water, and our understanding of green water storage is good.

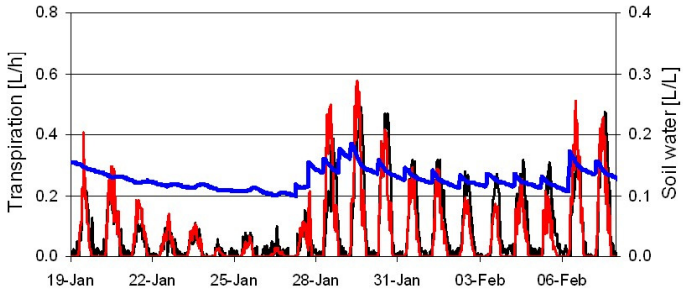

Figure 4. Measured soil water content (blue) and its impact on measured grape vine transpiration (black). The modelled plant transpiration is also shown (red)

What is less well understood is the biophysics of how plants extract water from this store, and we lack clear determination of when blue-water is needed. With limited water resources now being allocated to irrigation, relative to allocation for other ecosystem services, deficit irrigation practices are becoming more common. To manage irrigation efficiently, and to manage deficit irrigation effectively requires a high degree of understanding of soil physics and plant biophysics. New measurement techniques and modelling schemes are enabling the development of practices to minimise blue water use and reduce the virtual water contents of our primary products. In Figure 4 we show how the decline in soil water past the critical point can affect grape vine transpiration, and how rewetting of the soil can restore plant functioning. The key is to use the minimum of blue water to achieve the desired response in the plant – here, grape berries of high quality

Minimising leaching: Grey water production

We have comprehensive soil physical modelling schemes to predict the leaching of agrichemicals. But for the grey water volumes, there is a dearth of measurements available to corroborate our modelling. New measurements are providing us with the vision that is needed to provide our models with credibility, as well as defendability since non-point source pollution issues are inexorably making their way to the courts. Flux meters are one such new tool (Gee *et al.* 2009), and a version of these is shown in Figure 5

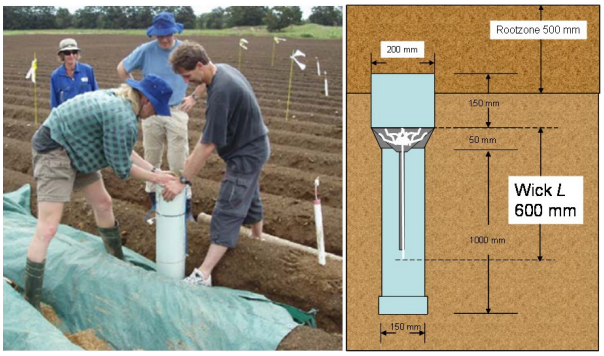

Figure 5. Installation of a fluxmeter into a field of potatoes (left), and the internal system of a fluxmeter showing the wick whose length *L* controls the suction at the soil interface, and the underlying reservoir to collect samples for analysis of leachate quality.

Conclusions

Quantitative soil physics modelling is a valuable means by which we can organise the new knowledge that arises from our better measurements and monitoring in the root zone. This can then be applied to minimise the green, blue and grey waters used in irrigated agriculture. From our new understanding we can develop policies and implement actions to protect the natural capital value of the ecosystem goods and services provided by our plant, soil and water systems. This will ensure sustainable and eco-efficient production from irrigated agriculture by minimising the virtual water content of our food, fibre and fuel products.

References

Allan JA (1998) Virtual water: A strategic resource global solutions to regional deficits. *Ground Water* **36**(4), 545-546.

Green SR, Clothier BE, van den Dijssel, Deurer M, Davidson P (2008) Measurement and modelling the stress response of grape vines to soil-water deficits in their root zones. In 'Modeling the response of crops to limited water: Recent advances in understanding and modeling water stress effects on plant growth processes', (Eds L Ahuja *et al.*) Chapter 15. Vol.12, pp.357-385. (Soil Sci. Soc. Amer. Mono)

Gee GW, Newman BD, Green SR, Meissner R, Rupp H, Zhang ZF, Keller JM, Waugh WJ, van der Velde M, Salazar J (2009) Passive-wick fluxmeters: Design consideration and field applications. *Water Resources Research* DOI 10.1029/2008WR007088

Hydrological and erosional responses in woody plant encroachment areas of semi-arid south–eastern Australia

Carlos Muñoz-Robles[A, *], Matthew Tighe[A], Nick Reid[A], Sue V. Briggs[B] and Brian Wilson[A, C]

[A]Ecosystem Management, School of Environmental and Rural Science, University of New England, Armidale, NSW 2351, Australia
Email cmunoz@une.edu.au
[B]NSW Department of Environment, Climate Change and Water, GPO Box 284, Canberra, ACT 2601, Australia
[C]NSW Department of Environment, Climate Change and Water, PO Box U221, Armidale, NSW 2351, Australia

Abstract
Resource retention is an important component of landscape function in semi-arid environments, with patches in the landscape serving as sink zones that capture runoff, sediments and nutrients sourced from inter-patch areas. The purpose of this rainfall simulation study was to compare hydrological and erosional responses in patches and inter-patches in woody encroachment areas (trees and shrubs >700 stems ha^{-1}) in semi-arid south-eastern Australia. Ground cover, hydrological and erosional responses differed consistently between patches and inter-patches. Inter-patches had low ground cover and produced more runoff and sediment than patches with medium to high ground cover. Patches displayed delayed initiation of runoff and a deeper soil wetting front. Litter, cryptogam cover and surface sand content were the main variables controlling average runoff rate, sediment concentration and total sediment production. The results indicated that patches and inter-patches are different functional units from an eco-hydrological perspective and influence the hydrologic and erosional characteristics of woody encroached areas.

Key Words
Soil erosion, shrub encroachment, invasive native scrub, patches, landscape function, semi-arid

Introduction
Semi-arid environments are often spatially organised in a two-phase mosaic, consisting of bands or patches of individual or aggregated plants interspersed in a low-cover matrix. Runoff and erosion dynamics are different in each phase and are controlled mainly by soil surface condition, particularly the nature of the surface crust and the amount and type of vegetative cover (Greene *et al.,* 1994). The low-cover matrix or inter-patch area is dominated by bare ground, although annual herbs, perennial grasses, woody plants or biological crusts are often present. Inter-patches generally have low infiltration rates and act as source zones of runoff, sediments and nutrients, whilst vegetated patches have higher infiltration rates and serve as sink zones for these resources (Ludwig and Tongway 1995). The type and spatial configuration of patches and inter-patches regulate the redistribution of resources and determine how effectively a landscape can retain resources, and therefore influence the hydrological and erosional processes in patchy semi-arid landscapes (Bergkamp 1998).

Shrub encroachment is a widespread phenomenon which has been reported in a range of arid and semi-arid environments. Encroachment generally refers to the increase in density, cover and biomass of woody plants, particularly shrubs, into former grassland or open woodland (Van Auken 2009), and is associated with declines in herbaceous forage production and livestock carrying capacity, reductions in biodiversity and socio-economic values (Graz 2008) and with increased runoff and erosion (Parizek *et al.,* 2002). Since the early 1900s, shrub and tree encroachment has increased in semi-arid New South Wales in south-eastern Australia (Gardiner *et al.,* 1998). Relationships between woody encroachment and runoff and erosion are not well understood in this region. In this study, we investigated hydrological and erosional responses using rainfall simulation in patches and inter-patches in six woody encroached sites. The objectives of this study were to: 1) investigate hydrological and erosional responses in two types of patches (e.g. under-shrub and medium vegetated) and in inter-patches; and 2) determine the effects of ground cover on runoff, sediment concentration and sediment production.

Methods
Study region
The study was conducted across three properties within the Cobar pediplain, New South Wales, Australia (Figure 1). Rainfall is highly variable, with a slight summer dominance and an annual mean of 400 mm (Bureau of Meteorology 2008). Average maximum and minimum temperatures are 26°C in January and 12°C in July, respectively. Soils are predominantly non-sodic Kandosols to Dermosols (Isbell 1996). Vegetation communities

1 – 6 August 2010, Brisbane, Australia. Published on DVD.

are mostly derived from *Eucalyptus populnea–Callitris glaucophylla* grassy woodlands (Noble 1997). Sites with a known history of encroachment were selected based on soil type and topography, and comprised areas of dense *C. glaucophylla* and *Eremophila sp.* (>700 stems ha^{-1}) with a scattered overstorey of *Eucalyptus populnea, Eucalytpus intertexta* or *C. glaucophylla.*

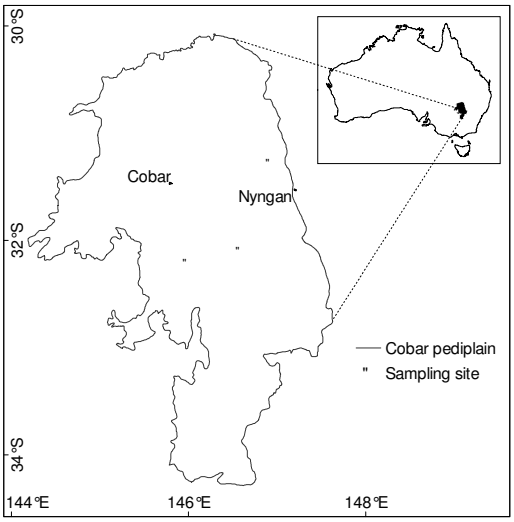

Figure 1. Location of the study area.

Identification of patches and inter-patches
Landscape function analysis (LFA) transects (Tongway and Hindley 2004) were used to define patches and inter-patches based on different amounts and components of ground cover. Patches and inter-patches were classified according to three levels of ground cover: 'Inter-patch' (<30% groundcover), 'Patches' comprising 'Medium vegetated' patches (30-65% groundcover) and 'Under-shrub' patches (>65% groundcover).

Surface characterisation and rainfall simulations
At each site, duplicate 1 m x 1 m plots were selected in each patch and inter-patch. Prior to rainfall simulations, percent herbaceous, litter and cryptogam cover were estimated visually in each plot, with their sum defining total ground cover. Duplicate soil samples (0–2 cm depth) were collected adjacent to the simulation plot using a hand-held soil corer (diameter 5 cm). Moisture content, oven dry bulk density and particle size distribution were determined for each sample. A Morin-type rotating-disc rainfall simulator (Morin and Cluff 1980) mounted on a trailer was used to apply rainwater to the plots for 30 min at 35
mm h^{-1}. Runoff and sediment samples were taken at regular intervals during each simulation, and time to runoff (min), average runoff rate (mm h^{-1}), average sediment concentration (g L^{-1}), total sediment production (g m^{-2}) and the depth of wetting front (cm) were also measured.

Data analysis
Mixed linear modelling with site as a random factor was used for analysis. Ground cover in patches and inter-patches and their hydrological and erosional responses were compared using pair-wise contrasts. Significance levels were set to $P < 0.05$, although P values < 0.10 were also noted. Forward stepwise multiple regression was used to explore the combined effect of rainfall simulation plot characteristics (ground cover components, bulk density and sand content as a proxy for texture values due to strong correlation between particle size components) on three hydrological and erosional responses (average runoff rate, average sediment concentration and total sediment production). Analyses were undertaken in R version 2.9.0 and SYSTAT version 12.

Results and discussion

Total ground cover was lowest in inter-patches followed in increasing order by medium vegetated patches and under-shrub patches (Table 1). Herbaceous cover was consistently low in both patches and inter-patches. Medium vegetated patches had the highest herbaceous cover, under-shrub patches had the highest litter cover, and cryptogam cover in inter-patches was higher than in patches.

Table 1. Mean ground cover (%) in patches and inter-patches. Values followed by different letters are significantly different ($P < 0.05$, or $P < 0.10$ if letters followed by *). n = 12 for each patch type and inter-patch.

Patch/Inter-patch	Herbaceous	Litter	Cryptogam	Bare soil	Total ground cover
Patch - Under-shrub	6.0b	52.6c	7.7a*	33.7a	66.3c
Patch - Medium vegetated	14.2c	22.5b	13.8b*	49.5b	50.5b
Inter-patch	0.7a	2.3a	28.2c	68.8c	31.2a

Bulk density and sand content were not statistically different between patches and inter-patches (data not shown). Hydrological and erosional responses varied consistently between patches and inter-patches (Table 2). Under-shrub patches had lower average runoff rates, total sediment production and greater depth of wetting front compared with medium vegetated patches and inter-patches, consistent with the effects of high ground cover on rainfall interception, microtopography and surface sealing (Renard *et al.,* 1996; Whitford 2002). Patches also exhibited delayed runoff initiation (Figure 2). In contrast, with their lower ground cover inter-patches had low infiltration and a rapid increase in runoff during the first 15 min of rainfall application (Figure 2). Patches and inter-patches had similar sediment concentration, indicating a similar susceptibility to soil particle detachment by rain drops, irrespective of differences in ground cover. Thus, the total sediment production of each patch and inter-patch was more closely related to the amount of runoff rather than any differences in sediment concentration. Total sediment production was markedly lower from under-shrub patches than inter-patches (Table 2), and once runoff began, the cumulative rate of sediment production was constant for each patch and inter-patch (Figure 2).

Table 2. Hydrological and erosional responses in patches and inter-patches. Values followed by different letters are significantly different ($P < 0.05$). n = 12 for each patch type and inter-patch.

Patch/Inter-patch	Time to runoff	Average runoff rate	Wetting front	Average sediment concentration	Total sediment production
	(min)	(mm h^{-1})	(cm)	(g L^{-1})	(g m^{-2})
Patch - Under-shrub	20.8b	3.3a	5.4c	2.04a	3.3a
Patch - Medium vegetated	12.7a	8.3b	3.8b	1.89a	7.5a
Inter-patch	9.6a	13.3c	2.8a	1.99a	13.0b

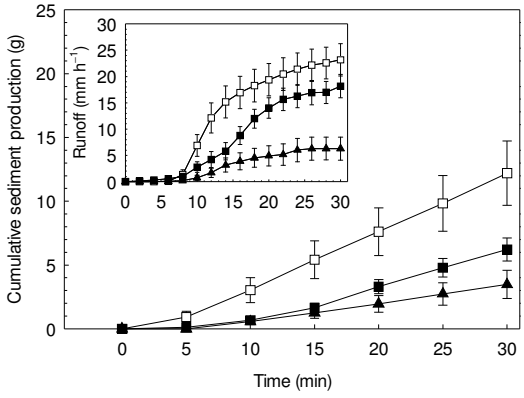

Figure 2. Mean cumulative sediment production and runoff rate (inset) in patches and inter-patches ▲= under-shrub, ■ = Medium vegetated, □ = Inter-patch. Bars represent ±1 SE.

Litter cover was the only significant predictor of runoff (Table 3). High cryptogam cover and sand content were associated with lower sediment concentration in runoff, but this relationship was weak, and the differences in cryptogam cover between patches and inter-patches did not translate into differences in sediment concentration. Total sediment production was best predicted by a combination of litter cover and sand content. These results indicated that the presence of ground cover components such as litter may partly compensate for the low herbage cover in woody encroached areas and provide soil stability and protection against raindrop impact, and in these areas of low herbaceous cover, litter plays a role in reducing total sediment production by reducing runoff.

Table 3. Stepwise multiple regression equations for average runoff (AR), average sediment concentration (ASC) and total sediment production (TSP).

Regression equation	Adjusted R^2	Model F	Significance P
$\sqrt{AR} = 3.41 - 0.03$ litter	0.44	$F_{1,34} = 28.54$	0.0001
$\sqrt{ASC} = 4.64 - 0.01$ cryptogam $- 0.04$ sand	0.35	$F_{2,33} = 10.21$	0.0001
$\sqrt{TSP} = 8.91 - 0.03$ litter $- 0.08$ sand	0.40	$F_{2,33} = 12.45$	0.0001

Conclusion

Due to consistent differences in hydrological and erosional responses, we consider that the patches and inter-patches in this patterned landscape are different functional hydrologic units that control the redistribution of runoff and sediments, in agreement with Ludwig *et al*. (2005). Inter-patches are more prone to runoff and sediment production than patches, and are probably the main drivers of runoff and erosion processes in woody encroached areas. The hydrological and erosional responses of patches and inter-patches are related to the occurrence of different ground cover components. Inter-patches have higher runoff and sediment production due to low ground cover, including low litter cover. Patches have high litter cover which appears to reduce total sediment production by reducing runoff. This effect of litter may be greater when more stable forms such as dead vegetation and large debris (i.e. logs) are considered.

References

Bergkamp G (1998) A hierarchical view of the interactions of runoff and infiltration with vegetation and microtopography in semiarid shrublands. *Catena* **33**, 201-220.

Bureau of Meteorology (2008) Climate statistics for Australian locations. Australian Government. http://www.bom.gov.au.

Gardiner DB, Tupper GJ, Dudgeon GS (1998) A quantitative appraisal of woody shrub encroachment in Western New South Wales. *Rangeland Journal* **20**, 26-40.

Graz PF (2008) The woody weed encroachment puzzle: gathering pieces. *Ecohydrology* **1**, 340-348.

Greene RS, Kinnell PI, Wood JT (1994) Role of plant cover and stock trampling on runoff and soil erosion from semi-arid wooded rangelands. *Australian Journal of Soil Research* **32**, 953-973.

Isbell RF (1996) 'The Australian Soil Classification.' (CSIRO,Melbourne, Australia).

Ludwig JA, Tongway DJ (1995) Spatial organisation of landscapes and its function in semi-arid woodlands, Australia. *Landscape Ecology* **10**, 51-63.

Ludwig JA, Wilcox BP, Breshears DD, Tongway DJ, Imeson AC (2005) Vegetation patches and runoff-erosion as interacting ecohydrological processes in semiarid landscapes. *Ecology* **86**, 288-297.

Morin J, Cluff CB (1980) Runoff calculation on semi-arid watersheds using a Rotadisk Rainulator. *Water Resources Research* **16**, 1085-1093.

Noble J (1997) 'The Delicate and Noxious Scrub.' (Lyneham).

Parizek B, Rostagno CM, Sottini R (2002) Soil erosion as affected by shrub encroachment in north-eastern Patagonia. *Journal of Range Management* **55**, 43-48.

Renard KG, Foster GR, Weesies GA, McCool DK, Yoder DC (1996) Predicting soil erosion by water: A guide to conservation planning with RUSLE. USDA handbook 703. US Department of Agriculture, Washington, D.C.

Tongway DJ, Hindley N (2004) 'Landscape Function Analysis: Procedures for monitoring and assessing landscapes.' (CSIRO Sustainable Ecosystems, Canberra).

Van Auken OW (2009) Causes and consequences of woody plant encroachment into western North American grasslands. *Journal of Environment Management* **90**, 2931-2942.

Whitford WG (2002) 'Ecology of Desert Systems.' (Academic Press, London, UK).

Hydro-pedotransfer functions for predicting the effective annual capillary rise

Gerd Wessolek[A], Klaus Bohne[B], Wim Duijnisveld[C] and Steffen Trinks[A]

[A]Technical University Berlin, Germany, Email: gerd.wessolek@tu-berlin.de
[B]University of Rostock, Germany, Email: klausbohne@googlemail.com
[C]Federal Institute for Geosciences and Natural Resources, Hannover, Germany, Email: wilhelmus.duijnisveld@bgr.de

Abstract
New hydro-pedotransfer functions for grassland are presented to calculate both annual capillary rise from the groundwater into the root zone and actual evapotranspiration for regional water balances. The functions i.e. the procedure has two advantages. Firstly, only easily available site information is necessary for the calculation, such as the soil texture class, groundwater depth, summer rainfall and potential evapotranspiration (ET_{pot}) according the FAO guideline. Secondly, we follow the principle idea to define the gain (G) of actual evapotranspiration (ET_{act}) caused by capillary rise from groundwater as an effective parameter to express both, the soil and climate dependent effective capillary rise for a given site. In order to define a reference, we used the actual evapotranspiration of a site without groundwater influence but with same soil hydraulic properties and climate conditions. In order to predict *G* without using the numerical model, a new hydro-pedotransfer concept was developed and tested for several regions in Germany, Europe.

Key Words
Capillary rise, actual evapotranspiration, hydro-pedotransfer functions, regional scale

Introduction
Recently, a set of hydro-pedotransfer functions was proposed to predict the annual percolation rate on a regional scale using easily available soil data (Wessolek et al. 2008). However, the above mentioned functions use a very simple approach to calculate the capillary rise from the groundwater into the root zone. Our aim was to improve the calculation in order to get an expression for a site specific capillary rise that enhances at least the actual evapotranspiration. We should keep in mind that the term “capillary rise” symbolizes an idealized flow pattern where drainage and capillary rise are imagined to be separated flow conditions in soil. In reality the flux at the bottom boundary changes magnitude and direction frequently due to actual conditions in the soil profile. For this reason we decided to express the effective capillary rise as a gain of actual evapotranspiration in order to make sure that capillary rise is not only dependent on soil hydraulic properties but also on climate and plant conditions such as rooting depth.

Methods
Firstly we used the numerical simulation model “SWAP” (Kroes et al. 1999) to simulate soil water dynamics for a broad spectrum of boundary conditions: in total we calculated water flow for four typical soil classes through 30 years using different values of groundwater depth. This was done for three different meteorological observation stations in Germany, one station with little rainfall and high potential evapotranspiration, the second one with average rainfall and average potential evapotranspiration, and the third one with high rainfall and low potential evapotranspiration. In total we obtained 1710 values of annual evapotranspiration. For each of the soil texture classes and observation stations one simulation was run without influence of groundwater. We compared this reference condition with simulation runs for various groundwater depths conditions. The latter indicate the increase in actual evapotranspiration. The increment was termed “gain” (G) and was attributed to so-called “effective capillary rise”.
Secondly, to predict gain without using the numerical model, functions were established to estimate gain from easily accessible data in two steps, (1) expressing the maximum capillary rise rate for a given soil and groundwater depth, and in step (2) we followed a suggestion after Visser (1968) to derive a gain (*G*= effective capillary rise rate) based on water supply (*S*), and water demand (*D*).

Results
In the first step the groundwater influence is denoted by steady-state flow rates, which only depend on soil hydraulic properties and the distance between groundwater table and the bottom of the root zone (*z*). These steady-state flow rates could be calculated using an arbitrary threshold of soil water potential. The selected value of ψ = -3200 hPa ensures obtaining a standard flow rate close to the maximum flow rate that would occur

1 – 6 August 2010, Brisbane, Australia. Published on DVD.

at the threshold $\psi = -\infty$. Using this threshold, the steady-state flow was evaluated numerically (Bohne, 2003) for various data points of $q(z_{max})$. In order to facilitate the results, the empirical function (1) was introduced to express $q_{max}(z)$.

$$q(z) = p_1 z^{p_2} \quad (1)$$

The parameters p_1 and p_2 could be easily gained for various soil texture classes (Table 1). Fig. 1 shows exemplarily how z controls the maximum flux rates at $\psi = -3200$ hPa for a sandy and a loamy soil (Lts).

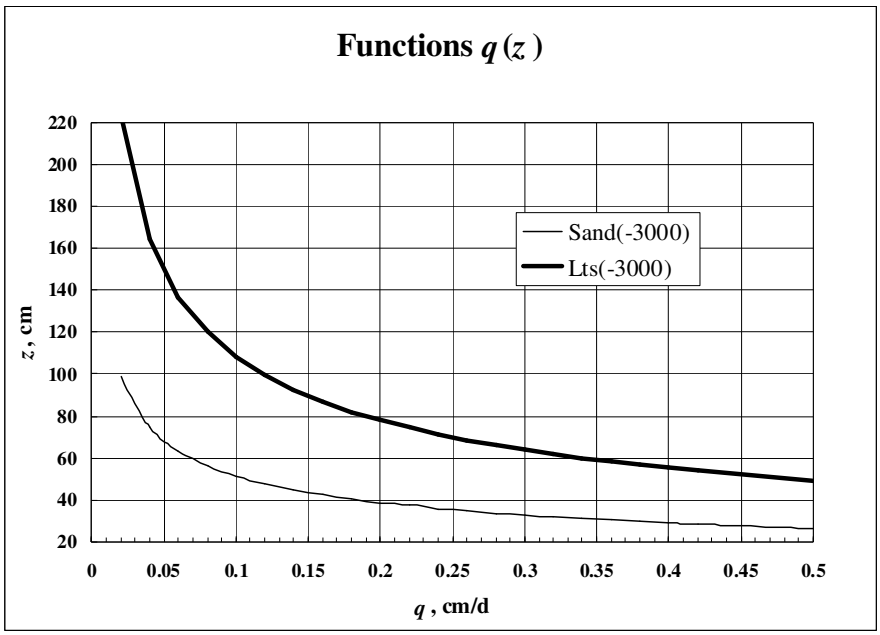

Figure 1. $q(z)$ functions for two soils, parameters of $p1$ and $p2$ are listed in Table 1.

Table 1. Parameters p_1 and p_2 of the empirical equation $q = p_1 z^{p_2}$ (cm/d).

Soil class	p_1	p_2	Soil class	p_1	p_2
Ss	1.5244E+03	-2.4467	**Uu**	9.6900E+03	-2.0996
Sl2	1.8344E+03	-2.3827	**Uls**	2.7659E+03	-1.9182
Sl3	5.8747E+03	-2.5284	**Us**	1.9477E+03	-1.8381
Sl4	5.1832E+02	-1.7925	**Ut2**	3.8354E+03	-1.9891
Slu	5.6573E+02	-1.7205	**Ut3**	3.7122E+03	-1.9858
St2	3.9707E+02	-1.4971	**Ut4**	3.0780E+03	-2.0077
St3	2.2651E+02	-1.8035	**Tt**	6.2126E+01	-1.8051
Su3	8.5042E+02	-1.7423	**Tl**	9.9199E+01	-1.8691
Su4	1.2992E+03	-1.7361	**Tu2**	9.8138E+01	-1.8643
Ls2	1.4856E+03	-1.5862	**Ts2**	2.2292E+02	-1.9629
Ls3	9.7394E+02	-1.7943	**Ts3**	8.5734E+02	-2.1027
Ls4	7.2012E+02	-1.7661	**Ts4**	2.0702E+02	-1.5199
Lt2	7.6150E+02	-1.7619	**fS**	3.0197E+03	-2.4811
Lt3	3.8861E+02	-1.6707	**mS**	1.5653E+03	-2.4537
Lts	2.2340E+03	-2.1450	**gS**	1.6850E+04	-3.4299
Lu	1.1664E+03	-1.8089			

As mentioned above, we intended to predict the increase of actual evapotranspiration (=gain, G) caused by capillary rise from the groundwater table using easily accessible soil and climate data. The gain is limited either by the water demand D or by the soil water supply S. Following a suggestion after Visser (1968) this condition leads to the equation:

$$(D-G)(S-G)=0 \tag{2}$$

Rearranging yields a quadratic equation with the solution

$$G=\frac{D+S}{\lambda_1}+\lambda_2\left[(D+S)^2-4DS\right]^{\lambda_3} \tag{3}$$

Where the λ_i are empirical fitting parameters and listed in Table 2.

Table 2. Parameters of Eqs.3, 4, 6 and 7.

Parameter	Value
λ_1	3.04093
λ_2	-0.22966
λ_3	0.52642
c_1	0.31273
c_2	0.46787
c_3	23.1155
c_4	0.94361
g_1	-0.601
g_2	0.02374
g_3	0.03529
g_4	0.07083
g_5	0.38338

Another empirical equation (4) was introduced to expressing the water demand and supply in terms of known data:

$$D=c_1+ET_{pot,summer}-P_{summer}-c_2 W_a \tag{4}$$

Where $ET_{pot,summer}$ denotes the grass reference evapotranspiration during summer, P_{summer} the precipitation in summer (April 1st – September 30th) and W_a is known as the amount of plant available soil water with

$$W_a = RD*(FC-PWP) \tag{5}$$

RD rooting depth
FC field capacity, taken here as $\theta_{(-63\ hPa)}$
PWP permanent wilting point, taken here as $\theta_{(-15800\ hPa)}$

c_2 provides the means to partition W_a so that only water that is easily available for evapotranspiration, it is include in calculation of *D*. The capability of soil to supply water is expressed by

$$S=c_3 q_{\max}^{\ c4} \tag{6}$$

Where q_{max} is the appropriate function value $q_{max}=q(GW-RD)$ of Eq.(1) for the texture class chosen and GW represents the depth to groundwater. After fitting the unknown parameters, the increase *G* of the actual evapotranspiration was calculated by Eqs. 3, 4, and 6. Based on 1710 comparisons, the root mean squared difference (*RMSD*) between G_{model} as calculated by the numerical simulation model and $G_{predicted}$ as calculated by Eq. (3) was *RMSD* =18.03 mm with a correlation coefficient of *R* =0.9025.
Actual evapotranspiration during summer depends on both potential evapotranspiration and on the amount of

water available for evapotranspiration. The amount of available water consists of precipitation during summer P_{summer}, the effect of groundwater and part of soil water storage at the start of summer.

Using the estimated Gain *G*, also the actual evapotranspiration during summer can be estimated by

$$ET_{act,summer} = ET_{pot,summer}(g_1 + g_2 P_{summer} + g_3 G + g_4 W_a)^{g5} \quad (7)$$

Eq. 7 estimates the actual evapotranspiration during summer with an accuracy of *RMSD*=23.73 mm (*R*=0.8884). The ratio ET_{act}/ET_{pot} has shown to be a good coefficient to assess water supply to crops.

Conclusions

The new hydro-pedotransfer functions for predicting the annual effective capillary rise and actual evapotranspiration lead to results which are in very good agreement with results of numerical simulation models. The method is applicable on a regional scale when easily available weather data and soil texture class are known. Since the equations are statistically based, they should not be used unverified in areas exhibiting climatic and soil conditions different from Central Europe.

References

Allen RG, Wright ME, Burman RD (1989) Operational estimates of evapotranspiration. *Agronomy Journal* **81**, 650-662.

Bohne K (2005) 'An introduction into applied soil hydrology'. (Catena Verlag: Reiskirchen). 231 pp.

Kroes JG, van Dam JC, Huygen J, Vervoort RW (1999). 'Simulation of water flow, solute transport and plant growth in the Soil-Water-Atmosphere-Plant environment: User's Guide of SWAP version 2'. Technical Document Nr. 53. (DLO Winand Staring Centre: Wageningen).

Renger M, Bohne K, Facklam M, Harrach T, Riek W, Schäfer W, Wessolek G, Zacharias S (2009) 'Ergebnisse und Vorschläge der DBG-Arbeitsgruppe „Kennwerte des Bodengefüges". Bodenökologie und Bodengenese, Heft 40'. 80pp. (Eigenverlag der TU: Berlin). (in German).

Visser WC (1968) Ein Ertragsmodell für günstige und schädliche Umweltfaktoren. *Studia Biophysica*, **11**, 227-236. (in German).

Van Genuchten MT (1980). A closed-form equation for predicting the hydraulic conductivity of unsaturated soils. *Soil Science Society of America Journal* **44**, 892-898.

Wessolek G, Duijnisveld WHM, Trinks S (2008) Hydro-pedotransfer functions (HPTFs) for predicting annual percolation rate on a regional scale. *Journal of Hydrology* **356**, 17-27.

Review Comments

The derivation of eqn (3) from eqn (2) is not correct. This means that estimates of *G* based on eqn (3) will not satisfy eqn (2). The empirical relationships that have been developed may still be useful but the authors will need to modify the manuscript to reflect the fact that these are not based on eqn (2).

Impact of conservation agriculture on runoff, soil loss and crop yield on a Vertisol in the northern Ethiopian highlands

Tesfay Araya[A], Wim M. Cornelis[B], Jan Nyssen[C], Bram Govaerts[D], Tewodros Gebregziabher[E], Tigist Oicha[E], Fekadu Getnet[E], Dirk Raes[F], Mitiku Haile[E], Ken D. Saire[D] and Jozef Deckers[F]

[A]Dept. of Crop and Horticultural Science, Mekelle University, P.O. Box 231, Mekelle, Ethiopia.
[B]Dept. of Soil Management - International Centre for Eremology, Ghent University ,Coupure links, 653, B-9000 Gent, Belgium.
[C]Dept. of Geography, Ghent University, Krijgslaan 281 (S8), B-9000 Gent, Belgium.
[D]International Maize and Wheat Improvement Centre (CIMMYT), A.P. 6-641, Mexico D.F. 06600, México.
[E]Dept. of Land Resources Management and Environmental Protection, Mekelle University, P.O. Box 231, Mekelle, Ethiopia.
[F]Dept. of Earth and Environmental Sciences, Katholieke Universiteit Leuven, Celestijnenlaan 200E, B-3001, Belgium.

Abstract
Conservation Agriculture (CA) can be a possible technique to mitigate the reduction in soil quality, to reduce runoff and soil erosion, and can increase in situ moisture conservation, thereby increasing crop yield. This study was carried out on a rainfed field in Tigray, northern Ethiopia. The objective was to evaluate the impacts of CA on runoff and soil loss, and crop yield improvements. The CA practices were introduced on farmers' fields on vertisols since 2005. The experimental layout was arranged according to a randomized complete block design with two replicates. Treatments included conventional tillage (TRAD) which was ploughed 3 times and residue removed, *Terwah* (TERW) ploughed 3 times, residues removed and furrows made at 1.5 m distance, and permanent beds (PB) with 30% residue retention, zero tilled and 60 cm wide bed size. All the ploughing and reshaping of the furrows was done using the local ard plough *maresha*. Data on soil loss, runoff and grain yield were collected. The crops in rotation were wheat and teff. There was significant reduction ($p<0.05$) in runoff in PB under wheat in 2005, whereas the reduction was non-significant in 2006 and 2007. The soil loss was significantly lower in PB in 2005 and 2006. Soil loss in 2005 under wheat was reduced by 76% in PB and 61% in TERW as compared to TRAD. Similarly, the reduction in soil loss in 2006 under teff was 86% in PB and 53% in TERW. There was no significant difference ($p<0.05$) for wheat yield in 2005 and 2007. However, there was a significant difference among treatments in 2006 with higher teff yield in TRAD followed by TERW. In summary, permanent bed reduced soil loss and runoff and hence increased yield of wheat. Yield of teff was, however, reduced with permanent beds.

Key Words
Conservation agriculture, Terwah, permanent bed, crop residue, wheat, teff

Introduction
Land degradation in northern Ethiopia is a great problem mainly aggravated by overpopulation in the highlands, over cultivation, soil erosion, and an unbalanced crop and livestock production system (Girma 2001). As a consequence of loss of the top fertile soil by erosion, there is severe decline in soil quality. The poor infiltration and water holding characteristics of the soil makes water a key limiting factor for crop yield in this area. The livelihood of 85 % of the population of Tigray depends on agriculture, mainly on crop production, and small units of land have been extensively cultivated by subsistence farmers for centuries. The rainfed farming agriculture is dominant and has low productivity. The rainfall in the region is erratic and insufficient during the growing season (Ermias *et al.* 2005). It is common to observe both water logging and drought in one cropping season (personal observation). Soil moisture in the Vertisols is insufficient due to periodic drought, low moisture holding capacity of the soils, high tillage frequency, and high runoff rates from sloping lands in case of periodic excess of rain water (Mati 2006). Tillage is done with a breaking plough locally known as *mahresha* with frequent ploughing before sowing which may result in compaction, poor drainage and crusting in Vertisols. Also, farmers harvest the straw of crops in order to feed their animals leaving no residues as soil cover. There is also free grazing of animals on the stubble residue after harvest. These operations have led to the long term reduction in soil organic matter content which consequentially increased soil erosion. Recent policy in Tigray region favours in situ water conservation, stubble management and the abandonment of free grazing. Vertisols are hard when dry, very sticky when wet and susceptible to erosion depending on how they are managed and on their top soil structure and texture (Deckers *et al.* 2001). McHugh *et al.* (2007) reported that ridges significantly increased soil moisture and grain yield and reduced soil loss in north Wollo, Ethiopia. Experiments conducted in Mexico by Govaerts *et al.* (2005) on a fine, mixed, thermic, Cumulic Haplustoll with zero tillage treatment combined with rotation and residue retention showed improvements in yield as compared to heavy tillage before

seeding, monocropping and crop residue removal. They reported that permanent bed with crop rotation and residue yielded the same as zero tillage. Various studies on CA outlined many benefits as it allows early sowing, growing long maturing crops/varieties, reduces runoff and evaporation, reduces soil loss, conserves soil moisture, increases labour efficiency, reduces oxen and straw demand, and enhances soil fertility (Nyssen *et al.* 2006). In contrast to traditional agriculture, conservation agriculture leaves residues from the previous crop on the surface. It may store a considerable amount of water and increases roughness, slowing down the runoff flow velocity (Findeling *et al.* 2003). However, comparison of conservation agriculture and traditional agriculture practices over different time periods have not been consistent across soils, climate, and experiments in different parts of the world (Ahuja *et al.* 2006). Conservation agriculture and other CA based resource conserving technologies practices like permanent bed and modified *terwah* tillage systems were introduced in Adigudom, Tigray, Ethiopia for the last three years since 2005 with the aim to conserve moisture, reduce runoff and soil loss on farmers' fields, hence increasing crop yields on Vertisols. In Tigray, farmers use to make contour furrows at 2-4 m interval, locally called *terwah*, usually on teff to trap water for later crop use instead of being lost as runoff. Therefore, the objective of this study was to evaluate runoff and soil loss, and crop yield under conservation and conventional agriculture in Tigray, northern Ethiopia. Short-term effects on physical soil quality are reported elsewhere (Oicha *et al.* 2010a,b).

Material and methods

Study site

The experiment was conducted under rainfed conditions starting in 2005 in Adigudom (13°14'N, 39°32'E), Tigray, Northern Ethiopia. Tigray is characterized by a cool tropical semi arid climate, with recurrent drought induced by moisture stress. The mean annual rainfall (26 yr) is 505 mm, with more than 85% falling from June to September. Rainfall intensity can be very high, with about 60% of the rain having intensities of over 25 mm/h. Mean annual temperature is 23 ^{o}C and mean annual evapotranspiration amounts to 1539 mm. Sowing begins in mid June and harvesting ends in December. The farming system in the region is a mixed farming system with both crop and livestock. The main crops grown in Adigudom are teff (*Eragrostis tef*.), wheat (*Triticum sp*.), barley (*Hordeum sp*.), hanfets (mixture of barley and wheat), sorghum (*Sorghum bicolor* (L).Moench), millet (*Eleusine coracana*), maize (*Zeamays L.*) and lentil. The sowing method is generally broadcasting manually.

Experimental layout

The experimental layout was arranged as a randomized complete block design with two replications. The plot size was 5 m wide and 19 m long. The sowing method was manual broadcasting for both crops (wheat and teff) that were grown during the three growing seasons under study (2005-2007). The slope gradient was 3%. The soil under the experimental trial is classified as Calcic Vertisol according to the FAO-UNESCO classification, pelli Calcic Vertisol according to WRB and Typic Calciustert according to Soil Survey Staff. The different treatments were: (1) conventional tillage (TRAD) ploughed three times without residue, (2) Terwah (TERW) ploughed 3 times without residue and with furrows made at 1.5 m distance interval along the counter, and (3) permanent bed (PB) with 30% residue, zero tilled and 0.6 m wide beds. All the ploughing and reshaping of the furrows was made using *maresha*. Fertilizer was applied uniformly to all treatments. Glyphosate was applied to control pre-emerged weed in PB treatment. However, hand weeding was used as post emergence weed control in all treatments.

Data collected

Parameters such as runoff, soil loss and grain yield were collected. Runoff and soil loss were measured in 4.5 m long, 1.5 m wide (at the top) and 1 m deep collection trenches, which were located at the down slope end of each plot and lined with 0.5 mm thick plastic sheets. Runoff amount was determined at 8:00 am after each rainfall shower that caused erosion by measuring the height of the water level in the middle and at both sides of the trench. The trenches were calibrated for their volume by relating a known amount of water to water depth at the same three locations. The collected runoff water was then stirred thoroughly and 4 liter was taken from each trench to determine sediment concentration. These were filtered in the laboratory using funnel and Whatman # 12 filter papers. The sediment in the filter paper was oven dried for 24 hours at 105 °C and weighed. Grain yield was determined from 2 m by 8 m and 2 m by 6 m harvestable areas.

Results

Runoff and soil loss

There was a significant difference ($p<0.05$) in runoff among all treatments in the first year (2005) for wheat, with less runoff recorded in PB followed by TERW. However, there was no significant difference for runoff among all treatments in the second and third year (2006 and 2007) when the crop was teff and wheat, respectively (Figure 1). Even though non-significant, in 2006, the PB treatment has revealed a reduction in 50% runoff followed by 16% in TERW. There was a very similar trend in 2007 when the crop was wheat as compared to 2006. There was significant difference ($p<0.05$) in soil loss in 2005 and 2006 in wheat and teff, respectively. The soil loss reduction in 2005 for wheat was 76% in PB while 61% in TERW as compared to TRAD. Similarly, the reduction in soil loss was 86% in PB and 53% in TERW as compared to TRAD in 2006 for teff (Figure 2).

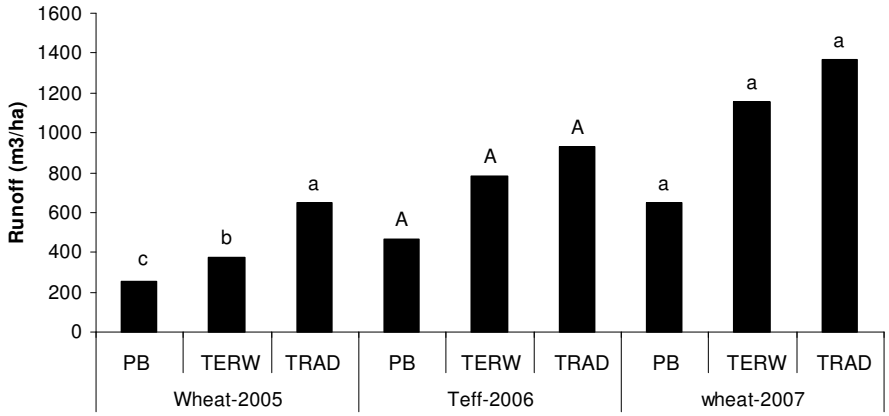

Figure 1. Average runoff amount from each treatment during the whole growing period across years in Adigudom. A letter on the top of each bar graph indicates the significant difference ($p<0.05$) among treatments per one year. PB = permanent bed tillage; TERW = *terwah* tillage; TRAD = conventional tillage.

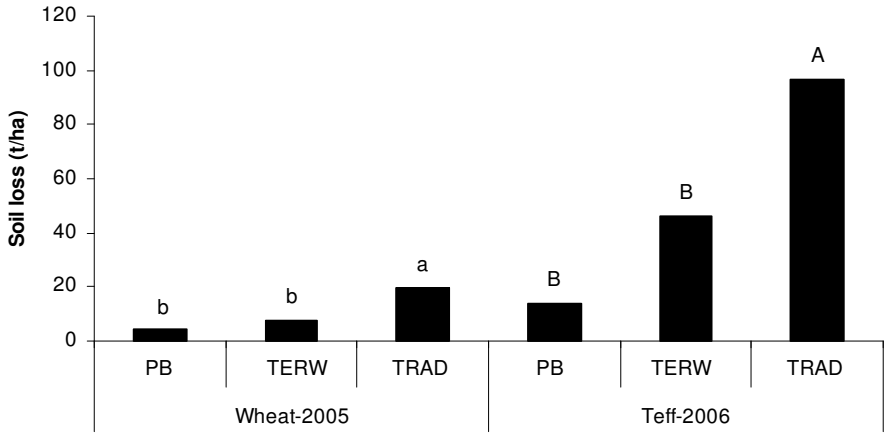

Figure 2. Average soil loss from each treatment during the whole growing period in 2005 and 2006 in Adigudom. A letter on the top of each bar graph indicates the significant difference ($p<0.05$) among treatments per one year. PB = permanent bed tillage; TERW = *terwah* tillage; TRAD = conventional tillage.

Yield performance

There was no significant difference ($p<0.05$) between treatments for wheat yield in 2005 and 2007. However, there was a significant difference among treatments in 2006 with higher teff yield obtained in TRAD followed by TERW. The lowest teff yield was recorded in PB. Although the difference was not significant, the yield of wheat in 2005 and 2007 showed that there was a higher yield record in PB followed by TERW. In contrast to the 2006 teff yield, the lowest wheat yield in both 2005 and 2007 was recorded in TRAD (Figure 3).

Conclusion

Based on the three years data, runoff was significantly reduced in PB followed by TERW as compared to TRAD in 2005. Although not significant, there was lower runoff in PB in 2006 and 2007. There was a significant difference for soil loss reduction which was lower in PB compared to TRAD. However, there was no significant difference for soil loss between PB and TERW. Although the difference was not significant, the yield of wheat

showed increment increase in both in 2005 and 2007. The yield of teff in 2006 was significantly lower in PB as compared to TRAD, which could be attributed to weed manifestation under PB and TERW. Specific attention should be paid to weed control while growing teff in PB and TERW systems.

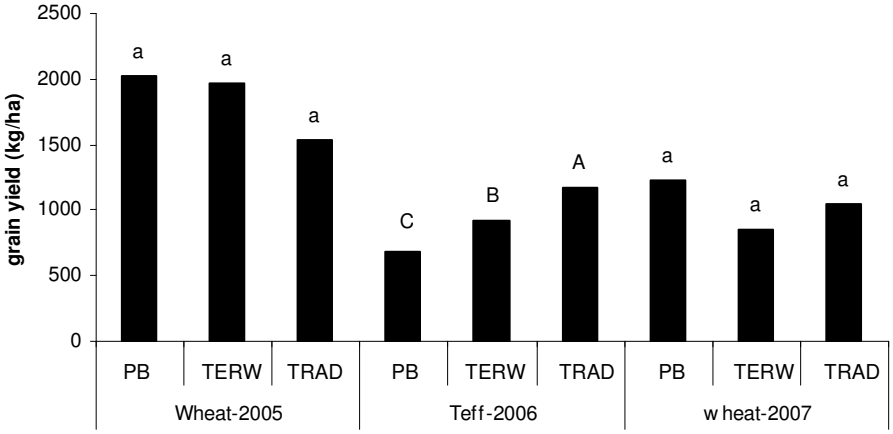

Figure 3. Average grain yield (kg/ha) trend in conservation and conventional agriculture across years in Adigudom. A letter on the top of each bar graph indicates the significant difference ($p<0.05$) among treatments per one year. PB = permanent bed tillage; TERW = *terwah* tillage; TRAD = conventional tillage.

References

Ahuja L , Ma L, Timlin D (2006) Trans-Disciplinary Soil Physics Research Critical to Synthesis and Modeling of Agricultural Systems. *Soil Science Society of America Journal* **70**, 311–326.

Deckers J, Spaargaren O, Nachtergaele F (2001). Vertisol: genesis, properties and soil scape management. In 'The sustainable management of Vertisols' (Eds K Syers, F Penning de Vries, P Nymundeza) pp. 3-20 (CABI publishing: New York).

Ermias A, Solomon A, Alemu E (2005) Small-scale reservoir sedimentation rate analysis for a reliable estimation of irrigation schemes economic lifetime. A case study of Adigudom area, Tigray, northern Ethiopia. Faculty of Dryland Agriculture and Natural Resources, Mekelle University.

Findeling A, Ruy S, Scopel E (2003) Modeling the effects of a partial residue mulch on runoff using a physically based approach. *Journal of Hydrology* **275**, 49-66.

Girma T (2001). Land Degradation: A Challenge to Ethiopia. *Environmental Management* **27**, 815-824.

Govaerts B, Sayre KD, Deckers J (2005) Stable high yields with zero tillage and permanent bed planting? *Field Crops Research* **94,** 33-42.

Mati BM (2006) 'Overview of Water and Soil Nutrient Management under Smallholder Rain-fed Agriculture in East Africa'. International Water Management Institute. Working Paper 105.

McHugh OV, Steenhuis TS, Abebe B, Fernandes E (2007) Performance of in situ rainwater conservation tillage techniques on dry spell mitigation and erosion control in the drought-prone North Wello zone of the Ethiopian highlands. *Soil and Tillage Research* **97**, 19-36.

Nyssen J, Govaerts B, Araya T, Cornelis WM, Bauer H, Haile M, Sayre K, Deckers J (2010) The use of the marasha ard plough for conservation agriculture in Northern Etiopia. *Agronomy for Sustainable Development* (in press).

Oicha T, Cornelis WM, Verplancke H, Nyssen J, Govaerts B, Behailu M, Haile M, Deckers J (2010a) Short-term effects of conservation tillage on soil (Vertisol) and crop (tef, *Eragrostis tef*) attributes in the northern Ethiopian highlands. In 'Proceedings of 19th World Congress of Soil Science, Soil Solutions for a Changing World, Brisbane'.

Oicha T, Cornelis WM, Verplancke H, Nyssen J, Govaerts B, Behailu M, Haile M, Deckers J (2010b) Short-term effects of conservation tillage on Vertisols under tef (*Eragrostis tef* (Zucc.) Trotter) in the northern Ethiopian highlands. *Soil and Tillage Research* **106**, 294-302.

Impacts of sodic soil amelioration on deep drainage

Lucy Reading[A], David A. Lockington[B], Keith L. Bristow[C] and Thomas Baumgartl[D]

[A]CRC for Irrigation Futures, University of Queensland, Queensland Department of Environment and Resource Management, 80 Meiers Rd, Indooroopilly, Qld 4072, Australia, Email Lucy.Reading@derm.qld.gov.au
[B]School of Civil Engineering, University of Queensland, St Lucia, Qld 4072, Australia, Email d.lockington@uq.edu.au
[C]CSIRO Water for a Healthy Country National Research Flagship and CRC for Irrigation Futures, PMB Aitkenvale, Townsville, QLD 4814, Australia, Email Keith.Bristow@csiro.au
[D]Centre for Mined Land Rehabilitation, University of Queensland, St Lucia, Qld 4072, Australia, Email t.baumgartl@uq.edu.au

Abstract
Groundwater tables are rising beneath irrigated fields in some areas of the Lower Burdekin in North Queensland, Australia. The soils where this occurs are predominantly sodic clay soils with low hydraulic conductivities. Many of these soils have been treated by applying gypsum or by increasing the salinity of irrigation water by mixing saline groundwater with fresh river water. While the purpose of these treatments is to increase infiltration into the surface soils and improve productivity of the root zone, it is thought that the treatments may have altered the soil hydraulic properties well below the root zone leading to increased groundwater recharge and rising water tables. In this paper we discuss the use of column experiments and HYDRUS modelling, with major ion reaction and transport and soil water chemistry-dependent hydraulic conductivity, to assess the likely depth, magnitude and timing of the impacts of surface soil amelioration on soil hydraulic properties below the root zone and hence groundwater recharge. In the experiments, columns of sodic clays from the Lower Burdekin were leached for extended periods of time with either gypsum solutions or mixed cation salt solutions and changes in hydraulic conductivity were measured. Leaching with a gypsum solution for an extended time period, until the flow rate stabilised, resulted in an approximately twenty fold increase in the hydraulic conductivity when compared with a low salinity, mixed cation solution. HYDRUS modelling was used to highlight the role of those factors which might influence the impacts of soil treatment, particularly at depth, including the large amounts of rain during the relatively short wet season and the presence of thick low permeability clay layers.

Key Words
Sodic soils, amelioration, gypsum, deep drainage

Introduction
In Australia, over 80% of the irrigated soils are sodic and irrigation management is closely linked with management of soil sodicity (Rengasamy and Olsson 1993). Sodic soils typically exhibit poor soil structural stability, low plant available water contents and low infiltration rates. Most of the irrigated soils in Australia need reclamation of sodicity, at least for the soil layers in the root zone (Rengasamy and Olsson 1993). When soils are successfully ameliorated, the leaching flux is expected to increase relative to surface runoff potentially increasing deep drainage rates (Rengasamy and Olsson 1993).

Sodic soils are prevalent in the Lower Burdekin irrigation area in North Queensland, Australia (Figure 1). While there are adequate supplies of fresh water for irrigation, there is a lack of sub-surface drainage and a number of areas have problems due to rising groundwater tables. Applications of gypsum or irrigation waters with increased salinity have been used to improve soil structural stability and hydraulic properties, but there is now a concern that the whole soil profile may be affected thus enhancing recharge and impacting groundwater tables. To assess the likelihood of this occurring, the expected magnitude, depth and timing of increases in soil hydraulic conductivity in response to these treatments needs to be determined.

Methods
Soil Properties
The soil used in this study was collected from an irrigated sugarcane field in the Lower Burdekin. The soil used was collected from the B horizon, 0.6 to 1.1 metres below the ground surface, by digging a soil pit and obtaining soil from the wall of the pit. The soils are clay soils with high sodicity levels (Table 1). The Exchangeable Sodium Percentage (ESP) of these soils places them in the strongly sodic category based on Australian soil classifications (Northcote and Skene 1972).

1 – 6 August 2010, Brisbane, Australia. Published on DVD.

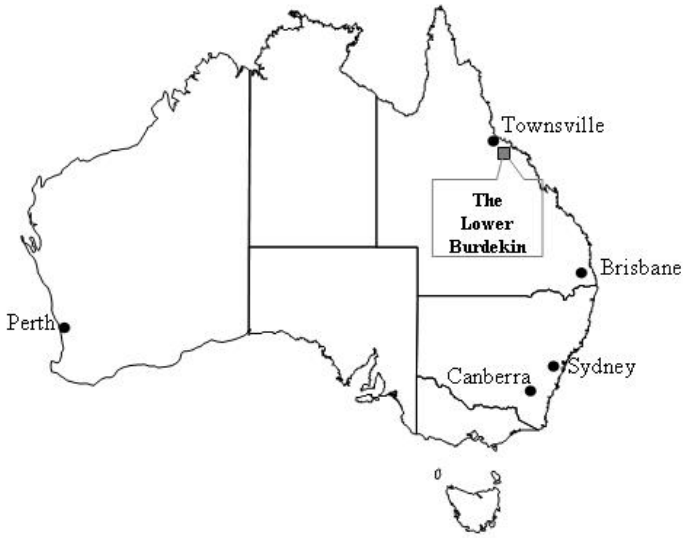

Figure 1. Location of the Lower Burdekin in North Queensland, Australia.

Table 1. Soil properties for the soils used in these experiments based on five samples from the same site.

Sample	pH†	Exchangeable Calcium (meq/100g)	Exchangeable Magnesium (meq/100g)	Exchangeable Sodium (meq/100g)	ESP‡ (%)	CEC (meq/100g)	Clay (%)
A	8.8	11.1	14.3	5.2	17.3	30	66
B	8.8	10.2	13.6	4.9	16.9	29	69
C	8.8	10.9	14.2	5.4	18	30	70
D	8.9	11	13.9	5.2	17.3	30	68
E	8.9	11.1	13.6	4.2	14.6	29	67
Mean	8.8	10.9	13.9	5	16.8	30	68
Standard deviation	0.1	0.4	0.3	0.5	1.3	1	2

† pH = pH of 1:5 soil solution extract
‡ ESP = Exchangeable Sodium Percentage
¶ CEC = Cation Exchange Capacity

Column leaching experiments
Column leaching experiments were used to investigate changes in hydraulic conductivity for sodic clays from the Lower Burdekin, in response to changes in applied solution chemistry. The soil columns were prepared by oven drying the soil, grinding it, sieving it to obtain the <2 mm fraction and packing it into columns with 5.4 cm diameter and 4 cm height. The soil columns were wet from the bottom using the percolating solution. Hydraulic conductivity was then determined by measuring the flow rate whilst continuing to apply the percolating solution using a constant head apparatus.

Two sets of experiments were conducted to determine the changes in soil hydraulic conductivity that occur when a) a saturated gypsum solution and b) mixed cation solutions of varying salinity are applied.
In the first set of experiments, a saturated gypsum solution was applied and the primary aim was to determine the potential for increases in hydraulic conductivity in response to gypsum applications. A low salinity irrigation water surrogate was used for comparison with the gypsum solution results.

As the measured field bulk densities were approximately 1.9 g/cm^3, much higher than the bulk densities typically used in laboratory experiments with repacked columns, the influence of bulk density was also investigated by using columns packed at two bulk densities, 1.3 g/cm^3 and 1.4 g/cm^3. Five replicates were used for each of these bulk densities.
The second set of experiments was designed to determine the influence of salt concentration on hydraulic conductivity after the methods of McNeal (1968). Measurement of hydraulic conductivity at two salt concentrations was recommended by McNeal (1968). In this study, 100 meq/L and 50 meq/L solutions containing calcium chloride, magnesium chloride and sodium chloride were used with three replicates for each salt concentration.

For both sets of experiments, the leaching was continued until a stable flow rate was achieved. The electrical conductivity, pH and cation concentrations of the leachate solutions were measured to determine when chemical equilibration with the applied solution had occurred.

HYDRUS modelling
HYDRUS-1D models were set up using the properties of the sodic clays used in the column experiments to determine whether the trends observed in the laboratory could be simulated using HYDRUS. Subsequent modelling efforts focused on determining the influence of the initial soil sodicity and hydraulic conductivity on deep drainage rates after amelioration. In addition, the influence of large amounts of rain during the wet season on soil properties and deep drainage rates was investigated.

Results
The bulk density of the repacked columns had a significant effect on the maximum hydraulic conductivity when saturated gypsum solutions were applied. The maximum hydraulic conductivity for the columns packed at 1.3 g/cm^3 was approximately five times greater than the maximum hydraulic conductivity for the columns packed at 1.4 g/cm^3 (Figure 2). The variability in the measurements was also significantly greater. The standard deviation for the columns packed at 1.3 g/cm^3 was approximately ten times greater than the S.D. for the columns packed at 1.4 g/cm^3.

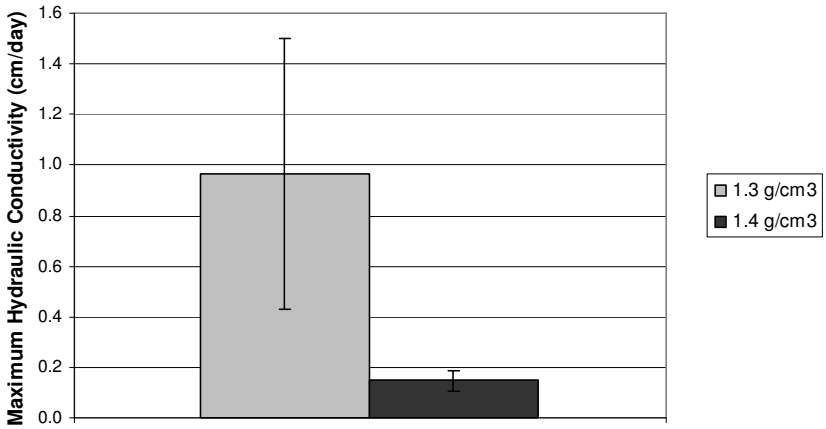

Figure 2. Maximum hydraulic conductivity with gypsum applied to soil columns packed at two different bulk densities. The mean and the standard deviation of the measurements are shown.

The maximum hydraulic conductivity measured for the columns leached with a saturated gypsum solution was approximately half of the maximum hydraulic conductivity measured for the columns leached with a 100 meq/L mixed cation salt solution, but approximately four times the maximum hydraulic conductivity measured for the columns leached with a 50 meq/L mixed cation salt solution (Figure 3). For the columns leached with a saturated gypsum solution, there was a gradual increase in hydraulic conductivity during the leaching period. This increase in hydraulic conductivity is due to the combined impacts of electrolyte effects and reductions in soil sodicity. The final hydraulic conductivity for the soil columns leached with a saturated gypsum solution was approximately twenty times larger than the final hydraulic conductivity for soil columns leached with a low salinity irrigation water surrogate.

Whereas the column experiments have been used to determine the maximum effects of varying solution chemistry on hydraulic conductivity after continuous leaching of the soils, HYDRUS modelling has been used to simulate a range of scenarios applicable to field conditions. For example, the depth of the profile affected as a result of the combined effects of irrigation, sporadic gypsum applications and intermittent rainfall was investigated. The results of the HYDRUS modelling indicate that the initial soil sodicity and the initial soil hydraulic properties have a large influence on the changes in deep drainage rates that would be expected in response to different soil treatments (Figure 4). For high initial sodicity levels, i.e. exchangeable sodium percentages of equal to or greater than 33.8, less of the profile was ameliorated and the corresponding deep drainage rates were much lower.

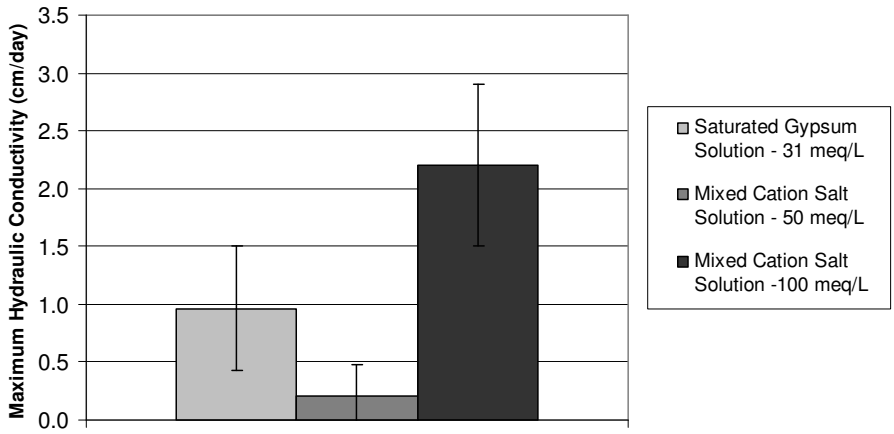

Figure 3. Maximum hydraulic conductivity with gypsum applied vs maximum hydraulic conductivity with mixed cation salt solutions applied. The mean and the standard deviation of the measurements are shown.

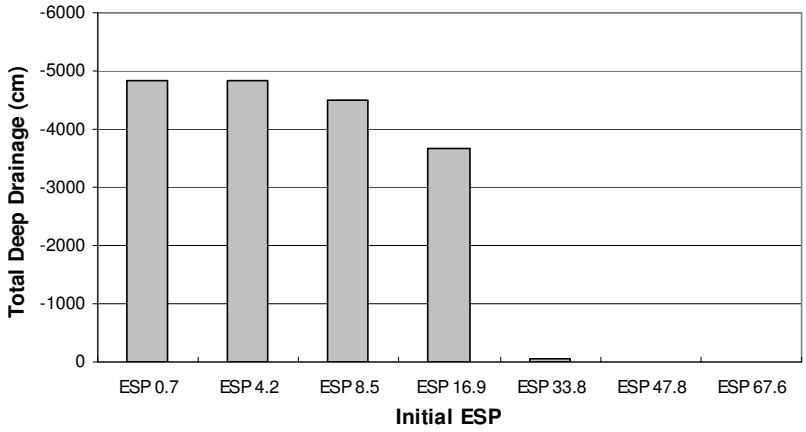

Figure 4. Impact of initial soil sodicity on total deep drainage rates after ten years of continuous gypsum applications.

Conclusion

The changes in hydraulic conductivity in response to gypsum applications and increased salinity waters were measured. Leaching with a saturated gypsum solution until the flow rate stabilised resulted in an approximately twenty fold increase in the hydraulic conductivity when compared with a low salinity, mixed cation solution. The maximum hydraulic conductivity when a 100 meq/L salt solution was applied was significantly higher than the maximum hydraulic conductivity when the saturated gypsum solution was applied.

Findings from the column experiments and HYDRUS-1D modelling are being used to improve understanding of the impact of long term treatment with gypsum or saline irrigation water on sodic soils. This is needed to test the validity of current practices in which water management in the Lower Burdekin is being informed by regional hydrology modelling with groundwater recharge estimated using static soil hydraulic properties.

References

McNeal BL (1968) Prediction of the Effect of Mixed-Salt Solutions on Soil Hydraulic Conductivity. *Soil Science Society of America Proceedings* **32,** 190-193.

Northcote KH, Skene JKM (1972) 'Australian Soils with Saline and Sodic Properties'. (CSIRO: Melbourne).

Rengasamy P, Olsson KA (1993) Irrigation and Sodicity. *Australian Journal of Soil Research* **31,** 821-837.

In situ soil water repellency is affected by soil water potential rather than by water content as revealed by periodic field observations on a hill slope in a Japanese humid-temperate forest

Masako Kajiura[A] and Takeshi Tange[B]

[A] Department of Forest Science, Graduate School of Agricultural and Life Sciences, University of Tokyo, 1-1-1 Yayoi, Bunkyo-ku, Tokyo, Japan, Email kajiura@fr.a.u-tokyo.ac.jp
[B] Department of Forest Science, Graduate School of Agricultural and Life Sciences, University of Tokyo, 1-1-1 Yayoi, Bunkyo-ku, Tokyo, Japan, Email tange@fr.a.u-tokyo.ac.jp

Abstract
To evaluate spatio-temporal occurrence of *in situ* soil water repellency in relation to soil moisture conditions, we periodically conducted field surveys in a humid-temperate forest in Japan. Measurements were made in 4 plots across a hill slope. Each plot contained 2 permanent quadrats (30 × 55 cm) with 48 measurement points per quadrat, where volumetric water content and water repellency of surface soil were measured. Most measurement points had critical water contents (CWC) below which soils repel water and above which soils were wettable. We assumed that the median CWC at 96 points per plot was the representative CWC (RCWC) for a plot, and estimated representative critical water potential (RCWP) from RCWC using water retention curves. RCWC differed, but RCWP was similar (pF = 3.5–4.0), between plots. Furthermore, water potential described the spatial fraction showing water repellency better than water content. These results suggest that water potentials, rather than moisture contents, are more indicative of the spatial occurrence of soil water repellency on hill slope areas. In the study site, surface soils on upper hill slopes tend to be drier and more frequently water repellent than lower parts, implying a greater tendency to generate surface runoff with rainfall events.

Key Words
Water repellent soil, water content, water potential, soil properties, spatial variability, temporal variability

Introduction
Soil water repellency, which has been observed worldwide, affects water movement such as surface runoff (DeBano, 2000; Doerr *et al*., 2000). Knowledge of water repellency distribution in soil surfaces would be useful in predicting the intensity of surface runoff on hill-slopes (Miyata *et al*., 2007). However, it is difficult to estimate water repellent areas by direct measurement when surface runoff occurs (Doerr and Moody, 2004), thus predictive indicators for water repellency need to be established.
Soil water potential might serve as a practical indicator for judging whether soil repels water without measuring water repellency *per se*. Disturbed soils that are potentially water repellent are reported to be so below water potentials of pF ≈3 and to be wettable above the water potentials (pF < ≈3) regardless of organic matter content or soil texture (de Jonge *et al*., 2007; Kawamoto *et al*., 2007; Kobayashi and Shimizu, 2007). We therefore postulated that soil water potential is indicative of water repellency across soils with varying physicochemical properties, even under field conditions. However, as most previous studies have used disturbed soil samples, there is inadequate information on the relationship between soil water potentials and water repellency under field conditions.
This study was undertaken to determine whether and how soil water potentials at soil depths of 0–5 cm indicated soil surface water repellency across a hill slope with varying soil properties; sites were within a humid-temperate forest in Japan. We also aimed to understand topographical conditions that influence water repellency within a hill slope.

Methods
Study site and soil properties
The study site was located in a humid-temperate forest administered by the Arboricultural Research Institute, University of Tokyo, Shizuoka, Japan (34°69′N, 138°8′E). Mean annual precipitation was 2,430 mm and mean annual temperature was 15.3°C in the period 2006–2007. We established 4 measurement plots located on different hill slope elements: P1 and P2 on a ridge, P3 on a shoulder, and P4 on mid-slope. The vegetation was secondary forest dominated by *Castanopsis sieboldii* (in all plots); *Alnus sieboldiana* and *Prunus jamasakura* also occurred in plots P2, P3, and P4.
We categorized soil structure by visual and hand inspection, and measured bulk densities using 100 cm^3 core

1 – 6 August 2010, Brisbane, Australia. Published on DVD.

samples to 5 cm depth. We took disturbed soil samples from the surface layer, (5 × 5 cm area, 1 cm depth) and ≈100 cm^3 samples from 0–5 cm depth. All samples were air-dried and dry-sieved through a 2 mm mesh. We determined soil textures, soil organic carbon (SOC) contents, C/N ratios, and soil pH (H_2O) of the 0–5 cm depth samples, and SOC contents and soil water repellency of the 0–1 cm depth samples. We performed particle size analysis by the wet sieving and pipette method (Gee and Or, 2002), and classified soil textures according to the system of the International Union of Soil Science. Total carbon and total nitrogen contents were measured with a NCS analyzer (NA 1500; Carlo Erba Instruments, Milan, Italy), and C/N ratios were calculated. The SOC was assumed to represent total carbon because soil samples were not calcareous. Soil pH (H_2O) was measured using a pH meter (D-24; Horiba Ltd., Kyoto, Japan) in 1:2.5 soil:water suspensions. Soil water repellency was measured by the molarity of ethanol droplets test (MED test) (King, 1981). We put subsamples >5 mm thick into plastic cups and dripped an ethanol solution (0–5 M range, applied at 0.2 M concentration intervals) through a pipette onto the flattened soil surface. We recorded the MED values as the lowest molarity of ethanol solution that was able to penetrate soil surfaces within 10 s. Water retention curves were made using the hanging water column method (pF = 0.0–2.1), the pressure plate method (pF = 2.1–3.7), and a psychrometer (pF > 3.7) (Dew Point Microvoltmeter HR-33T; Wescor Inc., Utah, USA) for soils sampled from 0–5 cm depth in mineral soils adjacent to quadrats in each plot (Dane and Hopmans, 2002a, b). The soil water potentials and soil water contents were fitted using the bimodal Kosugi soil water retention model (Seki, 2007).

Water repellency and water condition of surface soils

We established 2 permanent quadrats (each 30 × 55 cm) within each plot. At 48 points within each quadrat, we measured *in situ* water repellency and actual volumetric soil water content about twice a month during the period September 2006 to December 2007 (19–21 observations in total).We assumed that a soil was "water repellent" when water droplets remained on the surface for > 10 s (MED > 0 M), and was "wettable" when the retention time was < 10 s (MED = 0 M). We calculated the percentage of positions that were water repellent (proportion of 48 points) as a representative index of water repellency for each quadrate. Volumetric water content of the surface layer soil (0–5 cm depth) was measured using a soil moisture probe (ML2x Theta Probe; Delta-T Devices Ltd., Cambridge, UK) at points in quadrats adjacent to positions at which water repellency were measured. The sensor output was calibrated against water content for each plot. We determined the representative actual water contents of each quadrate (RAWC) as the median volumetric water contents of 48 points, and estimated the representative actual water potentials (RAWC) from RAWC and the soil water retention curve obtained for each plot.

Critical soil water conditions for soil water repellency

We determined the critical water content (CWC), above which the soil surface is wettable and below which it is water repellent, at every measurement point in each quadrate (48 points/quadrat). The CWC was calculated as the mean of the largest water content showing water repellency and the smallest water content when the soil was wettable. We determined the representative critical water content (RCWC) of each plot as the median CWC of 96 points (48 points × 2 quadrates) because there were similar frequency distributions of CWC in the 2 quadrats within each plot. We further estimated the representative critical water potential (RCWP, in terms of pF) from RCWC and the soil water retention curve obtained for each plot.

Results and discussion

Soil properties

Soil properties at 0–5 cm depth differed between plots; P4 had a less developed soil structure and a lower bulk density, P1 was less clayey and had a higher C/N ratio, and P2 had a lower SOC content than other plots (Table 1). All plots exhibited water repellency in air-dried 0–1 cm samples, except for one of 3 samples from P4 (MED = 0) (Table 1). The water retention curve of P1 differed from those of other plots, with lower soil water content at the same water potential when pF was >1.5. The relatively sandy texture in P1 may have caused this difference, as soil texture significantly affects water retention.

Table 1. Surface soil properties at each plot.

Plot ID	0–5 cm depth					0–1 cm depth	
	Soil structure	Bulk density (g cm^{-3})	Soil texture	SOC content (%)	C/N	SOC content (%)	Soil water repellency (M)
P1	Moderately granular	0.65 (0.03, n = 3)	Sandy clay loam	7.6 (1.6, n = 6)	24 (3, n = 6)	14 (4, n = 8)	2.7 (0.3, n = 8)
P2	Moderately granular	0.67 (0.03, n = 3)	Heavy clay	4.6 (0.9, n = 5)	13 (1, n = 5)	15 (5, n = 6)	2.9 (1.2, n = 6)
P3	Moderately angular blocky	0.69 (0.04, n = 2)	Heavy clay	7.5 (1.6, n = 6)	14 (1, n = 6)	12 (2, n = 3)	2.3 (1.1, n = 3)
P4	Weakly crumb	0.59 (0.07, n = 3)	Light clay	7.5 (1.1, n = 5)	14 (1, n = 5)	11 (2, n = 3)	0.5 (0.6, n = 3)

Representative critical water content (RCWC) versus representative critical water potential (RCWP)
The RCWC was 0.16, 0.29, 0.28, and 0.27 m^3 m^{-3} for P1, P2, P3, and P4, respectively. RCWC in P1 was markedly lower than the other plots. On the other hand, RCWP values were similar between plots; pF = ≈3.7; 3.8, 3.9, 3.6, and 3.5 for P1, P2 P3, and P4, respectively. These results, which are consistent with previous work on disturbed soils, indicate strongly that RCWP is a more robust indicator of water repellency than RCWC at our study site where soil characteristics (soil structure, bulk density, soil texture, SOM contents, C/N ratio) and topographic conditions differed between plots (Table 1) (de Jonge *et al*., 2007; Kawamoto *et al*., 2007).
We found a poor relationship between RCWC and SOC contents (p = 0.54). This is inconsistent with previous studies on disturbed soils that showed a positive relationship between critical water contents and SOM contents (Regalado and Ritter, 2005; de Jonge *et al*., 2007; Kawamoto *et al*., 2007). Differences in RCWC may be largely attributable to different water-retention capacities, which in turn depend not only on soil organic matter contents but also on soil texture or other soil properties.

Critical soil water condition as an in situ indicator of 50%-area water repellency
The drier the soil, the larger was the water-repellent area (Figure 1). The relationship between RAWC and areal fraction of water repellency in P1 differed from other plots (Figure 1-a), whereas the relationships with representative actual soil water potentials for a quadrat (pF) (RAWP) were similar for all plots (Figure 1-b). Hence, RAWP explains the proportion of water-repellent area on soil surfaces better than RAWC at this study site, where soils varied in physicochemical properties and topographical conditions. The percentage area that was water repellent was well approximated against pF by a sigmoidal curve: $y = \alpha - \alpha / (1+e^{(x-\beta)/\gamma})$ where α, β, γwere 100, 3.7, and 0.25, respectively, and R^2 was 0.79.
We expect that half an area may be water repellent when RAWP is close to RCWP, although it is *not* mathematically proven. Observed data showed that about half the area of a quadrat was water repellent when RAWP was RCWP (pF = ≈ 3.7) (Figure 1-b). This also indicates that RCWP is actually "representative" in the sense that it may inform us whether or not more than half the area is water repellent.
The parameter α in the regression curve corresponds to the fraction of area (%) having the potential for water repellency. We set α as 100 because most measurement points showed actual water repellency and most 0–1 cm depth samples showed water repellency when air-dried (Table 1, Figure 2). If α is smaller than 100, the water-repellent area at RCWP is <50%. In that case, the spatial fraction of water repellent area may be determined not only by soil water potentials but also by the fraction of area having the potential for actual water repellency.

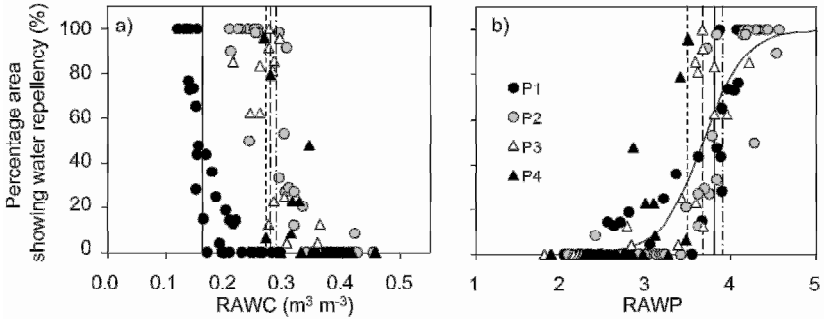

Figure 1. Percentage area showing water repellency as a function of soil water condition calculated from the number of water-repellent points divided by total observation points (48 points per quadrat). The x axis in (a) is representative water content for a quadrate (RAWC), which is identical to the median of 48 water contents in a quadrat; the x axis in (b) is representative water potential (pF) for a quadrat (RAWP) estimated from RAWC and water retention curves. Each point is a measure at each quadrat on each observation date. The same symbols are used for the 2 quadrates (a, b) in each plot. Solid line, dashed-dotted line, dashed line, and dotted line represent critical water conditions of P1, P2, P3, and P4, respectively. The sigmoidal curve was fitted against data for all plots, $y = 100-100/[1 + e^{(x - 3.7)/0.25}]$ ($R^2 = 0.79$).

Temporal distribution of water repellency as affected by topographic position
We estimated the common RCWP (50%-area water repellency) for all plots to be pF = 3.7 from the sigmoidal regression curve. Temporal fractions (against total observation dates) of RAWP drier than pF = 3.7 were highest at P1 and P2 (37% and 40%, respectively) which were located on ridges, were lower at P3 (15%) on the shoulder slope, and the lowest at P4 (0%) located on a mid-slope. These results were consistent with the temporal frequency in appearance of soil water repellency in each plot (Figure 2). Collectively, our results show that surface soils on upper hill slopes tend to be drier and, as a result, water repellent more than twice as often as lower slopes. This implies a greater tendency to generate surface-runoff with rainfall events at these topographic locations.

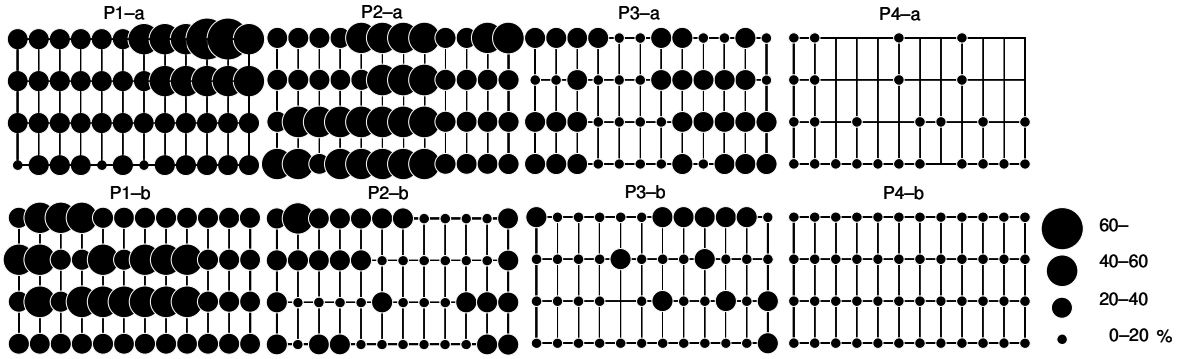

Figure 2. Proportion of occasions (percentage of 19–21 observations made between September 2006 and December 2007) when soils were water repellent at points within quadrats. Each lattice represents a quadrat within which measurements were made at 48 points. Each plot (P1–P4) consisted of 2 quadrats (a, b) . The size of each black circle represents the proportion of measurement occasions when soils were water repellent. The absence of a circle at lattice intersections indicates the soil was always wettable and was never water repellent at that position. P1 and P2 are located on a ridge, P3 on a shoulder slope, and P4 on a mid-slope.

Conclusion

Time-series field observations in a humid-temperate forest indicates that soil water potential, rather than soil water contents, at 0-5 cm soil depth is a practical indicator of the spatial occurrence of water repellency on soil surfaces in areas with varying physicochemical soil properties on hill slopes. We further suggest that the representative critical water potential (pF = ≈3.7) corresponds to a moisture condition with 50%-areal water repellency, given that the whole soil surface had a potential to repel water under certain water conditions, as observed in this study.

References

Dane JH, Hopmans JW (2002a) Hanging water column. In 'Methods of Soil Analysis Part 4. SSSA Book Series *5*' (Eds. Dane JH, Hopmans JW), pp. 680-683. Soil Science Society of America: Madison.

Dane JH, Hopmans JW (2002b) Pressure cell. In 'Methods of Soil Analysis Part 4. SSSA Book Series 5' (eds. Dane JH, Hopmans JW), pp. 684-688. Soil Science Society of America: Madison.

DeBano LF (2000) Water repellency in soils: A historical overview. *Journal of Hydrology* **231**, 4-32.

de Jonge LW, Moldrup P, Jacobsen OH (2007) Soil-water content dependency of water repellency in soils: effect of crop type, soil management, and physical-chemical parameters. *Soil Science* **172**, 577-588.

Doerr SH, Moody JA (2004) Hydrological effects of soil water repellency: on spatial and temporal uncertainties. *Hydrological Processes* **18**, 829-832.

Doerr SH, Shakesby RA, Walsh RPD (2000) Soil water repellency: its causes, characteristics and hydro-geomorphological significance. *Earth-Science Reviews* **51**, 33-65.

Gee GW, Or D (2002) Particle-size analysis. In 'Methods of soil analysis, Part 4. SSSA Book Series 5' (Eds. Dane JH, Hopmans JW), pp. 255-293. Soil Science Society of America: Madison.

Kawamoto K, Moldrup P, Komatsu T, de Jonge LW, Oda M (2007) Water repellency of aggregate size fractions of a volcanic ash soil. *Soil Science Society of America Journal* **71**, 1658-1666.

King PM (1981) Comparison of methods for measuring severity of water repellence of sandy soils and assessment of soil factors that affect its measurement. *Australian Journal of Soil Research* **19,** 275-285.

Kobayashi M, Shimizu T (2007) Soil water repellency in a Japanese cypress plantation restricts increases in soil water storage during rainfall events. *Hydrological Processes* **21**, 2356-2364.

Miyata S, Kosugi K, Gomi T, Onda T, Mizuyama T (2007) Surface runoff as affected by soil water repellency in a Japanese cypress forest. *Hydrological Processes* **21**, 2365-2376.

Regalado CM, Ritter A (2005) Characterizing water dependent soil repellency with minimal parameter requirement. *Soil Science Society of America Journal* **69**, 1955-1966.

Seki K (2007) SWRC Fit – A nonlinear fitting program with a water retention curve for soils having unimodal and bimodal pore structure. *Hydrology and Earth System Sciences Discussions* **4,** 407-437.

Increases in available water content of soils by applying bagasse-charcoals

Koji Kameyama[A], Teruhito Miyamoto[A] and Yoshiyuki Shinogi[A]

[A]Department of Agricultural Land and Water Resources, National Institute for Rural Engineering, National Agricultural and Food Research Organization, Tsukuba, Ibaraki, Japan, Email kojikame@affrc.go.jp

Abstract
Biochar is charcoal produced from pyrolysis of biomass. Application of biochar with fine pore structures to agricultural soil may enhance the availability of water to crops. Miyako Island (target area) is located in a subtropical zone and consists of highly permeable coral limestone. The land surface is covered with calcareous soil called "Shimajiri-Maji". Because the soil has low available water for crops, land application of biochar to the soil may be used to reduce irrigation water needed for crops. The main biomass resource on the island is sugarcane bagasse because agriculture is the main industry and sugarcane is cultivated in approximately 80% of the farmland. Therefore, increases in available water content of the Shimajiri-Maji soil and Toyoura sand by applying bagasse-charcoal was evaluated in this study. The results were as follows: (1) Available water contents of the two soils were increased by application of bagasse-charcoal. The available water contents did not significantly differ with carbonization temperatures. (2) Available water contents of the two soils were proportionally increased by application of more bagasse-charcoal. Therefore, the need for irrigation water can likely be proportionally reduced by application of more bagasse-charcoal to these soils.

Key Words
Biochar, water retention curve, soil amendment, cay-rich soil, sand

Introduction

Biochar is charcoal produced from pyrolysis of biomass. Biochar may affect soil physical properties such as soil water retention and these effects may enhance the water available to crops (Glaser *et al.* 2002). Miyako Island (target area) is located in a subtropical zone and consists of coral limestone with high permeability. The land surface is covered with calcareous soil that is called "Shimajiri-Maji". The soil is clay-rich and the available water content for crops is low. Therefore, application of biochar with fine pore structures to the soil is expected to increase the available water content and reduce irrigation water needed for crops. The main biomass resource on the island is sugarcane bagasse because agriculture is the main industry and sugarcane is cultivated in approximately 80% of the farmland. Clay-rich soils and sand-rich soils, including sand, have low available water content for crops. In addition, the properties of biochar differ depending on the pyrolysis conditions, especially pyrolysis temperature (Downie *et al.* 2009).Therefore, increases in available water content of clay-rich soil (Shimajiri-Maji) and sand (Toyoura sand) by applying bagasse-charcoals were evaluated. Subsequently, the effects of carbonization temperature of bagasse-charcoal on available water content of the two soils were also evaluated.

Methods

Preparation of samples

Sugarcane bagasse, the residue from pressing sugarcane stalks to extract juice in a sugar factory, were air-dried and heated in a batch-type carbonization furnace at three different carbonization temperatures (400, 600 and 800°C) with a holding time of 2 h. The bagasse charcoals were sieved with a 2 mm-mesh for measurements of the water retention curve. Shimajiri-Maji soil and Toyoura sand were also air-dried and sieved with a 2 mm-mesh for the water retention curve measurements. The physicochemical properties of the bagasse-charcoal and soils were also measured.

Water retention curves of charcoal-amended soils

The water retention curves express the relationship between water content and matric potentials. We used the hanging water column method to obtain the retention curves at high matric potentials (>-3 kPa) and the pressure extractor method to obtain the retention curves at low matric potentials (-3 ~ -1,500 kPa). Measurements were made for charcoal-amended soils. The gravimetric charcoal content in soils amended by bagasse-charcoals at 400, 600 and 800°C of carbonization temperature was 3 wt % to study effects of carbonization temperatures on water retention and available water content of soils. The gravimetric charcoal contents in soils amended by bagasse-charcoal at 800°C were 1, 3, 5 and 10 wt % to study effects of charcoal contents.

1 – 6 August 2010, Brisbane, Australia. Published on DVD.

Results

Physicochemical properties of bagasse-charcoal and soils

The physicochemical properties of bagasse-charcoal at different carbonization temperatures are shown in Table 1. The pH value of the bagasse-charcoal varied from 5.0 at 400ºC to 9.8 at 800ºC. The cation exchange capacity (CEC) decreased, while the total carbon (T-C) and particle density increased with increasing carbonization temperature. Assuming that the ranges of matric potential of available water for crops were -33 to -1,500 kPa, the diameter of the capillary pores corresponding with the matric potentials were calculated from 200 to 9,000 nm. Pore volumes for 200 to 9,000 nm of bagasse-charcoal were not significantly different with carbonization temperatures. The physicochemical properties of the two soils used in this study are shown in Table 2. Shimajiri-Maji soil contained a lot of clay, while Toyoura sand contained only sand.

Table 1. Physicochemical properties of bagasse-charcoal at different carbonization temperatures.

Carbonization temp.	pH[*1]	CEC(pH7)[*2]	Total-C	Total-N	Particle Density	BET surface area[*3]	Pore volume[*4] (200–9000 nm)
ºC		$cmol_c$ /kg	%	%	g/cm^3	m^2/g	cm^3/g
400	5	12.2	72.1	0.4	1.5	10.8	1.72
600	7.7	10.4	84.2	0.2	1.56	179	1.6
800	9.8	4.4	85.2	0.2	1.86	126	1.33

*1 charcoal:solution＝1 g:25 mL
*2 Shollenbergar method
*3 N_2 adsorption method
*4 Mercury intrusion method

Table 2. Physicochemical properties of Shimajiri-Maji soil and Toyoura sand.

	pH[*1]	CEC(pH7)[*2]	Org.-C	C/N	Particle Density	Sand (>0.02 mm)	Silt (0.002–0.02 mm)	Clay (<0.002 mm)
		$cmol_c$ /kg	g /kg		g/cm^3	%	%	%
Shimajiri-Maji	8.0	11.2	13.4	8.4	2.8	7.7	19.0	73.3
Toyoura sand	6.6	0.5	0	-	2.6	100	0	0

*1 soil : solution＝5 g:25 mL
*2 Shollenbergar method

Effects of carbonization temperature on water retention properties of soils

The water retention curves of Shimajiri-Maji soil and Toyoura sand amended with 3 wt % of bagasse-charcoals at three different carbonization temperatures are shown in Figures 1 and 2, respectively. Near saturation, volumetric water content of charcoal-amended soils was 400ºC<600ºC=800ºC. Tars that have water repellency remain in charcoal at low pyrolysis temperatures but are volatilized and almost disappear above 600ºC (Amonette and Joseph 2009).Therefore, the differences in volumetric water content near saturation may be caused by water repellency of tar. Except for near saturation, water retention properties of charcoal-amended soils did not significantly differ with carbonization temperature. At matric potentials less than -10 kPa, the volumetric water content of Shimajiri-Maji amended with charcoal were slightly lower than the original Shimajiri-Maji soil. The result showed that water in the pores of the charcoal is easily released while water adsorbed by clay in the soil is scarcely released at low matric potentials.

Available water content (-33 ~ -1,500 kPa) of Shimajiri-Maji soil and Toyoura sand amended with 3 wt % of bagasse-charcoal at three different temperatures is shown in Figure 3. Available water content of both clay-rich soil (Shimajiri-Maji) and sand (Toyoura sand) increased with application of bagasse-charcoal. In addition, the available water content of the two soils did not differ significantly with carbonization temperature. Therefore, the irrigation water needed for crops can likely be reduced by application of bagasse-charcoal to these soils.

Effects of charcoal content on water retention properties of soils

The water retention curves of Shimajiri-Maji soil and Toyoura sand amended with 0–10 wt % of bagasse-charcoal at 800°C are shown in Figures 4 and 5, respectively. The water retention of Toyoura sand was enhanced with application of more charcoal.

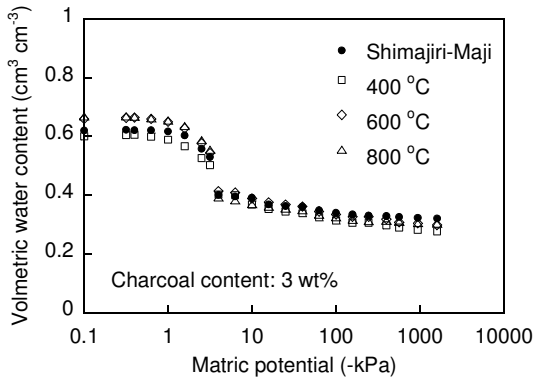

Figure 1. Water retention curves of Shimajiri-Maji soil amended with bagasse-charcoals at three different carbonization temperatures.

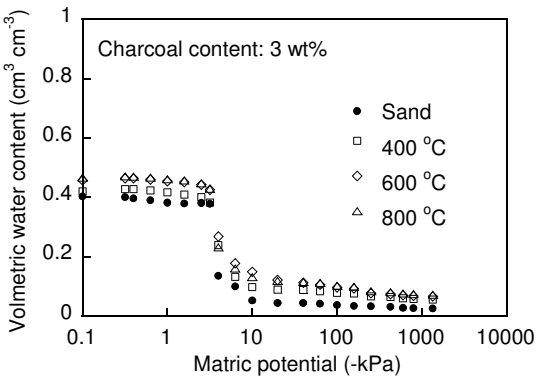

Figure 2. Water retention curves of Toyoura sand amended with bagasse-charcoals at three different carbonization temperatures.

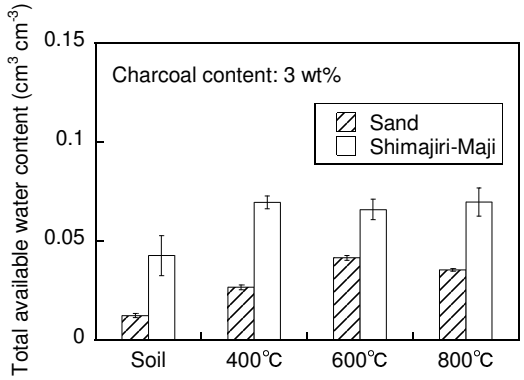

Figure 3. Available water content of soils amended with bagasse-charcoals at three different carbonization temperatures.

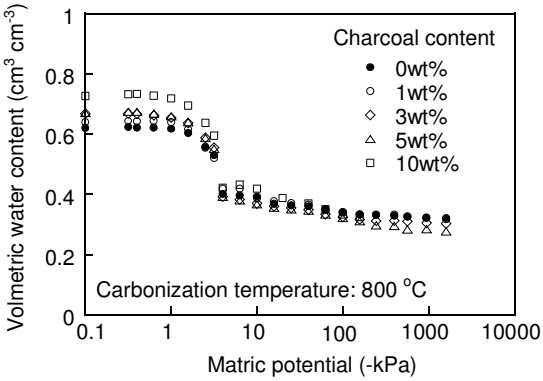

Figure 4. Water retention curves of Shimajiri-Maji soil amended with bagasse-charcoal at 800°C.

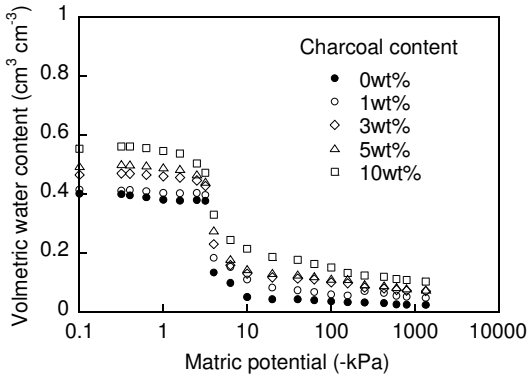

Figure 5. Water retention curves of Toyoura sand amended with bagasse-charcoal at 800°C.

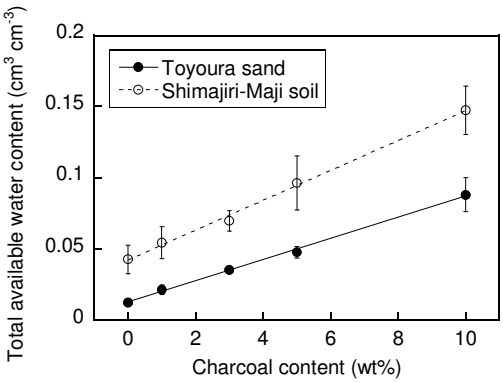

Figure 6. Available water content of soils amended with bagasse-charcoal at 800°C.

Available water content (-33 ~ -1,500 kPa) of Shimajiri-Maji soil and Toyoura sand amended with 0–10 wt % of bagasse-charcoal at 800°C is shown in Figure 6. Available water contents of the two soils were proportionally increased by application of more bagasse-charcoal. Therefore, irrigation water needed for crops can likely be proportionally reduced by application of more bagasse-charcoal to these soils.

Conclusion

Increases in available water content of the clay-rich soil (Shimajiri-Maji) and sand (Toyoura sand) by applying bagasse-charcoal were evaluated in this study. The results were as follows: (1) Available water contents of the two soils increased with application of bagasse-charcoal. The available water contents did not significantly differ with carbonization temperature. (2) Available water contents of the two soils were proportionally increased by application of more bagasse-charcoal. Therefore, irrigation water can likely be reduced by application of more bagasse-charcoal to these soils.

References

Amonette JE, Joseph S (2009) Characteristics of Biochar: Microchemical Properties. In 'Biochar for Environmental Management'. (Eds J Lehmann, S Joseph) pp. 33-52. (Earthscan).

Downie A, Crosky A, Munroe P (2009) Physical Properties of Biochar. In 'Biochar for Environmental Management'. (Eds J Lehmann, S Joseph) pp. 13-32. (Earthscan).

Glaser B, Lehmann J, Zech W (2002) Ameliorating physical and chemical properties of highly weathered soils in the tropics with charcoal – a review. *Biology and Fertility of Soils* **35,** 219-230.

Late season sugarcane performance as affected by soil water regime at the yield formation stage on commercial farms in northern Ivory Coast

Crépin B Péné, Marco H Ouattara and Sylvain G Koulibaly

SUCAF CI/Ferké Sugar mills, 01 P.O. Box 1967 Abidjan, Ivory Coast, Email cbpene@yahoo.fr

Abstract
A field trial was carried out in Ferké 2 Sugar mill located in northern Ivory Coast, in order to study sugarcane growth and yield response to deficit irrigation imposed at the yield formation stage. The crop used was a first ratoon Co957, a non flowering late season sugarcane variety. The experiment was completely randomized following a one-factor design with 4 water deficit treatments in 3 replicates. It came out that the optimum water deficit treatment was 20 %, i.e., 80 % of crop water requirements were satisfied through irrigation. That treatment gave 7.9 kg cane/m^3 or 0.98 kg sugar/m^3 as irrigation water use efficiency. More over, relatively low crop growth as well as low yields were obtained as a result of an intensive and persistent dry season occurring over the yield formation stage. Because of prevailing climatic conditions, cane juice quality measured was particularly high on Co 957 which used to be a moderate performing variety in Ferké 2 sugar mill.

Key Words
Deficit irrigation, yield formation, stalk growth, cane yield, Ivory Coast

Introduction

Previous studies carried out on commercial sugarcane plantations of Ferké 1 as well as Ferké 2 mills in northern Ivory Coast showed that water was the main yield limiting factor (Péné *et al*., 1997; Péné and Tuo, 1996). Water is seen as a complex factor as its availability is climate and soil texture dependent (Frère and Popov, 1987). To mitigate rainfall hazards and better meet sugarcane crop water requirements, sound irrigation investments are being made every year by the SUCAF-CI company. Nevertheless, sugar produced by the company through 2 mills at yearly basis is still strongly dependent on rainfall patterns. That's why water management efforts for a better impact of irrigation on cane yields are a major concern. Moreover, it was shown that late season sugarcane stalk growth and yield response to irrigation on Ivorian sugar mills was quiet low for most varieties under cultivation like Co 957, Fr 8069, R 570 (Péné and Kéhé, 2005; Péné and Koulibaly, 2007; Péné, 1999). The study objective was to impose deficit irrigation over the yield formation stage of late season sugarcane in order to increase crop water use efficiency.

Material and methods

Site characteristics

The study was carried out on a commercial field of Ferké 2 sugar mill in northern Ivory Coast which is located 40 km away from the city of Ferkessédougou (09°35'N, 05°12W, 330 m ASL). The prevailing climate is tropical dry with a unimodal rainfall pattern averaging 1200 mm/year. The 7-month rainy season takes place from April to October, August and September being highly wetted with a total rainfall of 500-600 mm. The 5-month dry season starting from November to March, is marked by a hot as well as dry wind originating from Sahara, namely the *harmattan* (or northern trade wind) which prevails from November to January with the highest magnitude of daily temperatures (+10-20 °C). The vegetation is Guinea savannah with some thin rain forests along waterways. Soils are mainly ferralsols with occasionally alluvial soils or hydromorphic soils in valley bottoms as well as in uplands where water infiltration is limited by impermeable layers. The Ferké 2 sugar mill covers a total cultivated land surface of 8000 ha which are mainly under sprinkler as well as drip irrigation.

Sugarcane crop

The cane variety investigated (Co 957) is widely grown in Ferké 2 sugar mill as a late season crop over about 40 % of total cultivated land (2300 ha). Only the first ratoon cane, harvested on March 20, 2007, was investigated. The plant crop was harvested on March 17, 2006.

Over a late season cane crop, the irrigation management involves 2 watering campaigns. The first one started at early growth stage and ended at the stem elongation stage in mid July. The second one took place at the yield formation stage which started from early November 2006 to late February 2007, i.e., approximately three weeks prior to harvest.

Experimental design

The study was laid out on the 10-numbered commercial field of 22 ha. Apart from the yield formation stage,

irrigation water was applied uniformly in the field following routine management practices. Four watering regimes were imposed over the yield formation stage as follows: T0: zero water deficit at yield formation (control); T20: 20 % water deficit at yield formation; T80: 80 % water deficit at yield formation; T100: 100 % water deficit at yield formation (control). The experiment was laid out following a RCB with 4 irrigation treatments in 3 replicates. Every plot was 1 ha area, i.e., 16 cane rows of 432 m in length with 1.5 m row spacing. Stalk elongation measurements were made twice a month (every two weeks) over a sample of 10 canes randomly chosen within all individual plots. All key agronomic factors, namely fertilization, weeding and soil tillage, were kept constant except for soil water regimes at the yield formation stage. Fertiliser rates applied in the field at early crop growth stage were 300 kg/ha of urea (46 % N), 100 kg/ha of super phosphate (45 % P_2O_5) and 350 kg/ha of potassium chloride (60 % K_2O).

Irrigation system

Watering was done following a full covering sprinkler irrigation system with 18 m x 24 m grid where PVC laterals as well as sprinklers were permanently installed over the crop cycle. Irrigation water was applied weekly following a climate-based water balance equation regarding the normal watering regime, i.e. zero water deficit, as indicated below: $I = K_c \times Pan_{Evap} - P$ Where: K_c, Pan_{Evap} and P stand for crop coefficient, class A pan evaporation and precipitation, respectively.

Sol water balance

Crop water uptake was assessed using a soil water balance model which is driven by the following simplified equation: $P + I - (ETa + D + R) = \Delta S$ over a given period Where: P (precipitation, measured), I (irrigation depth applied, as previously calculated), ETa (actual evapotranspiration, calculated), D (deep percolation, calculated by difference, the soil available moisture being determined), R (runoff which is neglected).

The soil in the experimental site was sampled over 30 cm depth at five different locations randomly chosen before setting up the trial in order to determine soil physical and chemical properties.

Field irrigation efficiency

The field irrigation efficiency, expressed in kg of cane or recoverable sucrose per cubic meter of water, is defined as the ratio of yield increase resulting from watering with respect to the rainfed treatment over the irrigation depth required. Therefore, the irrigation water use efficiency (IWUE) was assumed to be higher or at least equal to the irrigation water application efficiency (IWAE). Under good irrigation management practices, both irrigation efficiency data are supposed to be close for a given treatment:

$IWAE = (Y_i - Y_r) / (I_i - T_r)$ and $IWUE = (Y_i - Y_r) / (ETa_i - ETa_r)$ Water use efficiency (WUE) is defined as the ratio of cane stalk or recoverable sucrose yield over water uptaken by the crop (ETa): $WUE = Y_i / ETa_i$ where Y_i: yield of any irrigation treatment I_i; the semi-rainfed I_r included; Eta_i: Eta of any I_i, the semi-rainfed I_r included.

Results

Cane and sugar yields

Highly significant differences in cane as well as sugar yields were observed within irrigation treatments. Cane yields were affected by as much as 0, -18 and -69 % due to soil water deficit involving T20, T80 and T100 irrigation treatments respectively. Recoverable sugar yields were also affected by as much as -17.5, -21 and -69 % regarding T20, T80 and T100 irrigation treatments respectively. In contrast, all juice quality parameters were not significantly affected.

Cane yield response to soil water deficit

Cane yield response to irrigation deficit as well as ETa deficit has a decreasing parabolic shape, which suggests the moderately stressed T20% as the optimum level (Figure 1).

Crop growth response

Except for the non-irrigated treatment, water deficit at the yield formation stage did not significantly affect cane stalk growth. A lower stalk growth response to irrigation was observed over the yield formation stage with an elongation rate of 0.2 – 0.4 cm/day from December 2006 to march 2007, as opposed to 0.6 cm/day recorded in mid-November 2006 (Figure 2). A much lower stalk elongation rate was observed on the non-irrigated treatment T100 with 0.1 cm/day from December 2006 to March 2007, as opposed to 0.4 cm/d measured in November 2006.

Prevailing climatic conditions

Climatic conditions over the dry season in 2006/07 cropping season were quiet favourable for cane ripening as compared to that of 2005/06. Air moisture content and average temperature magnitudes were kept respectively lower (44 %) and higher (14.9 °C) in 2006/07 as compared to 2005/6 with 50 % and 13.9 °C. That might have affected cane growth response to irrigation water at the yield formation stage under investigation.

Soil physical and chemical properties

Soil in the experimental field is moderately acid (pH=6.5) and therefore optimum for sugarcane cultivation. It is also coarse textured, with total available moisture (TAM) of 70 mm.

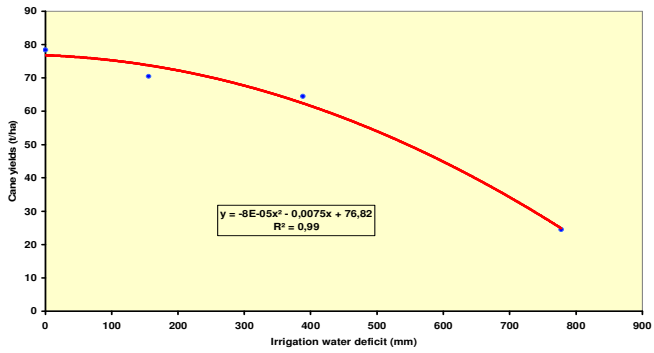

Figure 1. Cane yield response to irrigation water deficit imposed over the yield formation stage in Ferké 2 sugar mill (northern Ivory Coast).

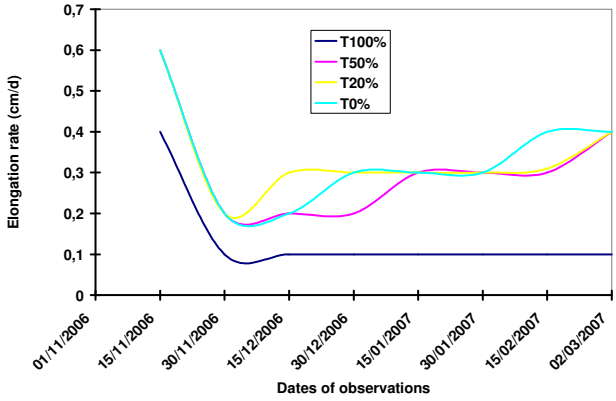

Figure 2. Cane stalk elongation rate over the yield formation stage of a late season variety (Co 957) in Ferké 2 sugar mill (northern Ivory Coast).

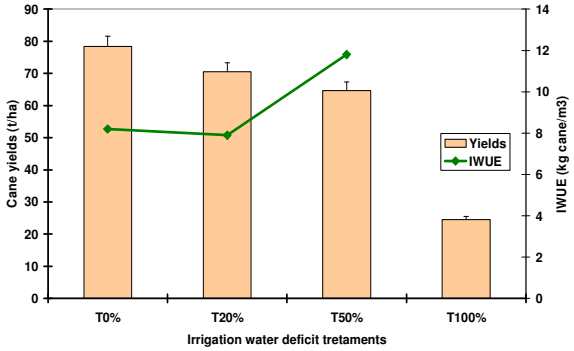

Figure 3. Cane yields and water use efficiency irrigation depending on water deficit treatments over the yield formation stage of a late season variety in Ferké 2 sugar mill (northern Ivory Coast).

The chemical status before setting up the trial was marked by a lower base saturation ratio (24 %) and a C/N ratio too high (15) which suggest a weathered soil with a slow organic matter mineralization process. Soil nitrogen and potassium contents were quiet low with 0.04 % and 0.13 meq/100 g respectively, resulting from, crop uptake but also from leaching and volatilization processes as far as nitrogen was concerned. In contrast, available phosphorous content was high (24 ppm) despite crop uptake, that element being much stable in the soil profile than nitrogen and potassium.

Field irrigation efficiency

Irrigation water use efficiency resulting from the non-stressed or fully irrigated treatment T0 (8.2 kg cane/m^3) was not significantly different from that of T20 irrigation treatment (7.9 kg canne/m^3). Therefore, additional irrigation water applied on T0 with respect to T20 in order to meet crop water requirements was not profitable (Figure 3).

Discussion

Climatic conditions and cane stalk elongation

Very low elongation rates observed over the yield formation stage despite watering of some treatments and Co 957 being a non-flowering variety, could be explained by an intensive drought enhanced by a longer lasting *harmattan* period which took place over 3.5 - 4 months instead of 1.5 – 2 as usual. As a result, a moderately performing variety like Co 957 gave high sucrose content in Ferké 2. On that site, the *harmattan* period used to be shorter (December-January) so that Co 957 could maintain a better growth rate at the yield formation stage and compensate its moderate sucrose content by higher cane yields.

Soil fertility and sugarcane yields

Lower cane yields obtained in the experiment regarding the fully irrigated treatment (78 t/ha) as well as several plantations in Ferké 2 (75 t/ha on average) might be explained partly by poor performing old varieties like Co 957, NCo 376, M 3145 and Q75 still under cultivation over about 60 % of total area, but also by soil fertility decline. That decline might have resulted from poor agricultural practices like cane burning at harvest and classical soil tillage under way more than 30 years ago. To mitigate that trend, mechanized green cane harvesting, cane trash blanketing, minimum soil tillage as well as sugarcane-based legume crop rotation system are being promoted on Ferké 2 plantations since 2006. Such a new farming system in sugarcane is of concern in most large sugarcane producing countries (Robertson, Thorburn, 2007a, 2007b; Pankhurst, Magarey *et al*, 2003;

Doerr, Cerda, 2005).

Cane yields and quality in commercial fields

Cane yield reduction with respect to yield predictions on late season varieties was high (10-20 %) due to exceptional climatic conditions over the yield formation stage in Ferké 2. In contrast, cane juice quality was quiet high with 16-17 % of sucrose content and 95-96 % of purity obtained in the field. This has mitigated sugar production loss as compared to initial estimates. Some extra sugar production (10-15 %) was obtained compared to estimates, as better cane yields and quality were achieved. Eventually, initial production estimates were met by 99 % on commercial plantations and by 112 % on village plantations.

Soil water deficit at yield formation of late season cane varieties. The study showed the relevance of 20 % water deficit imposed at the yield formation stage of Co957 as a non-flowering late-season cane variety in order to increase the field irrigation efficiency. This finding was not in line of results from similar study carried out on a neighbouring experimental station (Péné, Chopart *et al*., 2007) which suggested a normal watering regime at yield formation on the same variety because of its growth potential at that growth stage. This suggests the yield response of that variety to water deficit be dependent on the intensity as well as the duration of the *harmattan* period prevailing over the yield formation stage under late irrigation season. As far as some late cane varieties prone to flowering like M 3145 and R 570 were concerned, previous studies reported a limited yield response to irrigation at that growth stage and the profitability of managing a moderate water deficit by 20 to 30 %, in order to increase field irrigation efficiency and achieve some substantial water savings (Péné, Assa *et al*., 2001). In general, the study shows that cane yield response to water deficit is depending on variety, crop growth stage, pedo-climatic conditions as well as the watering strategy adopted (Gaudin, Brouwers *et al*., 1999; Martiné, 1999).

Conclusion

We found that 20 % water deficit was the optimum level which gave a field irrigation efficiency of 7.9 kg cane/m^3 of water, i.e., 0.98 kg sugar/m^3 of water. Also, lower cane stalk elongation rates as well as cane yields were obtained on a non-flowering late season variety like Co 957 as a result of an intensive and long lasting dry season observed over the yield formation stage. On the other hand, with drought enhanced by the *harmattan* period, a better cane juice quality was measured on Co 957 which used to be a moderately performing variety in Ferké 2 sugar mill. This finding is a sound contribution for a better water management strategy over the yield formation stage of late season cane varieties under cultivation in northern Ivory Coast.

References

Frère M, Popov GF (1987) Suivi agrométéorologique des cultures et prévision des rendements. *Etude FAO Production végétale et protection des plantes* 73.

Gaudin R, Brouwers M, Chopard JL (1999) L'eau utile et les caractéristiques hydrodynamiques des sols sous culture de canne à sucre. *Agriculture et Développement* **24**, 30-38.

Martiné JF (1999) Croissance de la canne et stress hydrique: Les apports d'un modèle plante. *Agriculture et développement* **24**, 21-28.

Ooerr SH, Cerda SH (2005) Fire effects on soil system functioning: new insights and futur challenges. *Inter. J. of Wildl. Fire* **14**(4), 339-342.

Pankhurst CE, Magarey RC, Stirling GR, Blair BJL, Bell MJ, Garside AL (2003) Management practices to improve soil health and reduce the effects of detrimental soil biota associated with yield decline of sugarcane in Queensland, Australia. *Soil & Til. Res*. **72**(2), 125-137.

Péné CB (1999) Diagnostic hydrique en culture cannière et gestion du risque climatique : cas de Ferké 2 et de Zuénoula, en Côte d'Ivoire. *Agricult. & Dév*. (n spécial sur la canne à sucre et l'eau) **24**, 74-80.

Péné CB, Assa DA, Déa BG (2001) Interactions eau d'irrigation-variétés de canne à sucre en conditions de rationnement hydrique. *Cahiers Agricultures* **10**, 243-53

Péné CB, Chopard JL, Assa DA (1997) Gestion de l'irrigation à la parcelle en culture de canne à sucre (*Saccharum officinarum L.*) sous climat tropical humide, à travers le cas des régions Nord et centre de la Côte d'Ivoire. *Sécheresse* **8**(2), 87-98.

Péné CB, et Kéhé M (2005) Performance de trois variétés de canne à sucre soumises au rationnement hydrique en prématuration au Nord de la Côte d'Ivoire. *Agron. Afr.* **17**(1), 7-18.

Péné CB, Tuo K (1996) Utilisation du diagnostic hydrique pour le pilotage optimal de l'irrigation de la canne à sucre en Côte d'Ivoire. *Sécheresse* **7**(4), 299-306

Robertson FA, Thorburn PJ (2007a) Decomposition of sugarcane harvest residue in different climatic zones. *Austr. J. Soil Res*. **45**(1), 1-11.

Robertson FA, Thorburn PJ (2007b) Management of sugarcane harvest residues: Consequences for soil carbon and nitrogen. *Aust. J. Soil Res*. **45**(1), 13-23.

Modeling of coupled water and heat fluxes in both unfrozen and frozen soils

Ying Zhao[A], Stephen Peth[A] and Rainer Horn[A]

[A]Institute of Plant Nutrition and Soil Science, Christian-Albrechts-University zu Kiel, Olshausenstr. 40, 24118 Kiel, Germany, Email yzhaosoils@gmail.com

Abstract
Accurate simulation of soil freezing and thawing behavior is critical to understand hydraulic processes in the vadose zone under cold and arid climatic conditions. Using an extended freezing code incorporated in the HYDRUS-1D model, this study was conducted 1) to verify the freezing model using field soil water and temperature data collected in Inner Mongolia grassland, and 2) to investigate the contribution of snowmelt or soil thawing to the seasonal water balance. The results showed that both the freezing model and the snow routine matched well the measured soil water and temperature under unfrozen conditions. However, under frozen conditions, the freezing model reflected the phase change of soil water better and substantially improved the simulation results than the snow routine. The freezing model did not produce surface runoff generated by snowmelt and soil thawing from frozen soil layers. Instead, it overestimated water content and thus underestimated surface runoff after spring snowmelt. We suggest that detailed knowledge of the soil-atmosphere processes is needed to improve the surface runoff algorithm in the frozen soil module.

Key Words
Frozen soil, modeling, water and heat fluxes, Inner Mongolia grassland

Introduction

Coupled water and heat movement in the vadose zone is a central process in many agricultural and engineering issues. In particular, in the cold and arid regions, snowmelt or lateral water movement on frozen soil layers have a non-negligible influence on seasonal water balance. However, although the importance of freezing and thawing processes are recognized widely, the mutual interactions of water and heat flow in frozen soil are limited in laboratory observation and theoretical analysis, and are rarely considered in field applications (Flerchinger and Saxton 1989; Smirnova *et al.* 2000; Hansson *et al.* 2004). This study addresses the field application of the hydrodynamic model HYDRUS-1D (Šimůnek *et al.* 1998). In the current version, an extended freezing code is incorporated, which numerically solves coupled equations governing phase change between water and ice and heat transport using a mass- and energy-conservative method (Hansson *et al.* 2004). Specifically, we will focus on following questions: 1) How well does HYDRUS-1D simulate soil water and temperature with and without the "frozen soil module"? 2) How does the frozen soil module affect soil temperature, soil moisture and runoff simulations?

Materials and Methods

The study was performed on a long-term experimental site of the Inner Mongolia Grassland Ecosystem Research Station (IMGERS, 43°37′50″N, 116°42′18″E). The site was protected from grazing since 1979 (24 ha). Since June 2004, soil moisture and temperature were recorded by a data-logger at 30-min intervals in summer and at 1-h intervals in winter. Soil water content was measured at 5, 20 and 40 cm depth by theta-probes (Type ML2x). When soil is frozen, the measured probe reading refers to the volumetric unfrozen water content. Soil temperature was measured at five soil depths of 2, 8, 20, 40 and 100 cm using Pt-100 probes. Precipitation and other weather variables were recorded by a micrometeorological station. To determine root length density, root samples were taken up to 100 cm soil depth. In addition, soil samples were taken at four depths of 4-8, 18-22, 30-34 and 40-44 cm to determine the water retention characteristics and hydraulic conductivities.

The model of coupled water and heat fluxes was performed with HYDRUS-1D. Variably saturated water flow for above- and sub-zero temperatures is described using the modified Richards equation (e.g., Hansson *et al.* 2004):

$$\frac{\partial \theta_u(h)}{\partial t} + \frac{p_i}{p_w}\frac{\partial \theta_i(T)}{\partial t} = \frac{\partial}{\partial z}\left[K_{Lh}\frac{\partial h}{\partial z} + K_{Lh} + K_{LT}\frac{\partial T}{\partial z} + K_{vh}\frac{\partial h}{\partial z} + K_{vT}\frac{\partial T}{\partial z}\right] - S \quad (1)$$

where θ_u [L^3/L^3] is the volumetric unfrozen water content (=$\theta+\theta_v$; θ and θ_v are the volumetric liquid and vapor water content, respectively), θ_i is the volumetric ice content, p_w and p_i is the density of liquid and ice water, respectively, t is time, z is the soil depth, h is the pressure head, T is the soil temperature, and S is a sink/source term normally considered as root water uptake. In Eq. 1, the first five terms on the right-hand side represent

1 – 6 August 2010, Brisbane, Australia. Published on DVD.

liquid flows due to gradient in pressure head (K_{Lh}, [L/T]), gravity, and temperature (K_{LT}, [L^2/T/K]), and vapor flows due to gradient in pressure head (K_{vh}) and temperature (K_{vT}), respectively. The hydraulic conductivity of frozen soil is significantly reduced by ice lenses, which is accounted for by an impedance factor, Ω (Lundin 1990), multiplied by Q, as follows:

$$K_{fLh} = 10^{-\Omega Q} K_{Lh} \quad (2)$$

the parameter Q is the ratio of the ice content to the total water content.

The governing equation for the movement of energy in soil is given by the following conduction–convection heat flow equation (e.g. Nassar and Horton 1992):

$$\frac{\partial C_p T}{\partial t} - L_f \rho_i \frac{\partial \theta_i}{\partial t} + L_0(T) \frac{\partial \theta_v(T)}{\partial t} = \frac{\partial}{\partial z}\left[\lambda(\theta) \frac{\partial T}{\partial z}\right] - C_w \frac{\partial q_l T}{\partial z} - C_v \frac{\partial q_v T}{\partial z} + L_0(T) \frac{\partial q_v}{\partial z} - C_w S T \quad (3)$$

where L_0 and L_f are the volumetric latent heat of water vaporization and freezing, respectively. C_p is the volumetric heat capacity of the bulk soil, which is determined as the sum of the volumetric heat capacities including solid, organic, liquid (C_w), ice, and vapor (C_v) phase multiplied by their respective volumetric fractions (De Vries 1963). The symbol λ(θ) denotes the apparent thermal conductivity and q the water flux density while T is the soil temperature. The phase change between water and ice is controlled by the generalized Clapeyron equation (e.g., Hansson *et al.* 2004), which defines a relationship between the liquid pressure head and temperature when ice is present in the porous material. Hence, the unfrozen water content can be derived from the liquid pressure head as a function of temperature when ice and pure water co-exist in the soil.

The initial condition was set based on measured water content and temperature. An atmospheric boundary condition and free drainage condition was imposed at the soil surface and bottom boundary of the flow domain, respectively. The soil profile was considered to be 100 cm deep. Root water uptake was simulated using the model of Feddes *et al.* (1978). The current HYDRUS-1D version including soil frozen module (denoted as freezing model) was modified to consider the subsurface soil freezing and thawing processes, as well as the surface energy and water balances. To verify the performance of freezing model, the "normal" version including snow hydrology only without soil frozen module (denoted as snow routine) was also run as a reference.

Results and Discussion

Soil water and heat fluxes are numerically simulated for the whole hydrological year in 2006 (Figure 1). Generally, the simulated and measured soil water contents (SWC) are comparable during the studied period in terms of root mean square error (0.02-0.07 cm^3/cm^3). Particularly, the freezing model simulates the diurnal water dynamics well which coincides with soil freezing and thawing processes, i.e. soil moisture increases with increasing soil temperature and vice versa (Figure 1b). However, the snow routine only fits soil water contents under unfrozen condition. Under frozen condition, there is a clear disparity between the liquid water content curve simulated by the freezing model and the total water content curve simulated by the snow routine (Figure 1a). This discrepancy is apparently caused by the program of two models, and therefore may be used to approximate the ice content in the soil. For example, the SWC simulated by the freezing model drops shortly after 6th November when the soil is freezing (Figure 1a). However, the SWC simulated by snow routine keeps constant. Hence the difference in water content between two models, i.e., ice content 0.07 cm^3/cm^3 can be estimated. In late March, due to above 0°C soil temperature, the SWC both measured and simulated by freezing model rise, while the SWC simulated by snow routine keep constant. This again suggests that the freezing model can predict the increase in SWC due to soil thawing well. An increase in SWC in the deep soil layers (20 and 40 cm) due to soil thawing is also clearly predicted (Figure 1). However, there is no indication of vertical water movement since soil water content is low and it can be held by soil.

In contrast to the soil water simulations, soil temperature is simulated well by either the freezing model or the snow routine (Figure 1), except that the freezing model is more accurate to reflect the diurnal dynamics of soil temperature (Figure 1c). This gives evidence of the impact of the frozen soil module on soil temperature simulations. When soil becomes freezing, soil temperature decreases and energy is released to warm up the cold soil. However, given the same total water content, the thermal conductivity of frozen soil is higher than that of unfrozen soil due to the presence of ice. Consequently, the upward soil heat flux is higher when the soil is frozen, thus it tends to cool the soil (Smirnova *et al.* 2000). Certainly, the energy released effect of high thermal conductivity of ice is smaller than that of water phase change. Consequently, the freezing model, that considers the both thermal transport processes, provides a more reasonably and realistic simulation of soil temperature.

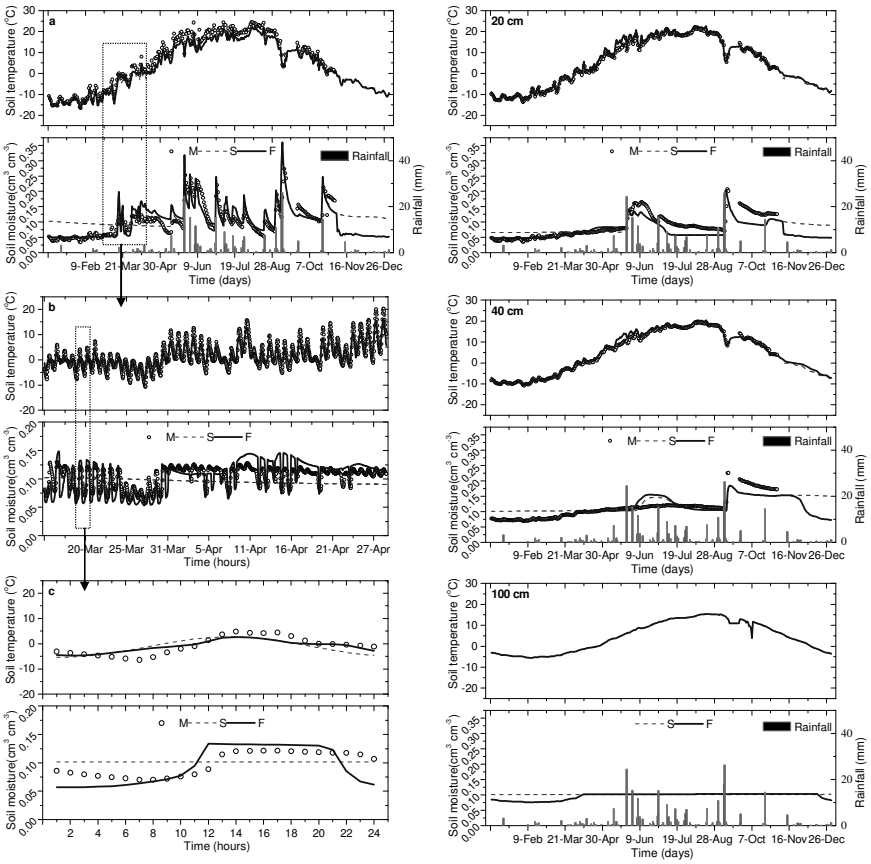

Figure 1. Measured and simulated soil moisture and temperature at 5 (a, b, c), 20, 40, and 100 cm depth during the whole year of 2006 (M: Measured liquid water content; S: Simulated total water content running snow routine; and F: Simulated liquid water content running freezing model).

The snow routine predicts up to 15 mm snow depth (Figure 2a), however, the simulated runoff after air temperature increasing above 0°C is negligible (Figure 2c). This might relate with that the snow routine does not account for surface runoff from the frozen soil layer, but it is likely that surface runoff is generated during snowmelt while soil is fully or at least partially frozen (Figure 2b).

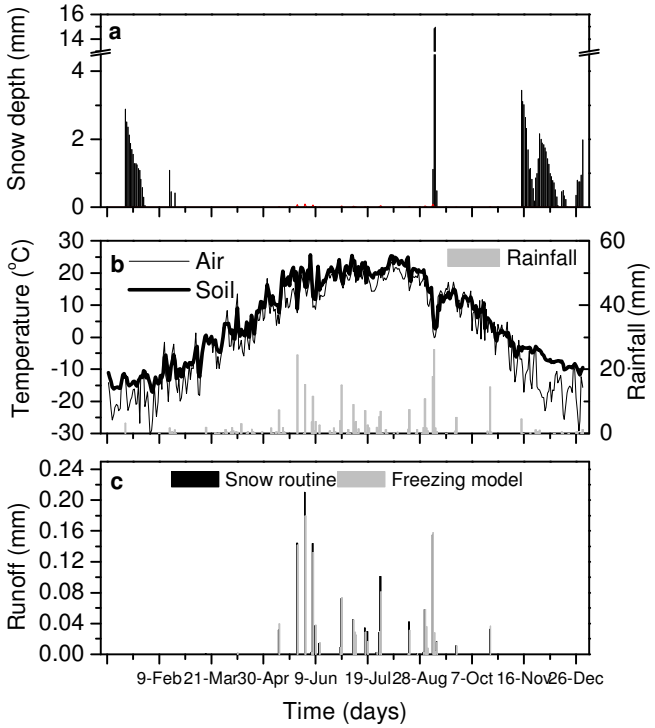

Figure 2. Rainfall, air and soil temperature, snow depth and runoff during the whole year of 2006.

Unexpectedly, the freezing model that can account for the subsurface freezing and thawing processes also does not produce surface runoff during winter (Figure 2c). Instead, we found that the freezing model simulated SWC is higher than the measured ones in the seasonal transition time when soil begins to thaw (Figure 1a). This implies that the freezing model might overestimate water content and thus underestimate surface runoff. Therefore, the freezing model seems still not sensitive enough to estimate surface runoff after spring snowmelt. This might relate to the fact that the freezing model we applied adopts soil surface temperature as the atmospheric boundary condition instead of air temperature, which undoubtedly lags energy transfer (Figure 2b). As a result, the freezing model may incorrectly partition all the snowmelt into infiltration as both soil thawing and snow melting happen simultaneously. Therefore, to solve this model problem, a transferable and double-layered boundary (e.g., one accounting for air temperature and other for soil temperature) is suggested. In addition, the current freezing model is possibly underestimated the reduction in infiltration capacity owing to the blocking effects of ice. Although the current frozen soil module has slight effect on the simulations of surface runoff, we suggest a detailed study on the soil-atmosphere processes and effects of boundary conditions to improve the surface runoff algorithm in the freezing code.

Conclusion

We used an extended frozen soil module of HYDRUS-1D, which solves water and heat transport under both frozen and unfrozen conditions simultaneously. The model was evaluated using field data of soil water and temperature at a long-term experimental site in Inner Mongolia grassland (North China). The results showed that both freezing model and snow routine reflect well the measured soil water and temperature under unfrozen condition, whereas the freezing model substantially improved the simulation results under frozen condition. In addition, the freezing model did not produce surface runoff generated by snowmelt or soil thawing from frozen soil layer. We suggest that seasonal water balance, especially considering rainfall water stored as snow, snow drift and the lateral water flow on frozen soil layers need to be investigated further because of the complicated interactions at the soil-atmosphere interface and thus effects of boundary conditions on the simulation.

References

de Vries DA (1963) The thermal properties of soils. In ‘Physics of plant environment’. (Ed RW van Wijk) pp. 210–235. (North Holland: Amsterdam).

Feddes RA, Kowalik PJ, Zaradny H (1978) ‘Simulation of Field Water Use and Crop Yield’. (John Wiley and Sons: New York, NY).

Flerchinger GN, Saxton KE (1989) Simultaneous heat and water model of a freezing snow-residue-soil system I. Theory and development. *Trans. ASAE* **32**, 565–571.

Hansson K, Šimůnek J, Mizoguchi M, Lundin L-C, van Genuchten MT (2004) Water flow and heat transport in frozen soil: numerical solution and freeze-thaw applications. *Vadose Zone Journal.* **3**, 693–704.

Lundin L-C (1990) Hydraulic properties in an operational model of frozen soil. *Journal of Hydrology* **118**, 289–310.

Nassar IN, Horton R (1992) Simultaneous transfer of heat, water, and solute in porous media: I. Theoretical development. *Soil Science Society of America Journal* **56,** 1350–1356.

Smirnova TG, Brown JM, Benjamin SG (1997). Performance of different soil model configurations in simulating ground surface temperature and surface fluxes. *Monthly Weather Review* **125**, 1870–1884.

Šimůnek J, Sejna M, van Genuchten MTh (1998) The HYDRUS-1D software package for simulating the one dimensional movement of water, heat, and multiple solutes in variably-saturated media. Version 2.0. IGWMC-TPS-70. (International GroundWater Modeling Center, Colorado School of Mines, Golden, CO).

Zhao Y, Peth S, Horn R, Krümmelbein J, Ketzer B, Gao YZ, Doerner J, Bernhofer C, Peng XH (2010) Modelling grazing effects on coupled water and heat fluxes in Inner Mongolia grassland. *Soil Tillage Research* doi:10.1016/j.still.2010.04.005.

Multi-TDR probe designed for measuring soil moisture distribution near the soil surface

Yuji ITO[A], Jiro Chikushi[b], and Hideki Miyamoto[c]

[A]Biotron Institute, Kyushu University, 6-10-1 Hakozaki, Higashi-ku, Fukuoka 812-8581, Japan, Email ito@agr.kyushu-u.ac.jp
[B]Biotron Institute, Kyushu University, 6-10-1 Hakozaki, Higashi-ku, Fukuoka 812-8581, Japan, Email chiku2@agr.kyushu-u.ac.jp
[C]Organization for the Strategic Coordination of Research and Intellectual Property, Meiji University, 1-1-1 Higashi-mita, Tama-ku, Kawasaki-shi, Kanagawa 214-8571, Japan. Email hidekim@isc.meiji.ac.jp

Abstract
To establish a method for monitoring the vertical profile of volumetric water content (θ) near a soil surface, a multi-TDR (time domain reflectometry) probe was designed and applied to θ-profile observations during the evaporation processes for sand soil and decomposed granite soil (DG soil). The multi-TDR probe consists of 8 sets of 3-line TDR probes, being on a print-circuit board with a low dielectric constant and able to measure dielectric constant ($\varepsilon_{\text{Multi-TDR}}$) at intervals of 3 mm. We individually calibrated the probes for sand with different moisture conditions and found that the probes can determine θ within acceptable accuracy. The effectiveness of the multi-TDR probe was examined in the evaporation processes for sand and DG soils. The observed θ-profiles showed that the moisture contents for sand at 3 and 6 mm depths decreased locally in the initial stage of the process, while the moisture contents for DG soil decreased uniformly at all depths. These results demonstrated the features of moisture content variation experienced in the evaporation process in these soils. We concluded that the newly designed multi-TDR probe would be useful for millimeter-interval measurements of vertical θ-profiles near a soil surface.

Key Words
Time domain reflectometry (TDR), Multi-TDR probe, Dielectric constant, Topp equation, Soil surface evaporation

Introduction
It is important to evaluate quantitatively the water content profile within 2 cm depth from the surface for understanding the hydrological processes of evaporation, runoff, and water infiltration near the soil surface. Two or three parallel metal rods are often used as a conventional time domain reflectometry (TDR) probe for measuring dielectric constant, while a variety of customized probes have been developed for different purposes (Selker *et al*., 1993; Inoue *et al*., 2001; Miyamoto and Chikushi, 2006). Although a vertical water content profile can be measured by setting several probes with different depths horizontally, the space between the probes should be at least a few centimeters to avoid interference between them (Inoue *et al*., 2001; Suleiman and Ritchie, 2003). However, for the evaporation process from soil composed of only coarse particles such as sand with no silt and clay, a dried thin layer with a steep gradient of water content profile can develop. Such a layer may affect the macroscopic water movement including the surface runoff and water infiltration. To understand temporal and spatial change in local water content in the layer, a down-sized probe has been required for measuring a water content profile with a limited space of only several millimetres. For the present paper, we developed a multi-TDR probe being able to measure water contents of small volumes and applied it to evaporation experiments for a sand soil and decomposed granite soil (DG soil). In the experiments we monitored the variation of water content profiles with time and examined the effectiveness of the probe based on the profiles obtained.

Materials and Methods
Figure 1 shows the schematic diagram of the multi-TDR probe we developed. The multi-TDR probe used in this study was made of a piled electrical board of a mixture of glass and epoxy resin, in which 17 copper lines (electrodes) 100 mm long, 0.2 mm wide, and 0.01 mm thick were aligned parallel at 1.6 mm intervals. These lines were used for constructing 8 sets of TDR probes by taking 3-lines from one end and shifting by the two lines to the other end. Thus, soil moisture measurements at 8 different points with 3.2 mm intervals can be conducted by setting the multi-TDR probe horizontally on its side. A cable tester (Textronix, 1502C) connected with a multiplexer (Campbell Scientific, SDMX50) was used to emit the step pulse and to receive its reflectance, from which the dielectric constants at the points can be estimated by using the software Win TDR (Or *et al*., 2004).

1 – 6 August 2010, Brisbane, Australia. Published on DVD.

To clarify the dielectric characteristics of the multi-TDR probe, we measured the dielectric constants for 9 different types of materials. As the materials we used distilled water at 24°C, ethanol-water mixtures with different ethanol concentrations (20, 40, 60, 80, and 100% in volume), a mixture of ethanol and vegetable oil with the ratio of 1 to 1, vegetable oil, and air. For each material, the multi-TDR probe was set up in the centre of a cylindrical container (7.5 cm in diameter and 15 cm in height) filled with the material. The dielectric constant was measured three times and they were averaged for every TDR probe in the multi-TDR probe (P1 to P8). For a comparison, a conventional three-wire probe (C3 probe) made of stainless steel rods 100 mm long and 1.2 mm in diameter was also used for the measurement.

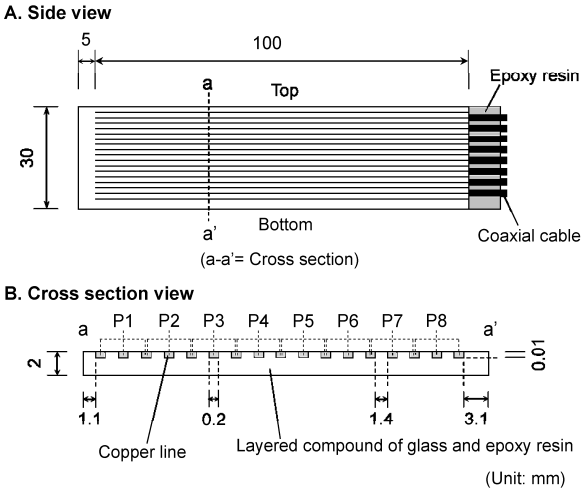

Figure 1. Schematic diagram of the multi-TDR probe (Diagram B shows the cross section view at the a-a' line in diagram A).

To calibrate the multi-TDR probe for the sand soil, we vertically fixed the probe in the centre of the plexiglass column (5 cm in diameter and 13 cm in height) and filled the column uniformly with the air-dried sand soil (No.6, grain size of 0.15-0.6 mm, Saitozaki Kousan Co., Ltd., Japan). Dielectric constants were measured after water sprayed on the soil surface had diffused uniformly. Simultaneously, soil water content of the sand was also measured gravimetrically by weighing the total weight of the column. By repeating the measurements at different moisture conditions, we investigated the relationship between the dielectric constant and water content for the probes.

To investigate the temporal variations of the water content profile in the evaporation processes of sand and DG soils, we fixed the multi-TDR probe (placing P1 at the top and P8 at the bottom) in a perpendicular container of poly-vinyl chloride sized 10 cm long, 20 cm wide, and 4 cm high. The container was filled with soil along with water, resulting in a water saturated medium. During the evaporation process under the condition of open soil surface, the dielectric constant profile was measured at 5 min intervals. The relationship between dielectric constant and volumetric water content was assumed to be the same for both sand and DG soils as suggested by Lin *et al*. (2001).

Results and discussion

Table 1 shows the dielectric constants measured by the C3 probe and the multi-TDR probe for the materials used. Thus, the measured values by the C3 probe effectively indicate the unique values for different solutions. On the other hand, the dielectric constants of different materials measured by the multi-TDR probe were about half of those done by the C3 probe. Since the calibration for each probe was conducted individually, there was little difference between the probes on the measurements of dielectric constant.

Figure 2 shows the relationship between the dielectric constant and the volumetric water content of sand measured by the multi-TDR probe and the thin line calculated by the Topp equation (Topp *et al*. 1980). The measurements disagreed generally with the estimation by the Topp equation. Thus, we need an alternative calibration equation instead of the Topp equation and proposed as,

$$\theta_{\text{Multi-TDR}} = a(\log \varepsilon_{\text{Multi-TDR}})^2 + b \log \varepsilon_{\text{Multi-TDR}} + c \qquad (1)$$

where $\varepsilon_{\text{Multi-TDR}}$ is dielectric constant measured by the multi-TDR probe, a, b, and c are fitting parameters, and $\theta_{\text{Multi-TDR}}$ is volumetric water content estimated by Eq. (1). The parameters were determined by the nonlinear least square method. The resulting calibration equations fitted well (solid and dashed lines in Figure 2) with the

observed data.

Table 1. Dielectric constants of distilled water, ethanol-water mixtures with different concentrations, ethanol-oil mixture, vegetable oil, and air measured by the 3-wire and the multi-TDR probe.

Material	Dielectric constant									
	Measured with 3-wire probe	Measured with multi-TDR probe								
		Average *	Differences from average							
			P1	P2	P3	P4	P5	P6	P7	P8
Distilled water	80.1	43.7	-1.0	-0.6	-0.3	0.0	0.5	-1.1	2.0	0.4
20%-ethanol solution	68.1	37.1	-0.7	-0.7	-0.4	0.0	0.6	-0.9	1.8	0.3
40%-ethanol solution	54.3	30.3	-0.7	-0.5	-0.2	0.1	0.5	-0.9	1.4	0.3
60%-ethanol solution	41.3	23.4	-0.5	-0.4	-0.2	0.0	0.3	-0.8	1.3	0.2
80%-ethanol solution	30.3	17.7	-0.5	-0.4	-0.1	0.1	0.4	-0.7	1.1	0.1
Ethanol	20.8	12.1	-0.4	-0.2	-0.1	0.1	0.3	-0.6	0.8	0.0
Ethanol-oil mixture	9.2	8.2	-0.2	-0.3	-0.2	-0.1	0.4	-0.4	0.8	-0.1
Vegetable oil	3.5	4.8	-0.2	-0.1	0.0	0.1	0.2	-0.3	0.5	0.0
Air	1.5	3.6	-0.1	-0.1	0.0	0.1	0.1	-0.3	0.3	0.0

* Average is a mean value of the dielectric constans measured by P1 to P8. Ethanol solutions were made by mixing different mass of ethanol in distilled water. Ethanol and vegetable oil were mixed in same mass when the mixture was made.

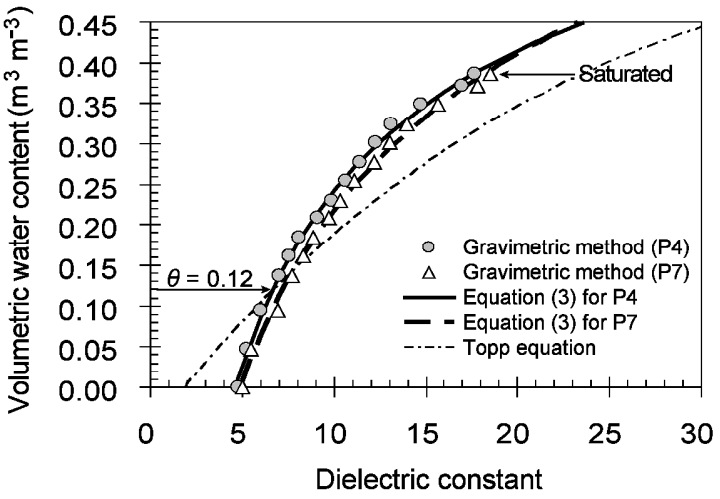

Figure 2. Relationships between dielectric constant and volumetric water content for sand.

Figure 3a shows the temporal variation of the water content profile in the evaporation process for sand. At the depths of 0.28 and 0.6 cm, volumetric water content abruptly decreased to about half during 2 hours following the start of the experiment. On the other hand, in the range of the depths 1.56 to 2.52 cm, the change in water content was little and thus did not depend on the evaporation. In the water content profile, it was confirmed that the content decreases from the top soil as evaporation proceeds and the drying front also goes down. After 12 hours from the initiation, the dry process proceeded in the whole profile. Finally after 168 hours (about 1 week) water contents at all the depths became constant to about 0 m^3/m^3.

Figure 3b shows the experiment results for DG soil. Volumetric water content for DG soil uniformly decreased with time in every depth. Thus, unlike with sand, the progression of the drying front with time was not observed. The comparison of water content between sand and DG soils after 12 hours from the start of the experiment shows that water was lost for sand faster than for DG soil in the region of 0.28-1.24 cm depth, while the difference between them was not so large in the region more than 1.56 cm in depth. During 12 to 24 hours from the initiation, the amount of water lost was higher for DG soil than for sand.

There are few reports on evaporation processes for different soils, especially on the water content close to the soil surface. However, Hillel (1977) showed that water content near the surface abruptly decreases for sand, while the decrease in the deeper zone is larger for loam than for sand. After soil water near the surface decreased, corresponding to at about 5-12 hours from the start of the experiment, water in the lower region tends to decrease for loam faster than for sand (Suleiman and Ritchie, 2003). Soil surface boundary conditions due to the difference in air temperature and humidity during the experiment may change the evaporation processes. The measured temporal changes in soil water profile revealed the difference of water content variation during

evaporation between sand and DG soils. Most of the studies on the measurement of soil water profile have been concerned with the surface zone of a few to several 10 cm (Richards *et al*., 1956; Bruckler *et al*., 1988; Inoue *et al*., 2001; Suleiman and Ritchie, 2003). Our study concentrates on the region of 0.28-2.52 cm in depth, which is closer to the surface than in the other studies. From the measured results, we can conclude that the multi-TDR probe is useful for investigating the water profile near the soil surface.

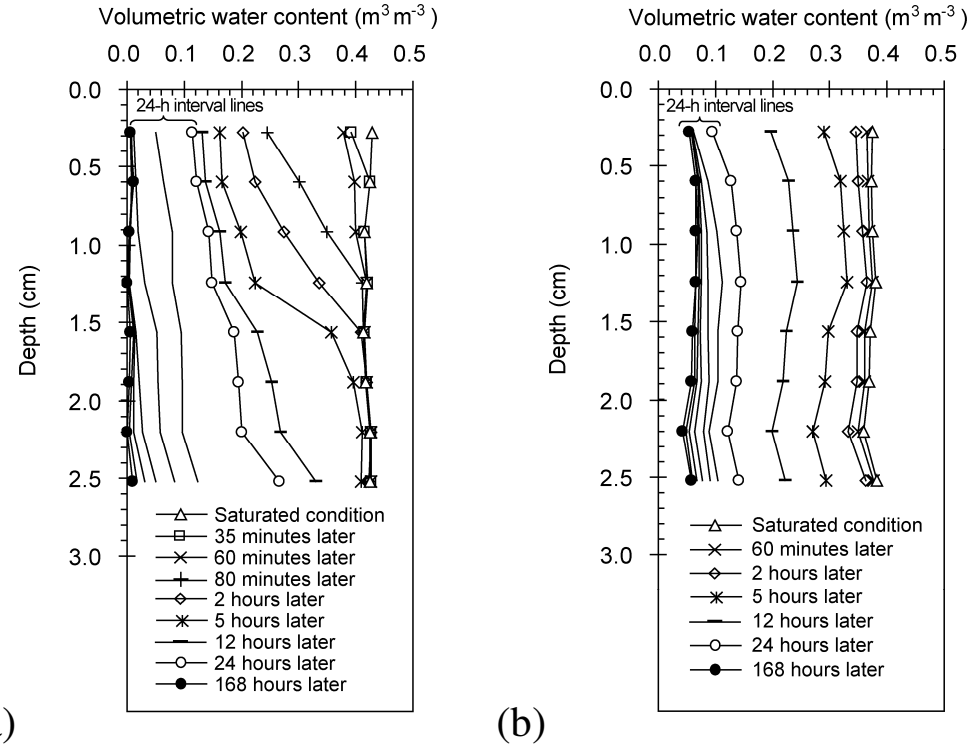

Figure 3. Temporal changes in vertical volumetric water content profiles. (a) Sand soil. (b) Decomposed granite soil (DG soil).

References

Bruckler L, Witono H, Stengel P (1988): Near surface soil moisture estimation from microwave measurements. *Remote Sensing of Environment* **26**: 101–121.

Hillel D (1977) 'Computer simulation of soil-water dynamics: a compendium of recent work'. pp.94–101, (International Development Research Centre: Ottawa).

Inoue Y, Watanabe T, Kitamura K (2001) Prototype time-domain reflectometry probes for measurement of moisture content near the soil surface for applications to "on-the-move" measurements. *Agricultural Water Management* **50**, 41–52.

Lin W, Yamaoka H, Sugita N, Takahashi M (2001) The effects of salinity of pore water on apparent dielectric constant and resistivity in sands. *Journal of the Japanese Society of Engineering Geology* **42(3)**, 140-148.

Miyamoto H, Chikushi J (2006) Calibration of column-attaching TDR probe based on dielectric mixing model. In 'Proceedings of TDR 2006: 3rd International Symposium on TDR for innovative soils applications', West Lafayette, USA.

Or D, Jones SB, VanShaar JR, Humphries S, Koberstein L (2004) 'WinTDR —Users Guide— for Ver. 6.1'. (Department of Plants, Soil and Biometeorology, Utah State University, Logan, Utah, USA).

Richards LA, Gardner WR, Ogata G (1956) Physical processes determining water loss from soil. *Soil Science Society of America Journal* **20,** 310–314.

Selker JS, Graff L, Steenhuis T (1993) Noninvasive time domain reflectometry soil moisture measurement probe. *Soil Science Society of America Journal* **57**, 934–936.

Suleiman AA, Ritchie JT (2003) Modelling soil water redistribution during second-stage evaporation. *Soil Science Society of America Journal* **67,** 377–386.

Topp GC, Davis JL, Annan AP (1980) Electromagnetic determination of soil water content: measurements in coaxial transmission lines. *Water Resources Research* **16**, 574–582.

Numerical Analysis of Coupled Liquid Water, Water Vapor, and Heat Transport in a Sandy Loam Soil

Sanjit K Deb, **Manoj K Shukla***, Parmodh Sharma

Plant and Environmental Sciences, New Mexico State University, Las Cruces, NM, USA-88003
*Tel: (575) 646-2324; Email: shuklamk@nmsu.edu

Abstract
Information on the coupled liquid water, water vapor and heat transport under arable field conditions is still limited, particularly in semi-arid unsaturated soils such as arid southern New Mexico. Hydrus-1D model was applied to evaluate various transport mechanisms associated with temporal variations in soil water content and soil temperature in the unsaturated zone of a sandy loam furrow-irrigated field located at Leyendecker Plant Science Research Center, Las Cruces. The model was calibrated and validated using measured soil water content and soil temperature in the sandy loam soil beds at four depths of 5, 10, 20, and 50 cm for a 19-day period from day of the year (DOY) 85 (26 March 2009) through DOY 103 (April 13 2009) and a 31-day period from DOY 104 (April 14 2009) through DOY 134 (14 May 2009), respectively. Measured soil hydraulic and thermal properties, and daily meteorological data were used in model simulations. Simulated results with the field experiment demonstrated that the model predicted soil water content and soil temperature and their temporal variations at all depths adequately. The total liquid water flux (comprised of isothermal and thermal liquid water) dominated the soil water movement during and early periods of an irrigation event, while the contribution of total water vapor flux (comprised of primarily thermal and much smaller isothermal water vapor) increased with increasing soil drying before and after irrigation. During the progressively soil drying process, the upward isothermal and thermal liquid water fluxes within 15 cm depth also served as potential sources of liquid water, which eventually changed to water vapor near the surface. Water vapor flux was much higher in the layer near soil surface and was approximately 10.4% of the total coupled water flux during the simulation period.

Key-Words
Water content, vapor transport, energy balance, unsaturated zone, hydrus, TDR

Introduction

Temporal variations in soil moisture in unsaturated soil zone due to temperature gradients, especially in arid and semiarid agricultural fields, may induce water fluxes in gas and liquid phase, which can play a key role in soil mass and energy transfer near the soil surface. As soil moisture contents near the soil surface are usually low in arid and semiarid regions water vapor movement continues an important part of total water flux and energy balance in unsaturated soils in agricultural and engineering applications (Parlange *et al.* 1998). The soil water near the soil surface governs the partitioning of precipitation into surface runoff and infiltration, and the partitioning of incoming solar and atmospheric radiation into latent and sensible heat fluxes into the atmosphere (Parlange *et al.* 1998). Along with solar radiation and soil nutrients, the availability of soil moisture in arable soils is of paramount importance for crop growth and agricultural production. The importance of soil moisture resulted in development of models that simulate water transport both in the liquid and vapor phase. Considering the microscopic structure of a porous medium most of these models is based on theories that account for the coupled energy and mass flow in soil (Philip and De Vries, 1957). Philip and de Vries (1957) developed a moisture migration model (henceforth the PDV model) with inhomogeneous soil temperature profiles to account for the effects of temperature gradients on moisture migration. After almost two decades of discussion, the PDV model still remains the basis for most soil-atmosphere continuum modeling. A considerable attention has been paid to analyzing water transport both in the liquid and vapor phase under field and laboratory conditions (Nassar and Horton, 1992; Cahill and Parlange, 1998). The complexity of the coupled liquid water, water vapor and heat transport in the unsaturated zone and the difficulties associated with field measurements especially near the soil surface necessitate the application of numerical models to analyze these processes. Despite of increasingly interest in numerical model development, information on the movement of liquid water, water vapor and heat under field conditions is still limited, especially under arable soil conditions in Las Cruces. The objective was to model the coupled liquid water, water vapor, and heat transport in the unsaturated zone of a sandy loam onion field in Las Cruces using a numerical code Hydrus-1D.

1 – 6 August 2010, Brisbane, Australia. Published on DVD.

Materials and Methods

Study Site and Field Measurements

Field experiment was carried out on a furrow-irrigated onion (*Allium Cepa*) field at the Leyendecker Plant Science Research Center (hereafter PSRC), New Mexico State University, New Mexico, USA (Latitude 32° 11.46′ N, Longitude 106° 44.40′ W, with an altitude ranged from 1128 to 1256 m above sea level). At the experiential field the dominant soil was a Harkey, which are characterized as deep, well-drained, formed on flood plains and low stream terraces along the Rio Grande Valley. The average annual temperature and precipitation for the experimental site are 17.7°C and 29.7 cm, respectively (Gile *et al.* 1981). During a 50-day measurement period from DOY 85 (26 March 2009) to DOY 134 (14 May 2009), field was irrigated 9 times under furrow irrigation systems during DOY 86, DOY 93, DOY 99, DOY 107, DOY 114, DOY 118, DOY 127, DOY 130, and DOY 132 .

Soil bulk density was determined by the core method (Blake and Hartge, 1986), saturated hydraulic conductivity by constant head method (Klute and Dirkson, 1986), soil water retention by pressure chamber method (Klute, 1986) and particle size distribution by the hydrometer method (Gee and Bauder, 1986). Temporal soil water content and soil temperature variations in the onion bed were measured using time domain reflectrometry (TDR) and temperature sensors (Campbell Scientific, Inc., Logan, Utah), respectively. Meteorological variables such as precipitation, solar radiation, air and soil temperatures, wind speed, and relative humidity were obtained from the local weather station. The daily average atmospheric transmission coefficient for solar radiation was estimated for the model input that incorporates transmission coefficients to calculate the daily potential global solar radiation (Campbell, 1985). Soil emissivity was estimated using the relationship given by van Bavel and Hillel (1976). The surface albedo was considered to depend on soil surface wetness according to the simple formulae given by van Bavel and Hillel (1976). When clouds are present the atmospheric emissivity on cloudy days was estimated by adding the energy emitted by the clear portions of the sky to the energy emitted by the clouds (Monteith and Unsworth, 1990), while the clear sky atmospheric emissivity was estimated based on equations given by Idso (1981).

Numerical Modeling

Nonisothermal uniform liquid vapor flow coupled with the heat transport in the unsaturated zone of a sandy loam field for a 50-day period from DOY 85 to 134, 2009 was simulated using the numerical model Hydrus-1D (Saito *et al.* 2006). Root water uptake was not considered.

Results and Discussion

Comparison of Hydrus-1D simulation with measurements

Simulated volumetric water content and soil temperature data are reasonably consistent with the field measurements and soil water content fluctuations predicted by the coupled model indicate that the field measurement is likely to account for both water and vapor flux. Despite a relatively consistent simulation of the temporal variation in soil water contents, Hydrus-1D slightly under predicted soil water contents at all depths during the validation period. Similarly, there was tendency for simulation to follow the measured temporal soil temperature variation and the model predicted systematically lower soil temperatures at all depths as compared to measured ones, especially during the validation period.

Vertical Profiles of Liquid Water and Water Vapor Flux

The isothermal and thermal liquid water and water vapor fluxes are upward (positive values) almost throughout the entire profile above 15 cm depth at 0000 h of the ‘dry’ day DOY 114 before irrigation (Figure 1). The upward movement of isothermal liquid water and water vapor fluxes within 15 cm was attributed to moisture gradients, while thermal liquid water and water vapor fluxes were upward because of steep temperature gradients. Below a depth of 15 cm, isothermal and thermal liquid water and water vapor fluxes were downward (negative values) when moisture and temperature gradients changed from upward to downward. The isothermal and thermal liquid water fluxes varied from +0.002 to +0.07 cm/d and +0.0003 to +0.04 cm/d throughout the profile above 15 cm, respectively, while the corresponding variation ranges of fluxes were between -0.003 and -0.05 cm/d, and -0.003 and -0.044 cm/d throughout the profile below 15 cm depth.

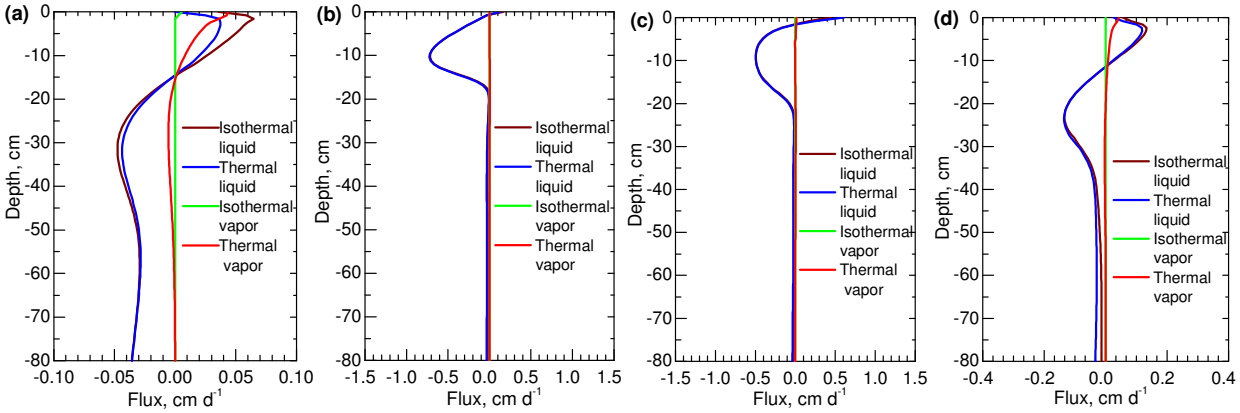

Figure 1. Simulated vertical distributions of the isothermal and thermal liquid water and water vapor fluxes during a typical 72-h period before and after an irrigation event at 1800 h of DOY 114: (a) at 0000 h of DOY 114 before irrigation, (b) at 0000 h of DOY 115 after irrigation, (c) at 1200 h of DOY 115 (DOY 115.5) after irrigation, and (d) at 0000 h of DOY 116 after irrigation. Positive and negative values of abscissa (x-axis) indicate upward and downward fluxes, respectively

The increasing upward isothermal and thermal liquid water fluxes above 15 cm indicated that liquid water in deeper layer was drawn to the surface by both moisture and temperature gradients. The variation ranges of the thermal water vapor flux were between +0.0014 and +0.044 cm/d above 15cm, while the corresponding variation of thermal vapor flux ranged from zero (no flux) to -0.01 below 15cm. The upward isothermal water vapor fluxes were markedly smaller in magnitude and almost negligible compared with thermal water vapor flux, which fluctuated mostly above 5 cm from zero (no flux) to +0.006 cm/d, while there was no isothermal water vapor flux below 5 cm. Both the upward total liquid water (both isothermal and thermal liquid water) and total vapor flux (mainly thermal water vapor) fluxes within 5 cm are responsible for the water vapor near the soil surface and thus the upward water transport at the experimental field. The total water vapor flux in this unsaturated soil layer of the furrow-irrigated sandy loam onion field contributed approximately 10.4% to total water flux.

Conclusions

Detailed analysis of vertical distributions of liquid water and water vapor fluxes indicated that both isothermal and thermal liquid water and thermal water vapor fluxes due to matric potential gradients associated with soil water content and soil temperature were responsible for water vapor near the soil surface at the experimental field. The liquid water flux dominated the soil water movement during and early periods of an irrigation event, while the contribution of vapor flux increased with increasing soil drying before and after irrigation.

Acknowledgments

Authors thank New Mexico State University for the support. Authors also thank USDA-SCRI for the financial support.

References

Blake GR, Hartge KH (1986) Bulk density. In 'Methods of soil analysis' Part 1, 2nd edn, Agron. Monogr. 9, (Ed A Klute) pp. 363-375. (American Society of Agronomy and Soil Science Society of America: Madison).

Campbell GS (1985) Soil physics with BASIC: Transport models for soil–plant systems. Elsevier, New York.

Cahill AT, Parlange MB (1998) On water vapor transport in field soils. *Water Resources Research* **43**, 731–739.

Gee GW, Bauder JW (1986) Particle-size analysis. In 'Methods of soil analysis' Part 1, 2nd edn, Agron. Monogr. 9, (Ed A Klute) pp. 383-411. (American Society of Agronomy and Soil Science Society of America: Madison).

Gile LH, Hawley JW, Grossman RB (1981) Soils and geomorphology in the basin and range area of southern New Mexico-Guide book to the Desert Project. New Mexico Bureau of Mines and Mineral Resources, Memoir 39.

Idso SB (1981) A set of equations for full spectrum and 8 to 14 µm and 10.5 to 12.5 µm thermal radiation from cloudless skies. *Water Resources Research* **17**, 295-304.

Klute A, Dirksen C (1986) Hydraulic conductivity and diffusivity: Laboratory methods. In 'Methods of soil analysis' Part 1, 2nd edn, Agron. Monogr. 9 (Ed A Klute) pp. 687-700. (American Society of Agronomy and Soil Science Society of America: Madison).

Klute A (1986) Water retention: Laboratory methods. In 'Methods of soil analysis' Part 1, 2nd edn, Agron. Monogr. 9, (Ed A Klute) pp. 635-662. (American Society of Agronomy and Soil Science Society of America: Madison).

Monteith JL, Unsworth MH (1990) Principles of environmental physics. 2nd edn, Edward Arnold, London.

Nassar IN, Horton R (1992) Simultaneous transfer of heat, water, and solute in porous media: I. Theoretical development. *Soil Science Society of America Journal* **56,** 1350-1356.

Parlange MB, Cahill AT, Nielsen DR, Hopmans JW, Wendroth O (1998) Review of heat and water movement in field soils. *Soil and Tillage Research* **47**, 5-10.

Philip JR, de Vries DA (1957) Moisture movement in porous materials under temperature gradients. *Transactions of the American Geophysical Union* **38**, 222-231.

Saito H, Simunek J, Mohanty BP (2006) Numerical analysis of coupled water, vapor, and heat transport in the vadose zone. *Vadose Zone Journal* **5**, 784-800.

van Bavel CHM, Hillel DI (1976) Calculating potential and actual evaporation from a bare soil surface by simulation of concurrent flow of water and heat. *Agricultural and Forest Meteorology* **17**, 453-476.

Numerical evaluation of inverse modelling methods for 1D and 3D water infiltration experiments in homogeneous soils

Laurent Lassabatere[A], Deniz Yilmaz[A], Rafael Angulo-Jaramillo[B,C], Jose Miguel Soria Ugalde[D], Isabelle Braud[E] and Jirka Šimůnek[F]

[A]Division Eau et Environnement, LCPC, Bouguenais, France, Email laurent.lassabatere@lcpc.fr, Deniz.Yilmaz@lcpc.fr
[B]Laboratoire des Sciences de l'Environnement, ENTPE, Vaulx-en-Velin, France, Email angulo@entpe.fr
[C]LTHE, Grenoble, France, Email angulo@entpe.fr
[D]Universidad de Guanajuato, Guanajuato, Mexico, Email josesoria@quijote.ugto.mx
[E] Cemagref, UR HHLY, Lyon, France, Email isabelle.braud@cemagref.fr
[F] Department of Environmental Sciences, University of California, USA, Email Jiri.Simunek@ucr.edu

Abstract
Modelling and understanding water fluxes in the vadose zone are important with regards to water management and require appropriate characterization methods of soil hydraulic properties. The present work studies three common methods for characterization of soil hydraulic properties based on the inverse modelling of water infiltration experiments at zero pressure head at surface (Beerkan method): the CI method for Cumulative Information method and two BEST methods for Beerkan Estimation of soil pedotransfer functions These methods estimate the soil sorptivity and saturated hydraulic conductivity by fitting infiltration data using infiltration models. The CI method directly fits the experimental cumulative infiltration to the usual short time expansion of the complete analytical model proposed by Haverkamp *et al.* (1994). The BEST methods are based on a specific algorithm that splits the experimental curves into two parts, the first part being fitted to the short time expansion and the second part to the long time expansion. To test the methods, several subsets of infiltration data were generated using the complete analytical model for several radii of the disc infiltrometer source and for times ranging from zero to several truncation times. The methods were then applied and the ratio between their estimations and the target values were evaluated to quantify their related accuracy. The results clearly demonstrated that the CI method must be used only to short time infiltration data. Yet, this method is usually used without any truncation of the experimental data, whereas the truncation should certainly be required. The BEST methods proved efficient and robust, provided the steady state was reached at the end of the infiltration experiment and both short and long time data solutions were used. The gain in accuracy of the BEST methods was all the more important when the disc radius was small.

Key Words
Soil characterization, unsaturated properties, BEST method, CI method, analytical modelling, infiltration.

Introduction
Modelling and understanding water fluxes in the vadose zone are important with regards to water management. They require accurate methods for the characterization of soil unsaturated properties. Water infiltration experiments and, in particular, Beerkan experiments (with zero water pressure at the soil surface) (Braud *et al.* 2005) have become a widely used practice for obtaining soil hydraulic properties. Several methods based on inverse modelling of Beerkan water infiltration data were developed to provide the sorptivity and the saturated hydraulic conductivity. This article aims at validating several common methods (i.e., the CI method for Cumulative Infiltration method (Vandervaere *et al.* 2000) and the BEST method for Beerkan Estimation of Soil pedoTransfer function (Lassabatere *et al.* 2006; Yilmaz *et al.* 2009) by using analytically generated data and comparing the estimated and target sorptivities and saturated conductivities. Estimator accuracy was studied as a function of the data subset (i.e., very short times, short times, short times plus steady state) for several geometric configurations (large and small disc radius).

Methods
Water infiltration models
Hydraulic characterization methods are usually developed using the following analytical models pioneered by Haverkamp *et al.* (1994) applied to infiltration from a disc free-water source into a homogeneous soil:

$$I_{3D}^{O(2)}(t,S,K_s) = S\sqrt{t} + \left(\frac{2-\beta}{3}\Delta K + K_0 + \frac{\gamma S^2}{r_d \Delta\theta}\right)t \qquad (1a)$$

$$I_{3D}^{+\infty}(t,S,K_s)=\left(K_s+\frac{\gamma S^2}{r_d\,\Delta\theta}\right)t+\frac{1}{2\,(1-\beta)}\ln\left(\frac{1}{\beta}\right)\frac{S^2}{\Delta K} \tag{1b}$$

$$q_{3D}^{+\infty}(S,K_s)=K_s+\frac{\gamma S^2}{r_d\,\Delta\theta} \tag{1c}$$

where S stands for sorptivity, K_s and K_0 for the saturated and initial hydraulic conductivities, ΔK and $\Delta\theta$ for the differences in conductivities and water contents between final and initial states, α and β are usually taken as 0.6 and 0.75, respectively, and r_d is the disc radius. These equations correspond to the short time (equation (1a)) and long time (equation (1b-c)) expansions of the implicit quasi-exact model proposed by Haverkamp *et al.* (1994):

$$\frac{2\Delta K^2}{S^2}t=\frac{1}{1-\beta}\left[\frac{2\Delta K}{S^2}\left(I_{3D}(t)-K_0t-\frac{\gamma S^2}{r\,\Delta\theta}t\right)-\ln\left(\frac{\exp\left(2\beta\frac{\Delta K}{S^2}\left(I_{3D}(t)-K_0t-\frac{\gamma S^2}{r\,\Delta\theta}t\right)\right)+\beta-1}{\beta}\right)\right] \tag{2}$$

Equations (1a) and (1b-c) were proved accurate provided their use was restricted to short and long time validity intervals, respectively (Lassabatere *et al.* 2009).

The CI method

The CI method consists in deriving directly the sorptivity and the saturated hydraulic conductivity from the fit of the equation (1a) with no *a priori* restriction to the experimental data. Several graphical methods were also proposed to provide additional information and validation of the use of the CI method (Vandervaere *et al.* 2000). This method is quite common and served as a basis of many characterization studies.

The BEST method

The BEST method refers to the Beerkan Estimation of Soil pedoTransfer parameters methods originally developed by Lassabatere *et al.* (2006). These authors proposed to fit the first part of the cumulative infiltration to the short time equation (1a) and the last part to the long time expansion (1c). In particular, they use the long time infiltration rate $q_{+\infty}^{\exp}$ to define the following constraint between the estimator for sorptivity ($\hat{S}$) and the estimator for the saturated hydraulic conductivity ($\hat{K}_s$):

$$\hat{K}_s=q_{+\infty}^{\exp}-\frac{\gamma\hat{S}^2}{r\,\Delta\theta} \tag{3}$$

Such a constraint allows the inversion of experimental data with regards to only the sorptivity $\hat{S}$; which increases the robustness of the inverse procedure (Lassabatere *et al.* 2006). Moreover, a specific algorithm allows the selection of the data that is fitted to the short time expansion (equation (1a)). The estimators $\hat{K}_s(n)$ and $\hat{S}(n)$ are estimated successively for the first n data points from five till the total number of the data points of the whole experimental dataset. Then, the maximum time $t_{\exp}(n)$ of the data set is compared to a maximum time $t_{\max}(n)$ that stands for the limit of the validity interval of the equation (1a):

$$t_{\exp}(n)\le t_{\max}(n)=\frac{1}{4(1-\beta)^2}\frac{\hat{S}^2}{\hat{K}s} \tag{4}$$

The chosen data correspond to the maximum number of points ensuring the relation (4). On that basis, Yilmaz *et al.* (2009) adapted such a method for highly sorptive soils, through considering the intercept of the long time expansion (equation (1b)) ($b_{+\infty}^{\exp}$) as a better constraint and neglecting the value for K_0, leading to:

$$\hat{K}_s=\frac{1}{2(1-\beta)}\ln\left(\frac{1}{\beta}\right)\frac{\hat{S}^2}{b_{+\infty}^{\exp}} \tag{5}$$

These methods differ from the CI method mainly by respecting the validity of the short time expansion *a priori* since they carry out the inverse modelling of only the short time data. The two methods developed by Lassabatere *et al.* (2006) and Yilmaz *et al.* (2009) are referred to as "BS" for the BEST Slope and "BI" for the BEST Intercept, respectively.

Methodology of method validation

The reference data were calculated using the equation (2) on the basis of several values for the target sorptivity (S_{ref}) and for the saturated hydraulic conductivity (Ks_{ref}) and assuming K_0 is negligible (dry initial conditions). The reference data were calculated from zero to sufficient time to include very short, short and long times. The maximum time was sufficient to reach the steady state conditions, i.e., to reach a constant infiltration rate (a constant value for the derivative of the generated cumulative infiltration). Then, the whole infiltration was truncated at several times to provide different data subsets. Moreover, calculations were performed for several radii from small to large radii. For the largest, quasi infinite radius, cumulative infiltration corresponds to 1D water infiltration (equation (2) with terms containing γ being zero). The smallest radius was taken as one fifth of the scale parameter for water pressure, which is on the order of a small disc source for most soils.

Different subsets were then analysed using the CI method and the BEST methods, leading to estimated values of $\hat{K}s$ and $\hat{S}$. Their accuracies were evaluated using the ratios between the estimated and target values:

$$R_S = \frac{\hat{S}}{S_0} \tag{6a}$$

$$R_K = \frac{\hat{K}s}{Ks_0} \tag{6b}$$

Ratios were plotted versus the scaled maximum time of the data set (Lassabatere *et al.* 2009):

$$t^* = \frac{2\Delta K^2}{S^2} t \tag{7}$$

Results

The results show that ratio values R_S and R_K do not depend on the values of the reference sorptivity (S_{ref}) and saturated hydraulic conductivity (Ks_{ref}), provided that the data subsets were truncated at the same scaled time (equation (7)). Presented results can then be considered as the rules for any values of S_{ref} and Ks_{ref}.

For the 1D infiltration data, the results clearly show that the CI method must be restricted to the analysis of short time data. The ratios R_S and R_K greatly diverge from unity when maximum times of data subsets (t^*) increase (Figure 1). In that case the CI method leads to the under-estimation of sorptivity and over-estimation of the saturated hydraulic conductivity. Such inadequacy results from not respecting the validity intervals of the short time expansions. Fitting long time data using the short time expansion leads to miss-estimations.

Concerning the BEST methods, both methods lead to very bad estimations when small data subsets are considered. The reference sorptivity is strongly underestimated ($R_S << 1$) and the hydraulic conductivity is strongly overestimated ($R_K >> 1$). This proves that the data modelled with the BEST methods must integrate quite long time data. When this is the case, the BEST methods are much better than the usual CI method and provide very accurate estimations of sorptivity and saturated hydraulic conductivity. Such accuracy results from the specific procedure that ensures the use of the right part of the cumulative infiltration to fit the short time expansion. In addition, it may be concluded that estimations of the sorptivity are usually better than of the saturated hydraulic conductivity. In all cases, the ratios are between unity and 1.05.

Calculations performed for the 3D case are presented for the optimal use of the methods: small time data ($t^* < 0.1$) used for the CI method and both short and long time data used for the BEST methods. For the CI method, the decrease in the radius, i.e. the increase in h_g/r_d, triggers no change for the estimation of the sorptivity but worsens the estimation for the saturated hydraulic conductivity (Figure 2). For the BEST methods, the decrease in the radius decreases the ratios of estimated and target sorptivities and hydraulic conductivities. The increase in the accuracy of the BEST methods compared to the CI method is all the more important when the disc radius is small. For instance, for a disc radius r_d equal to the fifth of the scale parameter for water pressure h_g, the BI method leads to R_S and R_K ratios of 1.005 and 1, respectively.

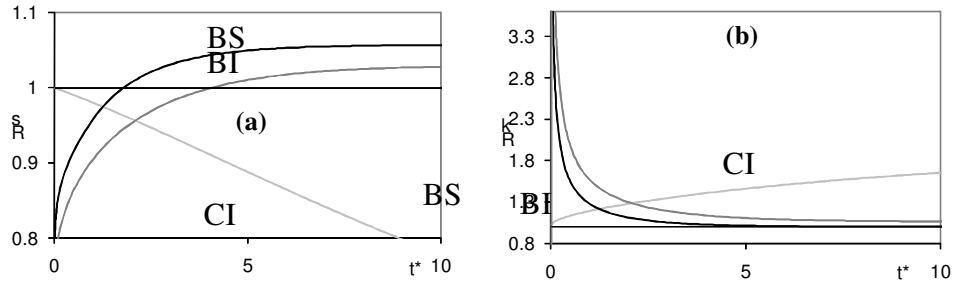

Figure 1. 1D infiltration data inverse modelling: ratios of estimated and target sorptivities –R_S- (a) and saturated hydraulic conductivities –R_K- (b) versus the scaled time (t^*).

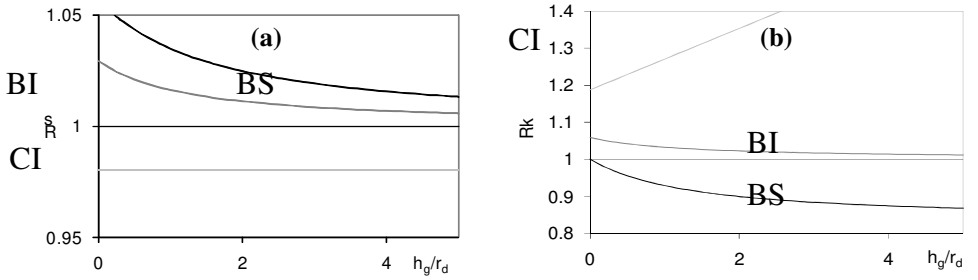

Figure 2. Ratios –R_S- (a) and –R_K- (b) versus the ratio of the scale parameter for water pressure (h_g) and the radius (r_d).

Conclusion

The presented work evaluates the accuracy of three methods involving the inverse modelling of water infiltration experiments. The CI method involves the direct fitting of the usual short time expansion of the complete infiltration model. The BEST methods fit the first part of the experimental infiltration data using the short time expansion and the second part of the infiltration data using the long time expansion. The methods include a specific procedure that splits the data into two parts. This procedure was developed to ensure the validity of the short time expansion for inverse modelling. In this study, the three methods were tested with regards to their adequacy to inversely model analytically generated reference data. The results proved that the CI method leads to an inaccurate estimation unless only the very beginning of the infiltration dataset is considered. This has a great disadvantage: only a small part of the cumulative infiltration may be used, requiring a great measurement precision for very small times. It must be noted that many methods based on the CI method (direct fitting) do not usually have any specific constraints to respect the validity of the short time expansion. On the contrary, the BEST methods provide quite accurate estimations, in particular for the sorptivity, provided that both short and long time data are used in the inverse procedure. Moreover they provide the complete set of unsaturated hydraulic parameters from the previous estimations of sorptivity and saturated hydraulic conductivity (Yilmaz *et al.* 2009). These methods appear to represent a suitable tool for the characterization of soil unsaturated hydraulic properties.

References

Braud I, De Condappa D, Soria JM, Haverkamp R, Angulo-Jaramillo R, Galle S, Vauclin M (2005) Use of scaled forms of the infiltration equation for the estimation of unsaturated soil hydraulic properties (Beerkan method). *European Journal of Soil Science* **56**, 361-374.

Haverkamp R, Ross PJ, Smetten KRJ, Parlange JY (1994) Three-dimensional analysis of infiltration from the disc infiltrometer. 2. Physically based infiltration equation. *Water Resources Research* **30**, 2931-2935.

Lassabatere L, Angulo-Jaramillo R, Soria Ugalde JM, Šimůnek J, Haverkamp R (2009) Analytical and numerical modeling of water infiltration experiments. *Water Resources Research* (in press).

Lassabatere L., Angulo-Jaramillo R, Soria Ugalde JM, Cuenca R, Braud I, Haverkamp R (2006) Beerkan Estimation of Soil Transfer parameters through infiltration experiments – BEST. *Soil Science Society of American Journal* **70**, 521-532.

Vandervaere, JP, Vauclin M, Elrick DE (2000) Transient Flow from Tension Infiltrometers: I. The Two-Parameter Equation. *Soil Science Society of American Journal* **64**, 1263-1272.

Yilmaz D, Lassabatere L, Angulo-Jaramillo R, Deneele D, Legret M (2009) Hydrodynamic characterization of basic oxygen furnace slag through an adapted BEST method. *Vadose Zone Journal* (in press).

Optimizing Water Use with High-Transpiration-Efficiency Plants

Prasanna Ayyaru Thevar[A], **M.B. Kirkham[B]**, Robert M. Aiken[C], Kenneth D. Kofoid[D], and Zhanguo Xin[E]

[A]Department of Agronomy, Throckmorton Hall, Kansas State University, Manhattan, Kansas 66506, USA. Now with Dow AgroSciences/Mycogen Seeds, York Nebraska 68467, USA, Email PAyyaruThevar@dow.com
[B]Department of Agronomy, Throckmorton Hall, Kansas State University, Manhattan, Kansas 66506, USA, Email mbk@ksu.edu
[C]Northwest Research-Extension Center, 105 Experiment Farm Road, Kansas State University, Colby, Kansas 67701, USA, Email raiken@ksu.edu
[D]Agricultural Research Center, 1232 240th Avenue, Kansas State University, Hays, Kansas 67601, USA; kkofoid@ksu.edu. Now with MMR Genetics, 3095 Co Rd 26, Vega, Texas 79092, USA, Email kdkofoid@mmrgenetics.com
[E]Plant Stress and Germplasm Development Unit, United States Department of Agriculture, Agricultural Research Service, 3810 4th Street, Lubbock, Texas 79515, USA, Email zhanguo.xin@ars.usda.gov

Abstract
High transpiration efficiency (TE) is one way to optimize water use. Plants with high TE produce more biomass per unit of water consumed than those with low TE. One novel solution to preserve water in soil is to identify plants with high TE. High TE is especially important in semi-arid regions where water is scarce. Grain sorghum (*Sorghum bicolor* Moench) is widely grown in these regions. Studies comparing sorghum lines known to have high and low TE have not been done. We grew in a greenhouse eight lines of sorghum, four known to have high TE and four known to have low TE, in pots with a commercial potting mix under well-watered and dry conditions. Relative water content, stomatal resistance, and pressure potential of the leaves were measured. High TE plants emerged better than low TE plants, which suggested that high TE lines have faster root growth. Under both watering regimes, relative water content, stomatal resistance, and pressure potential of high TE lines were similar to those of low TE lines. Because above-ground water relations did not distinguish high and low TE lines, the results suggested that research needs to focus on roots to determine why the lines differ in TE.

Key Words
Dry regions, plant root, drought, water-use efficiency, transpiration ratio, C_4 plant

Introduction
Grain sorghum is one of the most important crops grown in dry areas. Even though sorghum is classified as a drought-resistant species, the major environmental factor limiting its range of adaptation is drought (Gaosegelwe and Kirkham 1990). Genotypes of sorghum that make efficient use of water are needed for growth under drought in semi-arid regions. Water-use efficiency is defined the production of dry matter per unit of water consumed in evapotranspiration (water lost from soil and plants). Transpiration efficiency is defined as the production of dry matter per unit of water consumed in transpiration. Water lost from soil is excluded in the calculation. The reciprocal of transpiration efficiency is transpiration ratio, which is the ratio of weight of water transpired by a plant during its growing season to the weight of dry matter produced (usually exclusive of roots) (Glickman 2000). Understanding efficient water use is one of the most challenging problems facing scientists today (Zea-Cabrera *et al.,* 2006).

Almost a century ago, Briggs and Shantz (1913) showed that crop species differ in their transpiration efficiency. Since then, the C_3 and C_4 photosynthetic pathways have been elucidated, and differences in transpiration efficiency have been related to them. Plants with the C_4 type of photosynthesis have transpiration efficiencies that are about twice those of C_3 plants (Turner, 1993). However, within each species, differences in transpiration efficiency occur, including the C_4 plant, sorghum (Hammer *et al.,* 1997; Mortlock and Hammer, 1999).

An intensive breeding program has been carried out by personnel of the United States Department of Agriculture to screen for transpiration efficiency in sorghum (Xin *et al.,* 2009). In this work, 341 lines of sorghum have been screened for transpiration efficiency under greenhouse conditions. From these studies, the eight lines used in the current work were chosen. Four of them have high transpiration efficiency and four of them have low transpiration efficiency. However, because the plant-water relations of sorghum lines known to have high transpiration efficiency or low transpiration efficiency have not been compared, we measured their relative water content, stomatal resistance, and pressure potential to determine if they differed between high-TE and low-TE lines.

Materials and methods

Details of the experimental procedure are given by Thevar (2008). Briefly, the experiment was carried out between 3 December 2006 and 16 February 2007 in a greenhouse at Kansas State University in Manhattan, KS (39°08'N, 96°37'W, 314 m above sea level). The four lines with low TE were: PI257309 (from Argentina; Guinea-bicolor race; Nigricans-bicolor working group; Pedigree Mf.G.F:1228), PI295121 (Australia; Caudatum race; breeding material working group; Pedigree CAPRICORN), PI586381 (Cameroons; Guinea-caudatum race; Sumac working group; Pedigree IS 27595), and PI267532 (India; Kafir-caudatum race; Caffrorum-bicolor working group; Pedigree IS 2879). The four lines with high TE were: PI567933 (Beijing, China; Bicolor race; Nervosum-Kaoliang working group; Pedigree ER HUANG JIN), PI391652 (Shaanxi, China; race unknown; breeding material working group; Pedigree T'so 1MS), PI533946 (India; Durra-bicolor race; Durra-dochna working group; Pedigree MS385AXIS1008SA6473PB3R), and PI584085 (Uganda; Caudatum race; Caudatum-niricans working group; Pedigree 94USE9327).

Plants grew under greenhouse conditions in pots with a commercial greenhouse mix. Six seeds of each line, germinated in a Petri plate, were planted in a pot. Pots were covered with plastic, following the procedure of Xin *et al.* (2008), to prevent soil evaporation. Plants grew through holes cut in the plastic. Emergence was recorded on Day 3 (3 days after germination began), 4, 5, 8, 12, and 16. On Day 16, each pot was thinned to three seedlings. Harvest was 16 February 2007 (Day 75). None of the plants had reached reproductive stage by harvest. There were two watering regimes: wet and dry. Water was added by placing a funnel inside the hole in the plastic where a plant emerged. After an initial drenching of the pots with a fertilizer solution, each wet-treatment pot received about 700 mL of water and each dry-treatment pot received about 300 mL water. Relative water content was determined three times during the experiment by using the method of Barrs and Weatherley (1962). Abaxial stomatal resistance was measured 10 times during the experiment with a steady state diffusion porometer (Model SC-1, Decagon Devices, Pullman, Washington, USA). Pressure potential was determined at harvest (Day 75) on the most recently matured leaf using a portable plant water status console (Model 3115, Soilmoisture Equipment Corp., Santa Barbara, California, USA). The experiment was a completely randomized block design with eight sorghum lines, two treatments (wet and dry), and three replications. Data for relative water content and stomatal resistance taken during the experiment were averaged together to get means and standard errors. Data for pressure potentials, determined once at harvest, are presented with standard deviations.

Results and discussion

Plants with high transpiration efficiency (TE) emerged better than plants with low transpiration efficiency. By Day 16, an average of four plants with high TE had emerged and an average of three plants with low TE had emerged. Even though six germinated seeds were planted in each pot, no pot had six seedlings emerge. More of the low TE plants than high TE plants died in the soil before they could emerge. More research needs to be done to determine the difference in early (pre-emergence) root growth of high and low TE plants.

Relative water content, stomatal resistance, and pressure potential of plants with high TE did not differ from that of plants with low TE (Table 1). Because of the large variability in measurements, measurements made on well-watered plants did not differ from those of drought-stressed plants. Well-watered plants tended to have higher relative water contents, lower stomatal resistances, and higher pressure potentials, but differences were not significant. The number of seeds available for experimentation precluded more replications, which might have reduced the variability. Also, the relatively poor emergence of the plants limited the number of measurements.

In sum, because there were no differences in the water-relations of the shoots of the high and low TE plants, the data suggested that the difference in TE may be related to root growth. The fact that the high TE plants emerged better than the low TE plants indicates that the roots of the high TE plants may grow faster and penetrate a soil profile more quickly than roots of low TE plants. This would allow high TE plants to get water at depth that low TE plants cannot take up. It also would allow them to grow more in early development, without a large loss of water by transpiration because leaves are still small. With less transpiration, TE would be increased. Because only limited studies of sorghum roots have been done under field conditions (Krieg 1983, p. 362), it is not known if greater root growth at the seedling stage would continue into later stages. However, a small advantage in early growth is compounded during the life cycle of a plant (Blackman 1919). So a sorghum line with a large root mass at the seedling stage would likely have a large root mass at maturity. With more roots, a line can take up more water for transpiration and photosynthesis. Transpiration and photosynthesis are directly

related. When stomata are open, resulting in a high transpiration rate, more carbon dioxide can be taken up for photosynthesis. We plan to continue our pot studies with the lines differing in TE, as seeds of high TE and low TE plants become available. In these studies, we shall have more replications, so the high TE and low TE lines may show differences in relative water content, stomatal resistance, and pressure potential. Our future research also is going to focus on root growth under field conditions, where roots are not confined by pots. In these studies, we shall measure photosynthesis and transpiration. Preliminary work is already underway (Thevar, 2008). Our results reinforce the fact that one of the research challenges facing hydrology is the need for investigation not only of species-specific mechanisms of root water uptake (Rodríguez-Iturbe *et al.,* 2007) but also of line-specific mechanisms.

Table 1. Relative water content (g/g), stomatal resistance (s/cm), and pressure potential (MPa) of four lines of sorghum with low transpiration efficiency (TE) and four lines with high TE under well-watered or drought-stressed conditions. See text for details.

	Relative water content		Stomatal resistance		Pressure potential	
	Wet	Dry	Wet	Dry	Wet	Dry
Low TE						
PI257309	0.82±0.13	0.75±0.17	17.5±5.5	22.1±7.3	-1.72±0.35	-1.73±1.19
PI295121	0.83±0.11	0.92±0.04	24.1±28.0	11.3±3.1	-0.65†	-1.25†
PI586381	0.79±0.13	0.82±0.11	15.8±15.0	17.3±7.3	-2.55±0.07	-2.35±0.35
PI267532	0.83±0.13	0.71±0.19	21.1±12.0	18.6±15.6	-1.15±1.18	-2.23±1.52
High TE						
PI567933	0.84±0.06	0.78±0.16	26.1±13.4	32.5±24.1	-0.63±0.39	-2.22±0.55
PI391652	0.87±0.07	0.78±0.15	14.0±5.6	23.0±7.2	-1.73±0.74	-2.00±0.95
PI533946	0.90±0.06	0.79±0.11	23.7±12.7	23.2±9.8	-0.93±0.32	-2.30†
PI584085	0.79±0.20	0.77±0.17	19.0±12.1	25.0±23.2	-1.12±0.20	-1.90±0.35

†One value only

Acknowledgments

The research was funded by the Kansas Agricultural Experiment Station. This is Contribution No. 10-063-A from the Kansas Agricultural Experiment Station, Manhattan, Kansas 66506, USA.

References

Barrs HD, Weatherley PE (1962) A re-examination of the relative turgidity technique for estimating water deficits in leaves. *Australian Journal of Biological Sciences* **15**, 413-428.

Blackman VH (1919) The compound interest law and plant growth. *Annals of Botany* **33**, 353-360.

Briggs LJ, Shantz HL (1913) The water requirement of plants. I. Investigations in the Great Plains in 1910 and 1911. United States Department of Agriculture, Bureau of Plant Industry, Bulletin No. 284, 49 pp.

Gaosegelwe PL, Kirkham MB (1990) Evaluation of wild, primitive, and adapted sorghums for drought resistance. In 'Challenges in Dryland Agriculture. A Global Perspective.' (Eds PW Unger, TV Sneed, WR Jordan, RW Jensen), pp. 224-226. (Texas Agricultural Experiment Station: College Station, Texas).

Glickman TS (Ed) (2000) 'Glossary of meteorology.' Second ed. (American Meteorological Society: Boston, Massachusetts), 855 pp.

Hammer GL, Farquhar GD, Broad I (1997) On the extent of genetic variation for transpiration efficiency in sorghum. *Australian Journal of Agricultural Research* **48**, 6349-655.

Krieg DR (1983) Sorghum. In 'Crop-Water Relations.' (Eds ID Teare and MM Peet), pp. 351-388. (John Wiley & Sons, New York).

Mortlock MY, Hammer GL (1999) Genotype and water limitation effects on transpiration efficiency in sorghum. *Journal of Crop Production* **2**, 265-286.

Rodríquez-Iturbe I, D'Odorico P, Laio F, Ridolfi L, Tamea S (2007) Challenges in humid land ecohydrology: Interactions of water table and unsaturated zone with climate, soil, and vegetation. *Water Resources Research* **43**, W09301, doi:10.1029/2007WR006073.

Thevar PA (2008) Transpiration efficiency of eight grain sorghum lines [*Sorghum bicolor* (L.) Moench]. M.S. Thesis (Kansas State University: Manhattan), 53 pp.

Turner NC (1993) Water use efficiency of crop plants: Potential for improvement. In 'International Crop Science I.' (Eds. DR Buxton, R Shibles, RA Forsberg, BL Blad, KH Asay, GM Paulsen, RF Wilson), pp. 75-82. (Crop Science Society of America: Madison, Wisconsin).

Xin Z, Franks C, Payton P, Burke JJ (2008) A simple method to determine transpiration efficiency in sorghum. *Field Crops Research* **107**, 180-183.

Xin Z, Aiken R, Burke J (2009) Genetic diversity of transpiration efficiency in sorghum. *Field Crops Research* **111**, 74-80.

Zea-Cabrera E, Iwasa Y, Levin S, Rodríguez-Iturbe I (2006) Tragedy of the commons in plant water use. *Water Resources Research* **42** (Supplement), W06D02, doi:10.1029/2005WR004514.

Plant available water capacity of dryland cropping soils in the south-eastern Australia

Abdur Rab[AE], Peter Fisher[A], Nathan Robinson[B], Matt Kitching[C], Colin Aumann[A], Mark Imhof[D], Subhash Chandra[A]

[A] Future Farming System Research Division, Department of Primary Industries, 255 Ferguson Road, Tatura, Victoria, Australia 3616
[B] Future Farming System Research Division, Department of Primary Industries, Cnr Midland Hwy and Taylor Street, Epsom, Victoria, Australia 3554
[C] Future Farming System Research Division, Department of Primary Industries, 621 Sneydes Road, Werribee, Victoria, Australia 3030
D Future Farming System Research Division, Department of Primary Industries, 1301 Hazeldean Road, Ellinbank Victoria, Australia 3821
[E] Corresponding author; email: Abdur.Rab@dpi.vic.gov.au

Abstract
Field capacity (FC) and permanent wilting point (PWP) are two critical input parameters required in the APSIM model (Keating *et al*. 2003) which is currently being used nationally for predicting crop yield and fertiliser requirements at the paddock and landscape unit. FC and PWP were measured for three major soils which are used for dryland cropping in the Mallee and Wimmera regions. Plant available water capacity (PAWC) was determined as the difference FC and PWP. Data were grouped according to the three major soil suborders (Hypercalcic Calcarosols, HYC; Red Sodosols, RS; and Grey Vertosols, GV) and nine soil texture classes (ranging from sand to clay). FC, PWP and PAWC were found to be significantly higher for GV followed by HYC and RS. Overall, FC, PWP and PAWC varied from 0.063 to 0.495 and 0.018 to 0.378 m^3/m^3 respectively. PAWC ranged from 0.053 m^3/m^3 (sandy soils) to 0.147 m^3/m^3 (clay soils).

Key Words
Soil type, soil texture, soil hydraulic properties, paddock variability.

Introduction
Numerical models like APSIM (Keating *et al.* 2003) are currently being used nationally for crop yield and efficient allocation of resources (e.g. fertiliser input requirements) in farming systems at the paddock and landscape unit. FC and PWP are two critical input parameters required in most numerical models. The Mallee and Wimmera regions in Victoria produce about 90% of Victoria's grains. There is a lack of data on FC, PWP and PAWC for major soil types across these regions (see Cock 1985; Rab *et al*. 2009). The objectives of this study was to compare PAWC for three major soil suborders within the northern Wimmera and southern Mallee regions of north west Victoria.

Methods
The study area is located approximately 450 km north-west of Melbourne, in the southern Mallee and northern Wimmera regions of Victoria, SE Australia (Figure 1). The southern Mallee region is characterised by calcareous dunefields and plains (5.1.5 geomorphological unit), whilst the Wimmera region is typified by clay plains with intervening subdued ridges (5.4 geomorphological unit).

Two paddocks within each geomorphic unit were selected to capture the variability in PAWC across these significant cropping landscapes of north-west Victoria. Three sampling locations were established strategically to capture the inherent variability within each paddock. These sampling locations were chosen using paddock information including variability in (i) grain yield, (ii) electromagnetic induction (EM38), and (iii) elevation. Coordinates of the sample locations were recorded using a differential GPS with a horizontal accuracy of 10-20 cm. At each of the three sampling locations (within each paddock) three sampling points were randomly selected. At each sampling point undisturbed samples were taken from 0-10 cm and 20-30 cm soil depths.

Soil-water contents of the undisturbed samples were determined at −10 kPa (FC) using bubble tower ceramic suction plate apparatus. Soil-water content at –1500 kPa matric water potential (PWP) was determined using disturbed samples which were placed on a 15-bar ceramic plate in the pressure plate apparatus. Plant available water capacity (PAWC) was determined as the difference FC and PWP. Soils were classified according to the Australian Soil Classification - ASC (Isbell 2002).
Each soil property was modelled using residual maximum likelihood (ReML) based on a two-factor linear

1 – 6 August 2010, Brisbane, Australia. Published on DVD.

mixed model. The two factors were soil type (S, three levels) and soil depth (D, two levels). Wald tests were used to assess the significance of differences in soil properties between soil types, soil depths, as well as their interactions. All statistical analyses were conducted using GenStat 10.2 (Payne *et al*. 2007). The residuals reasonably satisfied the ReML assumptions of normality and constant residual variance. To study the effect of soil texture group on PAWC, data was analysed using one-way analysis of variance (ANOVA).

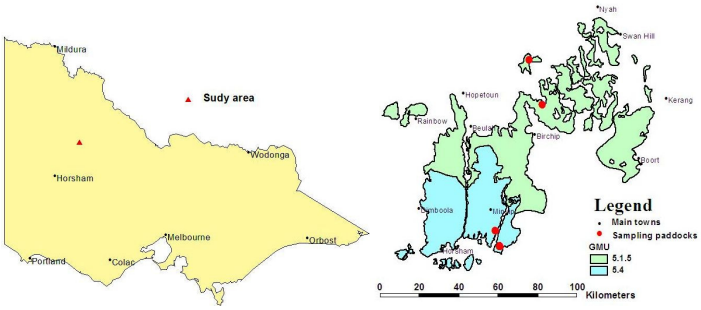

Figure 1. Location of study sites in the southern Mallee and Wimmera regions, SE Australia.

Results

Three major ASC soil suborders: Red Sodosols (RS), Hypercalcic Calcarosols (HYC) and Grey Vertosols (GV) were identified in this study area with nine soil texture classes were represented amongst these. There was a wide variation in soil texture across the three suborders; the RS dominated by coarse textures in the 0-10 cm and both coarse and medium textures in the 20-30 cm depth range; the HYC dominated by medium and fine textured soil in the 0-10 cm and 20-30 cm depth ranges respectively, and the GV dominated by fine textures.

Mean values of FC and PWP for three soil types are presented in Table 1. The effect of interaction (soil x depth) and soil suborder on FC and PWP was significant ($p<0.001$) but the effect of depth was non-significant ($P>0.05$). However, a plot of mean values shows that the nature of interaction was of a non-crossover type (data not shown) and at both depths, mean values for RS were consistently low compared to both HYC and GV. The LSD test showed that at 0-10 cm depth, differences in FC and PWP between soil types were significant while at 20-30 cm depth the difference in FC and PWP between HYC and RS was not significant. The LSD test also showed that for GV the FC and PWP was not significantly different between two soil depths while for HYC and RS the differences between depths were significant.

Table 1. FC, PWP and PAWC of three soil suborders at two depths in the Mallee and Wimmera regions of north-west Victoria, SE Australia.

Volumetric soil-water [A]	Soil types (S)[B]	Depth (D, cm)		Mean	Model term	F Prob	SEd
		0-10	20-30				
FC (% vol)	HYC	34	42	38	S	<0.001	2
	GV	46	42	44	D	0.369	1
	RS	17	23	20	S x D	<0.001	3
	Mean	32	36				
PWP (% vol)	HYC	19	28	23	S	<0.001	1
	GV	31	27	29	D	0.146	1
	RS	6	12	9	S x D	<0.001	2
	Mean	19	23				
PAWC (% vol)	HYC	17	14	15	S	0.001	1
	GV	15	14	14	D	0.314	1
	RS	11	11	11	S x D	0.552	2
	Mean	14	13				

[A] FC and PWP are water content at 10 and 1500 kPa matric potentials; PAWC is the difference between FC and PWP
[B] HYC, Hypercalcic Calcarosol; GV, Grey Vertosol; RS, Red Sodosol.

Both FC and PWP were significantly influenced by soil texture class. There were no significant difference in either FC or PWP found between loamy sand and sandy loam; between loam, sandy clay loam and clay loam; and between silty clay loam, silty clay and clay soils (Table 2). This suggests for practical purposes, these nine texture classes can be grouped in to four major texture classes, sandy soils, loamy sand, loams and clayey soils. The relationship between routinely measured soil properties and FC and PWP are presented in Table 3.

Table 2. FC, PWP and PAWC classified by soil texture groups in the Mallee and Wimmera regions of northwest Victoria, SE Australia.

	Volumetric soil water content (%)[A]					
	FC		PWP		PAWC	
Texture groups	Mean	Range	Mean	Range	Mean	Range
Sand	8	6-8	2	2-3	5	4-6
Loamy sand	20	17-23	7	7-8	13	11-15
Sandy loam	21	18-23	8	7-9	13	11-16
Loam	29	26-32	16	13-18	14	13-14
Sandy clay loam	33	31-34	19	18-22	14	12-15
Clay loam	35	30-39	21	15-25	14	11-17
Silty clay loam	44	32-49	29	19-35	15	12-17
Silty clay*	44		29		15	
Clay	45	40-50	30	25-38	15	10-17

* only one observation

[A] FC, Field capacity; PWP, permanent wilting point; and PAWC, plant available water capacity, is the difference between FC and PWP

Table 3. Regression models for predicting FC and PWP

	FC		PWP	
Variables[A]	**Models**	**R^2 (%)**	**Models[B]**	**R^2 (%)**
c	Y = 14.64 + 0.665(c)	82	Y=4.5+0.557(c)	82
z+c	Y = 12.90 + 0.473(z+c)	87	Y=3.11+0.395(z+c)	85
c, x	Y = 9.86+0.600(c)+7.67(x)	85	NS	
c, c^2	Y=6.17+1.50(c)-0.014(c^2)	93	Y=-1.32+1.13(c)-0.009$(c)^2$	89
c, c^2, x	Y=2.68+1.416(c)-0.0135(c2)+6.12(x)	95	NS	
z+c, $(z+c)^2$	Y=4.78+1.051(z+c)-0.007$(z+c)^2$	93	Y=-1.74+0.734(z+c)-0.005$(z+c)^2$	89
z+c, $(z+c)^2$, b	Y=2.15+1.023(z+c)-0.007$(z+c)^2$+4.5(x)	94	NS	

[A] z, silt (%); c, clay (%); x, organic carbon (%); b, and bulk density (Mg/m^3).

[B] NS, regression coefficient for the input variable, x is not significant.

Discussion

Knowledge of FC and PWP is essential for many plant and soil-water studies, especially those related to plant growth and deep drainage. The mean FC observed for HYC and GV in this study were lower than those reported by Murphy and Lodge (2001) for a Brown Vertosol (46 % vol) but higher than for a Red Chromosol (35 % vol). The PWP of the both HYC and GV found in this study were higher than by Murphy and Lodge (2001) for the Red Chromosol (11 % vol). However, the PAWC found in this study for all three soil suborders (11 – 15 % vol) were lower than those reported by Murphy and Lodge (2001) for a Brown Vertosol (23 % vol) and Red Chromosol (24 % vol).

The mean FC and PWP found for each of the soil texture class was higher than those reported by Jensen *et al.* (1990) for US soils except for sandy soils. For sandy soils, both the FC and PWP were lower than Jensen *et al.* (1990). However, PAWC (12 - 15 % vol) compared favourably with Jensen *et al.* (1990) (13 - 15% vol) except for sandy soils which were lower. The FC, PWP and PAWC found in this study also compare favourable with those found for other Australian soils based on field textures, FC (6 - 45 vol%), PWP (2-25 % vol) and PAWC (4 - 20 %vol), (Better Soils 2005). Hochman *et al.* (2001) found increase in field measured PAWC with increase in clay content with depth for both Black and Grey Vertosols while Ratliff *et al.* (1983) reported no significant increase in PAWC with increase in clay content from silt loam to clay. In our study, the FC and PWP for the HYC and RS increased with depth. However, it did not result in any significant increase in PAWC with depth. This was due to an increase in both FC and PWP with increasing clay content.

The relationships between clay content and FC and PWP found in this study are consistent with those reported for other soils (e.g. King and Stark 2005; Minasny *et al.* 1999; Iqbal *et al.* 2005). For example, Iqbal *et al.* (2005) found greater values of volumetric water content at paddock locations where the percentage clay content was high; an indication of the greater water holding capacity of soil micropores between clay-sized particles. Minasny *et al.* (1999) found a positive non-linear relationship between clay content and FC and PWP. The equations developed in this study can be used to predict FC and PWP for similar soil types. These samples used in this study (N=72) cover a wide range in soil textural composition but limited range in organic carbon content.

Therefore, further research, covering wide range of landuse systems, soil types and climatic conditions, is required to improve these predictive equations.

Conclusions

FC, PWP and PAWC were found to be significantly higher for GV followed by HYC and RS. FC was affected by both clay content and organic carbon (OC) content but PWP was only affected by clay content but not by OC. The developed equations can be used to predict FC and PWP for similar soils elsewhere. However, further research is needed to validate/improve the predictive models for a wider range of organic carbon content, soil types, soil texture and climatic conditions.

Acknowledgement

This research was jointly funded the Grains Research and Development Corporation and the Victorian Department of Primary Industries. The authors would like to thank A. Weidemann, I. McLelland, M. McLelland and R. Dunlop for the use of their paddocks.

References

Better Soils (2005) Better Soils. Module 5: Managing soil moisture, 5.1 Soil Water Holding Capacity. http://www.bettersoils.com.au/module5/5_1.htm

Cock GJ (1985) Moisture characteristics of irrigated Mallee soils in South Australia. *Australian Journal of Experimental Agriculture* **25**, 209-13

Hochman Z, Dalgliesh NP, Bell KL (2001) Contribution of soil and crop factors to plant available soil water capacity of annual crops on Black and Grey Vertosols. *Australian Journal of Soil Research* **52**, 955 -961.

Iqbal J, Read JJ, Thomasson AJ, Jenkins JN (2005) Relationships between Soil–Landscape and Dryland Cotton Lint Yield. *Soil Science Society of American Journal* **69**, 872-882.

Isbell RF (2002) 'The Australian Soil Classification.' (CSRIO Publishing: Collingwood, Vic.)

Jensen ME, Burman RD, Allen RG (1990) Evapotranspiration and Irrigation Water Requirements. ASCE Manuals and Reports on Engineering Practice No. 70. American Society of Civil Engineers, New York, NY.

Keating BA, Carberry PS, Hammer GL, Probert ME, Robertson MJ, Holzworth D, Huth NI, Hargreaves JNG, Meinke H, Hochman Z, McLean G, Verburg K, Snow V, Dimes JP, Silburn M, Wang E, Brown S, Bristow KL, Asseng S, Chapman S, McCown RL, Freebairn DM, Smith CJ (2003) An overview of APSIM, a model designed for farming systems simulation. *European Journal of Agronomy* **18**, 267-288.

King BA, Stark JC (2005) Spatial variability considerations in interpreting soil moisture measurements for irrigation scheduling. http://info.ag.uidaho.edu/pdf/BUL/BUL0837.pdf

Minasny B, McBratney AB, Bristow KL (1999) Comparison of different approaches to the development of pedotransfer functions for water-retention curves. *Geoderma* **93**, 225–253.

Murphy SR, Lodge GM (2001) Soil water characteristics of a red chromosol and brown vertosol and pasture growth. Proceedings of the 10th Australian Agronomy Conference, Hobart, 2001. http://www.regional.org.au/au/asa/2001/2/b/murphy1.htm?print=1

Payne RW, Harding SA, Murray DA, Soutar DM, Baird DB, Welham SJ, Kane AF, Gilmour AR, Thomson R, Webster R, Wilson GT (2007) 'The Guide to GenStat, Release 10. Part 2: Statistics.' (VSN International, Hertfordshire, UK).

Rab MA, Fisher PD, Armstrong RD, Abuzar M, Robinson NJ, Chandra S (2009) Advances in precision agriculture in south-eastern Australia. IV. Spatial variability in plant-available water capacity of soil and its relationship with yield in site-specific management zones. *Crops and Pastures* **60**, 885-900.

Ratliff LF, Ritchie JT, Cassel DK (1983) A survey of field-measured limits of soil water availability and related to laboratory-measured properties. *Soil Science Society of America Journal* **47**, 770–775.

Raised beds in South West Victoria: Pore structure dynamics deliver increased plant available water in sub-optimal rainfall years

Renick Peries[A], Abdur Rab[B] and Chris Bluett[C]

[A]Department of Primary Industries, P O Box 103, Geelong, Victoria 3220, Australia. renick.peries@dpi.vic.gov.au
[B]Department of Primary Industries, 255 Ferguson Road, Tatura, Victoria 3616, Australia abdur.rab@dpi.vic.gov.au
[C]Department of Primary Industries, 402-406, Mair St. Ballarat, Victoria 3350, Australia chris.bluett@dpi.vic.gov.au

Abstract
Soil physical properties were compared between raised beds and flat on two Vertosols (Vertisols in the USDA classification) at three and five years after establishment of beds where different crops and pasture rotations were managed to best practice. A black Vertosol (BV), which had superior structure prior to bedding, performed less favourably than a grey (and sodic) Vertosol (GSV) when their pore structure dynamics were compared. While the BV lost some of its micro-porosity in the 0–0.4 m in the first three years, there was some compensation at depth in the following two years but only at the 0.2–0.4 m depth. In comparison the GSV showed continuous improvement in its micro-porosity over the five years, thus improving in its water retention capacity by about 46% compared to only ~20% in the BV.

Key Words
Raised beds, Vertosols (Vertisols), Sodosols, pore structure, plant available water capacity

Introduction
Raised beds were adopted by farmers in this conventional grazing region, to overcome the risk of damage to crops through waterlogging during the long, cool winter growing season. Despite reliable growing season rainfall, the low permeability of these heavy clay soils can frequently restrict root growth and water movement, and can cause a severe perched water table (Belford *et al*.,1992). Under long-term pasture, these soils have been further compacted by livestock and uncontrolled trafficking of farm machinery. The Vertosols (Isbell 1996) that are representative of about 20% of the region are known to be generally more productive due to their better aeration and greater depth of aggregates (Sarmah *et al*., 1996) than the Grey Sodosols which are more widespread in the region. The work reported here is a part of a long-term trial where three different farming systems (rotations) were compared for productivity and sustainability on 1.7 m-wide and 0.20-0.25m high raised beds on two different Vertosol soils. One was a black cracking clay Vertosol (BV) and the other was a grey Vertosol, which was increasingly sodic at depth and referred to here as a Grey Sodic Vertosol (GSV). The aim of this study was to compare the two Vertosols for their plant available water capacity (PAWC) at three and five years of planned rotations on raised beds. This paper describes the dynamic of porosity changes in the two Vertosols which resulted in temporal differences in PAWC that could contribute to both survival of crops during sub-optimal rainfall conditions and increased productivity under average rainfall conditions.

Methods
The trial was conducted at Gnarwarre near Geelong (38^0 10'S, 144^0 08'E) at the eastern end of the West Victorian Volcanic Plains in Southern Australia in the 500+ mm high rainfall zone. The experiment consisted of 36 plots in a row–column design (6 rows by 6 columns), each devoted to a combination of three crops and pasture rotations on two raised bed systems; wide (20 m) and narrow (1.7 m) raised beds for the comparison of their productivity and sustainability. This paper deals only with the soil physical properties on 1.7 m narrow raised beds. The establishment of narrow raised beds involved several stages of tillage and mounding, starting from a flat perennial pasture. The soil was initially tilled to a depth of approximately 0.08- 0.1 m using a disk harrow, followed by cultivation to a depth of 0.2 m using a chisel plough. A three-bed bed forming machine was then used to mound the soil into beds of 1.7 m width and crumble rollers at the back of the machine lightly compacted the soil on the raised beds and aided in breaking larger clods. After initial cultivation and bed forming the only soil disturbance on the beds was the annual sowing operation using a cone seeder fitted with narrow knife points (minimum-till). Press wheels were used behind the sowing tines to ensure adequate seed–soil contact. The shallow grooves left on the beds by the press wheels act as a reservoir for water harvesting. The water moves through these grooves into the beds and, when bed height is saturated, moves into the main furrow between beds and is carried away from the paddock. Crops and pastures were sown annually on the raised beds and managed to local 'best practice' guidelines. Beds were established in April 1999 and were cropped under minimum tillage (MT) and controlled traffic (CT) for the next six years. Sheep were used to graze the plots during the pasture phases and 'tactical grazing' ensured that the sheep were removed from the plots when the soil was 'wet' to avoid compaction and

1 – 6 August 2010, Brisbane, Australia. Published on DVD.

pugging. The long-term perennial pasture state of the two Vertosols was determined at the commencement of the trial by collecting intact soil cores to a depth of 0.6 m, and using the process described by Gill *et al*. (2009) to determine the soil bulk density (BD), total porosity (P_t), macro porosity (P_m) and plant available water capacity (PAWC). P_m was measured by the difference in water held in the pores at saturation and the matric potentials of -10kPa. In April 2002 and May 2004, at the end of three and five years of planned rotations, all plots were again sampled to a depth of 0.4 m and analysed to determine the BD, P_t, P_m and PAWC experienced by the crops growing on the beds. The main comparison reported in this study is that of the soil environment experienced by crops and pastures growing on raised beds versus the soil environment on the flat, unimproved pasture system that was developed into a raised bed system. For this purpose the flat areas were sampled on each occasion that the beds were sampled and the assumption was made that these flat areas undergo little or no tillage at all while carrying an unimproved and grazed perennial pasture. The differences in soil physical parameters between the flat perennial pasture and the raised beds as experienced by the growing crops and sown pastures were analysed using the residual maximum likelihood procedure (REML) in Genstat 5.42 (GenStat Committee 2000).

Results and Discussion

The soil prior to raised beds

The soil physical parameters on flat, unimproved perennial pasture are shown in Table 1. The apparently higher soil BD in the GSV soil in the 0–0.3 m depth could impose a limitation to root growth and soil water extraction compared to the BV. These soils have been under perennial pastures for a long period (>10 years) and indiscriminately trafficked in their routine management. Despite the total PAWC to 0.4 m being very similar (~65 mm) in the two soils, the greater cracking and self-mulching nature of the BV soil and its lower density in the surface layers could contribute to its greater productivity compared to the GSV, as has been the experience of local farmers. The low self-mulching index of the GSV soil [53.0% compared to 60.3% for BV (Adcock 1998)], its higher BD in the subsoils as well as its sodic nature make this GSV very similar in behaviour at depth to the Sodosols which are extensively distributed across South-west Victoria. However, the measured soil physical parameters after three and five years of planned rotations on beds showed significant improvement in the GSV soil compared to the BV that could impact on temporal changes in crop performance on raised beds.

Table 1. Physical characteristics of the black Vertosol (BV) and the grey Vertosol (GSV) soils in their long-term perennial pasture state at the commencement of trial (1998)

	The black Vertosol (BV)				The grey (and sodic) Vertosol (GSV)			
Depth (m)	**Soil BD Mg m^{-3}**	**Total Porosity (%)**	**Macro Porosity %**	**PAWC% (mm/0.1m)**	**Soil BD Mg m^{-3}**	**Total Porosity (%)**	**Macro Porosity %**	**PAWC% (mm/0.1m)**
0–0.1	1.4	50.8	15.6	21.1	1.5	46.6	14.4	17.1
0.1–0.2	1.4	50.0	15.2	15.9	1.5	43.6	15.4	18.6
0.2–0.3	1.5	43.7	9.6	13.6	1.7	38.4	5.6	16.8
0.3–0.4	1.7	37.9	4.5	12.4(**63.0**)*	1.6	40.4	7.5	13.3(**65.8**)*

Note: BD-soil bulk density; PAWC-plant available soil water capacity; * The total PAWC (mm) to 0.4 m depth.

Figures1a & 1b show soil water storage responses to raised beds and farming systems at the end of three and five years respectively. The figures show soil water (in millimetres) held at -10kPa water potential down to 0.4 m depth in the profile, measured in two segments, 0–0.2 m and 0.2–0.4 m. At the end of the first three years, the differences between the raised beds and the flat system in soil water storage capacity (at -10kPa) of the BV, as experienced by crop roots, were significantly lower than those of GSV whereas at the commencement of the trial, the values of the two soils were very similar (Table 1). The consequence was a potentially higher PAWC (if the wilting point is assumed to remain unchanged) to 0.4 m depth in GSV compared to the BV, by the end of three years. The PAWC at the 0–0.2 m depth was also significantly different between the two soils although they were very similar in the 'flat, perennial pasture' state (Table 1). This difference appears to be the result of the loss of P_m in BV. The trend in the differences of soil water storage capacity continued through to five years (Figure 1b), with the GSV potentially holding more soil water down to 0.4 m depth compared to the BV. However, compared to the 2002 sampling, the latter sampling showed a positive difference in storage capacity in the BV at the 0.2–0.4 m depth. This was associated with the development of P_m at depth in the soil (Figure 1b).

Porosity changes impacting on PAWC

The dynamics in the development of porosity on beds led to the GSV holding more soil water than BV down to 0.4 m in the profile at both the 2002 and 2004 samplings. These cumulative differences are, for the purpose of this discussion, viewed in two segments, i.e. at or above the depth of tillage (0–0.2 m) and below the depth of tillage (0.2–0.4 m). Despite the beneficial differences measured in soil BD and P_t on raised beds, the P_m still remained sub-optimal (<15%) for optimum root function at depths below 0.2 m (~10.8–15.1) in the two soils. Table 2 shows

the measured differences in porosity at different depth intervals in the two soils and provides an explanation of the soil water storage differences in the two soils in response to cropping over time. While both BV and the GSV showed differences in soil BD (and therefore P_t) on beds compared to flat, the corresponding changes in P_m between soils were disproportionate. For example, for a 5.9% increase in P_t in the GSV, the corresponding difference in P_m was 21.8%. But in the BV, a 9.3% increase in P_t led to an almost 60% increase in P_m. Similarly a 12% difference in P_t in GSV was associated with 52.7% difference in P_m at the 0.2–0.4 m depth, while in the BV almost a 100% increase (98.6%) in P_m resulted with only18% increase in P_t. This disproportionate behaviour is very likely to be related to differences in the shrinkage properties of the two soils. While any micro-porosity increases associated with these changes would assist greater storage of water in the soil, a decrease in micro-porosity in BV (0–0.2 m) is likely to have contributed to the significantly higher soil water storage in GSV compared to BV in both 2002 and 2004 samplings. With a degree of break down of the pore structure through tillage and the wet-dry cycles the 'wilting point' of the soil may also have been lowered, thus contributing to enhanced PAWC. While any increase in P_m would certainly favour better drainage, it did correspond to a 12.9% loss in micro-porosity in BV resulting in an actual decrease in the capacity of the soil to store PAW.

Figure 1a **Figure 1b**

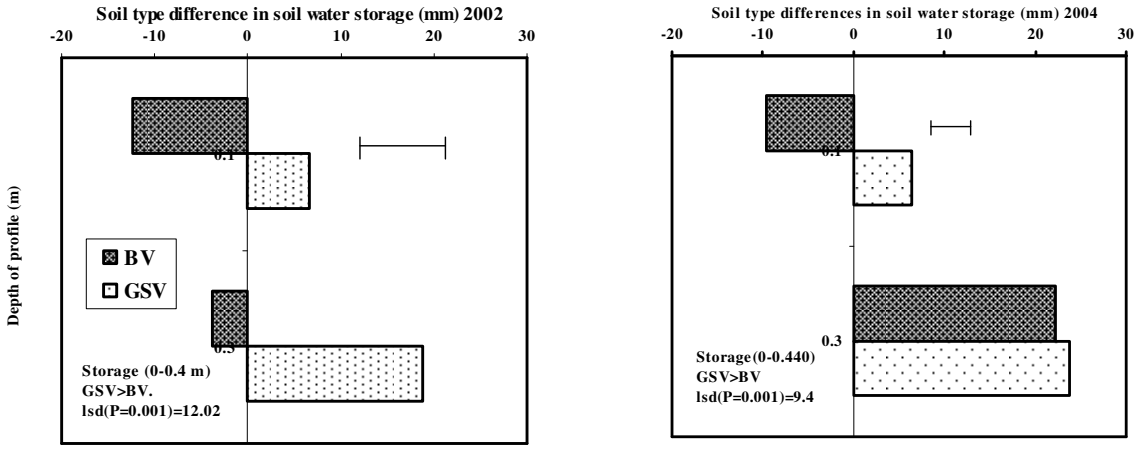

Figure 1. Soil type differences in soil water storage (at-10kPa) in the profile at depths 0-0.2 and 0.2-0.4 m at two samplings in 2002 (Fig. 1a) and 2004 (Fig. 1b). On the Y axis, the depths of 0–0.2 m and 0.2–0.4 m are denoted by their mid points 0.1 and 0.3 m respectively. The Y axis also denotes the soil water storage on the flat perennial pasture and the histograms are measured differences (in millimetres of water/0.2 m soil depth) between raised beds and flat. The horizontal bars are the lsd values for the 0–0.2 m depth.

Large increases in P_m in the BV both at the surface and the subsoil, while assisting drainage under heavy rainfall events, would have the negative effect in PAW storage because of the largely open nature of the resulting aggregates. This phenomenon is supported by the observation that pasture regeneration on raised beds of BV at the autumn break was a lot poorer than on the GSV. The greater P_m created is likely to have contributed to poor seed–soil contact at the bed surface and may also have resulted in more rapid evaporation of soil water compared to the GSV, in which the water would have been more tightly held. This would also lead us to the conclusion that the BV soil was less suitable than the GSV for raised beds and would have performed better under a system of controlled traffic and minimum tillage on flat ground. Once a controlled traffic system has been adopted, in the absence of further compaction the BV should be able to reverse or repair its compaction damage and improve its dense constitution without the use of raised beds, as shown by the experience of the croppers in south-east Queensland (McHugh, pers. comm.) on shrink–swell clays. These farmers have adopted controlled traffic farming without developing harmful levels of P_m that can reduce the PAWC of their soil. Some degree of biological drilling (McCallum *et al*., 2004) may also have contributed towards the differences in soil physical properties measured in this trial in both 2002 and 2004. However, it is difficult to separate the effects of the absence of compaction from those of biological drilling by plants roots and the contribution of other organisms or processes in the subsoil. The two processes may, however, be closely interrelated (Cresswell and Kirkegaard 1995) and the absence or abolition of compaction damage may be an essential trigger for soil biological processes to continue uninterrupted.

Upper limit of plant available water (response differential between soils)

Table 2. Measured differences (%) in the different components of soil porosity experienced by crop roots between raised beds and flat perennial pasture in the two soil types after five years of planned rotations. (While P_m was estimated by difference in soil water held at saturation at matric potential of -10 kPa, micro porosity was estimated as the difference between P_t and P_m).

		Black Vertosol (BV)	Grey Vertosol (GSV)
	Depth interval (m)	Measured difference 1998–2004	Measured difference 1998–2004
Total porosity (P_t)	0-0.2	9.3	5.9
	0.2-0.4	18.3	12.1
	0-0.4	13.3	8.8
Macro porosity (P_m)	0-0.2	59.7	21.8
	0.2-0.4	98.6	52.7
	0-0.4	71.9	31.2
Micro porosity	0-0.2	-12.9	-1.8
	0.2-0.4	1.4	4.1
	0-0.4	-5.8	1.2
Measured difference in soil water held at -10kPa (mm)	0-0.2	37.0 to 27.4	35.7 to 42.1
	0.2-0.4	26.0 to 48.2	30.1 to 53.9
	0-0.4	63.0 to 75.6	65.8 to 96.0
	Enhanced PAWC to 0.4 m depth (%)	20.0%	45.8%

Conclusion

Raised beds, five years on

For crops growing on raised beds, the best outcome from the data presented would appear to be the increased PAWC created over the years. This capacity was created mainly at depth, below the original tillage, and was mainly the result of enhanced macro and micro porosity. The results suggest that the BV soil lost some of its storage capacity in the 0–0.2 m depth of beds, through the development of excessive P_m, but the development of porosity below the depth of tillage still contributed to a ~20% enhancement in the overall storage of soil water compared to the flat. In the GSV however, the measured storage capacity was higher than the flat in both 2002 and 2004 in both depth intervals (0–0.2 and 0.2–0.4 m) thus contributing to an overall increase of approximately 46% in storage capacity at the end of five years. It would be this storage capacity that would act as insurance to crop productivity, ensuring yield stability to crops over time. With enhanced PAWC under beds, a rainfall event of, say 20 mm, which was previously worth 10 mm to the crops, is probably now worth 15 mm, thus offering that extra security to crops during critical stages of yield development. This is a good outcome for crops in South west Victoria that, even following a wet winter, frequently experience shortages of plant available water during Spring grain fill.

Acknowledgments

This work was jointly funded by the Victorian Department of Primary Industries and the Grains Research and Development Corporation, Australia.

References

Adcock D (1998) 'Gnarwarre soil survey. Project report for Graduate Diploma of Land Rehabilitation'. (University of Ballarat, Centre for Environmental Management: Ballarat).

Belford RK, Dracup M, Tennant D (1992) Limitations to growth and yield of cereal and lupin crops on duplex soils. *Australian Journal of Experimental Agriculture* **32**, 929-945.

Cresswell HP, Kirkegaard JA (1995) Subsoil Amelioration by Plant Roots – the Process and the Evidence. *Australian Journal of Soil Research* **33**, 221-239.

Genstat Committee (2000) 'GenStat for Windows. Release 4.2. Fifth Edition'. (VSN International Ltd.: Oxford).

Gill JS, Sale PWG, Peries RR, Tang C (2009) Changes in soil physical properties and crop growth in dense sodic subsoil following incorporation of organic amendments. *Field Crops Research*, doi:10.1016/j.fcr.2009.07.018.

Isbell RF (2002) 'The Australian soil classification.' (CSRIO Publishing: Collingwood, Vic.)

McCallum MH, Kirkegaard JA,Green TW, Cresswell HP, Davies SL, Angus JF, Peoples MB (2004) Improved subsoil macro porosity following perennial pastures. *Australian Journal of Experimental Agriculture* **44**, 299-307.

Sarmah AK, Pillai-McGarry U, McGarry D (1996) Repair of the structure of a compacted Vertosol via wet/dry cycles. *Soil and Tillage Research* **38**, 17-33.

Rapid estimation of soil water retention functions

Peter Fisher[A], Colin Aumann[A], Jasper Vrugt[B], Jan Hopmans[C], Abdur Rab[A], Matt Kitching[D] and Nathan Robinson[E]

[A]Future Farming Systems Research Division, Department of Primary Industries, 255 Ferguson Road, Tatura, Victoria, Australia, Email peter.fisher@dpi.vic.gov.au
[B]Los Alamos National Laboratory, Los Alamos, NM 87545 USA
[C]Department of Land, Air, and Water Resources, University of California, Davis, California 95616
[D]Future Farming Systems Research Division, Department of Primary Industries, 621 Sneydes Road, Werribee, Victoria, Australia
[E]Future Farming Systems Research Division,Department of Primary Industries, Midland Hwy and Taylor St, Epsom, Victoria, Australia

Abstract
Accurate and spatially dense data on the hydraulic functions that control water movement in soils is becoming increasingly important, particularly for crop models and farmer decision support tools. The paucity of this data is the result of the time consuming laboratory techniques involved. Inverse modelling of multistep outflow experiments (MSO) has been proposed as a rapid and accurate technique to obtain the soil water retention function, $\theta(h)$. In this study MSO experiments were carried out using modified Tempe cells and undisturbed soil cores from two depths and three soil types representative of the cropping areas in NW Victoria, Australia. Each core was run through seven desorption runs that varied in the number of pressure steps and the length of time each pressure step was maintained. The inverse modelling produced $\theta(h)$ curves that, except at the very wet end, resembled closely the shape of those produced from equilibrium data. However, the inverse modelled $\theta(h)$ curves over-estimated the air entry region which had the consequence of causing the $\theta(h)$ function to over-estimate the soil water content at all matric potentials. The choice of the number of pressure steps and the length of time maintained at each step had little effect on $\theta(h)$.

Key Words
Multistep outflow, inverse modelling, retention curve, water holding, PAWC

Introduction
The most important soil factor that controls yield in much of the Australian grain production regions is the quantity of plant available water (e.g. Rab *et al.* 2009). Prediction of the spatial distribution of soil water, and its availability to plants, will enable growers to make more informed production decisions that maximise profitability (e.g. the management of nutrients and crop canopies). For example, with accurate meteorological data and knowledge of the spatial variability in soil hydraulic properties, a dynamic soil water model can provide accurate soil water predictions. If this information is coupled with a spatial crop model it should be possible to provide a credible alternative to other techniques (such as real time NDVI prediction) for predicting the optimal spatial application of nutrients. However, the factors that control soil water retention are extremely spatially variable, both across the landscape and with depth. Despite the need for information on soil hydraulic properties there is generally a paucity of such data due to the time consuming and labour intensive techniques required for their accurate measurement. Therefore the objective of this work was to evaluate a relatively rapid and more automated methodology based on the inverse modelling of multistep outflow experiments (Hopmans *et al.* 2002).

Methods
Multistep outflow experiments were carried out using 20 individual pressure cells (Tempe cells, Soilmoisture Equipment Corp.) imported from the USA and modified for use with the metric soil cores used in Australia. They were also modified in a similar fashion to that suggested by Eching *et al.* (1994), incorporating a 6 mm diameter tensiometer inserted through the centre of the top of the Tempe cell that could then be inserted into the centre of the soil core. These micro-tensiometers were connected via a pressure transducer to a Smart Logger® (ICT International) to record the actual pressure within the soil matric. An inlet was added, off-centre, in the top of the cell and connected to a nitrogen cylinder via a pressure regulator and a pressure gauge. A pressure transducer connected to the Smart Logger® recorded the applied pressure from the nitrogen cylinder. The drainage connection at the bottom of each cell was connected to individual burettes and the water level was recorded by the Smart Logger® via a pressure transducer.

1 – 6 August 2010, Brisbane, Australia. Published on DVD.

The applied pressure, water outflow, and soil matric potential were recorded while an initially saturated soil core was subjected to a series of increasing pressure steps. To obtain the soil water retention function, $\theta(h)$, a numerical hydraulic model is coupled with a parameter optimisation algorithm to minimise the deviations between the observed and simulated flow variables in the objective function (e.g. Eching and Hopmans 1993). The Shuffled Complex Evolution Metropolis algorithm was used to solve the least-squares optimisation problem (Vrugt *et al.* 2003).

The inverse multistep outflow methodology was tested using three replicate intact cores from two depths (0-10 and 20-30 cm) from three representative soils found in the main cropping areas of the Victorian Wimmera/Mallee region (i.e. Red Sodosol, Hypercalcic Calcarosol, and Grey Vertosol, classified according to the Australian Soil Classification (Isbell 2002). The cores were run through a series of seven desorption runs and were re-saturated between each run. Each desorption run varied in either the number of pressure steps or the length of time each pressure step was maintained. For the initial run each pressure was maintained until the sample reached equilibrium.

Results

The three soils varied greatly in their soil texture (Table 1). The equilibrium data showed that the three replicates at each of the three soil types were very similar for the 20-30 cm depth, confirming the uniformity of the soil structure at that depth range at each site. While for the 0-10 cm depth, the variability between the replicates increased with increasing clay content. The experimental setup generally produced good data from the sensors during the multistep experiments. To ensure the inverse modelling obtained a unique solution, the possible range of the van Genuchten parameters were constrained to values that corresponded to three broad soil texture groups (sand, loam, and clay) depending on the approximate soil texture of the sample. However, greater inverse modelling experience with Australian soils is required to obtain the optimum restrictions on the search range used.

Table 1. Particle size analysis for soils at the study sites.

Location	Soil depth (cm)	Clay (%)	Silt (%)	Fine sand (%)	Coarse sand (%)
Red Sodosol	0-10	1	2	21	76
	20-30	2	2	38	58
Hypercalcic Calcarosol	0-10	20	8	26	45
	20-30	31	10	21	39
Grey Vertosol	0-10	49	30	14	7
	20-30	49	30	15	7

The inverse modelling produced a good fit between the actual and predicted values for matric potential and outflow (e.g. Figure 1). However, the values of the van Genuchten parameters (which define the soil water retention function) obtained from the inverse modelling resulted in the soil water content being over predicted at most of the matric potentials in the retention function (e.g. Figure 2). This was progressively worse the higher the clay content. The general shape of soil water retention curves produced from the inverse modelling match those from the equilibrium data, however the inverse modelled retention curves over-estimated the air entry region that is controlled by the van Genuchten alpha parameter and is related to the inverse of the air-entry pressure. It is thought that one possible cause of this over-estimation of the soil water contents in the inverse modelled retention curve is the exclusion of water outflow data from very low tensions (<4 kPa). This data was excluded to ensure that the cores were unsaturated at the start of the experiment. The benefits of including this data are now being considered. Despite this over-estimation, the gradient of the functions are similar for both the equilibrium and inverse modelling over most of the range of matric potentials and hence the estimated values of PAWC are relatively similar in both cases.

The inverse modelling technique resulted in very similar estimations of the retention curves irrespective of the seven different desorption runs. This suggests that the inverse modelling is extremely robust, irrespective of the exact combinations of the number of pressure steps or the time that the pressure is maintained (within the range tested). It is therefore anticipated that once the cause of the over-estimation in the air entry region is eliminated this experimental procedure is likely to produce reliable results and that just a few days will be required per test to obtain sufficient data for inverse modelling.

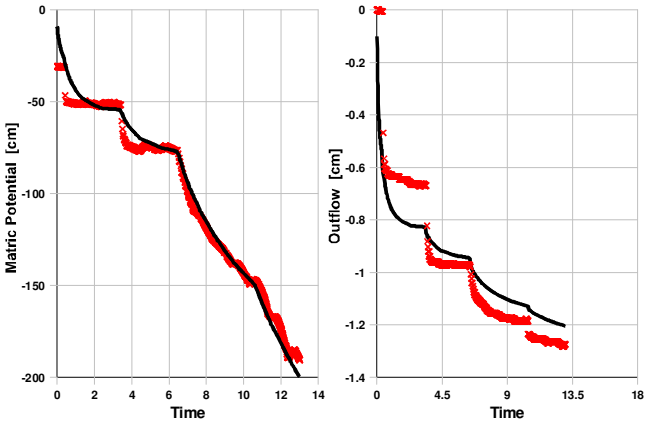

Figure 1. Measured matric potential and outflow (red markers) and the inverse modelled values (black lines) for the 0-10 cm Red Sodosol.

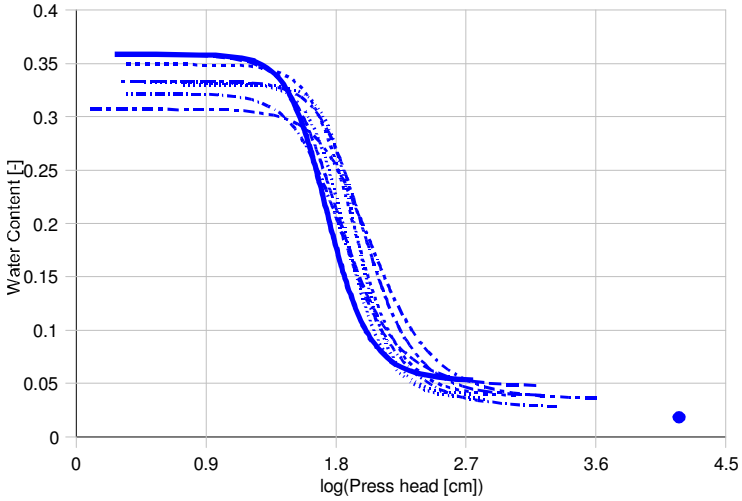

Figure 2. Best fit van Genuchten function curves for the equilibrium retention points for the 0-10 cm. Sodosol (solid line) and inverse modelling results for the 7 different desorption runs (broken lines). Dot marks the measured 1500 kPa retention point.

A further advantage of the data logging system used in this setup is that the outflow can be constantly monitored. In the soils tested, which ranged from 1 to 49% clay, the volume of outflow that occurred after pressure testing to 80 kPa in 4 days ranged between 65 and 88% of the quantity of outflow from the equilibrium test to 80 kPa (Table 2). The soil water content at each of the pressure steps in the rapid multistep outflow experiment provides pseudo retention points. Estimating the soil water retention curve using these pseudo retention points and the 15,000 kPa retention point resulted in retention curves that closely match the equilibrium retention function. This provides an alternative, or cross-checking, approach to the inverse modelling technique.

Table 2. Total outflow between the applied pressures of 4 and 80 kPa for the equilibrium desorption (Run 1) which consisted of a total of 6 pressure steps over 35 days and Run 2 which consisted of 4 pressure steps maintained for 1 day each (total of 4 days), and the fraction of outflow after 4 days compared to 35 day for each of the soil cores.

	Red Sodosol 0-10 cm			Red Sodosol 20-30 cm			Hyp. Calcarosol 0-10 cm			Hyp. Calcarosol 20-30 cm			Grey Vertosol 0-10 cm		Grey Vertosol 20-30 cm		
	Cumulative outflow (ml)																
Run 1	53.0	54.7	48.7	60.2	31.9	46.2	...	33.8	43.2	23.7	22.2	25.2	30.0	...	26.8	26.6	28.9	29.4
Run 2	42.6	46.5	42.7	42.9	26.5	37.2	22.8	23.9	33.3	17.6	17.7	17.2	20.0	18.2	19.2	17.5	18.7	19.9
	Cumulative outflow from Run 2 as a fraction of Run 1																
	0.8	0.85	0.88	0.71	0.83	0.8		0.71	0.77	0.74	0.79	0.68	0.67		0.71	0.66	0.65	0.68

Conclusion

This work has demonstrated that accurate estimation of the soil water retention function for intact cores can be reduced from several weeks of labour intensive work to a semi-automated test that can be completed in a few days. This test can therefore be integrated into a suite of rapid soil testing techniques (including mid-infrared and electromagnetic induction) to provide improved information about soil hydraulic properties for scientists and growers. Further research is required to validate the technique for Australian soils, especially those with high clay content and shrink-swell properties.

Acknowledgement

This research was jointly funded the Grains Research and Development Corporation and the Victorian Department of Primary Industries.

References

Eching SO, Hopmans, JW (1993) Optimization of hydraulic functions from transient outflow and soil water pressure data. *Soil Science Society of America Journal* **57**, 1167-1175.

Eching SO, Hopmans JW, Wendroth O (1994) Unsaturated hydraulic conductivity from transient multi-step outflow and soil water pressure data. *Soil Science Society of America Journal* **58**, 687-695.

Hopmans JW, Šimùnek J, Romano N, Durner W (2002) Simultaneous determination of water transmission and retention properties - Inverse methods. In 'Methods of Soil Analysis. Part 4. Physical Methods'. (Eds JH Dane, GC Topp). (SSSA: Madison, WI).

Isbell RF (2002) 'The Australian Soil Classification'. Revised Edition. (CSIRO Publishing: Victoria).

Rab MA, Fisher PD, Armstrong RD, Abuzar M, Robinson NJ, Chandra S (2009). Advances in precision agriculture in south-eastern Australia. IV. Spatial variability in plant-available water capacity of soil and its relationship with yield in site-specific management zones. *Crops and Pastures* **60**, 885-900.

Vrugt JA, Bouten W, Gupta HV, Hopmans JW (2003) Toward improved identifiability of soil hydraulic parameters: On the selection of a suitable parametric model. *Vadose Zone Journal* **2**, 98-113.

Seasonal variability of soil structure and soil hydraulic properties

Veronika Jirků[A], Radka Kodešová[A], Marcela Mühlhanselová[A] and Anna Žigová[B]

[A]Dept. of Soil Science and Soil Protection, Czech University of Life Sciences Prague, Prague, Czech Republic, Email kodesova@af.czu.cz
[B]Institute of Geology, Academy of Sciences of the Czech Republic, Prague, Czech Republic

Abstract
The study is focused on the assessment of the seasonal changes of soil structure, aggregate stability and hydraulic properties with respect to varying soil physical and chemical properties, soil management and climatic conditions. Seasonal variability of soil properties measured in surface horizons of three soil types (Haplic Cambisol, Greyic Phaeozem, Haplic Luvisol) was studied in years 2007 and 2008. Undisturbed and disturbed soil samples were taken every month to evaluate actual field soil-water content, saturated soil-water content, bulk density, porosity, pH_{H2O} and pH_{KCl}, humus content and organic matter quality expressed as A400/A600, aggregate stability using WSA index, and the soil hydraulic properties. Unsaturated hydraulic conductivity for h= -20 mm was measured directly in the field using the minidisk tension infiltrometer. In addition, micromorphological features of soil aggregates were studied in thin soil sections that were made from undisturbed large soil aggregates. Results show that the soil properties varied within the time. Aggregate stability and values of the soil properties were influenced by the climatic factors, biological activity, growth of plant roots and soil management. Values of pH slightly varied within both years at all localities. Organic matter content, organic matter quality and aggregate stability varied significantly during the first year. However, variability of those properties was considerably lower during the second year at all localities. Porosity and soil hydraulic properties were also more variable during the first year than during the second year.

Key Words
Soil structure, aggregate stability, soil hydraulic properties, micromorphological images, temporal variability

Introduction
Soil water regime is highly affected by soil structure and its stability. Various soil structure types may cause preferential flow or water immobilization (Kodešová *et al.,* 2006, 2007, 2008). Soil structure breakdown may initiate a soil particle migration, formation of less permeable or even impermeable layers and consequently decreased water fluxes within the soil profile (Kodešová *et al.,* 2009a). Soil aggregation is under control of different mechanisms in different soil types and horizons (Kodešová *et al.,* 2009b). Soil structure and consequently soil hydraulic properties of tilled soil varied in space and time (Strudley *et al.,* 2008). The temporal variability of the soil aggregate stability was shown for instance by Chan *et al.* (1994), and Yang and Wander (1998). While Chan *et al*. (1994) documented that temporal changes of aggregate stability were not positively related to living root length density, Yang and Wander (1998) suggested that the higher aggregate stability was found due to crop roots, exudates microbial by-products and wet/dry cycles. The temporal variability of the soil hydraulic properties (mainly hydraulic conductivities, *K*) were investigated for instance in following studies. Murphy *et al*. (1993) showed that *K* values at tensions of 10 and 40 mm varied temporally due to the tillage, wetting/drying, and plant growth. Messing and Jarvis (1993) presented that the *K* values decreased during the growing season due to the structural breakdown by rain and surface sealing. Somaratne and Smettem (1993) documented that while the *K* values at tension of 20 mm were reduced due to the raindrop impact, the *K* values at tension of 40 mm were not influenced. Angulo-Jaramillo *et al*. (1997) discovered that only the more homogeneous sandy soil under furrow irrigation exhibited significant decrease in sorptivity. Petersen *et al*. (1997) documented using the dye tracer experiment that cultivation reduced the number of active preferential flow paths. Azevedo *et al*. (1998) measured tension infiltration from 0 to 90 mm and showed that macropore flow decreased from 69% in July to 44% in September. Bodner *et al.* (2008) discussed the impact of the rainfall intensity, soil drying and frost on the seasonal changes of soil hydraulic properties in the structure-related range. Finally, Suwardji and Eberbach (1998) studied both, aggregate stability and hydraulic conductivities. They documented the lowest aggregate stability during the winter and increased in spring. The *K* values decreased during the growing season. The goal of this study is to assess the seasonal variability of the soil structure, aggregate stability and hydraulic properties with respect to each other and to varying soil physical and chemical properties, soil management and climatic conditions.

1 – 6 August 2010, Brisbane, Australia. Published on DVD.

Methods

The study was performed in 2007 and 2008 on Haplic Luvisol (parent material loess), Greyic Phaeozem (parent material loess) and Haplic Cambisol (parent material orthogneiss). Four soil horizons (Ap 0-35 cm, Bt_1 35-62 cm, Bt_2 62-102 cm , Ck 102-133 cm) were identified in Haplic Luvisol, four horizons (Ap 0-21 cm, Bth 21-28 cm, BCk 29-37 cm, Ck 37-80 cm) in Greyic Phaeozem and three horizons (Ap 0-32 cm, Bw 32-62 cm, Ck 62-97 cm) in Haplic Cambisol. Soil properties were measured every month in surface horizons. Actual field soil-water content, saturated soil-water content, bulk density and porosity were measured on the 100-cm^3 soil samples (10 soil samples per each location and sampling day) using standard methods (Dane and Topp 2002). Hydraulic properties (soil water retention and hydraulic conductivity curves) were measured on the 100-cm^3 soil samples (3 samples) using Tempe cells (Kodešová *et al.* 2006). Humus quality was assessed by the ratio of absorbances of pyrophosphate soil extract at the wavelengths of 400 and 600 nm (A_{400}/A_{600}) (3 repetitions). pH_{H2O} and pH_{KCl} were determined potentiometrically (3 repetitions). Organic carbon content (C_{org}) was determined oxidimetrically by a modified Tjurin method (see Sparks 1996) (3 repetitions). Unsaturated hydraulic conductivity at tensions of 20 mm, *K* (h = -20 mm), was measured directly in the field (2 measurements) using the minidisk tension infiltrometer (Decagon Devices 2006). Micromorphology of soil structure was studied on thin soil sections (2 section) prepared from large soil aggregates. Thin sections were prepared according to the methods presented by Catt (1990). The aggregate stability was studied using the indexes of water stable aggregates (Nimno and Perkins 2002) (3 repetitions). Soil aggregate stability within the soil profiles of soil types studied here was previously discussed by Kodešová *et al.* (2009a, 2009b).

Results

Seasonal changes of soil porosity (Figure 1), actual field soil water content (Figure 2), aggregate stability determined as water stable aggregates (Figure 3) and unsaturated hydraulic conductivity measured using the minidisk tension infiltrometer (Figure 4) are shown here as examples. Results showed that studied soil properties considerably varied within both one-year periods. In addition different values and trends were observed during different years. Organic carbon content (not shown), organic matter quality (not shown) and aggregate stability (Figure 3) varied significantly during the first year. However, variability of those properties was considerably lower during the second year at all localities. Porosity (Figure 1) and soil hydraulic properties (the *K* values shown only in Figure 4) were also more variable during the first year than during the second year. Values of pH_{H2O} and pH_{KCl} (not shown)slightly varied within both years at all localities.

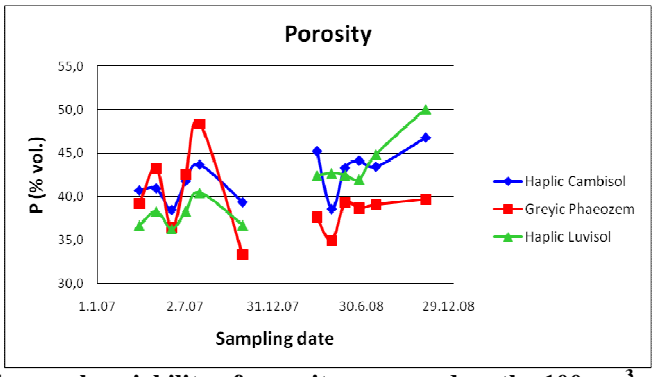

Figure 1. Seasonal variability of porosity measured on the 100-cm^3 soil samples.

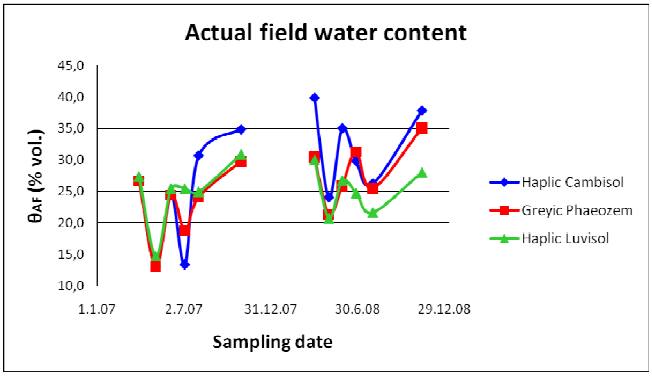

Figure 2. Seasonal variability of actual field soil water content measured on the 100-cm^3 soil samples.

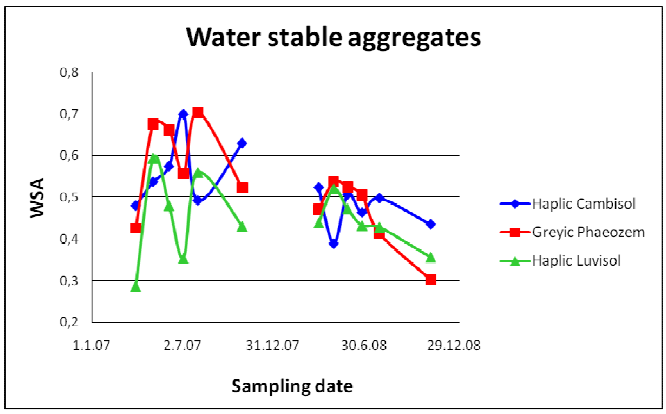

Figure 3. Seasonal variability of aggregate stability determined as water stable aggregates. Aggregate stability increases with increasing WSA value.

Soil aggregate stability depended (as also discussed by Chan *et al.,* 1994) on stage of the root zone development, soil management and climatic conditions. Larger aggregate stabilities and also larger ranges of measured values were obtained in the year 2007 than those measured in 2008. This was probably caused by lower precipitation and consequently lower soil-water contents observed at the beginning of the year 2007 than those measured during the same period in 2008. The highest aggregate stability was measured at the end of April in the years 2007 and 2008 in Haplic Luvisol and Greyic Phaeozem, and at the end of June in the year 2007 and at the beginning of June in 2008 in Haplic Cambisol. In all cases aggregate stability increased during the root growth and then decreased due to summer rainfall events. Aggregate stability reflected aggregate structure and soil-pore system development, which was also documented on micromorphological images (not shown). Hydraulic properties measured in the laboratory (not shown) reflected development of soil porous system. The fraction of larger gravitational pores increased with increasing root activity and decreased due to precipitation impact. As fractions of gravitation pores decreased fractions of capillary pores increased. Infiltration rates measured using the minidisc tension infiltrometer were impacted by the actual field soil-water content. High aggregate stability had positive influence on the infiltration rate.

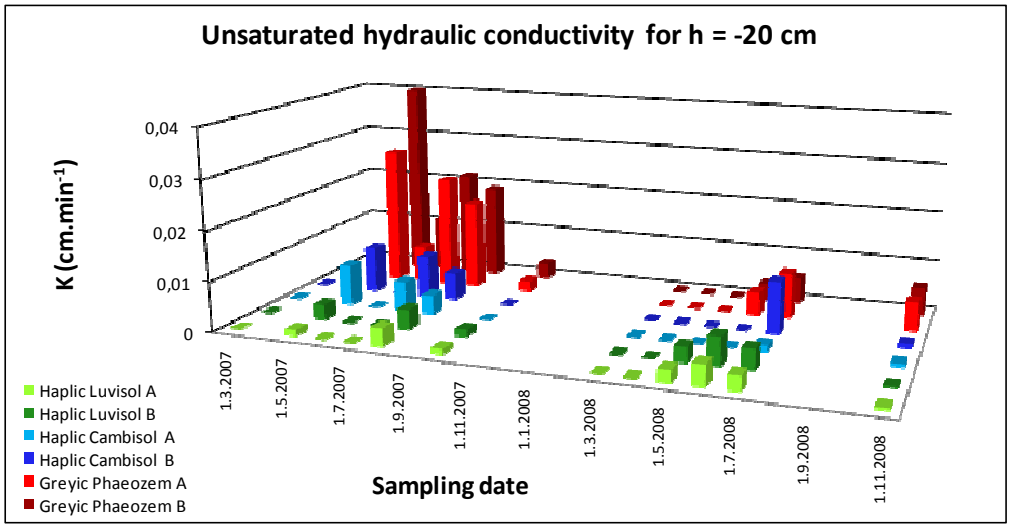

Figure 4. Unsaturated hydraulic conductivities measured for h= -20 mm using the minidisk tension infiltrometer.

Correlation coefficients (not shown) proved that the *K* (h = -20 mm) values measured using the minidisc tension infiltrometer were mostly impacted by the actual soil-water content. The *K* (h = -20 mm) values increased with the decreasing actual soil-water content. The soil aggregate stability was correlated negatively with the A_{400}/A_{600} values (e.g. incensed with the increasing humus quality) in Haplic Cambisol, and negatively with the actual field water content (e.g. increased with the decreasing actual field water content) in Greyic Phaeozem and in Haplic Luvisol. No relation between the soil aggregate stability and the organic carbon content, pH_{H2O} and pH_{KCl} values were found as expected based on previous studies carried out in these soils (Kodešová *et al.,* 2009b). Regression analysis did not show any other significant relationship between measured variables.

Conclusion

The field and laboratory tests were carried out to asses the seasonal changes of the selected soil properties in the surface horizons of three soil types. Similar seasonal trends were observed in all three soils. It was discussed that soil structure, aggregate stability and soil hydraulic properties are interrelated and depends on plant growth, rainfall compaction and tillage. However, it was also shown that climatic conditions dominantly influenced these properties. The drier conditions positively influenced the soil aggregate stability, porosity and hydraulic conductivity.

Acknowledgement

Authors acknowledge the financial support of the Grant Agency of the Czech Republic (grant No. GA CR 526/08/0434) and the Ministry of Education, Youth and Sports of the Czech Republic (grant No. MSM 6046070901).

References

Angulo-Jaramillo R, Moreno F, Clothier BE, Thony JL, Vachaud G, Fernandez-Boy E, Cayuela JA (1997) Seasonal variation of hydraulic properties of soils measured using a tension disc infiltrometers. *Soil Science Society of America Journal* **61**, 27-32.

Bodner G, Loiskandl W, Buchan G, Kaul HP (2008) Natural and management-induced dynamics of hydraulic conductivity along a cover-cropped field slope. *Geoderma* **146**, 317-325.

Catt JA (1990) Paleopedology manual. *Quaternary International* **6**, 1–95.

Chan KY, Heenan DP, Ashley R (1994) Seasonal changes in surface aggregate stability under different tillage and crops. *Soil and Tillage Research* **28**, 301-314.

Dane JH, Topp CT (Eds) (2002) 'Methods of Soil Analysis, Part 4 – Physical Methods'. (Soil Science Society of America, Inc.: Madison, USA).

Decagon Device (2006) 'Minidisc Infiltrometer – User's Manual, Version 3' (Decagon Device, Inc.: Pullman, USA).

Kodešová R, Kodeš V, Žigová A, Šimůnek J (2006) Impact of plant roots and soil organisms on soil micromorphology and hydraulic properties. *Biologia* **61**, S339–S343.

Kodešová R, Kočárek M, Kodeš V, Šimůnek J, Kozák J (2008) Impact of soil micromorphological features on water flow and herbicide transport in soils. *Vadose Zone Journal* **7**, 798–809.

Kodešová R, Vignozzi N, Rohošková M, Hájková T, Kočárek M, Pagliai M, Kozák J, Šimůnek J (2009a) Impact of varying soil structure on transport processes in different diagnostic horizons of three soil types, *Journal of Contaminant Hydrology* **104**, 107-125.

Kodešová R, Rohošková M, Žigová A (2009b) Comparison of aggregate stability within six soil profiles under conventional tillage using various laboratory tests. *Biologia* **64**, 550-554.

Messing I, Jarvis NJ (1993) Temporal variation in the hydraulic conductivity of a tiled clay soil as measured by tension infiltrometers. *Journal of Soil Science* **44**, 11-24.

Murphy BW, Koen TB, Jones BA, Huxedurp LM (1993) Temporal variation of hydraulic properties for some soils with fragile structure. *Australian Journal of Soil Research* **31**, 179-197.

Nimno JR, Perkins KS (2002) Aggregate stability and size distribution. In 'Methods of Soil Analysis, Part 4 - Physical Methods'. (Eds. JH Dane, GC Topp), pp. 317-328 (Soil Science Society of America, Inc.: Madison, USA).

Petersen CT, Hansen S, Jensen HE (1997) Tillage-induced horizontal periodicity of preferential flow in the root zone. *Soil Science Society of America Journal* **61**, 586-594.

Somaratne NM, Smettem KRJ (1993) Effect of cultivation and raindrop impact on the surface hydraulic properties of an alfisol under wheat. *Soil and Tillage Research* **26**, 115-125.

Sparks DL (Ed.) (1996) 'Methods of Soil Analysis, Part 3 – Chemical Methods'. (Soil Science Society of America, Inc.: Madison, USA).

Strudley WM, Green TR, Ascough II JC (2008) Tillage effects on soil hydraulic properties in space and time: State of the science. *Soil and Tillage Research* **99**, 4-48.

Suwardji P, Eberbach PL (1998) Seasonal changes of physical properties of an Oxic Paleustalf Red Kandosol) after 16 years of direct drilling or conventional cultivation. *Soil and Tillage Research* **49**, 65-77.

Yang XM, Wander MM (1998) Temporal changes in dry aggregate size and stability. *Soil and Tillage Research* **49**, 173-183.

Short-term effects of conservation tillage on soil (Vertisol) and crop (teff, *Eragrostis tef*) attributes in the northern Ethiopian highlands

Tigist Oicha[A], Wim M. Cornelis[B], Hubert Verplancke[B], Jan Nyssen[C], Bram Govaerts[D], Mintesinot Behailu[E,A], Mitiku Haile[A], Jozef Deckers[F]

[A]Dept. of Land Resource Management and Environmental Protection, Mekelle University, P.O. Box 231, Mekelle, Ethiopia
[B]Dept. of Soil Management - International Centre for Eremology, Ghent University ,Coupure links, 653, B-9000 Gent, Belgium
[C]Dept. of Geography, Ghent University, Krijgslaan 281 (S8), B-9000 Gent, Belgium
[D]International Maize and Wheat Improvement Centre (CIMMYT), A.P. 6-641, Mexico D.F. 06600, México
[E]Dept. of Natural Sciences, Coppin State University, MD, 21117, U.S.A
[F]Dept. of Earth and Environmental Sciences, Katholieke Universiteit Leuven, Celestijnenlaan 200E, B-3001, Belgium

Abstract
A conservation agriculture (CA) experiment was conducted in 2006 at Adigudom, Tigray, Northern Ethiopia, on experimental plots established in 2005 on a farmer's field. The objectives of this experiment were to evaluate the short term changes in soil quality of a Vertisol due to the implementation of conservation agriculture practices and to assess their effect on runoff and soil loss (not reported here), crop yield and yield components of teff (*Eragrostis tef* (Zucc.) Trotter). The treatments were permanent bed (PB), *terwah* (TERW) and conventional tillage (TRAD). Soil organic matter (SOM) was significantly higher in PB (2.49 %) compared to TRAD (2.33 %) and TERW (2.36 %). Although aggregate stability of PB (0.94) was higher than TRAD (0.83), the difference was not significant. PB had larger macroporosity (0.07) compared to the other treatments. The other soil physical quality parameters analysed showed, however, inconsistency between treatments. Moreover the plant available water content of all treatments was similar. Despite the above soil physical properties improvements, which most probably resulted in higher soil water storage in PB than in the other treatments, yield, biomass and plant height of teff were significantly higher in TRAD than PB. The significantly high weed dry matter at first weeding in PB, the types of weeds and their water uptake behaviour may have caused the reduced teff yield. Herbicides must be used while growing teff in CA experiments.

Key Words
Conservation agriculture, permanent bed, aggregate stability, runoff, soil loss, teff

Introduction

Agriculture in Ethiopia is dominated by rainfed farming of low productivity. Tigray, the northern-most region of the country, suffers from extreme land degradation as steep slopes have been cultivated for many centuries and are subject to serious soil erosion (Wolde *et al.* 2007). Rainfall is seasonal and erratic in Northern Ethiopia, particularly in Tigray. Consequently, there is strong seasonal (~8 months) moisture stress limiting the productivity of rainfed agriculture in the region (Haregeweyn *et al.* 2005). The conventional tillage that uses *maresha* as primary tillage, followed by repeated secondary shallow tillage, is aimed at control of weeds, moisture conservation and increased soil warming (Melesse *et al.* 2008).

In the study area, particularly since the widespread introduction of stone bunds in the late 1980s, ploughing is done parallel to the contour. The first furrow is made at the lower end of the field, and the oxen move upslope for each subsequent furrow. Around the central rift valley area of Ethiopia, however, the directions of any two consecutive tillage operations is usually perpendicular to each other in order to reach the untilled strip of land (Melesse *et al.* 2008). But these repeated operations, aimed to remove weeds and prevent crust formation, cause moist soil to move to the surface which favours loss of water by evaporation, exposes the soil to both wind and water erosion and causes structural damage (Melesse *et al.* 2008). Such detrimental effects can be improved to some extent by other management options like conservation agriculture (CA) practices, including permanent beds and semi-permanent beds.

Gebreegziabher *et al.* (2009) studied the effect of conservation tillage practices on the Adigudom Vertisol using wheat as an indicator crop. However, it is important to study how the treatments respond for teff. Tef is an endemic and major staple crop in Ethiopia. Traditionally, it is cultivated with intensive seed bed preparations with 3-5 passes in the semi-arid and 5-8 passes in the humid areas of the country with the ox driven local *maresha* aimed mainly to remove weeds. Due to the dominance of the vertic soils in the area, tillage is very difficult and farmers associate this with injuries on the shoulders of the oxen. More labour input is needed and longer time to accomplish the ploughing activity. In contradiction to the traditional belief, reduced tillage in

experiments conducted in the central highland Vertisols with high rainfall have shown higher yield although, it was not statistically significant (Balesh *et al.* 2008). A similar study in the Adigudom Vertisol also showed promising results for the use of minimum tillage for teff growth (Habtegebrial *et al.* 2007). However, most of these studies stress only crop parameters and the gross margin of teff. There is little information on the effect of tillage practices on soil physical quality. Therefore, the objective of this study is to evaluate the impacts of CA practice, permanent beds together with the traditional practice like *terwah* and traditional tillage, on changes in some soil physical quality indicators, teff yield and its yield components. Results on the effect of these practices on runoff and soil loss are reported elsewhere in this publication (Araya *et al.* 2010).*

Material and methods

Study site

The CA experiment begun in January 2005 in Adigudom, Northern Ethiopia (13°14' N and 39°32' E) located ~740 km north of Addis Ababa at an altitude of 1960 m a.s.l.. The area has a cool tropical semi-arid climate, characterized by recurrent drought induced by moisture stress. Rainfall in the study site is unimodal, with > 85% falling in the period of July -September. The mean annual rainfall (26 yr) is 504.6 mm and the mean annual temperature is 23 °C. The average annual evapotranspiration was estimated as 1539 mm. According to USDA soil classification, the soil has a clay content of 73% and 24% silt content with high calcium content (20%) and high $pH\text{-}_{H2O}$ (8.1). Together with the swelling and shrinking characteristic which is observed from very wide and deep cracks during the dry season, the soil is classified as Calcic Vertisol according to the FAO-UNESCO classification, pelli Calcic Vertisol according to WRB and Typic Calciustert according to Soil Survey Staff.

Experimental layout

The experiment was conducted on a farmer's field under rainfed conditions. All ploughing and reshaping of the furrows was done using *maresha* (as described by Gebreegziabher *et al.* 2009). Tef was sown by broadcasting in all plots on August 4, 2006. The sowing rate was 30 kg/ha and the fertilizer rate was 100 kg/ha DAP and 50 kg/ha Urea for all treatments. The moisture content at sowing was 0.291 kg/kg. The experimental design was a randomized complete block with two replications for each of the following treatments:

1. Traditional tillage practice (TRAD): The land was ploughed three times, once in May, once in July and the last time before sowing on the sowing date.
2. *Terwah* (TERW): This is a traditional water conservation technique in which furrows are made with *maresha* along the contour at an interval of 1.5-2 m. It is similar to TRAD except for the furrows at regular interval and is repeated yearly.
3. Permanent beds (PB): Beds and furrows of 60-70 cm width (middle of the furrow to the next one) were made after ploughing the plots. The furrows were reshaped after every cropping season without any disturbance on the top of the bed. In the current experiment, the furrows were reshaped in May and refreshed on the sowing date.

The whole experimental field was isolated from the upslope area by a 1.2 m wide and 0.5 m deep ditch to avoid any flow of water entering the upper side of the experimental field. The plots were separated from each other by a 0.5 m wide ditch, in order to avoid surface or subsurface hydrological 'contact' between them. The size of each plot was 19 x 5 m and they had a 3% slope. Wheat was sown in the summer 2005 rainy season and teff in the rainy season of 2006. Runoff collection ditches at the bottom of each plot collected runoff and sediment generated from the experimental plots (see Araya *et al.* 2010).

Soil sampling and analysis

Disturbed composite samples of 1.5 kg were collected from each plot from 0-20 cm in May 2006, before first ploughing for analysis of soil texture, soil organic matter (SOM), $CaCO_3$, soil shrinkage characteristic curve and aggregate stability. Undisturbed soil samples were collected from each plot at the same time from the same depth to determine the soil water retention curve (SWRC). Standard sharpened steel 100 cm^3 cylinders were driven into the soil using a dedicated ring holder. All soil properties were determined using standard procedures. From the soil water retention curve, we derived macroporosity (MacPOR), matrix porosity (MatPOR), soil air capacity (AC), plant available water capacity (PAWC) and Dexter's (2004) soil physical quality index S. Macroporosity was deduced from the water content at a matric potential of -6 kPa, corresponding to pores with a diameter >50 µm. For more details about the soil analysis, we refer to Oicha *et al.* (2010). We further collected agronomic parameters including plant height at maturity, teff dry matter, yield, and weed dry matter. For the determination of yield, harvestable areas of 2 x 8 m and 2 x 6 m were delineated. Hand weeding was performed 4 and 8 weeks after sowing. The weed dry matter was determined by air-drying the first weeding. The Harvest Index was also calculated as the ratio of grain yield to the dry above-ground biomass.

Results

Soil organic matter and aggregate stability

PB had significantly higher (p=0.0003) soil organic matter (SOM) than TRAD and TERW, while the later two do not have a significant difference (Figure 1). Although the stability index of aggregates in PB was higher than for the TERW and TRAD (Figure 1), the differences among the three treatments were not significant. There was also no significant difference among the different size classes for the three treatments too (data not shown).

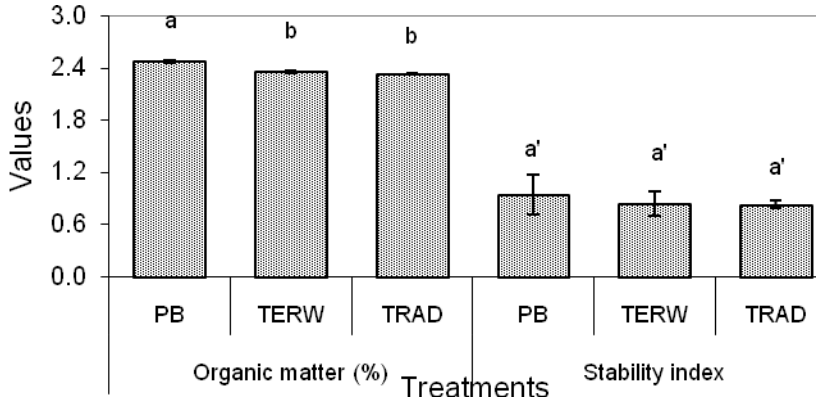

Figure 1. Soil organic matter and aggregate stability index for the three treatments for 0-20 cm soil depth

Soil water characteristic curve and derived soil physical quality parameters

Table 1 shows bulk density and soil moisture content at saturation (θ_s), S, MatPOR, MacPOR, θ_{PWP}, AC and PAWC values as calculated for the different treatments. PB and TRAD have relatively higher moisture content near saturation compared to TERW. The field-derived water content at field capacity was 0.510 m^3/m^3 for the site. This corresponds to matric potential values between -100 to -200 kPa, when using the SWRC (figure not shown). The bulk density and void ratio at oven dryness was 1.87 Mg/m^3 and 0.39, respectively (not shown). PB had higher MacPOR (0.070 m^3/m^3) compared to TRAD (0.063 m^3/m^3), while TERW (0.055 m^3/m^3) had the lowest value (Table 1). TRAD showed higher MatPOR followed by PB, whereas TERW had the lowest value. PB and TRAD had equivalent AC values, 0.087 m^3/m^3 and 0.088 m^3/m^3, respectively, which are higher than that of TERW (0.059 m^3/m^3). The θ_{PWP} of all the treatments is similar (~0.35 m^3/m^3). The PAWC of TERW (0.158 m^3/m^3) and TRAD (0.159 m^3/m^3) were slightly higher than PB (0.155 m^3/m^3).

Table 1. Bulk density and soil moisture at saturation calculated from SSCC, and soil physical quality index (S), matric porosity (MatPOR), macro porosity (MacPOR), water content at permanent wilting point (θ_{PWP}), plant available water content (PAWC) and air capacity (AC) calculated based on the van Genuchten (1980) parameters of the soil water retention curve for the different treatments. Values after ± are standard errors, α=0.05, n=6. Different letters indicate significant difference at p=0.05.

Treatments	Soil physical quality parameters							
	BD (Mg/m^3)	θ_s (m^3/m^3)	S	MatPOR (m^3/m^3)	MacPOR (m^3/m^3)	θ_{PWP} (m^3/m^3)	PAWC (m^3/m^3)	AC (m^3/m^3)
PB	0.98±0.031a	0.596±0.014a	0.067	0.527	0.070	0.355	0.155	0.087
TERW	1.05±0.004a	0.569±0.017a	0.060	0.514	0.055	0.352	0.158	0.059
TRAD	0.98±0.021a	0.598±0.009a	0.060	0.535	0.063	0.351	0.159	0.088

Crop yield and its components

PB resulted in the lowest grain yield, with a mean of 678 kg/ha (Table 2). There was also a significant difference in yield between TERW (mean yield of 925 kg/ha) and PB. There was significant difference (p=0.0016) among treatments in weed infestation. The mean mass of weed dry matter during the first weeding in the TRAD, TERW and PB was 77, 125 and 242 kg/ha, respectively. There was a significant (p<0.0001) negative correlation (r=-0.956, n=6) between weed dry matter and teff yield. Plant height at maturity was significantly higher for TRAD compared with both TERW and PB. The Harvest Index (HI) of PB and TERW was significantly (p=0.01) higher than TRAD (Table 2). Although there was a significant difference in yield between treatments, no difference in teff biomass was observed between PB and TERW.

Table 2. Teff yield, biomass, plant height, weed dry matter at first weeding and harvest index for the different treatments. Values between parentheses are standard deviation. Different letters indicate significant difference at p=0.05.

Treatment	Tef yield (kg/ha)	Weed dry matter (kg/ha)	Tef biomass (kg/ha)	Plant height at maturity (cm)	Harvest index
TRAD	1173 (50) a	77 (4) c	6.7 (0.18) a	44 (2.5) a	0.18 (0.007) b
TERW	925 (99) b	125 (10) b	4.5 (0.64) b	39 (3.5) b	0.21(0.007) a
PB	678 (73) c	242 (17) a	3.0 (0.69) b	31(1.7) b	0.22 (0.004) a

Conclusion

This short-term research showed improvement in SOM and aggregate stability in PB compared to the other treatments, although the difference was not significant. However, the SWRC shows that PB and TRAD had relatively higher moisture content near saturation compared to TERW. The relatively higher MacPOR of PB showed that the increase in the SOM and aggregate stability have contributed to this improvement. However, the PAWC of the treatments did not show a large difference. It is known that significant changes in some soil physical properties can be more prominent when the experiments are continued for longer periods of time. Despite the above improved soil physical properties, which most probably resulted in higher soil water storage in PB than in the other treatments, yield, biomass and plant height of teff were significantly higher in TRAD than in PB. The significantly high weed dry matter at first weeding in PB, the types of weeds and their water uptake behaviour may have caused the reduced teff yield. Herbicides must be used while growing teff in CA experiments.

References

Araya T, Cornelis WM, Nyssen J, Govaerts B, Gebregziabher T, Oicha T, Getnet F, Raes D, Haile M, Sayre KD, Deckers J (2010) Impact of conservation agriculture on runoff, soil loss and crop yield on a Vertisol in the northern Ethiopian highlands. In 'Proceedings of 19th World Congress of Soil Science, Soil Solutions for a Changing World, Brisbane'.

Balesh T, Jens AB, Fred JH, Bernand V (2008) The prospects of reduced tillage in tef (*Eragrostis tef* Zucca) in Gare Arera, West Shawa Zone of Oromiya, Ethiopia. *Soil Tillage Research* **99**, 58–65.

Dexter R (2004) Soil physical quality: Part I. Theory, effects of soil texture, density, and organic matter, and effects on root growth. *Geoderma* **120**, 201-214.

Gebreegziabher T, Nyssen J, Govaerts B, Fekadu G, Mintesinot B, Mitiku H, Deckers J (2009) Contour furrows for *in-situ* soil and water conservation, Tigray, Northern Ethiopia. *Soil Tillage Research* **103**, 257-264.

Habtegebrial K, Singh BR, Haile M (2007) Impact of tillage and nitrogen fertilization on yield, nitrogen efficiency of tef (*Eragrostis tef* (Zucc.) Trotter) and soil properties. *Soil Tillage Research* **94**, 55–63.

Haregeweyn N, Poesen J, Verstraeten G, De Vente J, Govers G, Deckers S, Moeyersons J (2005) Specific sediment yield in Tigray-Northern Ethiopia: Assessment and semi-quantitative modelling. *Geomorphology* **69**, 315-331.

Melesse T, Rockstrom J, Savenije HHG, Hoogmoed WB, Dawit A (2008) Determinants of tillage frequency among smallholder farmers in two semi-arid areas in Ethiopia. *Physics and Chemistry of the Earth* **33**, 183–191.

Oicha T, Cornelis WM, Verplancke H, Nyssen J, Govaerts B, Behailu M, Haile M, Deckers J (2010) Short-term effects of conservation agriculture on some soil physical quality indicators of Vertisol, soil erosion and agronomic parameters of tef (*Eragrostis tef* (Zucc.) Trotter) in the northern Ethiopian highlands. *Soil Tillage Research* **106**, 294-302.

Wolde M, Veldkamp E, Mitiku H, Nyssen J, Muys B, Kindeya G (2007) Effectiveness of exclosures to restore degraded soils as a result of overgrazing in Tigray, Ethiopia. *Journal of Arid Environments* **69**, 270–284.

Siberian Wildrye Grass Yield and Water Use Response to Single Irrigation Time in Semiarid Agropastoral Ecotone of North China

Hao Wang, Zizhong Li, Yuanshi Gong, and Weihua Zhang

Department of Soil and Water Science, China Agricultural University, NO. 2, YuanMingYuan West Road, Beijing, China, 100193. Email: wanghcau@gmail.com (H. Wang), zizhong@cau.edu.cn (Z. Li), gongys@cau.edu.cn (Y. Gong), zhangweihua.cau@163.com (W. Zhang)

Abstract
An irrigation experiment of Siberian wildrye grass (*Elymus sibiricus* L.) was conducted in the alpine cold areas of North China during 2006 to 2008 to compare forage yield (FY) and water use efficiency (WUE) between single irrigation before winter (WI) or at the elongating stage (EI), two irrigations at these two stages (WEI), and the WI treatment combining with mulching straw before next reviving (WMI). The results showed that the FYs under EI were increased by 66, 218, and 99%, and WUE was increased by 56, 134, and 81%, respectively, compared to no irrigation treatment (NI). The FYs under WI were increased by 40, 53, and 44%, and the WUE was increased by 30, 31, and 34%, respectively. No significant FY and WUE increments under WEI were found compared with EI during 2006 to 2007. In 2008, the FY and WUE under WMI were higher than those under EI. Therefore, EI, WMI and WI are the first, second and third choice to achieve relatively high production and WUE of Siberian wildrye grass, respectively. In addition, the elongating-heading stage was the most water sensitive period with significantly larger moisture stress sensitivity index and WUE.

Key Words
Forage yield, Water use efficiency, Irrigation, Agropastoral ecotone.

Introduction
Although forage yield could be increased significantly through irrigation, frequent or large amount of irrigation would hamper the sustainability of water resources and increase related equipment and labor cost. Crop yield and WUE could be increased significantly by irrigating during the critical growth stage (Demir et al., 2006). Wang et al. (2009) concluded that single irrigation at the elongating stage can achieve relatively high production and WUE in the semiarid agropastoral ecotone of North China (APENC).
Currently, almost all the crops were irrigated from May to August in the area, resulting in deficiency in irrigation water resources in this period. Thus, the farmers are facing difficulty to meet crop water demands during the growing season. Off-season irrigation was considered an alternate to improve the crop growth (Stone et al. 2008). In the APENC, most of soil water collected during the rainy season was evaporated due to the long-term bare soil at the regrowth stage. Soil moisture reached a low point before the winter when ample irrigation water is available. In addition, soil water storage changed very little due to the extreme cold weather throughout the whole winter. Thus, we hypothesized that storing soil water before winter might improve the soil moisture condition and enhance the yield and WUE in the following year. Mulching can maintain good soil water condition by reducing the water losses from soil surface. If the irrigated water before winter can be stored in the soil until the critical growth stage combining with mulching technology, the yield increase would be more significant.

Methods
Experimental Site
The field experiment was conducted at the Yu'ershan Demonstration Pasture of National Grassland Ecosystem Station located in Bashang Plateau (116°11´ E, 41°45´ N, elevation of 1460 m) during Oct. 2005–Oct. 2008. The area has a semiarid continental monsoon climate, and the annual precipitation is 300–400 mm, and about 279 mm falls during the growing season from May to September. The soil is a typical sandy loam (coarse loamy, mixed, superactive, calcic cryi-ustic Mollisols) in 0 to 60 cm soil profile based on the diluvial deposit. The primary soil properties can be found in Wang et al. (2009). The field capacity in the 0–60 cm soil profile (FC, 133 mm) and wilting point (WP, 42 mm) were measured at -0.3 and -1.5 MPa matrix potential.
Experimental Design and Field Management
(i) NI, no irrigation was applied. (ii) WI, a single irrigation was applied before winter to bring the soil water storage (SWS) in 0 to 60 cm to field capacity (FC). (iii) EI, a single irrigation was applied at the elongating stage to bring the SWS to FC. (iv)WEI, two irrigations were applied before winter and at the elongating stage. The WEI treatment was replaced by WMI (the irrigation before winter and mulched treatment with naked oats straw before the next reviving, 3 cm thick, 3000 kg ha^{-1}) in 2008.The grass was sown on 15 June 2005, at a seeding rate of 25 kg ha^{-1}. The plot size was 8 m wide by 20 m long. All plots were irrigated by a removable sprinkler system. The

1 – 6 August 2010, Brisbane, Australia. Published on DVD.

chemical fertilizers (75 kg ha^{-1} N and 20 kg ha^{-1} P) were tilled to subsoil before seeding in 2005 and applied on the soil surface every May from 2006 to 2008.

Measurements and Calculations

The 50 × 50 cm^2 aboveground biomass was collected at the end of each growing stage. The forage yield was calculated by 3 × 3 m^2 samples. The first harvest was generally in July and the second harvest was in late September with 5-cm height stubble. The biomass and yield samples were all dried at 75°C for 72 h in an oven. Soil volumetric water content was monitored by TDR. Evapotranspiration (ET) was determined from the soil water balance model, and water use efficiency (WUE) based on ET and Y was calculated.

The Jensen-model (Jensen 1968) was used to calculate the moisture stress sensitivity:

$$\frac{Y}{Y_{\mathrm{m}}} = \prod_{i=1}^{\mathrm{n}} \left(\frac{\mathrm{ET}_{\mathrm{a}i}}{\mathrm{ET}_{\mathrm{m}\,i}}\right)^{\lambda_{\mathrm{i}}} \qquad (1)$$

where Y is actual forage yield in kg ha^{-1}, Y_{m} is forage yield under non-stressed treatment in kg ha^{-1}, the maximum forage yield was used in this paper, ET_{ai} is actual crop evapotranspiration at growth stage "i", $\mathrm{ET}_{\mathrm{m}i}$ is the crop evapotranspiration under non-stressed treatment at growth "i", the maximum value was used in this paper, λ_i is Jensen's moisture stress sensitivity index at growth stage "i", n is the number of growth stages, and Π is a multiplicative sign.

Results

Soil Moisture Condition

There was little variation in soil water storage during winter due to the long-term frozen soil (from November to next April) (Figure 1). The water storage decreased rapidly during the reviving-elongating and the regrowing stage. Late June and late October were the two driest periods in the region. The moisture condition under NI was poor except during the short-term rainy season. The water storage of 0–60 cm soil layer in WI and WEI were relatively high during the reviving stage because the irrigated water before winter could be reserved until next spring. From late October to next late April, water storage under WI and WEI decreased by 11% on the average. In 2006–2008, about 42, 71, and 59% of the irrigated water before winter under WI were still stored in the soil until the reviving period, and 60, 62, and 56% under WEI. But soil water in the WI treatment decreased quickly from the early-May to mid-June. The irrigated water before winter could be stored until 23 May 2006, 10 June 2007, and 9 July 2008, respectively. The ample soil water in EI and WEI could be held until the rainy season because of the irrigation at the elongating stage. The ineffective evaporation could be reduced under mulching condition, so the soil water under WMI treatment in 2008 maintained in high level.

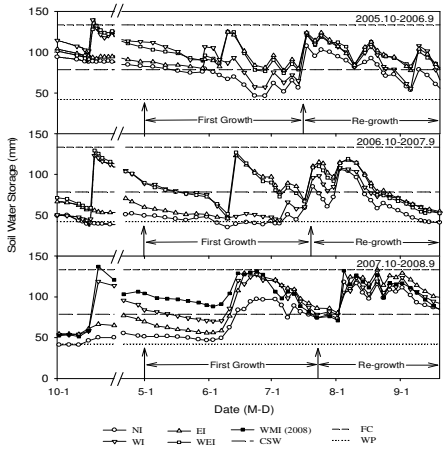

Figure 1 The dynamics of soil water storage in 0–60 cm during the 3-year (Oct. 2005-Sept. 2008). Where, NI: no irrigation; WI: irrigation before winter; EI: irrigation at the elongating stage; WEI: two irrigations before winter and at the elongating stage (Oct. 2005-Sept. 2007); WMI: irrigation before winter and mulched before the next reviving (Oct. 2007-Sept. 2008); FC: field capacity; WP: wilting point; CSW: the critical soil water storage, it was calculated by WP plus the 40% of the total available soil water storage.

Water Consumption

Significant ET difference existed among treatments (Table 1). Irrigation increased the total ET of the whole growing season considerably. Except for the dry year of 2007, no obvious difference was found among the three irrigation treatments. The ET of the first growth under NI in 2006–2008 was 146.6, 113.1, and 130.9 mm, respectively. The value under WI was increased by 15, 27, and 16% compared with NI. The ET under EI was increased by 15, 50, and 25% from NI. The ET under WEI (replaced by WMI in 2008) was increased by 27, 76,

and 16% compared with NI. The average ET under the two treatments irrigated before winter (WI and WEI) was 31.9 and 38.5 mm at the reviving and tillering stages, obviously higher than 22.4 and 27.5 mm for the treatments without winter irrigation (NI and EI). The average ET under the two treatments irrigated at the elongating stage (EI and WEI) reached 72.3 and 44.0 mm at the elongating and heading stages, significantly higher than 52.3 and 32.6 mm for the two treatments without irrigation at the elongating stage (NI and WI). No obvious increase was found under WMI in 2008 except at the heading stage. There was no significant ET difference among treatments during the regrowing stage. The ET at the regrowth in 2007, with less rainfall, was lower than that in 2006 and 2008.

Table 1 Growing stages and cumulative seasonal evapotranspiration (mm).

Year	Growing Stage	Reviving	Tillering	Elongating	Heading	Re-growth	Total
2006	NI	21.3 b	28.1 b	60.8 b	36.4 b	174.6 a	321.2 b
	WI	32.4 a	39.3 a	61.0 b	35.3 b	179.3 a	347.4 ab
	EI	19.0 b	29.8 b	72.7 a	47.5 a	173.5 a	342.5 a
	WEI	27.0 a	40.3 a	74.5 a	44.8 a	170.0 a	356.6 a
2007	NI	21.9 b	29.1 b	35.9 b	26.2 b	107.6 a	220.7 d
	WI	34.7 a	38.7 a	46.8 b	22.9 b	114.4 a	257.6 c
	EI	30.9 ab	27.6 b	68.3 a	42.5 a	131.0 a	300.4 b
	WEI	37.4 a	41.9 a	78.9 a	41.3 a	130.2 a	329.7 a
2008	NI	18.9 b	19.7 b	53.7 b	38.6 b	160.0 a	290.9 b
	WI	27.7 a	32.3 a	55.4 b	36.0 b	162.1 a	313.6 a
	EI	22.2 ab	30.7 a	67.0 a	44.1 a	155.8 a	319.8 a
	WMI	24.8 ab	22.4 b	57.4 b	42.3 a	164.6 a	311.4 a

Note: values followed by the same letter within a column in the same year are not significantly different among treatments for the same growing stage at the 0.05 probability level according to the least significant difference (LSD) test.

Forage Yield and Water Use Efficiency

Irrigation, especially at the elongating stage, played the most important role in yield increase. In 2006–2008, the total forage yield under EI achieved 6381, 6883, and 5763 kg ha^{-1}, increased by 66, 218, and 99% comparing with the NI. The WI increased the forage yield by 40, 53, and 44% comparing with NI. The WEI had the same effect on the total yield with the EI treatment. The first growth of Siberian wildrye grass resulted in the highest forage yield due to the poor ability of regrowth (Table 2). In the 3 yr, the forage yield of the first harvest under NI was 2250, 1085, and 2004 kg ha^{-1}, and that of the second harvest was 1595, 1076, and 896 kg ha^{-1}, respectively. Compared with NI, the yield of the first harvest under WI was increased by 53, 87, and 50%, and that of the second harvest was increased by 23, 20, and 33%. The first harvest of EI was increased by 104, 391, and 117%, and that of the second harvest was increased by 12, 44, and 57%. No obvious difference was found between WEI and EI in 2006 and 2007. Although the effect of yield increase at the first harvest under WMI was similar to EI, there was significant increase over EI yield (161% of EI yield) in the second harvest and the total yield was 6703 kg ha^{-1} in 2008. In addition, the forage yields of the first harvest under NI and WI in 2007 were decreased by 52% and 41% comparing to that of 2006 because of the dry year in 2007, whereas the yield of the EI treatment in 2007 increased. Clearly, the irrigation at the elongating stage was important in keeping the high and stable forage yield, while the forage yield of NI and WI fluctuated with rainfall. The forage yields of the first harvest under NI and WI in the wet year of 2008 increased slightly comparing to those of 2007, but were lower than that of 2006 due to the degradation of Siberian wildrye grass at its fourth growth year. As shown in Table 2, the WUE values during the 2006, 2007, and 2008 growing seasons under EI were 1.9, 2.3, and 1.8 kg m^{-3}, and were higher than 1.2, 1.0, and 1.0 kg m^{-3} under NI, and 1.6, 1.3, and 1.3 kg m^{-3} under WI. There was no difference between EI and WEI. The WMI treatment in 2008 increased WUE to 2.2 kg m^{-3} comparing to 1.8 kg m^{-3} under EI. The WUE at the first growth stage was much higher than that at re-growth stage. The NI in the first growth reached WUE of 1.5, 1.0, and 1.5 kg m^{-3}, respectively, in 2006, 2007, and 2008. The value under WI was increased by 34, 47, and 30% compared to that under NI. The WUE under EI treatment was increased by 77, 228, and 76% compared to under NI. No obvious difference was found between WEI and EI. The mulching treatment not only increased the first growth WUE, but the value at the regrowth stage was also improved. The WUE of WMI in 2008 was 3.0 and 1.4 kg m^{-3} in the first growth and regrowth stages, significantly higher than other irrigation treatments. In addition, the first growth WUE under the elongating stage irrigation treatments (EI and WEI) had less variation among years with coefficient of variation (COV) of 8.2% and 7.1% under EI and WEI, while the WUE under NI and WI fluctuated greatly among years (COV=21.7% under NI and 19.2% under WI).

Water Sensitivity and Production Function

We further calculated the water stress sensitivity index of each stage during the first growth using the Jensen model (1968).

$$\frac{Y}{Y_m} = (\frac{ET}{ET_m})^{0.07}_{Reviving} * (\frac{ET}{ET_m})^{0.20}_{Tillering} * (\frac{ET}{ET_m})^{1.08}_{Elongating} * (\frac{ET}{ET_m})^{0.96}_{Heading} \quad (2)$$

Where ET_m is the crop evapotranspiration under non-stressed treatment at each growth stage, the maximum value was used here. The water stress sensitivity indexes at the elongating and heading stage were 1.08 and 0.96, significantly larger than 0.20 at the tillering stage and 0.07 at the reviving stage.

Table 2. Forage yield and water use efficiency.

Year	Treatment	First growth		Re-growth		Whole season	
		Yield (kg ha^{-1})	WUE (kg m^{-3})	Yield (kg ha^{-1})	WUE (kg m^{-3})	Yield (kg ha^{-1})	WUE (kg m^{-3})
2006	NI†	2250 c‡	1.5 c	1595 a	0.9 a	3845 c	1.2 c
	WI	3443 b	2.0 b	1955 a	1.1 a	5398 b	1.6 b
	EI	4591 a	2.7 a	1790 a	1.0 a	6381 ab	1.9 a
	WEI	4909 a	2.6 a	1796 a	1.1 a	6705 a	1.9 a
2007	NI	1085 c	1.0 c	1076 c	1.0 c	2162 c	1.0 c
	WI	2025 b	1.4 b	1288 b	1.1 b	3313 b	1.3 b
	EI	5328 a	3.1 a	1555 a	1.2 ab	6883 a	2.3 a
	WEI	5649 a	2.8 a	1629 a	1.3 a	7278 a	2.2 a
2008	NI	2004 c	1.5 d	896 c	0.6 c	2900 d	1.0 d
	WI	3001 b	2.0 c	1189 bc	0.7 c	4190 c	1.3 c
	EI	4354 a	2.7 b	1409 b	0.9 b	5763 b	1.8 b
	WMI	4428 a	3.0 a	2275 a	1.4 a	6703 a	2.2 a

Note: values followed by the same letter within a column in the same year are not significantly different among treatments at 0.05 probability level according to the least significant difference (LSD) test.

Conclusion

Irrigation before winter improved the seasonal ET and the growth at the reviving-tillering stage. The yield under WI was increased by 40, 53, and 44% compared to NI in the 3 yr of study. Irrigation at the elongating stage improved the seasonal ET and the growth at the elongating-heading stage. The yield under EI was increased by 66, 218, and 99% over the NI treatment. There was no significant difference between WEI and EI in 2006 and 2007. The yield increase under WMI in 2008 was similar to EI at the first harvest, but the yield and WUE of the regrowth was increased by 61% and 53% compared to EI. Therefore, single irrigation at the elongating stage is the first choice to achieve relatively high production and WUE of Siberian wildrye grass, followed by a single irrigation before winter combining with mulching straw, and a single irrigation before winter. The water stress sensitivity indexes at the elongating and heading stages were 1.08 and 0.96, much higher than at other stages.

References

Demir AO, Goksoy AT, Buyukcangaz H, Turan ZM, Koksal ES (2006) Deficit irrigation of sunflower (*Helianthus annuus* L.) in a sub-humid climate. *Irrigation Science* **24**, 279-289.

Jensen ME (1968) Water consumption by agricultural plants. In 'Water deficits and plant growth. Vol. II'. (Ed. TT Kozlowski) pp. 1-22. (Academic Press: New York).

Stone LR, Lamm FR, Schlegel AJ, Klocke NL (2008) Storage efficiency of off-season irrigation. *Agronomy Journal* **100**, 1185-1192.

Wang H, Li Z, Gong Y, Wang Z, Huang D (2009) Single irrigation can achieve relatively high production and water use efficiency of Siberian wildrye grass in the semiarid agropastoral ecotone of North China. *Agronomy Journal* 101, 996-1002.

Influence of Soil Profile Characteristics on the Efficiency of Water Management Practice in Northeast Florida

Rao Mylavarapu, Subodh Acharya, Rao Mylavarapu

Email raom@ufl.edu

Abstract
The physical and hydraulic characteristics of a typical sandy soil profile lying in the Tri-County Agricultural Area (TCAA) of northeast Florida were studied. The efficiency of the conventional water management practice, called as 'seepage irrigation' was also investigated using a simple conceptual model of the field water balance based on the soil properties and the nature of the irrigation system. Seventy soil samples collected from 22.5cm, 45cm, 67.5cm, 90cm, and 120cm were studied for the particle size distribution (PSD), bulk density (D_b), saturated hydraulic conductivity (K_s), and water holding capacities. The results showed that the soils at the surface and near the crop-root zones had very low clay content, low water holding capacity and high saturated hydraulic conductivity. The results also suggested that the soil properties changed significantly at 120cm (below 90cm) depth indicating the presence of an argillic layer of low permeability in the soil profile. The results showed that the total amount of water loss from a during a typical potato season was as high as 77% which could go up to 87% depending on the amount of precipitation. Daily water losses by surface runoff ranged from 45-75% of the total irrigation supply depending on the time of the crop season while the water loss via SLF varied from 16% to 22%. The overall efficiency of seepage irrigation in 2006 and 2007 was 27% and 23% respectively suggesting that the system was highly inefficient despite it manageability and effectiveness in the sandy soil profiles of TCAA.

Key Words
Soil profile characteristics, water management practice, Florida

Introduction

Northeast region of Florida lying along the Atlantic coastline is the most important potato production area in the state. Majority of the potato farms in this region are concentrated in the Tri-County Agricultural Area (TCAA) spread in St. Johns, Putnam and Flagler counties. These potato farms are estimated to produce approximately 65% of the total potato production in the state annually (Mylavarapu *et al*., 2008). Soils in TCAA are mostly dominated by sand with a very small amount of clay and silt particles and therefore have a very low water holding capacity near the crop root-zone. Water management system in the area is typically based on a conventional seepage irrigation system which also covers most of the gravity-flow irrigated farms in Florida (Smajstrla and Haman, 1998). In this system, the water table is maintained near the crop root-zone during the entire cropping season (Campbell *et al*., 1978) with the help of open drainage ditches and appropriately spaced water furrows. Water is then supplied to the crop root zones by capillarity and subsurface lateral flow (Pitts and Smajstrla, 1989). This system is preferred to other systems because of its cost effectiveness and low maintenance requirement (Haman *et al*., 1989) while being simple to operate and effective for crop production (Bonczek and McNeal, 1996).

Despite the effectiveness and popularity, the efficiency of conventional seepage irrigation system is reported to be low, ranging from 20-70% (Smajstrla, 1991). The system requires continuous pumping of water into the field throughout the crop season as the water needs to be precisely maintained just below the crop root-zone. A large portion of water is lost by surface and subsurface runoffs not only reducing the efficiency by a great magnitude but also increasing the potential for nutrient leaching and subsequent water quality impacts.
This study investigated the physical properties of a typical seepage irrigated soil profile in the TCAA by collecting soil samples from five different depth up to 120cm. Based on the soil properties and the irrigation system. Daily amounts of water loss via surface runoff (RO) and subsurface lateral flow (SLF) from the seepage irrigated field was also estimated for 2006 and 2007 potato seasons with the help of a conceptual water balance model. The conceptual model was developed based on the soil physical properties and the nature of irrigation system and water loss calculations were performed using simple equations based on daily irrigation supply and evapotranspiration (Et) loss.

1 – 6 August 2010, Brisbane, Australia. Published on DVD.

Materials and Methods

The study was performed in a 4.7ha (approx.260m × 182m) seepage irrigated field of UF/IFAS' Research and Demonstration Site located at Hastings in St. Jones County, Florida. The field resembled a typical TCAA agricultural field and consisted 14 crop-beds each approximately 17.2m wide each of which was further divided into 16 rows raised approximately 25cm above the alleys (furrows between each crop row). Seventy soil samples were collected from a typical seepage irrigated field at five different depths: 22.5cm, 45cm, 67.5cm, 90cm, and 120cm using a core sampler and an auger. The measured physical properties included the particle size distribution (PSD), bulk density (D_b), saturated hydraulic conductivity (K_s), and volumetric water contents (θ_v) at different pressures.

Water balance components of the experimental field were recognized based on the nature of the soil profile and the irrigation method and a conceptual model (Figure 1) of the water balance for a typical seepage irrigated field was developed in order to estimate the total water loss from the field. The typical water balance of the field under water table control comprised five components. The inflow components, which consisted of irrigation supplied into the field, and lateral inflow from adjacent fields. The water loss component, on the other hand, comprised RO, SLF and Et losses. Vertical water movement is stopped during irrigation because of either the presence of the impermeable layer (perched water table condition) or the absence of the potential gradient in vertical direction due to the rise of ground water table. Therefore, it could be assumed that the system was in a steady state where the amount of irrigation applied was equal to the losses due to Et and the subsurface lateral drainage. Due to the nature of the irrigation system, subsurface lateral flow was considered to constitute the major portion of the total runoff in the field. Calculation of subsurface lateral flow (SLF) in a water table management system was given by Skaggs (1980) in the model DRAINMOD. Because of the high similarity of the water management system of the study site to the system described in DRAINMOD, the SLF was calculated using the equations given in the model. Once the SLF was calculated, the RO was obtained using the mass balance under the assumption of steady state condition. The rainfall and Et data necessary for the study were obtained from the Florida Automated Weather Network (FAWN, 2008).

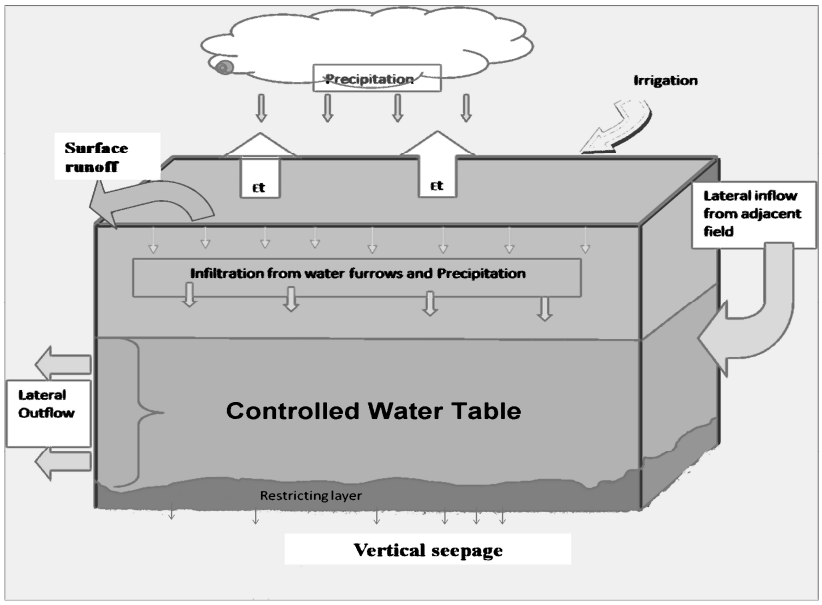

Figure 1. Conceptual representation of field water balance in a typical seepage irrigated field in TCAA.

Results and Discussion

The %clay, D_b and K_s changed significantly as the depth of the soil profile increased. Clay content at 90cm and 120cm were significantly higher than the first three depths (P-value < 0.001). The K_s of the soil decreased significantly at the 90 and 120cm depths while the K_s values of the first three sampling depths were similar. There was no significant difference in the water holding capacity of the soils up to 68cm depth from the surface which was possibly due to very low clay and organic matter content throughout the soil layers. The soil properties showed least variation at 120cm depth with an increase in variance at shallower sampling depths. Among the properties K_s showed the highest variability both within as well as between the sampling depths. The increase in %clay and D_b with decreased K_s values at deeper layers could be attributed to the continuously shallow water table environment. Soils in the TCAA are continuously wetted by the high water table at an

average depth of 40-50cm during most parts of the cropping seasons. Continuous flushing of the profile by fluctuating water table enhances illuviation of clay from upper soil layers which deposit in the lower soil layers. Deposition of fine clay particles tends to decrease K_s of a soil horizon because these fine particles occupy the void spaces between coarse sand particle sand reduce the porosity of the medium.
During 2006 and 2007 growing seasons, the average daily water supply into the field was approximately 583,200 L, out of which a major portion was lost drainage (RO and SLF). The average daily, water-loss from the field during the 100 days potato season was approximately 421,860L in 2006 and 444,500 L in 2007 which respectively represented 73 % and 77% of the total irrigation supply. The amount of water loss was highest at the beginning of the season, with the water loss volume of as high as 90% of the irrigation supply. This was because of the low Et losses from the field as there is little or no vegetative cover at the field surface.

Surface runoff losses accounted for approximately 53% of total irrigation in 2006 and 57% in 2007 while SLF losses were estimated approximately 20% for both seasons ranging from 16% to 22%. Surface runoff from the water furrows decreased as the growing season advanced while SLF did not change significantly. In February 2006, average daily RO loss was 456,815 L which reduced to 348,937 L in March and during the last two months the quantities of RO losses were less than the average daily losses observed during previous months by a magnitude of more than100,000 L. A similar water loss trend was observed in 2007 as well. Surface runoff was as high as 450,000 L per day in February which continuously decreased during the following months. This suggested that as the Et rate increased with the crop growth, hydraulic gradients in the soil also increased and as a result more water was drawn into the soil consequently reducing the RO volumes. It was further supported by average SLF observations that showed little change from February to May. In 2006 average daily SLF loss in February was 94,231L while in May it was 128,066L. The results were similar for the 2007 growing seasons as well. Evapotranspiration and RO showed an inverse relationship across the growing period while SLF showed statistically insignificant yet a gradual increase. These results suggested that, although the changes in average SLF were very small from February to May, it increased with increase in Et form areas around the border of the field. Since Et losses occur also from the surrounding road surfaces it can increase the gradient across the border causing more water to flow laterally towards the ditch or the adjacent fields.

Conclusions

This study showed that the soil properties in the TCAA changed significantly in terms of the texture, bulk density, water holding capacity, and the soil water movement with increasing depth. Presence of an argillic layer with low permeability was evident in the results which showed significant increase in clay content and D_b, and decrease in the K_s at 120cm depth. Observations of the low water holding capacity along with very high K_s of the soil near the crop root-zone also suggested that subsurface seepage irrigation system was highly relevant for the potato and vegetable farming practices in TCAA. Precise control of the water table near the root-zone, avoids any moisture stress to the crops which would be highly likely to occur under other irrigation systems.

The study also estimated that the total amount of water loss from a typical seepage irrigated field during a 100 day cropping season was up to 77% of the total irrigation supply under little or no rainfall conditions. Under normal rainfall conditions, the water loss could be as high as 87% of the total water received by the field. The average efficiency of irrigation water use was approximately 27% in 2006 and 23% in 2007. Water loss by surface runoff from the water furrow was highly dependent on the Et rate, showing an inverse relationship. Despite the manageability and effectiveness of seepage irrigation, the aspects of water use efficiency under seepage irrigation should not be overlooked as it could potentially hasten the loss of nutrients and chemicals into the drainage waters. The results obtained from this study have therefore provided a basis for further research towards developing better water management alternatives to meet the best management practice (BMP) goals implemented in TCAA. The estimated results of water loss are however preliminary and need to be confirmed with the field measured water los data. Currently further studies on the development of a water table management model in the TCAA are under way.

References

Bonczek JL, McNeal BL (1996) Specific gravity effects on fertilizer leaching from surface sources to shallow water tables. *Soil Sci. Soc. Am J.* **60**, 978-985.

Campbell KL, Rogers JS, Hensel DR (1978) Water table control for potatoes in Florida. *Trans. ASAE.* **21**(3), 701-705.

FAWN (2008) Florida Automated Weather Network. http,//fawn.ifas.ufl.edu

Haman DJ, Smajstrla AG, Zazueta FS, Hensel DR (1989) Water recycling in seepage irrigation of potatoes. SJ 89-SP1. St. Johns River Water Manage. Dist. Palatka, FL.
Mylavarapu RS, Hutchinson CM, Li YC, Acharya S (2008) Measurement of lateral water flow in a subsurface seepage irrigation potato production system in the tri-county agricultural area. St. Johns. River Water Manage. Dist. Report.
Pitts DJ, Smajstrla AG (1989) Irrigation systems for crop production in Florida: descriptions and costs. Circular 821. Fl. Coop. Extension Service Gainesville, Florida, 32611.
Skaggs WS (1980) DRAINMOD Reference Report. Method for design and evaluation of drainage-water management system for soils with high water table. US Department of Agriculture, Raleigh.
Smajstrla AG, Hensel DR, Harrison DS, Zazueta FS (1984) Improved seepage irrigation efficiency by controlled water applications. *Proc. Fla. State. Hort. Soc.* **97**, 181-187.
Smajstrla AG, Boman BJ, Clark GA, Haman DZ, Harrison DS, Izuno FT, Pitts DJ, Zazueta FS (1991) Efficiencies of Florida agricultural irrigation systems. Bul. 247. Cooperative Extension Service, University of Florida, Gainesville, Florida, 32611.
Smajstrla AG, Haman DJ (1998) Irrigated acreage in Florida- A summary through 1998. Cir 1220. Cooperative Extension Service, University of Florida, Gainesville, Florida, 32611.

Soil resistance to penetration under the dynamic and predictive perspective of restriction to crop yield

Paulo Ivonir Gubiani[A], José Miguel Reichert[A], Dalvan José Reinert[A] and Neiva Somavilla Gelain[A]

[A]Soils Department, Federal University of Santa Maria (UFSM), RS, Brazil, Email dalvan@ccr.ufsm.br

Abstract
Crop yield is related to soil compaction and water availability. In periods with scarcity of rains, water deficit to plant and soil resistance to root penetration are the main factors which cause yield loss. The way they affect biological processes in crops is already well understood; nevertheless, when and with what intensity they act are difficult questions to answer, above all in relation to resistance penetration, since studies do not duly consider its dynamic behavior. The declared hypothesis is that the time for the resistance penetration to reach a restrictive value is a consequence of the state of compaction and is related to plant response. The penetration resistance was estimated throughout the growing phase of the bean plant crop (*Phaseolus vulgaris*) as a function of soil moisture at different compaction levels (chisel plowed; no-till and no-till with additional compaction). The results obtained confirm the hypotheses of this study. Data showed that the time for the resistance to penetration to reach the value of 2 MP is different among the compaction levels and is directly related to the grain yield. Chisel plowing provides a significant increase in grain yield when the soil is high compacted. The analysis of time for the evolution of resistance to penetration at a critical value is a promising strategy with predictive potential for the effect of soil compaction on crops.

Key Words
Compaction, no-till, bean crop, soil moisture

Introduction

The expansion of no-till system in the world has been accompanied by increasing use of agricultural machinery, whose continued traffic intensifies soil compaction, especially in inappropriate soil moisture conditions and can reduce crop production. Reductions in yield of bean greater than 50% were observed in the no-till when it was compacted by traffic (Collares 2005). Reduced production due to soil compaction has been reported in several other crops (Secco *et al.* 2005; Freddi *et al.* 2008). On the other hand, attempts to reduce soil compaction by plowing or chiseling not always were advantageous (Secco *et al.* 2004; Marcolan and Anghinoni 2006). Various physical properties have been related to crop response in the attempt to define critical physical limits. Using crop yield as a reference, Reinert *et al.* (2001) established restrictive values of soil bulk density as a function of the clay content. These levels have been refined with the association of studies of various other researchers who studied the physical quality of the soil by means of the least limit water range (LLWR) (Reichert *et al.* 2009), which associates information of critical aeration porosity and resistance to penetration. The great difficulty has been in establishing limits for these indicators which characterize a state of compaction which is harmful to crops. More than that, the greatest challenge has been in describing relations between one indicative piece of data and plant response, in a way that the relationship or model preserves the sensitivity between the cause and the effect in other situations of its application. The hypothesis is that values which indicate restriction from resistance to penetration occur at different times among the compaction levels, and there is a relationship between the grain yield of the bean plant and the time for resistance to penetration to reach restrictive conditions.

The objectives of this study are: (i) to generate equations of soil resistance to penetration as a function of soil moisture and estimate soil resistance to penetration during the bean plant growth period; (ii) quantify the period of time which passes for soil moisture to decrease from a moisture condition after rain or irrigation up to the moisture condition in which resistance to penetration reaches a critical value; (iii) relate grain yield with the period of time which passes for resistance to root penetration to reach a critical value.

Methods

An experiment was implanted in the experimental area of the Soils Department of the Federal University of Santa Maria (29º 43’ 14” S, 53º 42’ 18” W), Rio Grande do Sul, Brazil. Soil at the location is classified as a typical Red Dystrophic Argisol, with a sandy loam surface texture with 150 g/kg of clay, 238 g/kg of silt, and 612 g/kg of sand, at the layer from 0 to 0.30 m. The area has been cultivated under no-till for 16 years.

In 12 experimental units (5 m long x 3 m width) distributed in four blocks, the treatments were randomized which consisted of three compaction levels: (1) soil under no-till along 16 years (NT), (2) soil under no-till along 16 years that received mechanical compaction (C-NT) and (3) soil under no-till along 16 years that was chisel plowed (CP). The C-NT was defined by means of the successive traffic of an agricultural tractor (approximate mass of 3.8 Mg), with a disk plow connected to increase the load on the soil. Four sequences of traffic were performed over the subplot, with parallel passing, at a distance from one another of half the width of the rear tractor tire. This operation was performed when the soil presented moisture of 0.14 kg/kg.
The CP was defined by means of chisel plowing performed with a subsoiler, with shanks 0.5 m apart, to a depth of 0.25 m. Chisel plowing was performed when soil moisture was around 0.11 kg/kg. Compaction and chisel plowing were performed after chemical dissecation and spontaneous plant senescence present in the area (*glyphosate*, at a dose of 1,230 g.a.i./ha). Seeding of the beans, BRS Valente cultivar, was performed on January 30, 2008 (second crop), at a density of 280,000 seeds/ha.

For purposes of characterization of the compaction levels, porosity and soil bulk density were measured at 5 DAS, corresponding to 20 and 13 days after the operations of chisel plowing and compacting respectively. Soil samples were collected with their structure preserved in metallic rings of 0.06 m diameter by 0.05 m height in the layers of 0-0.1; 0.1-0.2; 0.2-0.4 m. The soil resistance to penetration (PR) was determined at 23, 25, 26, 35 and 36 DAS, with a manual penetrometer with electronic data storage and a conical point with a 30º angle of penetration. Determinations of the PR were used to generate PR regression equations as a function of the soil moisture. These equations were used to estimate the daily PR throughout the crop cycle based on the moisture data measured with TDR. The time which passed until the PR reached the value of 2 MPa ($Days_{[PR<2MPa]}$) was calculated by means of the estimates of PR throughout the crop cycle. The measurement $Days_{[PR<2MPa]}$ was quantified in the period from 33 to 52 DAS, when the rainfall had practically ceased. Time zero was considered when the soil moisture was near field capacity (33 DAS, Figure 3). The intensity of PR was also quantified, measured by the difference between the maximum values of PR in the period analyzed minus the value of 2 MPa ($\Delta PR_{[PRmax-2MPa]}$). The value of 2 MPa was chosen as the critical value, due to its generalized use by most researchers.

Results
Changes in soil moisture were greatest from 32 to 52 DAS due to extremely low rainfall. Soil moisture variations were more pronounced at the layer ranging from surface to the depth where the effects of different levels of compaction were observed, especially in the 0-0.10 m layer, both within and among levels of compaction. However, the moisture measured 24 hours after significant rainfall (θ_{24h}), which occurred at 14 and 33 DAS, was not significantly affected by the levels of compaction. As of 33 DAS, soil moisture in CP was always less than in the other compaction levels, mainly in the layer from 0-0.10 m. As the θ_{24h} was similar in the different compaction levels, which confers a similar quantity of water in the profile, the more accentuated reduction of soil moisture in the CP must be associated with a greater depth of the root system of the crop, which allowed greater access and, consequently, greater water extraction of soil. In the C-NT, greater soil moisture indicates less access to water by the crop, limited by the high PR. The PR profile of the C-NT at 36 DAS (Figure 1), two days after a period of intense rainfall, and considering 2 MPa as restrictive, clearly indicates that the PR must have limited crop growth even when the soil had elevated moisture. The PR profile of the C-NT shows the occurrence of PR greater than 2 MPa in the layer from 0-0.10 and near this value in the layer from 0.10-0.20. This indicates that the first factor to limit crop growth was the moisture in the CP, and the PR in the PDC. In the PD, moisture and PR must have affected in conjunction, but both at lesser intensities and with non-additive effects.

The time which passed for the PR to reach the value of 2 MPa, or the time in which it remained above this value, to the extent that soil moisture decreased, was different among the compaction levels, as well as among the soil layers (Figure 2). The time which passed for the PR to reach the value of 2 MPa ($Days_{[PR<2MPa]}$) was on mean 2 and 7 days for the C-NT and PD, respectively, in the 0-0,10 m layer and 3, 4 and 13 days for the C-NT, NT and CP respectively in the 0.15-0.25 m layer. The intensity of the PR measured by the difference between the maximum value of the PR in the period analyzed minus the value of 2 MPa ($\Delta PR_{[PRmax-2MPa]}$) was on mean 0.5 and 1.0 MPa for the NT and the C-NT respectively, in the 0-0.10 m layer and 0.4, 1.2 and 1.4 MPa for the CP, NT and C-NT respectively in the 0.15-0.25 m layer. At the time in which the estimated PR was equal to 2 MPa, the soil moisture was in the domain of the functions of the estimate of PR. Soil moisture which corresponds to the lower limit of the domain of the functions occurred at the time indicated by the dotted vertical line (Figure 2).

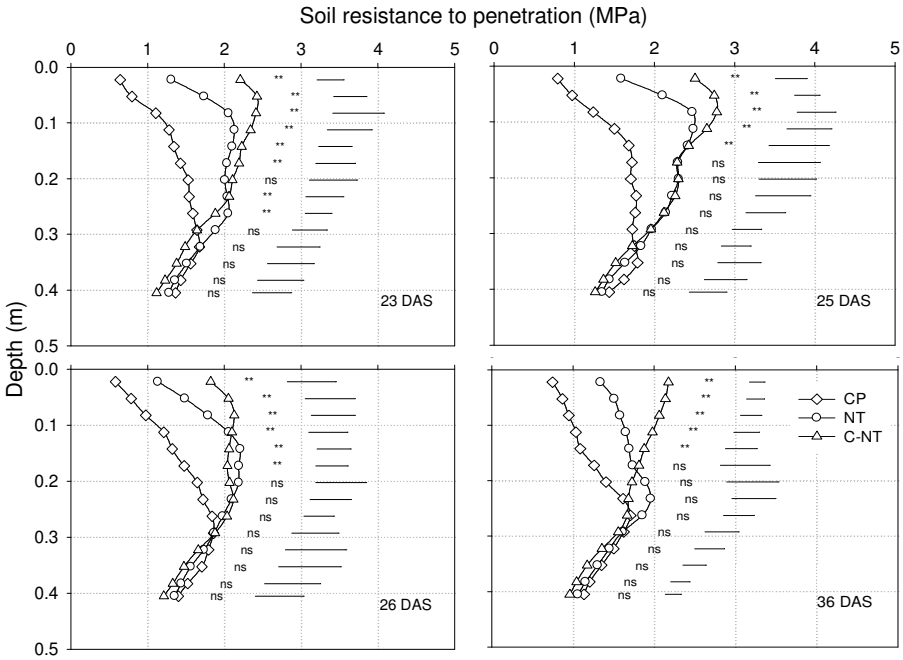

Figure 1. Soil resistance to penetration measured at different days after seeding (DAS). The horizontal lines represent the least significant difference of the Tukey test at 0.05 and compare the means of the treatments in each layer. CP = chisel plowed; NT = no-till; C-NT = compacted no-till; * = significant; ns = not significant.

Therefore, one verifies that the $\Delta PR_{[PRmax-2MPa]}$ calculated is the result of extrapolations of the functions to values beyond the interval over which they were generated. Nevertheless, the lower limit of moisture of the domain of the general function in the 0-0.10 m layer was 0.07 cm^3/cm^3, less than the moisture of the wilting point (0.09 cm^3/cm^3), and the best adjustment of the PR as a function of moisture was the linear. Thus, one expects that in the 0.15-0.25 m layer, if the soil moisture used for the adjustment of the function had decreased as in the 0-0.10 m layer, the linear model would be that which would best adjust a function to the data.

Therefore, the extrapolation used in this study may be considered as an acceptable risk. Comparison of the values of $Days_{[PR<2MPa]}$ with the PR profile at 36 DAS, two days after a period of intense rainfall, shows that the PR in the C-NT had reached the value of 2 MPa, while in NT it would take some days; however, it would not be possible to foresee how many days it would delay. For the 0.15-0.25 m layer, one would also expect that the value of 2 MPa would first occur in the C-NT and NT and then in the CP. Knowledge of the increase of the PR as a function of the daily rate of soil water extraction requires sequential or strategic measurements which allow one to foresee the evolution of the PR and the occurrence of levels which are critical to the plants. The strategy used in this study has potential for this purpose.

The average grain yield was greater in the CP and in the NT (2,807 e 2,791 kg/ha, respectively) which differed from the C-NT (2,254 kg/ha) by the Tukey test at 0.05 (Figure 3). Many studies have shown that when compaction is induced by intense traffic, crops decrease yield in relation to no-till. However, when no-till is compared with soil mobilization, whether by chisel plowing, moldboard plowing or disking, crop response has been varied. At times the yields are greater in mobilized soil, and other times in no-till, or without a difference between soil management systems. In this study, the bean plant grain yield showed that chisel plowing was not a beneficial option compared to the NT; however, it may significantly increase the yield when soil compaction is high (C-NT).

The results of this study confirm the hypothesis that the indicative values of restriction of resistance to penetration (2 MPa) occur at different times among distinct levels of compaction. The PR of 2 MPa occurred at 33 and 40 DAS in the C-NT and NT respectively (0-0.10m layer), and at 37 DAS in the C-NT and NT and at 47 DAS, in the CP (0.15-0.25 m layer). The hypothesis that there is a relationship between grain yield and the time for the PR to reach a restrictive value was also confirmed. Thus, temporal analysis of the PR may be a good study strategy of the effect of soil compaction on crops. In addition, this strategy presents PR predictive potential and may come to be a good guiding instrument for making decisions in regard to physical soil management.

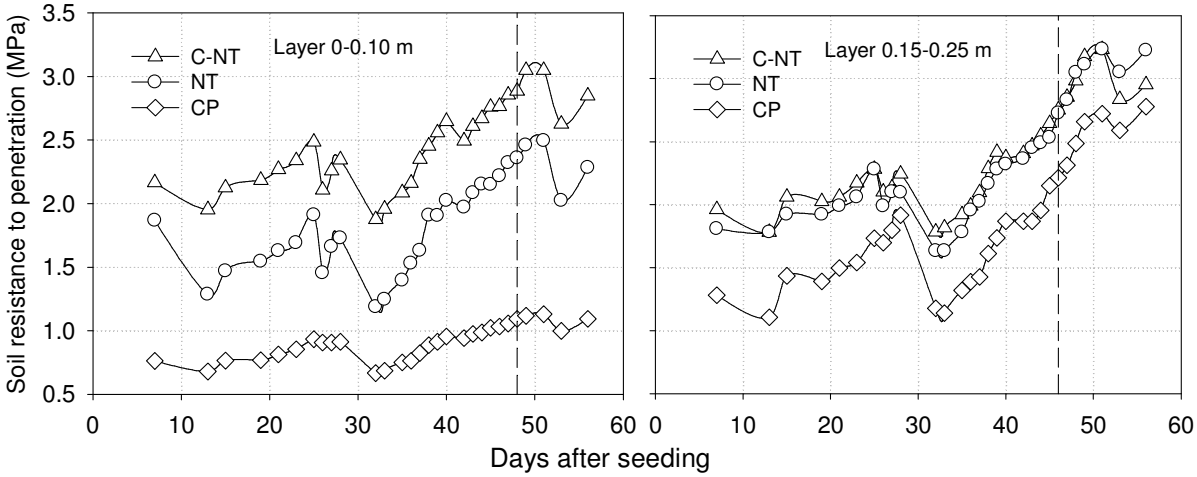

Figure 2. Variation of the soil resistance to penetration at different compaction levels. The vertical line indicates the time at which the soil moisture (Figure 3) decreased beyond the domain of the soil resistance to penetration estimate functions. CP = chisel plowed; NT = no-till; C-NT = compacted no-till.

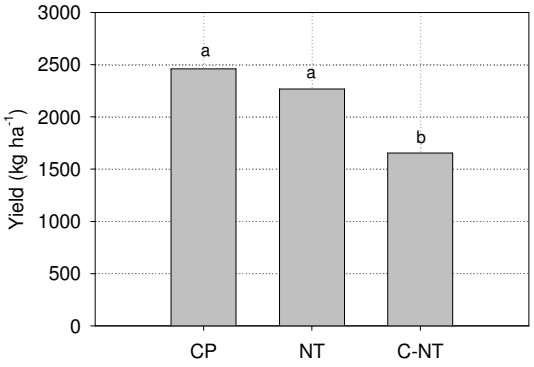

Figure 3. Average yield of bean plant crop. Columns followed by the same letter do not differ statistically by the Tukey test at 0.05 probability of error. CP = chisel plowed; NT = no-till; C-NT = compacted no-till.

Conclusion

The time for resistance to penetration to reach the value of 2 MPa is affected by the state of compaction. In soils with a high state of compaction, plants suffer restriction to growth earlier and with greater intensity through resistance to root penetration than through water deficit. In contrast, in mobilized soils or not very compacted soils, resistance to penetration is much less important than water deficit. The analysis of time for the evolution of resistance to penetration to a critical value is a promising strategy and has predictive potential regarding the effect of soil compaction on crops.

References

Collares GL (2005) Compaction in Oxisols and Argisols and relations with soil and plant. PhD thesis, Federal University of Santa Maria, Santa Maria, RS, Brazil.

Freddi OS da *et al.* (2008) Soil compaction and least limiting water range as related to corn growth and productivity. *Irriga, Botucatu* **13**, 272-287.

Marcolan AL, Anghinoni I (2006) Soil physical attributes of a Alfisol and crop productivity as function of soil mobilization in no-tillage. *Revista Brasileira de Ciência do Solo, Viçosa* **30**, 163-170.

Reinert DJ, Reichert JM, Silva VR (2001) Soil physical properties in irrigated no-tillage system. In 'Irrigation in the Rio Grande do Sul state. Santa Maria'. (Eds R Carlesso, MT Petry, GM Rosa, CA Ceretta) pp. 114-133 (Sprinkler).

Reichert JM, Suzuki LEAS, Reinert DJ, Horn R, Hakansson I (2009) Reference bulk density and critical degree-of-compactness for no-till crop production in subtropical highly weathered soils. *Soil and Tillage Research* **102**, 242-254.

Secco D *et al.* (2004) Soybean productivity and soil physical properties of a Oxisol under management systems and compaction. *Revista Brasileira de Ciência do Solo, Viçosa* **28**, 797-804.

Secco D, Ros Da CO, Secco JK, Fiorin JE (2005) Physical attributes and crop productivity in a Oxisol under management systems. *Revista Brasileira de Ciência do Solo, Viçosa-MG* **29**, 407-414.

Subsoil manuring with different organic manures increased canola yield in a dry spring

J.S. Gill, J. Byrne, P.W. Sale and C. Tang

Department of Agricultural Sciences, La Trobe University, Bundoora, Vic, Australia, Email jsingh@latrobe.edu.au

Abstract
A field study was undertaken in 2007 to examine the effects of subsoil manuring, with different rates of organic amendments, on the growth and yield of a canola crop. The crop was grown on a Sodosol with dense sodic subsoil, in a high rainfall region (long-term average annual rainfall 576 mm) of Victoria. Amendments were applied at a rate of 5, 10 or 15 t/ha. Minimal rain fell during the late winter and early spring, but then significant rain fell in the late spring. The crop was sown late (mid June) and cool winter conditions delayed the germination and early growth of crop until spring. There were no treatment differences in canola biomass during vegetative growth or at anthesis. The control plots experienced water deficit stress during October and began to senesce. However the plots with organic amendments remained green during October, and were able to respond to the rain that fell in the late spring. All organic amendment treatments, apart from the low rate of pig manure, produced higher canola yields, than the control treatment. Yields generally increased linearly with increasing in rates of organic amendments. A key finding was that the poultry manure used in this study was equivalent in effectiveness to the lucerne pellets.

Key Words
Canola, Deep ripping, Pig manure, Poultry Manure, Subsoil constraints

Introduction

There is now a widespread awareness that the dense clay subsoil in Sodosol soils can limit the performance of crops grown on these soils (Wong and Asseng 2007). The soils tend to become waterlogged on top of the relatively impermeable clay layer early in the growing season when winter rainfall exceeds evaporation (Gardner *et al*. 1992), and yet there may not be sufficient plant-available water above the clay for the crops to reach their potential yield at the end of the growing season, particularly if there is a dry finish to the season. It is not surprising therefore that many crops in the high rainfall zone (HRZ) of southern Australia do not yield more than one third of their potential (Riffkin and McNeil 2005).

Research from our laboratory has led to the development of subsoil manuring technology. This involves the placement of large quantities of organic amendment (such as 20 t/ha of lucerne or Dynamic Lifter® pellets) in the upper layers of the clay B horizon in Sodosol soils (Gill *et al.* 2009). Substantial increases in wheat yield (50-70%) and water extraction (up to 70 mm of additional subsoil water) from the clay subsoil during post-anthesis crop growth, have occurred at sites in the high rainfall zone of south west Victoria (Gill *et al.* 2008, 2009). These increases in crop performance were closely correlated with improvements in the physical properties of the subsurface layers that received the amendments (Gill *et al.* 2009). However the amendments used in these experiments were expensive and limited in availability. The issue is whether low-cost animal manures are effective as organic amendments for subsoil manuring. The manures are widely available in Victoria.

In this paper we discuss the effects of different rates (5, 10, and 15 t/ha) of pig and poultry manures, for their effects on the growth and yield of canola grown at Ballan in south west Victoria in 2007. The performance of these manures will be compared with equivalent rates of the lucerne pellets that were used in the earlier subsoil manuring experiments.

Methods

A field trial was carried out in 2007 on a Sodosol soil at Ballan in a high rainfall region of Victoria (long-term average annual rainfall 576 mm). The soil had a dense sodic subsoil (ρ_b = 1.4-1.6 g/cm^3; ESP=17-21%). The trial had a randomized complete block design with nine treatments (Table 2) in three replicated blocks. Each plot was situated on a raised bed (1.7 m wide) and was 10 m long, with a buffer bed between two treatment beds and a 3 m buffer space between two treatments on the same bed. Two beds were left as a buffer between blocks. The amendments (Table 1) were applied at the depth of 30-40 cm using a custom-modified twin-ripper implement, with a 20 cm diameter pipe located behind each ripper shank. An attached hydraulic-operated fan

1 – 6 August 2010, Brisbane, Australia. Published on DVD.

was used to move the materials down through the pipes. The organic amendments were fed into the pipes manually. The lucerne pellets contained 2.8% N, 0.9% P, and 1.4% K, poultry manure contains 3.2% N, 1.8% P and 2.1%K while pig manure contains 1.8% N, 1.2% P, and 1.3% K. Treatments were applied one week before sowing of the crop.

Canola (*Brassica napus*) was sown in mid June, 2007. Daily rainfall events in 2007 are presented in Figure 1. This shows that a dry spring occurred with minimal rainfall from mid-August to the end of October. Canola shoots, cut from a 0.5 m^2 quadrat, were sampled for biomass and N concentration determination on 19th September and at flowering on the 15th October 2007. The N concentration in a ground subsample of dried shoots was measured using an Elementar CN analyzer (Elementar Analysensysteme GmbH, Hanau, Germany). Grain yield was determined from mature shoots, harvested (15th Dec 2009) from the 0.5 m^2 quadrat, on the raised bed. Significant differences between treatments were determined by analysis of variance using Genstat 5 (Lawes Agricultural Trust, Rothamsted, UK).

Table 1. Description of the treatments used in the field trials

Treatment	Amendment	Rate (t/ha)
1	Lucerne pellets	5
2	Lucerne pellets	10
3	Lucerne pellets	15
4	Pig manure	5
5	Pig manure	10
6	Pig manure	15
7	Poultry manure	5
8	Poultry manure	10
9	Poultry manure	15
10	Control	Deep ripped only

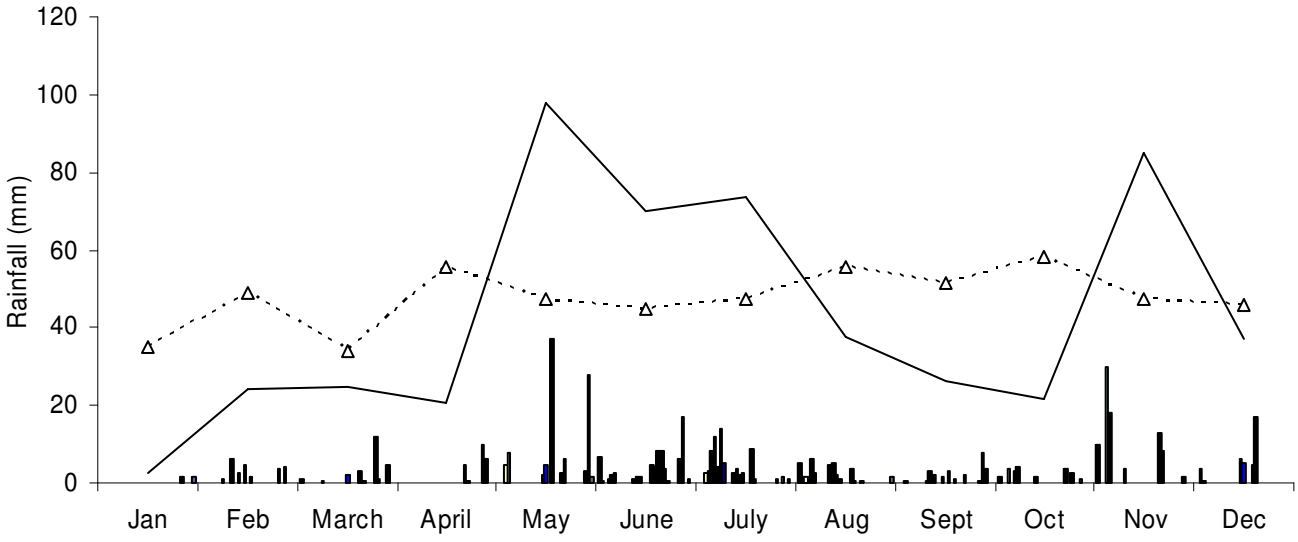

Figure 1. Daily rainfall events (bars) during 2007 at the trial site, together with the actual (continuous) and long-term monthly rainfall means (dashed lines).

Results and Discussion

Crop growth

The crop was sown late because of an infestation of annual ryegrass in paddock. Low temperatures followed during the winter months (maximum daily temperatures were around 12^{o}C while minimum temperatures were generally < 5^{o}C) with frequent frosts and one snowfall event. Germination and growth of crop were slow during this time. There was no differences in shoot biomass between treatments at the first harvest (mean 101 g/m^2),

taken at rosette stage of growth. Biomass results (data not shown) for the harvest at flowering showed trends of increasing biomass in the treated plots, but no significant differences occurred.

Nitrogen concentration in canola shoots

There were no significant differences between treatments in shoot N concentrations at the 1st harvest (mean 5.1 %N). However there were differences between treatments and the control in the shoot N concentration at flowering (Figure 2). Here the three rates of the poultry manure had significantly higher shoot N concentrations ($P<0.05$) compared to the control, as did the two higher rates of lucerne pellets. No pig manure treatments differed from the control in shoot N concentration at flowering.

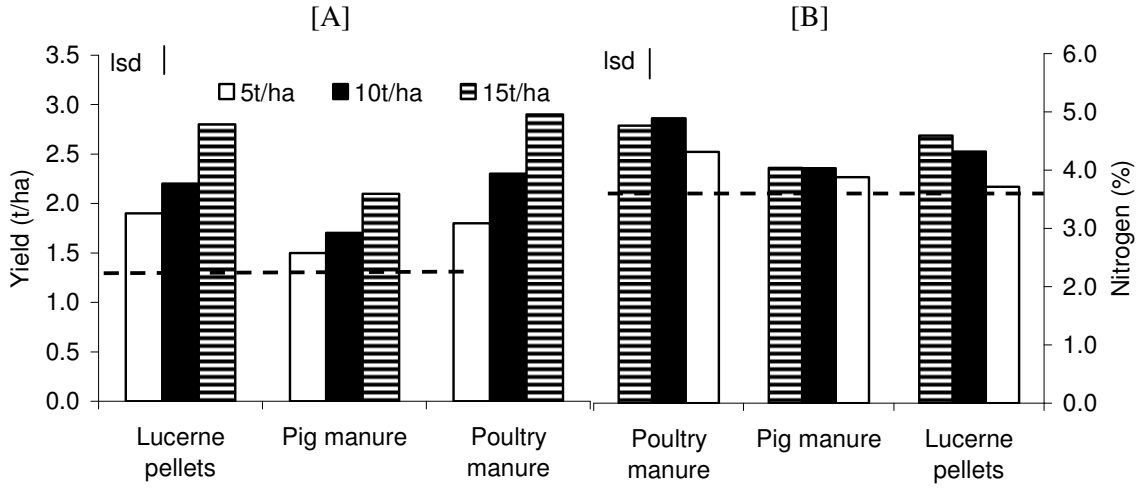

Figure 2. Canola grain yield (A) at harvest and the shoot N concentration at flowering (B). Dotted line shows values for the control treatment.

Crop performance and grain yield

Grain yield from the canola plots was significantly higher in all the organic-manure-treated plots, apart from the pig manure application of 5 t/ha. (Figure 2). Yields increased linearly with increases in rate of application of lucerne pellets and both manures from 5 t/ha to 15 t/ha. Increase in rate of application of pig manure from 10 t/ha to 15 t/ha also increased the yield significantly. The grain yield of canola was 115% higher with the 15 t/ha of lucerne pellets or poultry manure plots compared to the control plots (Figure 2).

The high rainfall events during May to July period (242 mm) would have increased the soil water status in the profile. This meant that there was adequate soil water to sustain the rapid increase in canola growth in all treatments in the early spring. However the dry conditions, resulting from the lack of significant rainfall events from late July to the end of October (Figure 1), began to restrict canola growth in the control plots during the mid spring period. Another subsoil manuring trial with canola had been established next to this field experiment, where access tubes for monitoring soil water with a neutron probe had been installed (Gill *et al.* 2008). Soil water measurements from the adjacent trial (data not presented) indicated that more soil water below the depth of 40 cm had been used by the canola plants from organic-amended plots, compared to the control plots, by the end of October. Thus it is likely that the canola plants in the organic-amended plots in this study were able to extract more subsoil water than the plants growing in the control plots. Large rainfall events occurred in early November during the latter part of the podfilling period (Figure 1); the canola plants in the organic-amended plots had not suffered any moisture stress prior to this rain and were able to benefit more from the rain. In contrast, the control plants had been showing symptoms of severe moisture deficit stress during October, and had begun to senesce when the November rain occurred. Consequently they did not respond to this late rain.

The poultry manure used in this study was equal in effectiveness to the lucerne pellets, when used as an organic amendment for subsoil manuring. This is encouraging for grain growers in the HRZ (High rainfall zone) as poultry manure is considerably cheaper and is more available than lucerne pellets. The pig manure however was less effective than the other two amendments, at all rates of incorporation. It is likely that the lower N concentrations in the pig manure reduced the N status of the canola plants relative to the other amendments (Figure 2), and this contributed to the lower canola yields.

References

Gardner WK, Fawcett RG, Steed GR, Pratley JE, Whitfield DM, van Rees H (1992) Crop production on duplex soils in south-eastern Australia. *Australian Journal of Experimental Agriculture* **32,** 915-927.

Gill JS, Sale P, Tang C (2008). Amelioration of dense sodic subsoil using organic amendments increases wheat yield more than using gypsum in a high rainfall zone of southern Australia. *Field Crops Research* **107**, 265-275.

Gill JS, Sale P, Tang C (2009) Changes in soil physical properties and crop root growth in dense sodic sub soil following incorporation of organic amendments. *Field Crops Research* **114**, 137-146.

Riffkin P, McNeil D (2006) Plant characteristics associated with wheat yields in the high rainfall zone of southern Australia. In 'Proceedings of the 13th Australian Agronomy Conference', Perth, Western Australia. http://www.regional.org.au/au/asa/2006/poster/agronomy/ 4608_riffkinpa.htm.

Wong MTF, Asseng S (2007) Yield and environmental of ameliorating subsoil constraints under variable rainfall in a Mediterranean environment. *Plant and Soil* **297**, 29-42.

The effect of drip emitter rate on bromide movement in a drip irrigated vineyard

Jonathan Holland[A] and Philip Charlton[B]

[A]National Wine and Grape Industry Centre, Charles Sturt University, Wagga Wagga, NSW, Australia, Email jholland@csu.edu.au
[B] School of Computing and Mathematics, Charles Sturt University, Wagga Wagga, NSW, Australia

Abstract
A field-scale solute transport experiment was undertaken using a bromide tracer to understand leaching in soils of drip irrigated vineyards. The effect of applied irrigation volume was investigated with 3 distinct emitter rates (treatments) of 1 L /h (T1), 1.6 L /h (T2) and 2.3 L /h (T3). Depth concentration profiles of bromide and the recovered mass of applied bromide showed just one significant difference (times 2) between the irrigation volume treatments. Soil water content remained very high throughout the experiment, which indicates that antecedent soil moisture is a major factor that strongly influences soil leaching rates and patterns. These results on bromide movement are indicative of nitrate and salt movement and suggest that close attention needs to be placed on irrigation timing and soil water content to avoid excessive leaching, especially when fertiliser is applied so that nutrients are kept within the root zone.

Key Words
Drip emitter rate, irrigation volume, bromide tracer, field solute transport, nutrient movement, soil water

Introduction
Scarcity of water in many parts of the world has led to increased interest and indeed greater need for improvements in the management and distribution of water resources for irrigation. In some countries the water situation is critical and it is necessary to increase global food production to reduce the widespread hunger. Increasing water use efficiency can be achieved by several means, including system design, soil moisture monitoring, irrigation scheduling and reducing loss pathways such as drainage beyond the root zone. In an irrigated production system nutrient use efficiency is strongly related to water use efficiency. Indeed fertilizer is often applied at the same time or close to when a field is irrigated. While soil water and nutrient supply are often separated into two distinct problems, they are actually closely associated. We believe that for many irrigated agricultural production systems there is a great need to focus on soil nutrient status and soil water together.

To further understand the relationship between soil water dynamics and nutrient movement a study was undertaken on a drip irrigated vineyard in the Riverina wine region of NSW Australia. Recently, this region has experienced constraints on water allocations for irrigation and irrigation water costs have risen. In addition, over the last 10 years there has been a large increase in the area of drip irrigation systems (while the area of furrow irrigated vines has declined). Hutton *et al.* (2007) report that there are large differences in the application rates of fertilizer and evidence of inefficient fertilizer application practices. Therefore, there is a major need for improved understanding on fertilizer application for drip irrigation systems. This paper seeks to increase understanding on the movement of nutrients and solutes from drip irrigated vineyards. In that context, this work aims to investigate the effect of irrigation volume on the leaching characteristics of a tracer during the growing season. A tracer approach was chosen as it relates to the movement of nutrients (such as nitrate) and salts. The objectives of this experiment were to: 1) observe the spatial and temporal leaching characteristics from a surface applied drip source; 2) calculate the water and nutrient use efficiency of different irrigation volumes; and 3) estimate the risk of nutrient and solute leaching.

Methods
Site description and instrumentation
The experimental site is located within a 2.7 ha commercially managed vineyard near Griffith, NSW, Australia (34^{o} S, 146^{o} E). The vineyard is drip irrigated and was planted with Chardonnay grapes in 2002 at a row spacing of 3.6 m and vine spacing of 2.5 m using a single cordon, spur pruned growing system. This site has low relief which is typical for the extensive Riverine plains that are distributed across the south and west of NSW. The landscape contains deep alluvial sediments with some sandy prior streams which were deposited by the action of ancient streams. At the surface (0 – 15 cm) the soil is a clay loam texture and below this the profile becomes a sandy clay loam. The soil at the experimental site is classified as a Brown Dermosol (Isbell 2002). This soil drains well and is commonly found across this region. The soil bulk density was measured using the core

method (McKenzie *et al.* 2002) and the soil particle size analysis was determined using the hydrometer method. Soil chemical and physical properties at 6 depths are given to characterise the experimental site (Table 1).

Table 1. Soil chemical and physical properties by depth for the field experimental site

Depth (cm)	EC (dS/m)	pH (1:5 water)	Bulk density (g/ cm3)	Sand (per cent)	Silt (per cent)	Clay (per cent)
0-10	0.13	7.09	1.40	48.5	8.9	42.6
10-20	0.21	7.19	1.40	40.3	7.9	51.9
20-45	0.48	7.24	1.46	28.9	7.7	63.3
45-60	0.64	8.21	1.27	27.9	11.3	60.9
60-75	0.46	8.91	1.30	31.6	10.5	57.9
75-100	0.36	9.44	1.37	40.1	11.8	48.2

Irrigation was controlled by the vineyard property owner and was scheduled and managed on a commercial basis. The decision to irrigate was determined according to weather conditions and crop condition, although at certain times the irrigation schedule was fixed. There were three irrigation treatments (T1, T2 and T3) that were established and varied according to different drip emitter rates (1.0, 1.6 and 2.3 L /h). Each treatment received irrigation for the same period of time. Irrigation commenced on 26 September 2008 and finished on 30 April 2009. A randomised complete block design was chosen and each irrigation treatment was replicated four times. Each plot was 25 m long and three vine rows wide. To maintain regular observations on the dynamics of the soil moisture granular matrix resistance sensors (Watermark Irrometer Co. USA) were installed on 26 September 2008 at three depths (0.25, 0.5 and 0.75 m) in the middle row of each plot. These sensors recorded soil matric potential (kPa) every 2 h which was stored on a field-based data logger.

Tracer application

Bromide (Br^-) was applied as an aqueous solution at 32 mg Br^-/cm^2 (as KBr) on 7 November 2008 (close to flowering when fertilizer is typically applied). This is a comparable level to that used in other tracer studies (Tilahun *et al.* 2005). An animal health vaccinator (NJ Phillips Pty Ltd) was used to inject 5 ml doses 5 cm apart in a square grid layout (625 cm^2) at a depth of 20 mm below the soil surface. The centre of the injection grid was placed directly underneath a drip emitter. There were 15 injection sites in each plot to allow for a total of 5 separate sampling times. Due to the destructive nature of the soil core sampling there was no repeated sampling.

Soil sampling and laboratory analysis

Soil core samples were taken at predetermined locations along each plot on five occasions (7, 26, 46, 83 and 131 days after the Br^- was injected) during the 2008/ 09 growing season. Each coring point was directly under the centre of the Br^- injection grid and was taken using a tractor-mounted hydraulic ram to a 1 m depth. The core samples (50 mm diameter) were segmented into 8 depth increments: 0-5, 5-10, 10-20, 20-30, 30-40, 40-60, 60-80 and 80-100 cm and stored in zip-lock plastic bags. Bentonite powder was poured into the cored hole to prevent a preferential pathway developing at each sample point. Soil core samples were oven dried (48 h at 105°C) and the gravimetric water content was determined. Samples were crushed and passed through a 2 mm sieve. An aqueous soil extract solution (1:1 ratio) was prepared using 20 g of dried soil and 20 ml of deionised water. Each solution was shaken with a rotating laboratory shaker, then centrifuged and filtered (0.48 µm) into vials and analysed for Br^- using ion chromatography (Dionex ICS-2500 system).

Transfer function modelling, statistical analysis and mass balance

A least squares optimisation technique was used to calculate the best fit of observed values of field-averaged normalised Br^- concentrations from 8 depths with a probability density function (pdf) at 5 different sampling times. Two pdf's were investigated, the convective dispersion equation (CDE) and the convective lognormal transfer function (CLT) (Butters and Jury 1989):

$$f_l(z) = \left[1/(2\pi)^{1/2}\sigma z\right]\exp\left[-\left(\ln\left(\frac{lL}{z}\right)-\mu\right)^2/2\sigma^2\right] \quad [1]$$

where μ = mean, σ^2 = variance. The CLT provided a much better fit to the data than the CDE. Analysis of variance (ANOVA) was used to check for differences between the treatments at each sampling time. Then a Bonferroni multiple comparison was used to determine whether there was a significant difference of the mean travel depth of Br^- between treatment pairs (i.e. T1 vs. T2 etc.). The mass of Br^- recovered from the soil core samples was compared with the applied mass of Br^- less the small background concentration of Br^-. The percentage recovery of the applied Br^- solute is an important calculation to check that the solute is adequately accounted for.

Results

Bromide concentration profiles

The depth concentration profiles of Br^- clearly showed that there was a great amount of solute movement during the first 3 weeks after the start of the experiment. Figure 1 shows a depth concentration profile for T1 for the 5 sampling times during the course of the experiment. After sample time 2 (26 days) there was much less Br^- measured and it is thought that it was mostly leached from the soil profile.

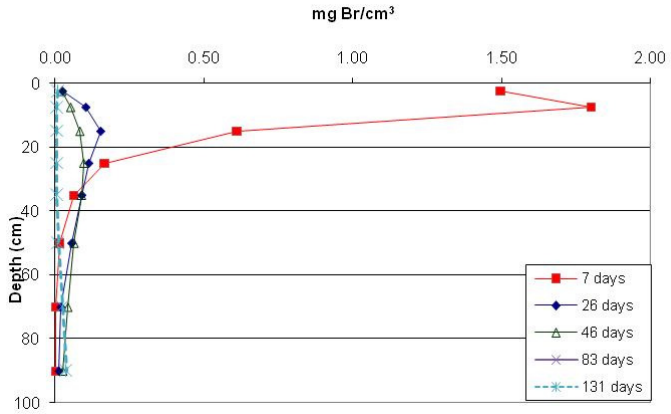

Figure 1. Bromide concentration (mg Br^-/ cm^3) by depth for treatment 1 at 5 sampling times during 2008/09

Using a convective lognormal (CLT) model for solute transport it was found that the level of applied irrigation volume produced a significant difference (P = 0.04) in the average depth reached by the solute at time 2 only, while at times 1 and 3 there was no significant difference. At times 4 and 5 there were significant differences in the variability of the depth reached by the solute, however these data are not conclusive since by time 4 a large proportion of the solute mass had leached beyond the measurement region. The difference in the depth concentration profile of Br^- for all treatments at sample time 2 is given in Figure 2.

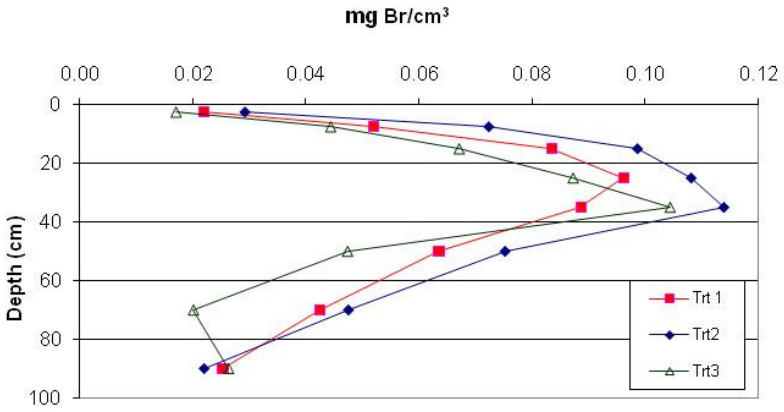

Figure 2. Bromide concentration (mg Br^-/ cm^3) by depth for all treatments (T1, T2, T3) at the sample time 2

Mass balance

The mass balance is the amount of Br^- that was recovered as a percentage of the amount applied (Figure 3). These results support and further emphasise that there was no significant difference between the treatments. Most Br^- was recovered after 7 days (time 1), but by sample time 2 >70 % of the applied Br^- had been leached. By the end of the experiment the Br^- concentrations were close to the background levels.

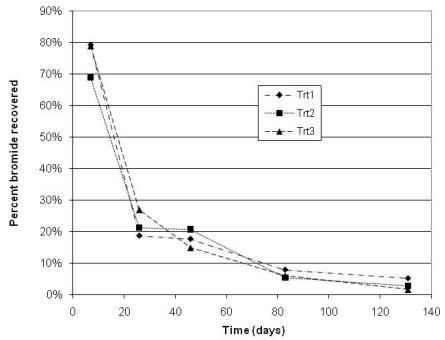

Figure 3. The percentage bromide recovered as a percentage of the amount applied at 5 sampling times for 3 different irrigation volume treatments (T1 = 1 L /h, T2 = 1.6 L /hand T3 = 2.3 L /h)

Soil moisture

The soil moisture status was very wet from the start of the experiment and remained wet for all the treatments (T1, T2 and T3) for the period until the end of 2008. In fact, for much of this period there was little difference between the treatments, for example the soil water potential is shown at 50 cm depth (Figure 4). These data agree with other measurements of soil water content (data not shown) taken at time 1-5.

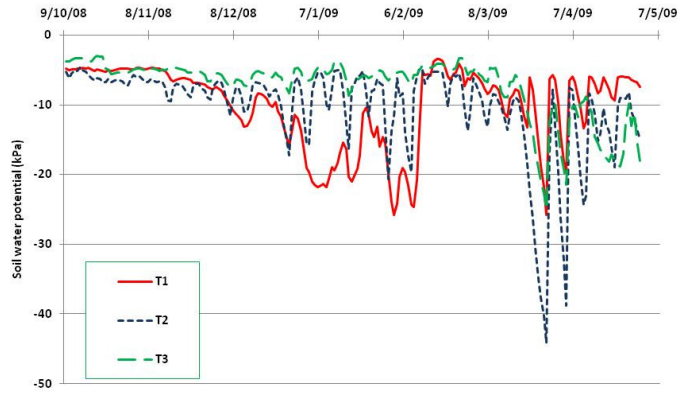

Figure 4. Soil water potential (kPa) at 50 cm depth for the 3 applied irrigation volume treatments during 2008/09

Conclusion

The applied irrigation volume was only once found (time 2) to have a significant effect on the average depth concentration of Br. At other times there was either no significant difference (time 1 and 3) or a difference could not be observed due to leaching beyond the depth of measurement. This suggests that the drip emitter rate and ultimately the irrigation volume is not a dominating factor on the leaching of Br. The soil water content plays an important role on leaching and appears to be more important than irrigation volume. Analysis of solute transport parameters using a transfer function modelling approach confirms this interpretation. Therefore, we believe that greater attention needs to be placed upon the soil moisture than drip emitter rate or irrigation volume to avoid excessive nutrient leaching.

References

Butters G, Jury W (1989) Field scale transport of bromide in an unsaturated soil 2. Dispersion modelling. *Water Resources Research* **25**, 1583-1589.

Hutton R, Holzapfel B, Smith J, Hutchinson P, Barlow K, Bond WJ (2007) Influence of irrigation and fertilizer management on the movement of water and nutrients within and below the rootzone of vines for sustainable grape production. *CRC for Viticulture - Final Report*.

Isbell RF (2002) 'The Australian Soil Classification.' Revised edition (CSIRO Publishing: Melbourne).

McKenzie NJ, Coughlan KJ, Cresswell HP (2002) 'Soil physical measurement and interpretation for land evaluation.' (CSIRO Publishing: Melbourne).

Tilahun K, Botha JF, Bennie ATP (2005) Transport of bromide in the Bainsvlei soil: Field experiment and deterministic/stochastic model simulation. I. Continuous water application. *Australian Journal of Soil Research* **43**, 73-80.

The effect of tillage and nitrogen application on soil water retention, hydraulic conductivity and bulk density at Loskop, KwaZulu-Natal, South Africa

Terri Bassett[A], Louis Titshall[A], Jeffrey Hughes[A] and Guy Thibaud[B]

[A] Soil Science, School of Environmental Sciences, University of KwaZulu-Natal, Pietermaritzburg, South Africa. Email 204500593@ukzn.ac.za; Titshall@ukzn.ac.za; Hughesj@ukzn.ac.za
[B] Soil and Analytical Services Division, Department of Agriculture, Cedara, South Africa. Email Guy.Thibaud@dae.kzntl.gov.za

Abstract
The effects of agricultural management practices on soil physical parameters provide fundamental information for assessing sustainability. Tillage and fertilizer rates were evaluated for their effects on soil bulk density (P_b), water retention characteristics and saturated hydraulic conductivity (K_s) on a clay loam (Typic Haplustox). The field experiment was initiated in 2003 and planted to dry-land maize. Tillage regime and limestone ammonium nitrate (LAN) application rate significantly affected soil physical properties in the topsoil (0 - 5 cm). Under no-till (NT) the P_b, saturated water content and K_s were considerably lower than under conventional tillage (CT) and greater plant available water was retained under NT. At 200 kg N/ha P_b, water retention and K_s was significantly lower than at the lower rates of LAN application, especially under NT. These results suggest there is a need to re-evaluate the sustainability of using high rates of LAN to increase crop yields, especially under NT systems.

Key Words
Soil quality, soil physical properties, conservation tillage, nitrogen fertilizer

Introduction
Soil quality is linked to human health and environmental sustainability. As such, there is a need to evaluate the effect of agroecosystems on soil quality (Janke and Papendick, 1994). Tillage alters the physical, chemical and biological properties of soil ecosystems (Doran, 1980) and thus it is an agricultural practice of particular interest in its effect on soil quality. A large body of literature has accumulated on the sustainability of various agricultural practices and their long-term effects on soil and environmental quality (e.g. Jackson *et al*., 2003; Spedding *et al*., 2004; Riley *et al*., 2008; Fuentes *et al*., 2009). Much of the published literature focuses on the role of different tillage systems with an emphasis on conservation tillage in commercial farming systems in developed countries. However, there is a deficit of similar research on the African continent, where agro-ecological and socio-economic conditions differ markedly from those experienced in developed countries (Fowler and Rockstrom, 2001). In view of this, an investigation was undertaken of the effects of nitrogen application and tillage practice on soil physical properties, as part of a wider study, at a field experiment in KwaZulu-Natal, South Africa.

Field experiment
The field experiment was established in 2003 at Gourton Farm, near Loskop (KwaZulu-Natal Province, South Africa) to investigate the combined effects of cultivation methods (no-till and conventional tillage) and nitrogen application (urea and limestone ammonium nitrate (LAN)) on maize yield and soil fertility. The field trial includes three tillage treatments, namely no-till (NT; direct seeding into undisturbed soil), annual conventional tillage (CT1; annual ploughing with a moldboard plough to a depth of 30 cm, followed by disking) and conventional tillage (CT5; conventional tillage after every four seasons of no-till). Nitrogen is applied at five rates to each tillage treatment as either urea or LAN. In the 2008/2009 season nitrogen was applied at application rates of 0, 50, 100, 150 and 200 kg/ha (previously 0, 40, 80, 120 and 160 kg/ha) due to a linear response in maize production to the fertilizer application rate used in the 2007/2008 season. Lime is applied at a rate of 2 Mg/ha every second season to the entire trial. The trial is arranged as a split plot design; with randomized tillage strips forming whole plots and N source and rate of application forming sub-plots which are randomized within the whole plots. Each treatment is replicated three times (three blocks). Each sub-plot has 12 rows each of 9.5 m of maize at a density of 70 000 plants/ha. The area is cropped to dry-land maize in the summer and stands fallow in the winter. Wheels from mechanized equipment are restricted to inter-rows 1, 3, 5, 7, 9 and 11.

1 – 6 August 2010, Brisbane, Australia. Published on DVD.

Materials and methods

The soil is classified as Hutton form (Soil Classification Working Group, 1991); Typic Haplustox (Soil Survey Staff 2003) with a clay-loam texture. Only the plots under NT and CT1 were investigated with N (applied as LAN) application rates of 0, 100 and 200 kg/ha (6 treatments). Three undisturbed soil cores (50 mm height x 75 mm diameter) were collected from the topsoil (0 - 5 cm) in each plot and a single core was collected from each of inter-rows 4, 8 and 10 (unaffected by wheeled traffic). Cores were collected 20 weeks after planting. The cores were prepared and analysed for water retentivity characteristics, saturated hydraulic conductivity (K_s) and bulk density (P_b) using the method of Moodley *et al*. (2004). Water retention characteristics were determined at 0, -1, -2, -4, -6, -8 -33 and -100 kPa matric potential using a tension table and pressure plate apparatus (Avery and Bascomb 1974), after which K_s was determined prior to oven drying for determination of P_b. A value of -33 kPa was used to represent field capacity (Givi *et al.,* 2004). Wilting point (-1500 kPa) moisture content was determined in a high pressure chamber apparatus using <2 mm soil samples.

To determine K_s an empty core was taped to the soil core to increase the length and the soil sample was re-saturated by capillary wetting. The core was then placed on a steel mesh held inside a funnel and K_s measured by the constant head method (Klute and Dirksen, 1986).

Treatment effects on P_b , K_s, total porosity, moisture content at field capacity and wilting point were analysed by ANOVA (GENSTAT, 12th edition). Where significant overall effects were found, means were compared by LSD at the 5% level of significance.

Results and discussion

Tillage has a considerable impact on the soil physical properties in the upper 5 cm of the soil profile. Bulk density is significantly ($p = 0.015$) greater under NT than under CT (Table 1).

Table 1. The effect of no-till (NT) and annual conventional tillage (CT) on bulk density and saturated hydraulic conductivity in the topsoil (0 - 5 cm) at different application rates of nitrogen fertilizer.

Fertilizer application rate (kg N/ha)	Bulk density (g/cm^3)		Saturated hydraulic conductivity (mm/hr)	
	NT	CT	NT	CT
0	1.40	1.35	220	426
100	1.38	1.32	212	395
200	1.53	1.38	121	157

Under CT the bulk density in the plough layer is lowered by the mechanical inversion of the soil during tillage which creates macropores and increases soil porosity. Many authors (e.g. Osunbitan *et al*., 2005; Bescansa *et al*., 2006) have found that bulk density in the top 5 to 20 cm of soil is greater under conservation tillage compared to CT up to 10 years after conversion to conservation tillage. Higher bulk density under NT corresponds to the significantly ($p = 0.008$) lower saturated water content (Figure 1) and lower K_s (Table 1) under NT compared to CT. Tillage-induced macropores allow more water to be held at saturation. However, plant available water is greater under NT than under CT, which had a significantly ($p = 0.024$) higher volumetric water content under NT at field capacity (-33 kPa; Figure 1). This is due to a higher proportion of mesopores which is a consequence of increased aggregate stability that allows for the maintenance of soil structure.

The application rate of LAN fertilizer also has a marked effect on the soil physical properties in the soil surface. An application rate of 200 kg N/ha significantly increased bulk density (Table 1) and lowered the water retention (Figure 2) at all matric potentials, especially under NT .Comparisons by LSD(5 %) indicate that the volumetric water content at 0 kPa and -33 kPa in the 200N treatment is significantly ($p < 0.001$) lower than the 100N and 0N fertilizer treatments. In addition, there is a decrease in K_s at 200 kg N/ha under both NT and CT compared to the lower rates of nitrogen fertilizer application (Table 1). It is proposed that the high application rate of fertilizer on the soil surface is an irritant to soil fauna and thus pore formation and aggregate stability are reduced leading to higher bulk density and lower moisture retention. Under CT the negative effect of 200 kg N/ha is less marked as the effect of ploughing dominates leading to greater soil macroporosity.

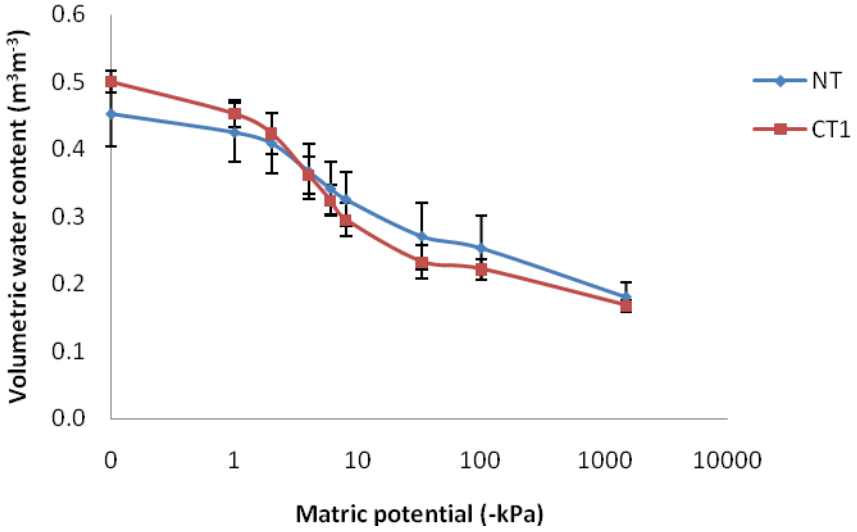

Figure 1. The overall effect of no-till (NT) and annual conventional tillage (CT) averaged across fertilizer treatment (n = 9) on the water retention characteristics for the topsoil (0 - 5 cm).

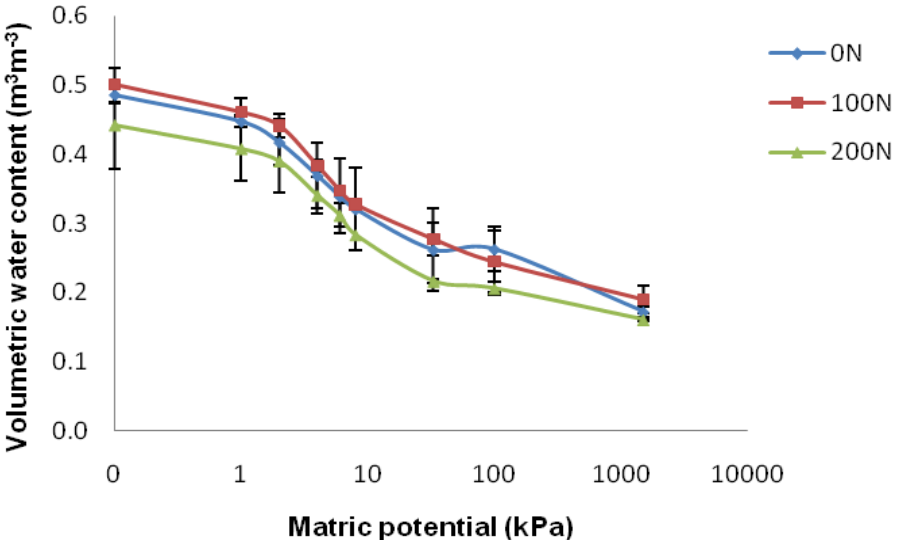

Figure 2. The overall effect of limestone ammonium nitrate (LAN) fertilizer application rate (0 kg N/ha (0N), 100 kg N/ha (100N) and 200 kg N/ha (200N) averaged across tillage treatment (n = 6) on the water retention characteristics for the topsoil (0 – 5 cm).

Conclusion

Although soils under CT have greater saturated water content and lower bulk density the water retained within the plant available range (-33 to -1500 kPa) is greater under NT. Furthermore, plant growth under NT is not adversely affected by reduced porosity and therefore NT is the preferred tillage practice to provide long-term sustainability and soil quality without causing negative soil structural properties for crop productivity in the short-term. In addition although the increased levels of nitrogen fertilizer results in higher yielding maize plants, the effect of high application rates of LAN result in a negative effect on the soil physical properties. This suggests that the mechanisms for these negative impacts need to be investigated.

References

Avery BW, Bascomb CL (1974) Soil Survey Laboratory Methods. Rothamsted Experimental Station, Harpenden.

Bescansa P, Imaz MJ, Enrique A, Hoogmoed WB (2006) Soil water retention as affected by tillage and residue management in semiarid Spain. *Soil and Tillage Research* **87**, 19-27.

Doran JW (1980) Soil microbial and biochemical changes associated with reduced tillage. *Soil Science Society of America Journal* **44**, 765-771.

Fowler R, Rockstrom J (2001) Conservation tillage for sustainable agriculture: An Agrarian revolution gathers momentum in Africa. *Soil and Tillage Research* **61**, 993-1007.

Fuentes M, Govaerts B, De Leon F, Hidalgo C, Dendooven L, Sayre KD, Etchevers J (2009) Fourteen years of applying zero and conventional tillage, crop rotation and residue management systems and its effect on physical and chemical soil quality. *European Journal of Agronomy* **30**, 228-237.

Givi J, Prasher SO, Patel RM (2004) Evaluation of pedotransfer functions in predicting the soil water contents at field capacity and wilting point. *Agricultural Water Management* **70**, 83-96.

Jackson LE, Calderon FJ, Steenwerth KL, Scow KM, Rolston DE (2003) Responses of soil microbial processes and community structure to tillage events and implications for soil quality. *Geoderma* **114**, 305-317.

Janke RR, Papendick RI (1994) Preface. In `Defining soil quality for a sustainable environment`. (Eds JW Doran, DC Coleman, DF Bezdicek, BA Stewart), pp. ix-xi. (SSSA, Madison).

Klute A, Dirksen C (1986) Hydraulic Conductivity and Diffusivity: Laboratory Methods. In `Methods of Soil Analysis, Part 1`. (Ed A Klute) (ASA, SSSA, Madison).

Moodley M, Johnston MA, Hughes JC, Titshall LW (2004) Effects of water treatment residues, lime, gypsum, and polyacrylamide on the water retention and hydraulic conductivity of two contrasting soils under field conditions in KwaZulu-Natal, South Africa. *Australian Journal of Soil Research* **42**, 273-282.

Osunbitan JA, Oyedele DJ, Adekalu KO (2005) Tillage effects on bulk density, hydraulic conductivity and strength of a loamy sand soil in southwestern Nigeria. *Soil and Tillage Research* **83**, 57-64.

Riley H, Pommeresche R, Eltun R, Hansen S, Korsaeth A (2008) Soil structure, organic matter and earthworm activity in a comparison of cropping systems with contrasting tillage, rotations, fertilizer levels and manure use. *Agriculture, Ecosystems and Environment* **124**, 275-284.

Soil Classification Working Group (1991) Soil classification: a taxonomic system for South Africa. Department of agricultural development. Pretoria. p. 241.

Soil Survey Staff (2003) Keys to Soil Taxonomy. 9th edition, USDA, Natural Resources Conservation Service, U.S. Government Printing Office, Washington, DC.

Spedding TA, Hamel C, Mehuys GR, Madramootoo CA (2004) Soil microbial dynamics in maize-growing soil under different tillage and residue management systems. *Soil Biology and Biochemistry* **36**, 499-512.

The *matric flux potential* as a measure of plant-available water in soils restricted by hydraulic properties alone

Cameron D Grant[A], Pieter H Groenevelt[B], Neville I Robinson[C] and Sukhpal Singh Chahal[A]

[A]School of Agriculture Food & Wine, University of Adelaide, Urrbrae, SA, Australia, Email cameron.grant@adelaide.edu.au
[B]University of Guelph, Guelph, Ontario, Canada, Email pgroenev@lrs.uoguelph.ca
[C]School of Chemistry, Physics & Earth Sci, Flinders University, Bedford Pk, SA, Australia, Email neville.robinson@flinders.edu.au

Abstract
In a soil for which the plant available water is restricted solely by its hydraulic properties (i.e. not by high soil strength, nor poor aeration and salinity) the amount of plant available water as defined by the integral water capacity which is shown to be equal to the differential matric flux potential.

Key Words
Integral water capacity, plant available water, hydraulic conductivity, matric flux potential.

Introduction

Groenevelt *et al.* (2001, 2004) introduced the theoretical framework to calculate how much soil water might be available to plants. There, the differential water capacity, C(h), was obtained from the water retention curve, θ(h), and then weighted for various soil physical limitations (e.g. excessively rapid or slow drainage or aeration, high soil strength, salinity, and low hydraulic conductivity). The method allowed any number of physical limitations to be incorporated to obtain a net amount of plant available water. In the present study we are primarily interested in evaluating the sole contribution of low unsaturated hydraulic conductivity common in most coarse-textured soils. This paper describes the theory required to allow such an analysis.

Theory

The *integral water capacity*, IWC, was defined by Groenevelt *et al.* (2001) in terms of the matric head, h:

$$\mathrm{IWC} \equiv \int_{h_f}^{h_i} \left(\prod_{j=1}^{n} \varpi_j(h) \right) \frac{d\theta}{dh}\, dh \qquad [1]$$

in which h_i and h_f are the initial and final matric heads, $h_f > h_i$, and the $\omega_j(h)$ are weighting functions designed to reduce the *differential water capacity*, $C(h) \equiv d\theta/dh$, based upon a number of limiting soil physical properties, j = 1 to n. In this context we focus here solely on soil hydraulic limitations, which arise partly from the inability of the soil matrix to release water and partly from its inability to transport water from one point to another. The limiting 'water release' component is found in the differential water capacity, dθ/dh, and the limiting 'transport' component is found in the unsaturated hydraulic conductivity function, K(θ), both of which can be combined to formulate the so-called 'diffusivity' function, $D(\theta) \equiv K(\theta)/C(h)$.

If as a first approximation we define a weighting function, $\omega(h) \equiv D(\theta)$, its substitution into Eqn [1] gives:

$$\mathrm{IWC} = \int_{h_f}^{h_i} \left(K(\theta) \Big/ \frac{d\theta}{dh} \right) \frac{d\theta}{dh}\, dh \qquad [2]$$

It can be seen that equation [2] reduces to:

$$\mathrm{IWC} = \int_{h_f}^{h_i} K(\theta)\, dh = \Phi(h_i) - \Phi(h_f) \qquad [3]$$

which is simply a difference in the *matric flux potential* (or the Kirchhoff potential) as outlined for example by Klute (1952) and Raats (1970). An important consequence is that for soils in which nothing but hydraulic properties restrict water uptake by plants, the *integral water capacity* is identical to the *differential matric flux potential*.

1 – 6 August 2010, Brisbane, Australia. Published on DVD.

It is common to express h and K(h) as functions of the water content, which allows the integral in Equation [3] to be written as:

$$\mathrm{IWC} \equiv \int_{\theta_f(h_f)}^{\theta_i(h_i)} K(\theta)\frac{dh}{d\theta}d\theta \qquad [4]$$

To evaluate this integral, we note that $dK(\theta)/d\theta$ is often available, derived from $K(\theta)$ in integral form, which allows Equation [4] to be integrated by parts:

$$\int_{\theta_f(h_f)}^{\theta_i(h_i)} \frac{d[K(\theta)h]}{d\theta}d\theta = \int_{\theta_f(h_f)}^{\theta_i(h_i)} \left[K(\theta)\frac{dh}{d\theta}\right]d\theta + \int_{\theta_f(h_f)}^{\theta_i(h_i)} \left[h\frac{dK(\theta)}{d\theta}\right]d\theta \qquad [5]$$

Rearrangement gives a more amenable integral:

$$\int_{\theta_f(h_f)}^{\theta_i(h_i)} \left[K(\theta)\frac{dh}{d\theta}\right]d\theta = \int_{\theta_f(h_f)}^{\theta_i(h_i)} \frac{d[K(\theta)h]}{d\theta}d\theta - \int_{\theta_f(h_f)}^{\theta_i(h_i)} \left[h\frac{dK(\theta)}{d\theta}\right]d\theta \qquad [6]$$

Now the first part of the integral in Equation [6] is relatively simple:

$$\int_{\theta_f(h_f)}^{\theta_i(h_i)} \frac{d[K(\theta)h]}{d\theta}d\theta = h_i(\theta_i)\,K_i(\theta_i) - h_f(\theta_f)\,K_f(\theta_f) \qquad [7]$$

The second part, however, is somewhat more difficult to evaluate and requires assumptions about the form of the θ–h relationship and the nature of its integration. In this work we assume a version of the θ–h relationship proposed by Groenevelt and Grant (2004) and offer a solution to the second part of the integral using incomplete gamma functions. As the work is currently under review for publication, the results will be presented at the Congress or can be obtained from the authors directly.

Conclusion

In the limited circumstances where growth and water-uptake by an 'average' plant are restricted by the hydraulic properties of the soil and nothing else, it is possible to calculate the amount of water that plants can remove from the soil (the integral water capacity) by computing the matric flux potential. An evaluation of this approach is currently underway using different types of plants grown at different planting densities under different environmental conditions.

References

Groenevelt PH, Grant CD (2004) A new model for the soil-water retention curve that solves the problem of residual water contents. *European Journal of Soil Science* **55**, 479-485.

Groenevelt PH, Grant CD, Murray RS (2004) On water availability in saline soils. *Australian Journal of Soil Research* **42**, 833-840.

Groenevelt PH, Grant CD, Semetsa S (2001) A new procedure to determine soil water availability. *Australian Journal of Soil Research* **39**, 577-598.

Klute A (1952) A numerical method for solving the flow equation for water in unsaturated materials. *Soil Science* **73,** 105-117.

Raats PAC (1970) Steady infiltration from line sources and furrows. *Soil Science Society of America Proceedings* **34**, 709-714.

The relationship between field soil water content variability and soil moisture deficit prediction from meteorological data

Anthony Kerebel[A], Rachel Cassidy[B], Philip Jordan[BC] and Nicholas M. Holden[A]

[A]Biosystems Engineering, UCD School of Agriculture, Food Science and Veterinary Medicine, University College Dublin, Belfield, Dublin 4, Ireland, Email anthony.kerebel@ucd.ie
[B]School of Environmental Sciences, University of Ulster, Cromore Road, Coleraine, BT52 1SA, Northern Ireland
[C]Teagasc, Environment Research Centre, Wexford, Ireland

Abstract
The Hybrid Soil Moisture Deficit (SMD) model (Schulte *et al*., 2005) was designed to predict soil moisture conditions as a function of water balance for agro-climatic regions in Ireland. It is assumed to work between the field scale (1,000 m^2) and the regional scale (100 km^2) and is being developed to predict runoff at the field scale. However soil physical properties that affect the water balance vary significantly at field scale. This study provides preliminary evidence of how a point estimation of SMD can be used as a predictor of a field water balance. Point SMD predictions calculated from meteorological data measured on farm were compared with continuous time series point volumetric water content (θ_p) and periodic observations of variation in field volumetric water content (θ_f) both measured by time domain reflectometery. The θ_p and θ_f trends were relatively similar.

Key Words
Soil, water, model, prediction, spatial, drainage

Introduction
The Hybrid Soil Moisture Deficit (SMD) model (Schulte *et al*., 2005) was designed to predict soil moisture conditions as a function of water balance for agro-climatic regions in Ireland. It is a point model because it uses input data from a specific meteorological observation location; however it has always been tacitly assumed that it predicts water balance over an unspecified spatial extent thought of as a "field". Additionally, the model is effectively dimensionless with no defined support (i.e. defined length, width and depth over which it functions). It was not designed to predict soil water contents, rather to predict when the soil was at a state of wetness, expressed relative to field capacity, with units of mm rainfall deviation from field capacity. Furthermore, the model has potential as the basis of farm decision support tools because it requires little data to run (soil classified into one of three classes, rainfall, wind speed, temperature and solar radiation), yet during development gave reliable predictions of relative soil water status for a range of grassland fields.

The SMD model is being developed as the core of a demonstration sustainable nutrient management decision support system. As part of its testing and development, it is necessary to understand more about the spatial scale over which the model applies, and how point predictions relate to field scale spatial variability on the farm. As it was not designed as a physical model, soil variations are captured via 3 operational drainage classes: well, moderate and poorly drained. Although a field is assigned to a class, two drainage classes may occur in the same field, so it is imperative to ensure that each area of a field is allocated to the correct class. For practical purposes, it has been decided that the minimum area to be considered will be 4,000 m^2, which equates to the area of spreading for one full slurry tanker. Although the weather is a main factor affecting nutrient transport from the field to watercourses, the soil physical properties can also have a large impact on leaching and runoff events. The objective of this work was to evaluate the relationship between Time Domain Reflectometry (TDR) estimates of soil volumetric water content (θ_p) at a fixed location associated with the farm weather stations, spatial variability θ_f of water content in the field, and point prediction of SMD on the farm weather stations.

Methods
Sites
Ten sites representative of the three grassland soil drainage classes were selected to evaluate the SMD model and the larger decision support system as a whole. They were selected based on geographical distribution (north to south climate gradient) and the range of drainage classes they encompassed. For this paper, examples from two sites are presented representing poor and well drained soil classes.

1 – 6 August 2010, Brisbane, Australia. Published on DVD.

Soil moisture deficit calculation
Meteorological stations were installed at each site therefore weather data from synoptic stations, interpolation or Numerical Weather Prediction (NWP) were not required. Daily SMD was calculated from weather data using maximum and minimum temperature (°C), rainfall (mm), wind speed at 10m (m s^{-1}) and radiation (J cm^{-2}) on a daily basis. The SMD model also requires spatial co-ordinates (latitude and longitude) and previous SMD state (the model is initialised in mid-winter to ensure wet soil conditions). In the past it has been found that the SMD model relates best to a 15 cm tensiometer, which represents rooting zone in a grassland soil.

Volumetric water content (θ)
In order to evaluate SMD predictions, the point soil volumetric water content (θ_p) was measured by a time domain reflectometer (TDR) at fixed locations relative to the weather station. Four continuously logged TDR probes were inserted into the wall of two pits. Each pit has one probe inserted at 10 cm and another one at 20 cm and at least 24 cm apart.

The spatial variation in soil water content (θ_f) was assessed on specific days by handheld TDR. Waveguides 12 cm long were used to measure the volumetric water content across the soil surface. Variation in θ_f was then compared to θ_p and maps were created to visualise how representative the fixed TDR was of the sites being used to test the DSS.

Handheld and fixed time domain reflectometers were calibrated by collecting volumetric water content samples for laboratory analysis. Soil samples (3 × 13.7 cm^3 at 10 cm and 20 cm depths) were taken on a monthly basis during visits to each site. These samples were dried at 65°C until the dry mass was constant and the volumetric water content was calculated as the mass of water per unit volume soil sampled.

Results
Although the volumetric water content, θ, has not been determined for the soil surface, the soil surface θ and the TDR θ_p at 10cm depth have the same trends but slightly different absolute values (Figure 1). It can be expected that the soil surface will have a more rapid change in θ than at 10 cm depth: on the well-drained soil, the soil surface is drier or wetter than at 10 cm depth on respectively drier or wetter periods of the year; on the poorly-drained soil, the soil surface usually remained wetter than at 10 cm depth but the θ range was much greater at the soil surface than at 10 cm.

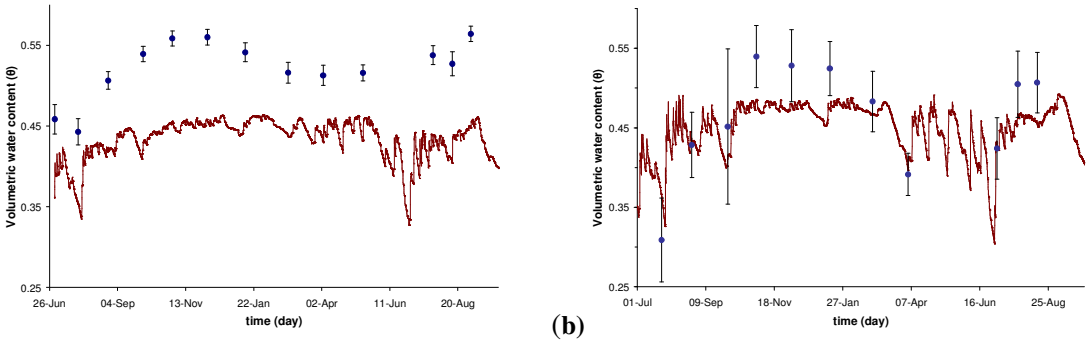

Figure 1. The volumetric water content over 13 months on a poorly-drained soil (a) and a well-drained soil (b) in Ireland. Fixed TDR time series are measured on a daily basis (-) while field observations with standard deviation of spatial variation (●) are made on a monthly basis.

At a given location, SMD prediction was related to volumetric water content measurement, θ (fixed TDR or handheld TDR). On average, at a given point, the linear regression of θ_p and SMD was significant if SMD data were grouped into classes of 5 mm (Figure 2). This means that small differences in SMD were smoothed out. The linear regression of mean of θ_f and SMD was also significant (Figure 2). However, the standard deviation was much larger for the well-drained soil than for poorly-drained soil, perhaps due to differences in soil depth or topography at the sites.

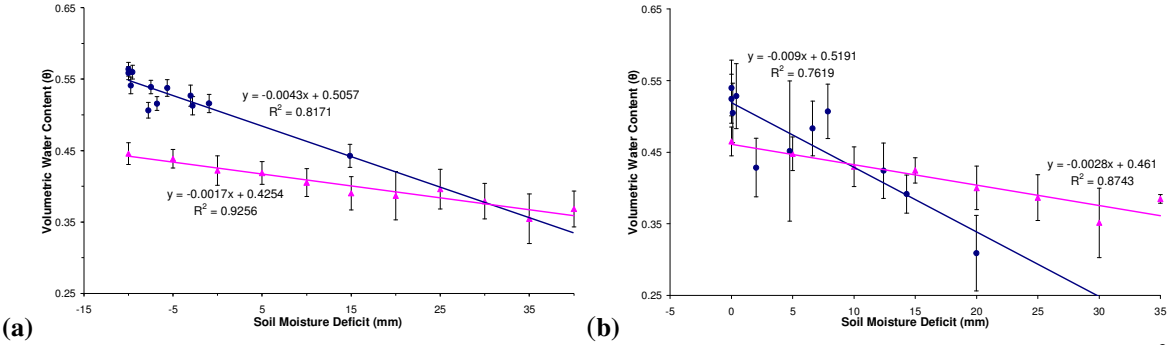

(a) (b)

Figure 2. Comparison of soil moisture deficit (mm) predictions with soil volumetric water content (cm^3H_2O/cm^3soil) measurements (by fixed TDR (▲) and by handheld TDR(●)) on a poorly-drained soil (a) and a well-drained soil (b).

Even though the SMD model is effectively dimensionless, SMD predictions were good estimates of the soil wetness. In addition to comparing θ versus SMD, the spatial variation of θ was also considered. These data showed that soil moisture variations at the field scale were small (Figure 3). However the application of the SMD model to some areas should be considered carefully. While it is recognised that these example fields do not capture all variability that might be found on grassland farms, these preliminary data do indicate that the SMD model should be able to correctly capture trends in soil water balance, thus permitting a forecast of when gravity moveable water, i.e. runoff, will occur in a field based on soil wetness.

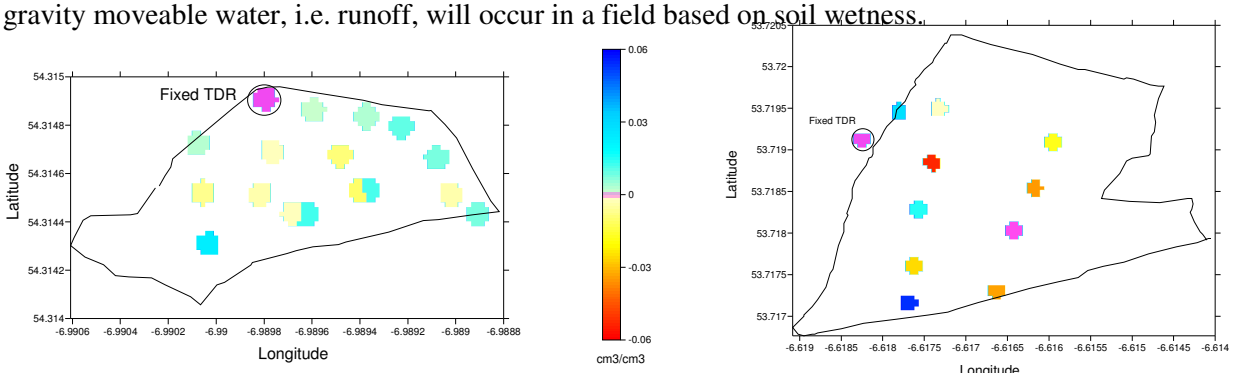

(a) (b)

Figure 3. Volumetric water content variation (θ) across the field on a poorly-drained soil (a) and a well-drained soil (b).The colour scale represent the average difference of volumetric water content between the fixed TDR location and other points (blue is wetter and red is drier).

Conclusions

It was found that:

- The trend in θ was similar for the point observation and the mean of the field observations over time. This means that the point field observation is characteristic of the field it represents, but that absolute value does not necessarily reflect all that might be happening in the field.
- SMD and θ were significantly related. While SMD is not a prediction of θ it is necessary that it reflects the trend in θ correctly in order to give confidence to the use of SMD to predict when a condition of gravity moveable water exists in a field.
- Small changes in SMD are probably not that meaningful at the field scale. SMD classes of 5 mm were required to clearly see trends between SMD and θ.
- The relationship between SMD and θ was different at the surface as a spatial average (as measured around the field) when compared at a given location in the field. This reflects the fact that the SMD model is a mixing bucket model that works over a non-defined depth. The trends indicate that the SMD model should work at the farm scale.

References

Schulte RPO, Diamond J., Finkele K, Holden NM and Brereton AJ (2005) Predicting the soil moisture conditions of Irish grasslands. *Irish Journal of Agricultural and Food Research* **44**, 95-110.

Toward improving estimates of field soil water capacity from laboratory-measured soil properties

Attila Nemes[A], Yakov Pachepsky[B], Dennis Timlin[C]

[A]Department of Plant Science and Landscape Architecture, University of Maryland, College Park, MD, USA, Email attila.nemes@ars.usda.gov
[B]Environmental Microbial and Food Safety Lab, USDA Agricultural Research Service, Beltsville, MD, USA, Email yakov.pachepsky@ars.usda.gov
[C]Crop Systems and Global Change Lab, USDA Agricultural Research Service, Beltsville, MD, USA, Email dennis.timlin@ars.usda.gov

Abstract
Different recommendations exist world-wide on which – if any - pressure head should be used in laboratory measurements to approximate the 'field capacity' (FC) of the soil. Literature often deems any such pressure heads to be inadequate to approximate FC for soils of all textures. We used a data collection from the literature to evaluate if corrections can be made to improve the estimation of FC from -33 kPa water retention (W33). Regression tree modeling coupled with jack-knife cross validation was used to identify the best predictors – sand, silt, clay and the measured W33 value – to estimate the difference between W33 and FC. Such predictions were then successfully used to adjust the W33 value as the estimate of FC. An improvement in estimating FC was seen in general statistical terms, and texture specific bias was also greatly reduced. Such a solution may allow the reliable use of a single pressure head in the laboratory to approximate FC, which may be the only feasible option for large scale studies.

Key Words
Field capacity, drained upper limit, pedotransfer function, regression tree, jack-knife, re-sampling

Introduction

Field capacity (FC) - i.e. the content of water remaining in a soil that has been wetted with water and after free drainage is negligible - is an important soil hydraulic parameter that has multiple uses in hydrological, meteorological, agronomical, and environmental predictions and modelling. Measurement of FC is unfeasible in large scale projects, therefore estimating FC is common practice. The customary way to estimate FC is to equate it to soil water contents measured in the laboratory at a predefined soil water pressure head. Different values of such pressure head have been employed in different countries, e.g. -5 kPa in United Kingdom (White, 2006) and France (Le Bas *et al*., 2007), -6 kPa in Brazil (Ajayi *et al*., 2009), -10 kPa in Australia (White, 2006) and Sweden (Kätterer *et al*., 2006) and even varied among different authors in the same country. In the United States the recommended value of such pressure head is -33 kPa (Kirkham, 2005).

There have been continual reports that the laboratory measured water content at -33 kPa can be a poor predictor of FC (e.g., Haise *et al*., 1955; Rivers and Shipp 1978). The objective of this work was to use a sizeable data collection (a) to evaluate the accuracy of using laboratory measured water content at -33 kPa as the predictor of FC, and (b) to develop corrections to laboratory measured water content at -33 kPa - via examining the prediction residuals - that may allow a more reliable estimation of FC.

Materials and Methods

We used the data collection described and used by Ratliff *et al*. (1983), Cassel *et al*. (1983) and Ritchie *et al*. (1987). Data were assembled in 15 U.S. states for 61 soil profiles representing 6 soil orders. For each soil profile, the in-situ drained upper limit (DUL) and lower limit (LL) were measured at various depths. Following the field capacity concept (Veihmeyer and Hendrickson, 1931), DUL can be interpreted as the equivalent of FC. Cassel *et al*. (1983) report a wide range of soil properties that have been measured in the National Soil Survey Laboratory (Lincoln, NE) for these locations using standard procedures (USDA-NRCS SCS, 1972).

We categorized the field collected information and laboratory measured properties into three groups. *Field observations* comprised data on depth, US taxonomy order, master soil horizon notation, land use type, drainage and permeability classes. *Simple laboratory based data* included 3 particle-size classes (sand, silt, clay), texture classes derived from those classes, organic carbon content, bulk density, coefficient of linear extensibility (COLE) and the ratio of clay content to water retention measured at -1500 kPa pressure (CLratio). *Detailed laboratory based data* included additional details about the particle-size distribution (PSD) by describing PSD using 8 particle-size classes. Water retention measured at -33 kPa pressure was used as a separate individual

variable. Total of 243 samples had all the abovementioned data. The distribution of samples by USDA texture classes are shown in Table 1.

Table 1. Number of samples and texture class-wise differences in laboratory measured water retention at -33 kPa (W33) and field measured drained upper limit (DUL). (s - sand; ls – loamy sand; sl – sandy loam; scl – sandy clay loam; sc – sandy clay; l – loam; cl – clay loam; sil – silt loam; si – silt; sicl – silty clay loam; sic – silty clay; c – clay).

	s	ls	sl	scl	sc	l	cl	sil	si	sicl	sic	c
n	1	8	13	11	0	39	40	63	4	39	19	6
mean(W33-DUL) [vol. %]	-3.96	-3.36	-1.31	-2.25	-	0.24	0.21	2.67	3.40	1.80	1.54	3.94
st.dev.(W33-DUL) [vol. %]	N/A	4.15	2.44	3.46	-	4.07	6.85	5.27	6.58	3.58	4.80	3.09

We used regression tree modeling to find ways of improving the estimation of DUL using the selected data. Regression tree modelling is an exploratory technique that uncovers structure in data by first partitioning data into two groups. Each group is then further subdivided into two subgroups, providing groups as homogeneous as possible at each of the levels (Clark and Pregibon, 1992). Regression trees can use both categorical and numerical variables as predictors and have been used in the estimation of soil properties by e.g. McKenzie and Jacquier (1997), Rawls and Pachepsky (2002) and Lilly *et al*. (2008).

The optimal use of a tree model requires a criterion to halt further partitioning of the data to avoid over-fitting. In preliminary runs, we used random re-sampling combined with a trial-and-error approach and root-mean-squared residuals (RMSR) as decision criterion to optimize tree pruning for the current task, i.e. to estimate DUL. The ratio of the development and test data set size had also been optimized simultaneously. As a result, in the subsequent sections of this study, tree development will be stopped when the tree reaches 10 terminal nodes and calculations that involve re-sampling are performed using a training data set (N=220) and an independent test data set (N=23) that are used in a recurrent "jack-knife" cross validation scheme (i.e. randomized subset selection without replacement). In order to facilitate the estimation of uncertainty of our subsequent findings, calculations are performed on one hundred alternative training/test data set pairs.

Results and Discussion

Figure 1a shows the 1:1 comparison of W33 and DUL values in the data set, and a simple linear regression equation that best describes the data. There is considerable scatter around the 1:1 line as well as some bias; W33 tends to underestimate DUL where DUL is small and overestimate it where DUL is large. Typically coarse textured soils retain less water at a given suction than finer textured ones; hence the lower values in Figure 1a are those mostly of sands and other sandy soils. Table 1 also reflects such underestimation of DUL by W33 for the coarse textured samples. This observation agrees with the general recommendation reflected in literature; i.e. that in order to approximate DUL for coarse textured soils, a higher pressure should be used in laboratory measurements (e.g. Cassel and Nielsen, 1986 and therein).

If the root mean squared residual (RMSR) and mean residual (MR) is calculated directly from the scatter data in Figure 1a, an RMSR of 5.18 vol. % and an MR of -1.03 vol. % is found. To test various alternatives to improve the DUL estimates from W33, the first choice was to use the simple linear equation in Figure 1a as the correction factor. When DUL is calculated as 0.7433*W33+6.7746, the obtained RMSR is 4.715 and the overall bias is removed (MR=0), which are both improvements. One other solution to account for variation by texture is to correct the W33-based estimate of DUL according to the mean difference between W33 and DUL in each texture class, as shown in Table 1. When that is done, we obtain an RMSR of 4.58 and an MR of 0.04 (vol. %). To test such correction on independent data, we also generated the RMSR and MR using the re-sampling and cross-validation scheme outlined above. In each of the 100 alternative runs, 220 samples were analyzed for statistical differences between W33 and DUL and the texture class-based correction was then applied to the 23 independent test samples. The mean RMSR and MR for the independent test data set were 4.83 and 0.07 (vol. %) respectively.

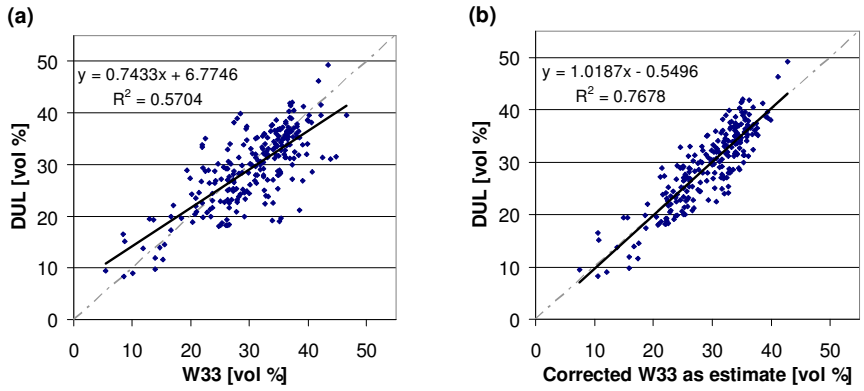

Figure 1. (a) Laboratory measured water retention at -33 kPa (W33) vs. field measured drained upper limit (DUL) for the 243 samples. Solid line and equation represent the best fit linear equation. (b) Estimate formulated after correcting W33 by the best regression tree description of ε, where ε=DUL-W33.

Table 2. Estimation RMSR and ME (and their standard errors) in estimating ε - formulated as ε=DUL-W33 (vol. %) - using various input groups. (W33 - laboratory water retention at -33 kPa; DUL - field measured drained upper limit).

Lab	Lab	Field	W33	TEST DATA				TRAINING DATA			
(simple)	(detailed)			RMSR	ST. ERR	ME	ST. ERR	RMSR	ST. ERR	ME	ST. ERR
x				4.900	0.087	-0.025	0.118	3.989	0.012	0	0
x		x		5.013	0.083	-0.091	0.119	3.984	0.012	0	0
x			x	4.412	0.064	-0.010	0.102	3.652	0.008	0	0
x		x	x	4.465	0.063	-0.018	0.108	3.647	0.009	0	0
x	x			5.092	0.086	-0.213	0.120	3.885	0.013	0	0
x	x	x		5.223	0.086	-0.284	0.125	3.857	0.013	0	0
x	x		x	4.808	0.074	-0.146	0.115	3.765	0.016	0	0
x	x	x	x	4.891	0.076	-0.167	0.121	3.757	0.015	0	0
			x	4.855	0.085	-0.067	0.114	4.404	0.011	0	0
		x		5.167	0.097	-0.039	0.121	4.513	0.014	0	0
		x	x	4.548	0.079	0.022	0.103	3.929	0.009	0	0
			x	4.855	0.085	-0.067	0.114	4.404	0.011	0	0
x(†)			x	4.367	0.063	-0.015	0.102	3.655	0.008	0	0
x(‡)			x	4.377	0.066	-0.028	0.101	3.693	0.009	0	0

†: sand, silt, clay, org. carbon, clay/-1500kPa water retention ratio used only ‡: sand, silt, clay used only

We then calculated ε for each sample as ε=DUL-W33. The value of ε is the correction needed to adjust W33 as the estimate of DUL. We evaluated the use of a hierarchically decreasing amount and variety of input variables to estimate ε (Table 2). Of the initial grouping of input data, using the *simple laboratory* data group and W33 itself gave one of the most accurate (training data) – and the most reliable (test data) – results. Use of more input data clearly had no advantage and signaled 'over-fitting' even for the training data. We then reduced the amount of data to sand, silt, clay content and W33, the error-estimates did not get worse. The three-class particle-size distribution appears to control much of the explainable variability in W33-DUL, while information related to e.g. soil depth (depth, horizons), taxonomic grouping or drainage/permeability classification could not explain any additional variability. When W33 is adjusted by using the texture+W33 model to estimate the W33-DUL difference, using re-sampling and the cross-validation scheme, a mean RMSR of 4.25 and MR of 0.01 (vol. %) is obtained, which is a substantial improvement from the direct estimation of DUL from W33. Moreover, the general texture related bias could be virtually eliminated, as seen in Figure 1b.

Conclusions

The use of the water content at -33 kPa as a practical approximate to DUL (and FC) is driven by early recommendations in literature and also by national preference and data availability. Inadequacy of that value to represent DUL for some soil texture groups has been noted in the past – and the use of other water retention point(s) have been recommended. In this study we examined the general suitability of W33 as an estimate to DUL and explored some possibilities to improve such estimate. It appears that a regression tree based grouping of the initial W33-DUL difference by soil particle-size fractions (sand, silt, clay) and W33 can result in a

correction that generally improves the initial estimate, while also removes most of the texture based bias noted already in early literature. The presented methodology is also usable to test water contents at other pressure heads or to be tested on data from other parts of the World. More research is planned about the comparison of this technique with an improved direct estimation of DUL, testing of additional potentially influential environmental variables, as well as the extension of the approach to LL and available water content. An international effort seems to be desirable to improve and standardize the estimation of the field capacity value that is widely used in evaluations of the magnitude and consequences of global change.

References

Ajayi AE, de Souza Dias M Jr, Curi N, Araujo CF Jr, Aladenola O, Teixeira Souza T, Vasconcellos Inda A Jr. (2009) Aplicação de diferentes métodos para estimar a resistência de cinco solos. (Comparison of estimation methods of soil strength in five soils). *Revista Brasileira de Ciência do Solo* **33**, 487-495.

Cassel DK, Ratliff LF, Ritchie JT (1983) Models for estimating in-situ potential extractable water using soil physical and chemical properties. *Soil Science Society of America Journal* **47**, 764-769.

Cassel DK, Nielsen DR (1986) Field capacity and available water capacity. In 'Methods of Soil Analysis, Part I.: Physical and Mineralogical Methods', Agronomy Monographs No. 9. (Ed. Klute A), pp. 901-926. (Agronomy Society of America and Soil Science Society of America, Madison, Wisconsin).

Clark LA, Pregibon D (1992) Tree-based models. In 'Statistical Models in S' (Ed. Hastie TJ), pp. 377-419. (Wadsworth, Pacific Grove, CA).

Haise HR, Haas HJ, Jensen LR (1955) Soil moisture of some Great Plains soils. II. Field capacity as related to 1/3-atmosphere precentage and "minimum point" as related to 15- and 26-atmosphere percentages. *Soil Science Society of America Proceedings* **19**, 20-25.

Kätterer T, Andrén O, Jansson P-E (2006) Pedotransfer functions for estimating plant available water and bulk density in Swedish agricultural soils. *Acta Agriculturae Scandinavica* B **56**, 263-276.

Kirkham MB (2005) Principles of Soil and Plant Water Relations. Elsevier.

Le Bas C, King D, Daroussin J (1997) A Tool for Estimating Soil Water Available for Plants Using the 1:1,000,000 Scale Soil Geographical Data Base of Europe. *ITC Journal*, 3–4.

Lilly A, Nemes A, Rawls WJ, Pachepsky YaA (2007). Probabilistic approach to the identification of input variables to estimate hydraulic conductivity. *Soil Science Society of America Journal* **72**: 16-24.

McKenzie NJ, Jacquier DW (1997). Improving the field estimation of saturated hydraulic conductivity in soil survey. *Australian Journal of Soil Research* **35**: 803–825.

Ratliff LF, Ritchie JT, Cassel DK (1983) Field-measured limits of soil water availability and related laboratory-measured properties. *Soil Science Society of America Journal* **47**, 770-775.

Ritchie JT, Ratliff LF, Cassel DK (1987) Soil laboratory data, field descriptions and field measured soil water limits for some soils of the United States. ARS Technical Bulletin.

Rivers ED, Shipp RF (1978) Soil water retention as related to particle size in selected sands and loamy sands. *Soil Science* **126**, 94-100.

Rawls WJ, Pachepsky YaA (2002) Soil Consistence and Structure as Predictors of Water Retention. *Soil Science Society of America Journal* **66**, 1115-1126.

USDA-NRCS Soil Conservation Service (1972) Soil Survey Laboratory Methods and Procedures for Collecting Soil Samples. Report No. 1. U.S. Government Printing Office, Washington D.C.

Veihmeyer FJ, Hendrickson AH (1931) The moisture equivalent as a measure of the field capacity of soils. *Soil Science* **32**, 181-194.

White RE (2006) Principles and practice of soil science: the soil as a natural resource. 4th Ed. Wiley-Blackwell.

Use of simulation modeling and pedotransfer functions to evaluate different irrigation scheduling scenarios in a heterogeneous field

Attila Nemes[A], Erik Czinege[B], Csilla Farkas[C]

[A]Dept. Plant Sci. and Landscape Architecture, University of Maryland, College Park, MD, USA, Email attila.nemes@ars.usda.gov
[B]Yara Hungaria Kft, Berhida, Hungary, Email erik.czinege@yara.com
[C]Bioforsk, Norwegian Institute for Agricultural and Environmental Research, Ås, Norway, Email csilla.farkas@bioforsk.no

Abstract
Increasing water use efficiency in agriculture is a multi-faceted optimization problem which could benefit from the use of a pro-active planning process. Simulation models are tools that can facilitate such planning, but their parameterization may be a difficult and costly task. Pedotransfer functions (PTFs), however, can provide important soil physical data at relatively low cost. Few studies, however, explore what contributions PTFs can make to land-use planning, in terms of being applied to evaluate the expected outcome of changes in management. We use an exploratory research approach using simulation modeling to evaluate benefits and risks posed while using different irrigation scenarios to a heterogeneous field. We also evaluate the applicability of pedotransfer functions to parameterize the simulation model for this task. Using this research approach we provide quantitative answers to several "what if" type questions, allowing the distinction of trends and potential problems. The approach may help increase water use efficiency while evaluating potential associated risks.

Key Words
Irrigation scheduling, heterogeneity, pedotransfer function, simulation model, SWAP, Hungary

Introduction
Large areas in the world face either a shortage of (irrigation) water or a decline in available water resources; while the demand for water by agricultural, industrial and municipal users keeps increasing. To keep up with the demand, it is necessary to find ways to increase water use efficiency in agriculture. Natural, technical or financial limitations of using different irrigation systems combined with the potential shortage or high cost of irrigation water poses a complex problem for practitioners in quest of maximizing yield and profit without posing avoidable risks the environment.

Field experimentation with different management scenarios is time consuming, costly and sometimes can even be risky. Changing land management, irrigation or fertilization practices can carry undesired and hazardous risks. However, given that a suitable model is available, exploratory ('what if?') simulation modeling offers an alternative that is quicker and easier to execute, and may give at least indicative answers about trends that are expected to occur without risk to the environment.

Plant-soil-atmosphere models need input on soil hydraulic properties, regardless of their complexity. However, measurement of these properties is relatively time-consuming and costly, especially when data are needed for large areas of land. Extensive research exists on pedotransfer functions (PTFs) that can estimate such properties from easily or routinely measured soil properties (e.g. Pachepsky and Rawls, 2004 and other papers therein), but few studies go further to evaluate the functionality of PTFs in field applications (e.g. Wösten *et al*., 1995; Soet and Stricker, 2003). Well tested PTFs can assist such modeling by providing low-cost and low-risk input data.

In this study we explore the use of a simulation model and estimated soil hydraulic properties to evaluate different irrigation scheduling scenarios in a heterogeneous field. The specific objectives of this study are (1) to examine the effect of different irrigation scheduling scenarios on selected soil water balance components and the soil's ability to supply the vegetation with water; (2) to examine the effect of apparent soil heterogeneity on those water balance components at the selected site; and (3) to evaluate the functionality and effectiveness of using a cost saving soil hydraulic pedotransfer function to parameterize the applied simulation model.

Materials and Methods
Three soil profiles were sampled in central Hungary within 50 meters from each other in a field that has a history of heterogeneity in crop yield (Czinege, 2000). The profiles had 2 to 4 distinct horizons. Textural and other differences among the top 120 centimeters of the three profiles can be seen in Figure 1.

1 – 6 August 2010, Brisbane, Australia. Published on DVD.

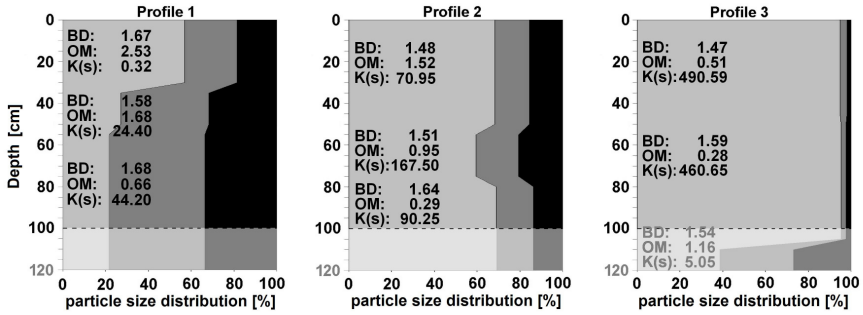

Figure 1. Physical properties of the top 120 cm of the soil profiles. The depth of 1 meter was considered as the bottom of the simulated profile. Light grey: sand (0.05-2mm); dark grey: silt (0.002-0.05mm); black: clay (<0.002mm) content. BD: bulk density [g/cm^3]; OM: organic matter content [%]; K_s: saturated hydraulic conductivity [cm/day].

Simulations of one-dimensional flow were carried out on a daily basis, using the SWAP model (van Dam *et al*., 1997). This model has previously been tested under Hungarian climatic and soil conditions (e.g. Farkas and Rajkai, 2002; Nemes *et al*., 2003). Groundwater levels were recorded at variable time intervals and were used as lower boundary condition for the simulations. Simulated weather data were used as upper boundary condition. The stochastic weather generator of Semenov and Barrow (1997) was used to generate one-year-long data sets of daily average temperature, solar hours and amount of precipitation. These were used to calculate daily values of potential evapotranspiration (ET_{pot}) using an empirical equation developed for the Hungarian Great Plain area (N. Fodor, pers. comm., 2002). Three drier and warmer than average years were simulated. The average annual precipitation was 416.5 (SD=29.2) mm, annual average temperature was 11.47 (SD=0.25) °C, and the calculated sum of annual ET_{pot} was 1280.6 (SD=71.5) mm; yielding considerably long periods of dry soil conditions. The simple crop growth routine of SWAP was used with grass as cover crop. Factors to characterise plant growth were derived by adjusting general factors suggested by van Dam *et al*. (1997), and FOCUS (2000) to local conditions. Soil hydraulic properties were described using the four parameter van Genuchten water retention model - with m=1–1/n - combined with Mualem's solution to describe unsaturated hydraulic conductivity, *K(h)* (van Genuchten, 1980). The M9 neural network PTF of Nemes *et al*. (2003), developed from Hungarian data, was used to predict the van Genuchten model parameters for all soil horizons. Soil texture, BD and OM content were used as input to a neural network model to predict saturated hydraulic conductivity (K_s) (A. Nemes, pers. comm., 2004). Predicted K_s, coupled with an assumed L=*0.5* was used to describe *K(h)*. Laboratory measured water retention and K_s data were used in alternative simulation runs to validate the PTF driven results.

Three different irrigation scheduling scenarios were evaluated for each of the three profiles. A "simple" (empirical) irrigation scheduling scenario was based on simple decision criteria that relied on daily weather observations as follows: (1) From May to September, 20 mm of irrigation water was applied on a particular day if the average daily temperature of the preceding five days was >20 °C, and the sum of the precipitation for the same period was <1 mm; (2) The same amount of irrigation was applied when daily average temperature was 17-20 °C for the preceding 8 days, with <1 mm of precipitation. Hence, irrigated days were at least 6 days apart to account for the need to rotate the irrigation equipment between fields. The alternative ("advanced") irrigation scheduling technique used decision criteria based on a preceding run of the simulation model. Using the available weather data, the model calculated when the vegetation started to suffer from water stress. When daily actual plant transpiration fell below 85% of the potential transpiration, we applied 20 mm of irrigation water, considering the same rule to rotate irrigation equipment as above. As the three profiles are physically close enough to each other to fall within the same irrigation unit in reality, we calibrated the latter scheduling technique to the profile with the intermediate texture (Profile 2) and applied the resulting irrigation schedule to all three soil profiles. As a control, we also ran simulations for each profile without any irrigation.

Results and Discussion

An average of 293 (SD=23.1) mm irrigation water was applied during the irrigated period annually following the "simple" irrigation scheduling system; while a total of 353 (SD=23.1) mm irrigation water was applied to the field following the "advanced" irrigation scheme. This gives a possible indication that the "simple" system does not supply enough water or proper timing to cover the needs of the vegetation.

Table 1. Water deficit for the vegetation (a); number of days with soil water pressure below –80 kPa in the top 50 cm of the soil (b); and flux balance of the soil profiles (c) in the period May 15 – October 15 under different irrigation schemes. Different letters indicate significant differences at 95% confidence level. First letters compare soil profiles within each irrigation scheme; second letters compare irrigation schemes within each profile; third letters compare results between pedotransfer function (PTF) and measured water retention (WRC) within the same profile and irrigation scheme.

irrigation	Pedotransfer function						Measured water retention and hydraulic conductivity					
	Profile 1		Profile 2		Profile 3		Profile 1		Profile 2		Profile 3	
scenario	MEAN	(STD)	MEAN	(STD)	MEAN	(STD)	MEAN	(STD)	MEAN	(STD)	MEAN	(STD)
						a) Water deficit [mm] for the vegetation						
no	544.7	(52.6) ^{a,a,a}	413.7	(49.2) ^{b,a,a}	172.6	(76.6) ^{c,a,a}	569.7	(54.4) ^{a,a,a}	436.7	(56.0) ^{b,a,a}	221.8	(83.6) ^{c,a,a}
simple	317.3	(23.6) ^{a,b,a}	144.4	(20.5) ^{b,b,a}	14.2	(20.1) ^{c,b,a}	343.3	(32.1) ^{a,b,a}	166.1	(25.3) ^{b,b,a}	37.8	(38.2) ^{c,b,a}
advanced	296.2	(16.7) ^{a,b,a}	100.9	(10.5) ^{b,c,a}	2.3	(0.2) ^{c,b,a}	323.5	(25.8) ^{a,b,a}	121.1	(17.6) ^{b,b,a}	4.6	(2.5) ^{c,b,a}
						b) Number of days with soil water pressure below -80kPa in the top 50cm						
no	153.0	(0.0) ^{a,a,a}	129.3	(13.0) ^{b,a,a}	51.3	(13.1) ^{c,a,a}	152.7	(0.6) ^{a,a,a}	128.0	(12.0) ^{b,a,a}	61.3	(12.7) ^{c,a,a}
simple	135.7	(6.4) ^{a,b,a}	71.7	(13.0) ^{b,b,a}	7.0	(12.1) ^{c,b,a}	140.3	(8.5) ^{a,a,a}	69.0	(13.5) ^{b,b,a}	18.3	(19.1) ^{c,b,a}
advanced	100.3	(13.3) ^{a,c,a}	31.3	(7.2) ^{b,c,a}	0.0	(0.0) ^{c,b,a}	101.7	(16.7) ^{a,b,a}	26.7	(5.1) ^{b,c,a}	1.7	(2.1) ^{c,b,a}
						c) Flux balance of the soil profiles [mm, negative downwards]						
no	-0.4	(0.5) ^{a,a,a}	76.2	(3.3) ^{b,a,a}	235.7	(21.6) ^{c,a,a}	-5.0	(0.3) ^{a,a,b}	36.1	(1.8) ^{b,a,b}	184.3	(25.7) ^{c,a,a}
simple	-0.5	(0.5) ^{a,a,a}	73.4	(3.9) ^{b,a,a}	133.2	(23.6) ^{c,b,a}	-5.1	(0.2) ^{a,a,b}	33.9	(3.6) ^{b,a,b}	100.6	(24.1) ^{c,b,a}
advanced	-0.5	(0.5) ^{a,a,a}	75.4	(3.2) ^{b,a,a}	88.7	(18.1) ^{c,b,a}	-5.1	(0.3) ^{a,a,b}	36.0	(1.8) ^{b,a,b}	75.7	(14.6) ^{c,b,a}

We used eight different output measures to evaluate the result of different irrigation schemes, of which we show and discuss three measures. Water deficit to the vegetation, as the difference between potential and actual transpiration (expressed in mm), was added up for the period from 15th May to 15th October. Flux balance – defined as the sum of daily bottom fluxes - at the depth of 1 meter in the profiles was summarized for the same period; and days were counted, when the average matric potential in the top 50 cm of soil – representing the root zone – was below the suggested starting point of water stress for grass (–80 kPa, FOCUS, 2000).

Table 1a shows that for each soil, irrigation significantly decreased water stress for the vegetation, calculated using the PTF estimates. For the heaviest textured Profile 1, using the simple irrigation scheduling scenario reduces plant water deficit by a predicted ~40% compared to using no irrigation. For Profile 2 such improvement is by ~65%, and for Profile 3 it nearly removes all water deficit. Using the advanced irrigation scheme resulted in further significant improvement for Profile 2. For Profiles 1 and 3 any such improvement was not significant. Differences between respective values for the three profiles are significant in all cases. Differences between respective values obtained using PTFs or measured soil hydraulic data are not significant in any of the cases.

The number of days with the average pressure in the top 50 cm below -80 kPa, were significantly different for the three profiles and were significantly reduced by both irrigation schemes (Table 1b). For Profile 3, the simple scheme reduced the presence of such stress condition to the plant to only 7 days a year. Additional improvement by the advanced irrigation scheme proved insignificant. Despite the coarse texture and thus low water holding capacity in the top 100 cm, Profile 3 had the least amount of water deficit. The overlying horizons greatly benefited from the favorable hydraulic properties of loamy material beneath 105 cm. That layer retains a considerable amount of water that later may partially be available by upward flux during water redistribution. Differences between results obtained using measured or estimated soil hydraulic data were not significant.

Table 1c summarizes the flux balance of each profile at the depth of 1 meter. Some of the water/soluble that flow below this depth may still reach shallower horizons by capillary rise during water redistribution, but most will end up in the subsoil and/or ground water. Only Profile 3 with its very coarse texture in the top 1 meter showed to be sensitive for the irrigation treatments. Differences between simulated results using PTF estimates and measured soil hydraulic properties were small in absolute values, but significant for two of the three profiles. None of the applied irrigation schemes had any influence on the leaching pattern of Profiles 1 and 2, but the amount of water leached into the subsoil increased significantly for Profile 3 (not shown). This signals an increased risk of subsoil/groundwater pollution introduced locally at the coarse part of the field by the application of extra water. Such leached pollutants will redistribute in the subsoil and groundwater due to the three-dimensional nature of water flow in field soils.

Conclusions

We used predicted soil hydraulic properties in exploratory simulation modeling to quantify the benefits and risks of using different irrigation scheduling scenarios. Studies of these kinds can be used to extend expert knowledge by giving a quantitative dimension to the outcome of planned or implemented changes. A simulation-assisted "advanced" irrigation system is more complicated, but for some soils, it brings further improvement in terms of plant water supply as compared to a simple "empirical" irrigation system. However, we also showed some dilemmas soil heterogeneity may cause: one action optimal for part of a management unit may be far from optimal for other parts, and the extent of the differences may be large. We quantified a major reason for the observed heterogeneity in crop yield, and showed that while one part of the field is sensitive for leaching; other parts are sensitive for drought. For most water balance components, and for at least two of the three soils, simulation results using PTF estimates and measured soil hydraulic properties did not differ significantly. Using well tested PTFs to provide soil hydraulic data appears to be a reasonable, reliable and cheap alternative to sampling and laboratory measurements; especially since laboratory measurements themselves are not error-free. PTFs appear to be useful in planning sustainable, productive and environmentally sound management systems.

Results of this demonstration are based on a limited number of simulation years. The presented approach can be further broadened and improved by running simulations using a larger number of years of different weather scenarios or by involving e.g. simultaneous yield estimation, estimation of cost-effectiveness, or assessment of uncertainty in the inputs. Besides quantifying different risk factors, such studies can also support the delineation of new management units that better balance contradictory demands within fields.

References

Czinege E (2000) Extension of soil information and knowledge of site-specific nutrient management consulting. PhD Thesis. University of Gödöllő, Gödöllő, Hungary. (in Hungarian).

Farkas C, Rajkai K (2002) Moisture regime with respect to spatial variability of soil hydrophysical properties. *Agrokémia és Talajtan* **51,** 7-16.

FOCUS (2000) Focus groundwater scenarios in the EU pesticide registration process. Report of the FOCUS Groundwater Scenarios Working Group, EC document.

Nemes A, Schaap MG, Wösten JHM (2003) Functional evaluation of pedotransfer functions derived from different scales of data collection. *Soil Science Society of America Journal* **67,** 1093-1102.

Pachepsky YaA, Rawls WJ (2004) [Eds.] Development of pedotransfer functions in soil hydrology. Developments in Soil Science, Vol 30. Elsevier, Amsterdam. ISBN 0-444-51705-7.

Semenov MA, Barrow EM (1997) Use of a stochastic weather generator in the development of climate change scenarios. *Climatic Change* **35,** 397-414.

Soet M, Stricker JNM (2003) Functional behaviour of pedotransfer functions in soil water flow simulation. *Hydrological Processes* **17,** 1659-1670.

van Dam JC, Huygen J, Wesseling JG, Feddes RA, Kabat P, van Walsum PEV, Groenendijk P, van Diepen CA (1997) SWAP version 2.0, Theory. Simulation of water flow, solute transport and plant growth in the Soil-Water-Atmosphere-Plant environment. Technical Document 45, DLO Winand Staring Centre, Wageningen.

van Genuchten MT (1980) A closed form equation for predicting the hydraulic conductivity of unsaturated soils. *Soil Science Society of America Journal* **44,** 892-898.

Wösten JHM, Finke PA, Jansen MJW (1995) Comparison of class and continuous pedotransfer functions to generate soil hydraulic characteristics. *Geoderma* **66,** 227-237.

Visualising and quantifying rhizosphere processes: root-soil contact and water uptake

Sonja Schmidt[A, B], Peter J. Gregory[A], A. Glyn Bengough[A], Dmitri V. Grinev[B] and Iain M. Young[C]

[A]Scottish Crop Research Institute, Invergowrie, Dundee, DD2 5DA, Scotland, UK, Email Sonja.Schmidt@scri.ac.uk
[B]University of Abertay Dundee, SIMBIOS Centre, Bell Street, Dundee, DD1 1HG, Scotland, UK
[C]The School of Environmental & Rural Science, University of New England, Armidale, NSW 2351, Australia

Abstract
Root-soil contact is vital for water transport via liquid films. X-ray microtomography potentially makes it possible to study the root-soil interface non-invasively. This paper presents first attempts to quantify the contact areas of roots with the three phases of soil systems using X-ray microtomography. Root-particle contact was investigated producing 3D volumetric images of maize in soil and vermiculite wetted to matric potentials of -0.03MPa and -1.6MPa. Root-soil contact was calculated to be greater in soil than in vermiculite. Water volumes in artificial porous media, formed by cellulose acetate beads, were determined by weighing samples before and after wetting and by image analysis of 3D volumetric images. Image analysis underestimated the water volume by about 10%. Contact between an artificial root (porous glass fibre tube) and the solid, liquid and gaseous phases in sand were calculated from 3D volumetric images. The total sum of contact areas was about 8% greater than the estimated surface area of the root. Results of repeated image analysis of root-particle contact revealed that changes in threshold values influenced the final results by up to 12%. Thus, whilst this method has clear potential for investigating the root-soil interface, there remain several limitations that are being addressed.

Key Words
X-ray microtomography, 3-D visualisation, root-soil interface, root-contact surface area

Introduction
Knowledge of root contact with the soil solution is essential for understanding water and nutrient adsorption by plants. The contact is influenced by soil and root properties, such as particle size, soil bulk density, root diameter, soil matric potential and volumetric water content (Tinker 1976; Nye 1994). In water saturated and heavily compacted soils, problems with gas exchange can occur (Veen *et al.,* 1992). Conversely, incomplete root-soil contact due to soil structure or root shrinkage can reduce the uptake of water and nutrients (Veen *et al.,* 1992). A thin section technique was used by Noordwijk *et al.* (1992) to derive the degree of root-soil contact in 2D slices. An increase in root-soil contact with increasing bulk density was investigated by Kooistra *et al.* (1992). A decrease in water and nitrate uptake per unit root length was associated with smaller root-soil contact (Veen *et al.,* 1992). Neutron and X-ray computed tomography have been used to provide a non-invasive methodology to visualise and quantify roots growing in opaque soils (Heeraman *et al.,* 1997; Lontoc-Roy *et al*., 2006; Tumlinson *et al.,* 2007; Oswald *et al.,* 2008; Moradi *et al.,* 2009; Carminati *et al.,* 2009) and establish an approach to examine root-soil contact. Root-soil contact dynamics of lupin plants under drying and wetting cycles were investigated by Carminati *et al.* (2009). Changes of water contents around roots were detected with neutron radiography. A non-uniform water uptake around the root was observed (Oswald *et al.,* 2008). Quantification of the spatial distribution of solid, liquid and gaseous phases using X-ray computed tomography was achieved by a cluster analysed segmentation method (Wildenschild *et al.,* 2002).
In this paper, the use of X-ray microtomography to study the root-soil interface will be discussed and preliminary data on root-soil contact and water distribution will be presented. Processes for quantifying the solid, liquid and gaseous phases around the root surface will be reviewed with both artificial and natural systems.

Methods
X-ray microtomography
3D volumetric images were obtained using a Metris X-Tek HMX CT scanner with a Varian Paxscan 2520V detector with a 225kV X-ray source and a molybdenum target. 3D volumetric images were reconstructed with the Metris software CT-Pro v2.0. VGStudioMAX v2.0 was used to analyse the 3D volumetric images.

Water visualisation
3D volumetric images of water in packed cellulose acetate beads of 1mm and 3mm diameter were obtained. A 0.75g/100g sodium iodide-spiked solution was used as a wetting fluid to obtain a greater contrast between the water and solid phases. A high absorption was achieved through the sodium iodide rendering the water and solid phase separable. Samples were scanned before and after wetting, using a beam with energy of 65kV and a current of 486µA. 2855 projections were acquired. A resolution of 21µm (isotropic voxel size) was attained. Typically, scans took approximately 150 minutes.

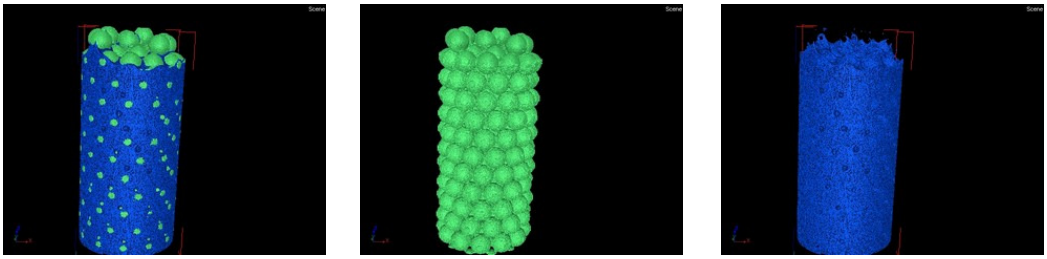

Figure 3. False coloured 3D volumetric images of wetted cellulose acetate beads (3 mm diameter; left), extracted beads (middle) and extracted water (right).

The volume of water was segmented using 3D volume segmentation tools, which identify and extract voxels belonging to calculated ranges of greyscale values (representing water phase in the sample). As a control the sample was weighed before and after wetting.

Contact areas of the root with the water, air and solid phases of the growth medium
Root-particle contact was estimated for 3D volumetric images of maize seeds growing in soil and vermiculite at matric potentials of -0.03MPa and -1.6MPa. The pre-germinated seeds were grown for 2 days at 20ºC in darkness. The samples were scanned using a beam with energy of 145kV and a current of 140µA. 2987 projections were acquired. Typically, scans took 180 minutes. Three replications of each treatment were analysed twice by the same operator. The sample size was 3 cm in diameter and 10 cm high. To differentiate the contact areas of the root with air, water and solid phase, an artificial root (porous glass fibre tube of 1.5 mm in diameter) in sand was scanned. The sand was wetted with 0.75% sodium iodide solution (see above) and drained by applying suction to the artificial root. The sample was scanned with energy of 85kV and a current of 296µA with 2855 projections acquired. The sample was 1.5 cm in diameter and 10 cm high. Resolutions of 35µm for the samples in soil and vermiculite and 18µm for the sample in sand were attained.

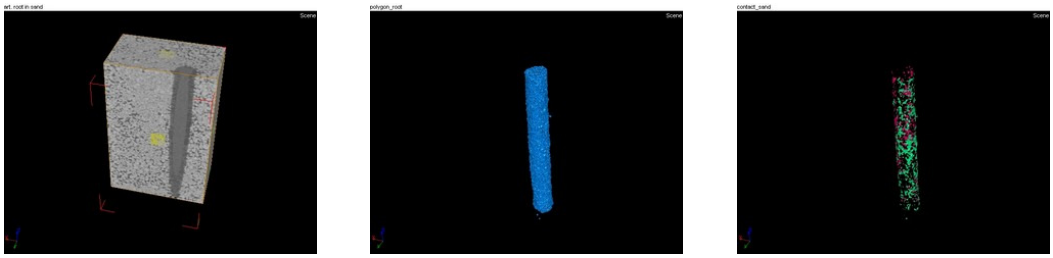

Figure 4. Region of interest with artificial root in sand (partly drained; left), polygonal mesh of root volume for calculating the root surface area (middle) and polygonal mesh of root sand contact surface area (right).

Image analysis was performed to determine the contact areas of liquid, air and solid phases with the root. For calculating the root surface and contact surface area, the root volume was segmented. Advanced calibration and 3D volume segmentation tools, which identify and extract voxels belonging to calculated ranges of greyscale values (representing root, water, air and solid particle) were used to segment the root volume. The surface area of the root was determined for the extracted root volume. The contact surface area of root with the three different phases of the sample were investigated, by subtracting voxels representing each phase which were adjacent to voxels of the root volume from the volumetric region of the root.

Results

Water visualisation
In Figure 3 the volumes of water added to the packed cellulose acetate beads (1 mm and 3 mm diam.) and calculated from 3D images are shown. Image analysis underestimated the volume of water by 11% for 1 mm beads and 8% for 3 mm beads.

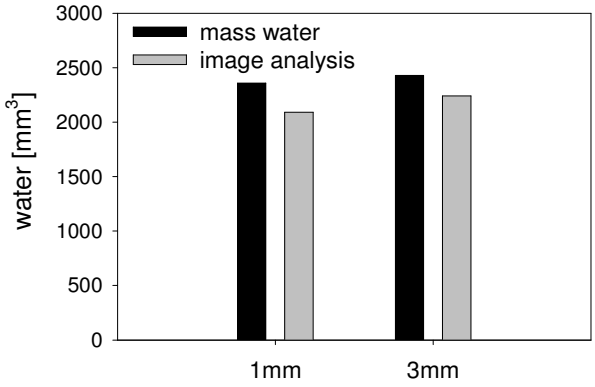

Figure 5. Water volume determined by weighing samples before and after adding water to cellulose acetate beads of 1mm and 3mm size and by image analysis with VGStudioMAX v2.0.

Root-soil interface contact areas

The results for root-particle contact of maize in soil and vermiculite at -0.03MPa and -1.6MPa are shown in Figure 4. The determination of root-particle contact in VGStudioMAX v2.0 was done twice. The second time (VGStudio MAX (2)) the root-soil contact for all samples except maize in vermiculite at -1.6MPa was greater than that determined in the first attempt (VGStudio MAX (1)). The results for both investigations showed greater root-particle contact in soil than in vermiculite.

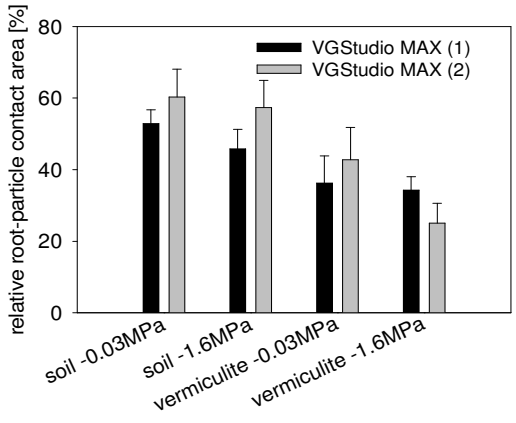

Figure 4. Root-particle contact of maize in soil and vermiculite at matric potentials of -0.03MP and -1.6MPa analysed in VG Studio MAX v.2.0 a two time points, average differences between the 1st and 2nd attempt are ca. 6-11% (left).

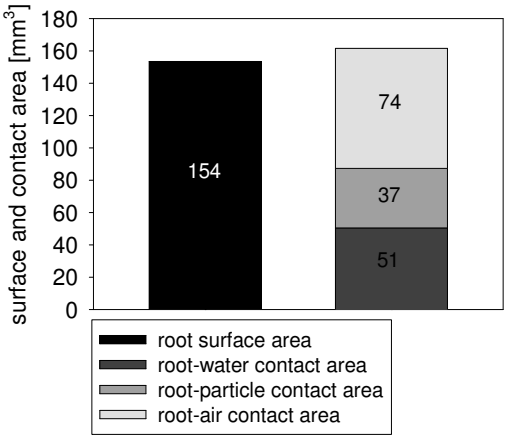

Figure 5. Surface area of artificial root (black) and contact surface areas of artificial root in contact with water, solid and air (grey; right).

The contact surface areas of an artificial root with air, water and sand particle are shown in Figure 5. The total root surface area of the root volume was 154 mm^2. The total contact surface area was 162 mm^2 according to the image analysis in VGStudioMAX, where the water phase contributed the greatest part at 74 mm^2 and the solid phase the smallest part at 37 mm^2.

Discussion and Future Work

These studies investigated the use of X-ray microtomography for quantifying contact areas of roots in a three phase system. The water, air and solid phases could be clearly distinguished. It was possible to segment voxels containing water in a bead system using a contrast enhancer (NaI). The concentration of the contrast enhancer was kept as small as practicable, resulting in relatively small contrast between solid and liquid phase, making discrimination between water and solid voxels difficult. A small proportion of voxels containing water might have been counted as voxels representing beads. However, the water volume was underestimated by 8-11%. To better quantify this source of uncertainty, we intend comparing the volume of the beads in dry samples (two phase system, big contrast) with the volume estimated with water present to help specify the effects of decreasing contrast. A similar approach was used by Culligan *et al.* (2004) where partially saturated images

were registered with the dry image to create tertiary volume in which the solid, liquid, and air phase were quantified.

Image analysis of root-particle contact of maize grown in soil and vermiculite showed a greater root-soil contact than in vermiculite. This was expected because of the greater particle sizes of vermiculite and smaller bulk density (Kooistra *et al.,* 1992). Yet, repeating the image analysis on the same samples showed a variation of 6 to 12% in the relative root-particle contact. This was probably because the contrast between root and solid particles was relatively poor and partial volume effects made it difficult to specify the borders between root and solid phase. In the procedure, several parameters are changed manually to extract the different phases and define the root-particle contact areas. A sensitivity analysis of those parameters on a model system of known dimensions is underway to help improve the methodology. Extracting the three phases and calculating the contact areas with an artificial root in sand was possible but a greater cumulative contact surface area resulted – this is probably because voxels were classified non-uniquely, with certain voxels being double-counted as both root-solid and root-water interfaces. This may also have been associated with partial volume effects making the segmentation of the phases more difficult and adding to this double counting. We are currently modifying the procedure to reduce this source of error.

In conclusion, X-ray microtomography and 3D image analysis algorithms are useful tools to study the root-soil interface and determine contact areas, but require both careful optimisation of image quality and the development of rigorous image analysis protocols that minimise elements of subjectivity.

Acknowledgements

PhD Studentship for Sonja Schmidt was funded by SCRI and University of Abertay Dundee. SCRI receives funding from the Scottish Government Rural and Environmental Research and Analysis Directorate.

References

Carminati A, Vetterlein D, Weller U, Vogel HJ, Oswald SE (2009) When roots lose contact. *Vadose Zone Journal* **8**, 805-809.

Culligan KA, Wildenschild D, Christensen BSB, Gray WG, Rivers ML, Tompson FB (2004) Interfacial area measurements for unsaturated flow through a porous medium. *Water Resources Research* **40**, W12413.

Heeraman DA, Hopmans JW, Clausnitzer V (1997) Three dimensional imaging of plant roots in situ with X-ray computed tomography. *Plant and Soil* **189**, 167-179.

Kooistra MJ, Schoonderbeek D, Boone FR, Veen BW, Van Noordwijk M (1992) Root-soil contact of maize, as measured by a thin-section technique 2. Effects of soil compaction. *Plant and Soil* **139,** 119-129.

Lontoc-Roy M, Dutilleul P, Prasher SO, Han L, Brouillet T, Smith DL (2006) Advances in the acquisition and analysis of CT scan data to isolate a crop root system from the soil medium and quantify root system complexity in 3-D space. *Geoderma* **137**, 231-241.

Moradi AB, Conesa HM, Robinson B, Lehmann E, Kuehne G, Kaestner A, Oswald S, Schulin R (2009) Neutron radiography as a tool for revealing root development in soil: capabilities and limitations. *Plant and Soil* **318,** 243-255.

Noordwijk M, Kooistra MJ, Boone FR, Veen BW, Schoonderbeek D (1992) Root-soil contact of maize, as measured by a thin-section technique. I. Validity of the method. *Plant and Soil* **139**, 109-118.

Nye PH (1994) The effect of root shrinkage on soil-water inflow. Philosophical Transactions of the Royal Society of London Series B-Biological Sciences **345**, 395-402.

Oswald SE, Menon M, Carminati A, Vontobel P, Lehmann E, Schulin R (2008) Quantitative imaging of infiltration, root growth, and root water uptake via neutron radiography. *Vadose Zone Journal* **7**, 1035-1047.

Tinker PB (1976) Roots and water - transport of water to plant roots in soil. *Philosophical Transactions of the Royal Society of London Series B-Biological Sciences* **273**, 445-461.

Tumlinson LG, Liu H, Silk WK, Hopmans JW (2008) Thermal neutron computed tomography of soil water and plant roots. *Soil Science Society of America Journal* **72,** 1234-1242.

Veen BW, Van Noordwijk M, De Willigen P, Boone FR, Kooistra MJ (1992) Root-soil contact of maize, as measured by a thin-section technique 3. Effects on shoot growth, nitrate and water-uptake efficiency. *Plant and Soil* **139,** 131-138.

Wildenschild D, Hopmans JW, Vaz CMP, Rivers ML, Rikard D, Christensen BSB (2002) Using X-ray computed tomography in hydrology: Systems, resolutions, and limitations. *Journal of Hydrology* **267**, 285-297.

Water exchange between the fine earth and pebbles in remoulded soil samples

Marion Tétégan[A, B], Nathalie Korboulewsky[A,C], Alain Bouthier [B] and Isabelle Cousin[A]

[A] INRA, UR 0272 Science du Sol, Centre de recherche d'Orléans, 2163 Avenue de la Pomme de Pin, CS 40001 Ardon 45075 Orléans Cedex 02, France. Email Marion.Tetegan@orleans.inra.fr
[B] Arvalis – Institut du Végétal, Domaine expérimental du Magneraud 17700 Saint Pierre d'Amilly, France. Email a.bouthier@arvalisinstitutduvegetal.fr
[C] Aix-Marseille Université, IMEP, UMR CNRS-IRD - Centre Saint-Charles, case 4, 3 place Victor Hugo 13331 Marseille Cedex 03, France. Email nathalie.korboulewsky@univ-provence.fr

Abstract
Stony soils cover about 30% of the surface soils of Western Europe, and 60% in Mediterranean areas. Rock fragments may alter the physical, chemical and agricultural properties of soils. In particular, the stony phase may participate in the water supply of crops and change the storage capacity of soil water. This implies the existence of water transfer between rock fragments and fine earth. To better understand the interaction between the fine earth and rock fragments, we studied the transfer of water between the pebbles and the fine earth on remoulded soils in the presence and absence of plants.

Key Words
Stones, fine earth, water content, water exchange.

Introduction
Lots of physical and chemical exchanges occur in the rhizosphere between the soil, plant roots and micro-organisms. The physico-chemical, biochemical and biological processes that take place at the soil-root interface affect water transfer and fluxes of many elements, macro- nutrients like potassium and phosphorus or micro-nutrients like iron. But rock fragments are also a potential reservoir of water and nutrients for plants (Poesen and Lavee 1994; Coile 1953; Gras 1994; Cousin *et al*. 2003), suggesting that the stony phase of soil can participate in water supply to crops and affect the storage capacity of soil water. Some water exchanges between the rock fragments and the fine earth should then exist. The understanding of these exchanges between the rhizosphere and the soil would be a significant progress and would improve the existing "soil-plant" models. It is then necessary to understand mechanisms taking place between the different phases of soil: fine earth and stones. Our experiment, conducted on remoulded samples during one season under controlled conditions, aimed to analyse the water transfer between stones and fine fractions of soil and the effects of the proportion (0, 20, 40% in volume) of rock fragments and of the rhizosphere (with or without plants).

Methods
Experiments in controlled conditions (artificial light and 22°C in a greenhouse) with remoulded soils in containers (3 L) were conducted. Rock fragments and fine earth were collected separately from the Ap horizon of a calcareous lacustrine limestone silty soil located in the central region of France. The fine earth was sieved at 2 mm and air-dried. The rock fragments were sieved at 2-5 cm, which corresponds to the pebble fraction, washed under tap water and dried at 105°C during 2 days in an oven. The pebbles' bulk density was about 1.98 g/cm^3. Pebbles were mixed with the fine earth to reach a bulk density of the fine earth of 1.1 g/cm^3. Four modalities of remoulded soil, with different percentage in volume of pebbles, were created:

"0%p": 0 % pebbles + 100 % fine earth + plant
"20%p": 20 % pebbles + 80% fine earth + plant
"40%p": 40 % pebbles + 60% fine earth + plant
"40%": 40 % pebbles + 60% fine earth

Fifteen containers were created for each modality and cuttings of *Populus robusta* were planted in the three first modalities. All containers were saturated, then irrigated by capillarity and controlled to maintain a moderate water stress continuously. After three months, the containers were again saturated and then allowed to dry. At that time, plants were from 27 cm to 43 cm height depending on the modality. Soil samples were collected at 5 dates following this second saturation: D0, Day 2 = D0 + 2 days, Day 4 = D0 + 4 days, Day 7 = D0 + 7 days, Day 11= D0 + 11 days, where D0 corresponds to the soil water content equal to the Available Water Content. At each sampling date, the fine earth and the pebbles were separated at five depths inside each container. The gravimetric water content of the fine earth (Wfe) and the gravimetric water content of the pebbles (Wp) were measured; and the gravimetric water content of the soil (Wsoil) was calculated, knowing the volume percentage

of fine earth and pebbles. Three containers of each modality were used at each date. Differences in water content between the pebbles and fine earth, and between the dates, were analysed by a variance analysis (ANOVA with a threshold of 5%).

Results

During drying, the water content decreased in both the fine earth and the pebbles, and differences between modalities were observed for each phase (Figure 1).

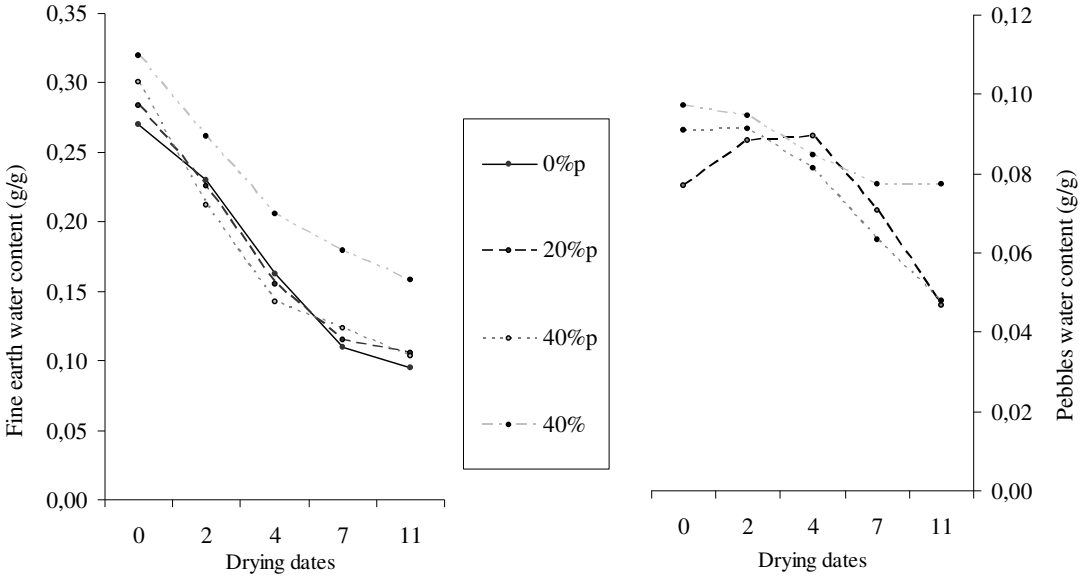

Figure 1. Temporal evolution of water content of fine earth (left) and pebbles (right).

The pebbles' effect

To study the effect of the proportion of pebbles, a statistical comparison was made between the modalities "0%p", "20%p" and "40%p".

The water content of fine earth in all modalities decreased from the beginning but the rate of decrease was less rapid from Day 4 to Day 11 (Table 1 and Figure 1). In contrast, the water content of the stony phase stayed stable at the beginning, and decreased after Day 7 for the modality "20%p", and after Day 4 for the modality "40%p".

There were significant differences in water content of the fine earth from the 4th day between the modalities (Table 2). The stony phase shows no differences for the modalities concerned (20%p and 40%p).

These results show that the fine earth of the modality without pebbles (0%p) lost water faster compared to modalities with pebbles ("20%p" and "40%p") from the 7th day. Meanwhile, pebbles lose water only from the 4th day or 7th day. This suggests a water transfer from the pebbles towards the fine earth occurs when drought starts to be severe which would explain the higher water content in fine earth for modalities with pebbles.

Table 3. Statistical analysis results on the temporal evolution of mass water content (g/g) by phase and by modality. The table reads left to right. Letters in group column correspond to differences between dates within a modality.

Fine Earth	Day 0			Day 2			Day 4			Day 7			Day 11		
	Average	Standard Deviation	Group	Average	Standard Deviation	Group	Average	Standard Deviation	Group	Average	Standard Deviation	Group	Average	Standard Deviation	Group
0%p	0,270	0,016	a	0,230	0,019	b	0,162	0,007	c	0,110	0,003	d	0,095	0,005	d
20%p	0,283	0,038	a	0,226	0,021	b	0,155	0,010	c	0,115	0,003	d	0,105	0,002	d
40%p	0,301	0,021	a	0,212	0,014	b	0,143	0,005	c	0,123	0,003	cd	0,103	0,006	d
40%	0,320	0,014	a	0,261	0,029	b	0,206	0,012	c	0,179	0,007	cd	0,158	0,004	d

Pebbles	Day 0			Day 2			Day 4			Day 7			Day 11		
	Average	Standard Deviation	Group	Average	Standard Deviation	Group	Average	Standard Deviation	Group	Average	Standard Deviation	Group	Average	Standard Deviation	Group
20%p	0,077	0,015	a	0,088	0,017	a	0,090	0,005	a	0,071	0,011	a	0,047	0,002	b
40%p	0,091	0,009	a	0,091	0,005	a	0,081	0,004	a	0,063	0,002	b	0,048	0,006	c
40%	0,097	0,006	a	0,095	0,008	a	0,085	0,007	ab	0,077	0,009	b	0,077	0,004	b

Table 4. Statistical analysis results on the daily comparison of water content (g/g) by phase between modalities. The table reads vertically. Letters in group column correspond to differences between modalities within a date.

Fine Earth	Day 0			Day 2			Day 4			Day 7			Day 11		
	Average	Standard Deviation	Group	Average	Standard Deviation	Group	Average	Standard Deviation	Group	Average	Standard Deviation	Group	Average	Standard Deviation	Group
0%p	0,270	0,016	b	0,230	0,019	ab	0,162	0,007	b	0,110	0,003	c	0,095	0,005	c
20%p	0,283	0,038	ab	0,226	0,021	ab	0,155	0,010	bc	0,115	0,003	bc	0,105	0,002	b
40%p	0,301	0,021	ab	0,212	0,014	b	0,143	0,005	c	0,123	0,003	b	0,103	0,006	bc
40%	0,320	0,014	a	0,261	0,029	a	0,206	0,012	a	0,179	0,007	a	0,158	0,004	a

Pebbles	Day 0			Day 2			Day 4			Day 7			Day 11		
	Average	Standard Deviation	Group	Average	Standard Deviation	Group	Average	Standard Deviation	Group	Average	Standard Deviation	Group	Average	Standard Deviation	Group
20%p	0,077	0,015	a	0,088	0,017	a	0,090	0,005	a	0,071	0,011	a	0,047	0,002	b
40%p	0,091	0,009	a	0,091	0,005	a	0,081	0,004	a	0,063	0,002	a	0,048	0,006	b
40%	0,097	0,006	a	0,095	0,008	a	0,085	0,007	a	0,077	0,009	a	0,077	0,004	a

The plant's effect

In order to study this effect, modalities "40%p" and "40%" were statistically compared. The water content decreased at a similar rate for the fine earth and we noted the same water content from the 7th sampling date for the fine earth for the 2 modalities (Table 1 and Figure 1). For the stony phase, significant differences from this 7th date onward were observed.

The day by day comparison between modalities (Table 2) showed that the water content of the fine earth of the "40%p" modality was significantly greater than the "40%"modality after Day0. Similarly, the drying of the rock fragments was more pronounced with a plant by Day 11.

These results indicate that, whatever the percentage of stones, the moisture of the fine earth reduces on average 1.3 times faster with a plant (modality "40%p") than without a plant (modality "40%p").

Conclusion

Results showed different behaviour for water loss between fine earth and pebbles during a drying period of 11 days. While water content of fine earth decreased from the beginning and onward, pebbles only started to lose water several days after. Plants enhanced the drying processes due to their transpiration but did not seem to modify the water transfer trends.

Evolution of water content in the fine earth and the coarse fraction suggests the existence of water exchange between the two phases to establish a water balance. In the future work we aim to determine the water exchanges using water retention curves of pebbles and fine earth to determine the radii of pores involved in this exchange.

References

Coile TS (1953) Moisture content of small stone in soils. *Soil Science* **75**, 203-207.

Cousin I, Nicoullaud B, Coutadeur C (2003) Influence of rock fragments on the water retention and water percolation in a calcareous soil. *Catena* **53(2)**, 97-114.

Gras R. (1994) 'Sols caillouteux et production végétale'. (INRA Editions).

Poesen J, Lavee H (1994) Rock fragments in top soils: significance and processes. *Catena* **23**, 1-28.

Water retention estimation and plant availability for subtropical Brazilian soils

José Miguel Reichert[A], Jackson Adriano Albuquerque[B], Dalvan José Reinert[C], and Douglas Rodrigo Kaiser[D]

[A]Department of Soil Science, Federal University of Santa Maria (UFSM), Brazil, Email reichert@smail.ufsm.br
[B]Department of Soil Science, State University of Santa Catarina (UDESC), Brazil, Email jackson@cav.udesc.br
[C]Department of Soil Science, UFSM, Brazil, Email reinert@ccr.ufsm.br
[D]Graduate Program in Soil Science, UFSM, Brazil, Email douglasrodrigokaiser@gmail.com

Abstract
Limited databases on water retention and availability in soils to generate pedotransfer functions are available for tropical and subtropical soils. The objectives of the study were to generate and evaluate pedotransfer functions for soil water retention in soils from subtropical Brazil; and to estimate plant available water based on soil particle size distribution. Two databases were set up for soil properties including water retention: one had 725 data and the other 253 data. From the literature database, pedotransfer functions were generated, nine pedofunctions available in the literature were evaluated and the plant available water capacity was calculated. Pedotransfer functions for selected sections generated for the soils had coefficients of determination ranging from 0.56 to 0.66. Pedotransfer functions generated with soils from other regions were not appropriate for estimating the water retention. Plant available water content varied with soil texture class, from 0.089 kg kg^{-1} for the sand texture class to 19.6 kg kg^{-1} for the silty clay class. These variations were more dependent on sand and silt content than on clay content. The soils with a greater silt/clay ratio, that were less weathered and had a greater quantity of smectite clay minerals, possessed greater water retention and plant available water capacity.

Key Words
Pedotransfer functions, moisture retention, field capacity, permanent wilting point, tropical soils, ferralsols

Introduction
Plant available water in the soil is essential for adequate development of crops and is dependent on soil properties. To overcome difficulties in water retention and availability determinations, researchers have proposed mathematical models to estimate soil water retention (Saxton *et al*., 2006), known as pedotransfer functions or equations (pedofunctions). These models estimate water retention by means of soil properties that are more easily obtainable or available in the literature, which are related to water retention, and are generally related to capillarity and water adsorption phenomena (Rawls *et al*., 1991).
Models were initially developed for temperate regions, where the edaphoclimatic properties are different from tropical regions, which may make their use for these regions unviable (Tomasella *et al*., 2000). In Brazil, some pedotransfer functions have already been established for estimating soil water retention (Arruda *et al*., 1987; Masutti, 1997; Giarola *et al*., 2002; Oliveira *et al*., 2002), but their validity for other soils different from the database soils has been little studied, which makes one question the degree of efficiency of generalized use of these equations.
The objectives of this study were: to generate pedotransfer functions to estimate soil water retention at different tensions from easily obtainable soil properties; to evaluate the efficiency of pedotransfer functions generated in other regions for the estimation of water retention in subtropical soils from southern Brazil; and to calculate plant available water capacity based on soil particle size distribution of Brazilian subtropical soils.

Methods
The pedotransfer functions for the soils were generated from data obtained from the 25 literature sources. These studies were generated from samples collected from soil classes and horizons which represent various regions of the state, giving a total of 725 sets of data, which include water retention curves, organic matter content, clay, silt and sand, and bulk and particle density.
Retention data was available for up to eight tensions. The water retained at the tension of 10 kPa was denominated as field capacity and that of 1,500 kPa as permanent wilting point. The option was made to standardize the estimation of water retention at 10 kPa, determined in the laboratory, in spite of the concept of field capacity for a given tension being questionable.
Based on the database, multiple regression analyses were made for obtaining the pedofunctions using the stepwise option. This method selects the independent variables, sand, silt, clay, organic matter, bulk density, particle density and the sum of the clay fractions plus silt (soil properties) and generates the respective coefficients that compose each pedofunction to estimate the water content retained by the soil at the tensions of 6, 10, 33, 100, 500 and 1,500 kPa. Pedofunctions to estimate water retention for the tensions of 10, 33 and

1,500 kPa were also generated simply from particle size distribution data, necessary for databases that do not have the organic matter content and the bulk and particle densities.
To evaluate the accuracy of other available equations, those that estimate the gravimetric soil water content were used, such as those proposed by Arruda *et al*. (1987), Oliveira *et al*. (1992), Bell & van Keulen (1995) and Masutti (1997), and others that estimate the volumetric soil water content, such as those from Gupta & Larson (1979), Rawls *et al*. (1982), Saxton *et al*. (1986), Van den Berg *et al*. (1997) and Giarola *et al*. (2002), with data of organic matter, bulk density and clay, silt and sand content. Estimated moisture was correlated with the moisture measured for each model.
Water content at field capacity (10 kPa) and at the permanent wilting point (1,500 kPa) and plant available water capacity (between 10 and 1,500 kPa) were calculated for each sample. The results were grouped by textural class and the mean of each class was presented in a textural triangle. For these properties, regression analysis and path analysis were done. In this analysis, the data were submitted to descriptive statistics, Pearson correlation analysis and multicollinearity. Variables with high and severe multicollinearity were not included in the path analysis.

Results

Soil physical properties and water retention

The clay contents varied from 0.01 to 0.82 kg/kg, silt from 0.01 to 0.78 kg/kg and sand from 0.01 to 0.99 kg/kg. The organic matter content varied from 0.01 to 0.10 kg/kg and the bulk density from 0.86 to 1.85 kg/dm^3. This ample variation is favorable and necessary for the generation of pedotransfer functions (Pachepski & Rawls, 1999). Thus, water retention also varied, as exemplified for the tension of 1,500 kPa, with levels from 0.01 to 0.48 kg/kg. These differences reflect the material of origin and the degree of weathering and thus the physical, chemical and mineralogical properties of the soil.
Water retention had a positive correlation with the clay content, because this fraction favors the occurrence of micropores and menisci, which generate capillary forces. In addition, clay increases the specific surface area of the soil matrix and, consequently, water adsorption. These two phenomena, capillarity and adsorption, determine the matric potential and are responsible for soil water retention.

Estimation of water retention and validation of the pedofunctions

The independent variables included in the equations were the same as the model presented by Gupta & Larson (1979) and Rawls *et al*. (1982), and the coefficient associated with bulk density also had a negative signal, as in that study, which is due to the fact that sandier soils, with low water retention, are denser.
The pedofunctions generated have coefficients of determination (R^2) that vary from 0.56 at the tension of 500 kPa to 0.67 at the tensions of 6 and 10 kPa, all significant at the 1% level. Nevertheless, there are overestimates for low tensions and underestimates for high tensions of water retention, differences expressed in the angular coefficient (slope of the equation), always less than one, with variation from 0.56 to 0.67. The pedofunctions generated only with particle size distribution data had R^2 from 0.44 to 0.54, less than those of the equations that also use organic matter and bulk density, when only the particle size distribution data are available.

Evaluation of pedofunctions from the literature

Of five models tested that of Masutti *et al*. (1997) for the tension of 33 kPa and of Oliveira *et al*. (2002) for the tensions of 33 and 1,500 kPa were those that resulted in the best estimation of water retention, in spite of underestimating water retention for greater tensions. The model from Arruda *et al*. (1987) presents a gravimetric soil water content estimated at approximately 0.32 kg/kg at the tension of 33 kPa, while the measured contents are much higher than this level. All the models underestimate water retention for high tensions, which may be observed by the b coefficient of the determined equation, which frequently has a value of less than 0.5. The model from Bell and van Keulen (1995) estimated with greater precision the retention measured for the soils of Rio Grande do Sul. Nevertheless, the b coefficient of the equation was 0.61, different than 1 from the straight line 1:1. This indicates that for low tensions there was an underestimation of water retention.
Models developed from soils of the temperate climate region, such as those from Gupta & Larson (1979), Rawls *et al*. (1982) and Saxton *et al*. (1986), also had under or overestimation in water retention; nevertheless, variability was high. With the exception of the model from Saxton *et al*. (1986) for the tension of 33 kPa, the other models had R^2 less than the models developed from the soils of tropical regions. This may be due to differences in mineralogy between the soils of the tropical regions and the temperate climate regions.
To evaluate the accuracy of the model proposed, the estimated results were compared with those estimated by the models from Oliveira *et al*. (1992) and from Masutti (1997), which were generated with data from the State

of Pernambuco. The water retention estimation from the proposed model, compared to that estimated by the model from Oliveira *et al*. (1992) has a higher R^2 (0.93 for 33 kPa to 0.92 for 1,500 kPa), but the model proposed overestimates water retention at the tension of 1,500 kPa. For the Masutti (1997) model, the R^2 were 0.46 for 33 kPa and 0.94 for 1,500 kPa. In addition, the angular coefficient at the tension of 1,500 kPa was only 0.42, very different from the unit value, which indicates a significant underestimation.
With the objective of making equations available when there is only information regarding particle size distribution, three water retention equations were generated for the tensions of 10, 33 and 1,500 kPa. For the tensions of 33 and 1,500 kPa, it was possible to evaluate the equations with the data available for soils from an irrigation system. It may be seen that at the tension of 33 kPa, the R^2 between the estimated moisture and the measured moisture was 0.73, while for 1,500 kPa it was 0.76.

Plant available water
Through path analysis, the direct and indirect effects of soil properties on water retention were evaluated. For water retention at field capacity (10 kPa), direct and positive effects are seen from clay and silt, and a negative effect from bulk density. The direct effect of clay (R=0.71) is greater than its total effect (R = 0.62) due to its indirect effect through silt content (R = -0.23). In the more clayey soils, the silt content had a negative relationship with clay (R = -0.42) and the lower direct contribution from the silt fraction to water retention (R=0.54) diminishes the total effect from the clay in that retention.
The total effect of bulk density was negative (R = -0.65), a result of its direct effect (R = -0.27) and indirect effect via the clay content (R = -0.34). In denser soils, the volume of larger pores diminishes, affecting water retention at field capacity. With an increase in sand content, bulk density increased (R = 0.51); thus in the denser and sandier soils, water retention was less, which resulted in an indirect effect from particle size distribution in reduction of field capacity in the denser soils. The organic matter content had a total positive effect on water retention at field capacity, with a correlation coefficient of 0.41. Nevertheless, the direct effect was low (R = 0.14), while the indirect effect through clay (R = 0.04), silt (R = 0.15) and bulk density (R = 0.09) were responsible for the total effect.
Similar effects to those discussed for field capacity were observed for the permanent wilting point, however with different correlation coefficients, primarily by the lower direct effect from the silt fraction. Furthermore, for bulk density, the negative effect on water retention (R = -0.44) was principally indirect via clay content (R = -0.33) and from organic matter (R = -0.04).
The water content retained at field capacity varied from 0.141 kg/kg in the sand class to 0.477 kg/kg in the silty clay class, while the permanent wilting point varied from 0.050 kg/kg in the sandy loam textural class to 0.286 kg/kg in the silty clay textural class. Both the field capacity and the permanent wilting point increased in similar magnitude with the increase in clay content, which caused the plant available water capacity to change little with the increase of clay content in the soil.
The mean plant available water capacity for the soils evaluated was 0.130 kg/kg, with less retention in the sand textural class and greater in the silt-clay textural class (Figure 1). Other classes with greater retention were silty clay loam (0.158 kg/kg) and the silty loam (0.176 kg/kg). In the other textural classes, the plant available water capacity varied little with the particle size distribution, from 0.116 kg/kg, in sandy clay loam, to 0.137 kg/kg, in sandy clay soil. The lower plant available water capacity in the sand textural class is related to the low specific surface area of these soils, while the greater availability in the silt-clay class is related to the greater presence of clay and silt, with a greater specific surface area. When the three classes with greater retention are examined, it is observed that these soils are less weathered and with a greater silt clay ratio and, thus, greater contribution to water retention by 2:1 type minerals.
The path analysis showed that the plant available water capacity had positive total correlation with the silt content (R = 0.22) and organic matter (R = 0.19), and negative with bulk density (R = - 0.30). For the silt content and bulk density, the effects were direct, while for organic matter, the direct effect was small (R = 0.04) and the total effect was dependent on the indirect effects via the silt content (R = 0.06) and bulk density (R = 0.10). Soils with greater organic matter content were those with greater silt content (R = 0.22); thus, the greater water retention of these soils was also via silt. Low correlation coefficients among soil properties and plant available water capacity have frequently been related (van den Berg *et al*., 1997; Giarola *et al*., 2002), probably due to the interactions with positive and negative effects among the soil properties, which could be verified through path analysis.

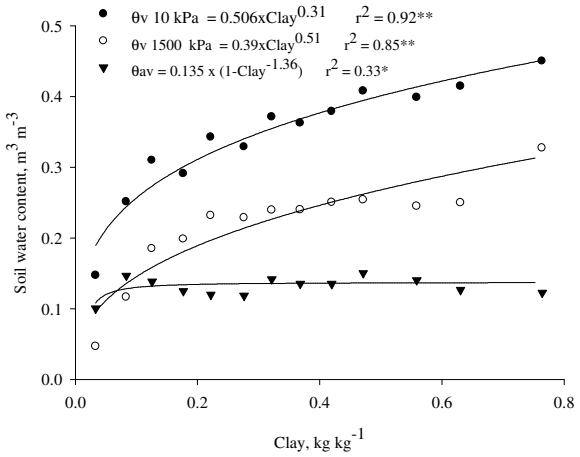

Figure 1. Relationship between clay content and moisture at field capacity (UV 10 kPa), permanent wilting point (UV 1500 kPa) and available water (UV10 - UV 1500 kPa) for the subtropical soils.

Conclusion

Pedotransfer functions generated from soils from other geographical regions were not adequate for estimating water retention for the soils of southern Brazil and, for the soils evaluated, the proposed equations generally included the variables of organic matter, bulk density and the sum of the clay plus silt fractions.

The contents of clay, silt and organic matter had total positive correlation with soil water content at field capacity and at permanent wilting point, whereas bulk density had negative correlation with water content in field capacity. Part of the correlation was due to an indirect effect, as a consequence of interrelationships which exist among soil properties.

The lowest level of plant available water capacity was in the sand textural class due to the low specific superficial area, while the greatest level was observed in the classes with a greater silt content and, therefore in those with a greater silt/clay ratio, indicative of less weathered soils with a greater quantity of 2:1 type clay minerals.

References

Arruda FB, Julio Jr J., Oliveira JB (1987) Parâmetros de solo para cálculo de água disponível com base na textura do solo. *Brazilian Journal of Soil Science* **11**, 11-15.

Bell MA, van Keulen H (1995) Soil pedotransfer functions for four Mexicans soils. *Soil Science Society of America Journal* **59**, 865-871.

Giarola NFB, da Silva AP, Imhoff S (2002) Relações entre propriedades físicas e características de solos da região sul do Brasil. *Brazilian Journal of Soil Science* **26**, 885-893.

Gupta SC, Larson WE (1979) Estimating soil water retention characteristics from particle size distribution, organic matter percent, and bulk density. *Water Resources Research* **15**,1633-1635.

Massuti MM (1997) Caracterização da água disponível a partir de parâmetros físico-hídricos em solos da zona da mata do estado de Pernambuco. Recife, Universidade Federal Rural de Pernambuco. 69p. (Master's Dissertation).

Oliveira LB, Riveiro MR, Jacomine PKT, Rodrigues JJV, Marques FA (2002) Funções de pedotransferência para predição da umidade retida a potenciais específicos em solos do estado de Pernambuco. *Brazilian Journal of Soil Science* **26**, 315-323.

Rawls WJ, Brakensiek DL, Saxton KE (1982) Estimation of soil water properties. *Transaction of the American Society of Agricultural Engineering* **25**, 1316-1320.

Rawls WJ, Gish TJ, Brakensiek DL (1991) Estimating soil water retention from soil physical properties and characteristics. *Advances in Soil Science* **16**, 213-234.

Saxton KE, Rawls WJ (2006) Soil water characteristic estimates by texture and organic matter for hydrologic solutions. *Soil Science Society of America Journal* **70**, 1569-1578.

Saxton KE, Rawls WJ, Romberger JS, Papendick RI (1986). Estimating generalized soil-water characteristics from texture. *Soil Science Society of America Journal* **50**, 1031-1036.

Tomasella J, Hodnet MG, Rossato L (2000) Pedotransfer functions for the estimation of soil water retention in Brazilian soils. *Soil Science Society of America Journal* **64**, 327-338.

van den Berg M, Klamt E, van Reeuwijg LP, Sombroek WG (1997) Pedotransfer functions for estimation of moisture retention characteristics of Ferralsols and related soils. *Geoderma* **78**, 161-180.

What are the chances of successfully replacing buffel grass with native plant communities in central Queensland's coal mine rehabilitation sites?

Hendry Baiquni, Thomas Baumgartl, David Mulligan and David Doley

The University of Queensland, Centre for Mined Land Rehabilitation (CMLR), St Lucia, QLD, Australia, Email: h.baiquni@uq.edu.au

Abstract
It is sometimes desired to establish native plant species on rehabilitated minesites of central Queensland that are occupied by exotic pasture grasses such as *Cenchrus ciliaris*, which is more effective than native plant species in utilising the limited available soil moisture. Investigations were conducted on the hydrological characteristics of the mine site soils and on the water requirement for germination of selected native species. Rainfall simulation experiments using established pastures of different ages showed that pastures increased the infiltration rates and water retention capacities of soils as compared with bare surfaces. Germination experiments exposed non-dormant seeds of six native tree and shrub species and five grass species to decreasing osmotic water potentials (OWPs). Each species varied in its rates of imbibition, radicle elongation and germination, as well as their tolerance to dehydration during germination. Imbibing seeds of all species would germinate only if they reached critical minimum water contents, regardless of the OWPs imposed during imbibition.
Coupled with the knowledge on the rainfall characteristics of the region, this study demonstrates the possibility of increasing the success of native species establishment on rehabilitated minesites in central Queensland by identifying environmental conditions that must be provided in order to achieve successful germination.

Key Words
Runoff, erosion, water content, bulk density, coal industry, grazing

Introduction
While grazing may continue to be a practical option as a post-mining land-use in some areas, the mining industry in central Queensland has, in the past two decades, turned towards the establishment of native plant communities or bushland as one of the alternative post-mining land-uses (Emmerton and Elsol, 1998; Williams, 2001). Native trees and shrubs have been seen by many mine operators as useful in providing shade and shelter for native fauna, as well as potentially providing useful forest timbers and assisting in erosion control (Roe et. al., 1996). It is assumed that once established, native vegetation communities can be self sustaining and maintenance-free. On the other hand, grazed pastures are thought to form plant communities that lack diversity and are less resilient to environmental disturbances (Walker *et al*., 1999).
However, following reshaping of the mined land and placement of growth media to support vegetation, the slower growing native species are exposed to intense competition for water, nutrients and light from fast-growing weed species and exotic pasture grasses such as *Cenchrus ciliaris* (buffel grass), and thereby tend to be excluded from the site (Mulligan, 1993). Moreover, only limited work has been done where exotic pastures that have been established for two or more years were replaced with native species sown into media with much higher organic matter concentrations and vastly improved physical characteristics than would have existed if the pasture phase had not been established initially. Therefore, the replacement of well established exotic pastures under the relatively dry and erratic climate of central Queensland requires that the seeds of native species can germinate and become established before the limited available soil moisture is exhausted. This study examines three factors involved in seedling establishment: water characteristics of the soil, germination characteristics of the seeds of native species and the rainfall distribution of the region. Defining conditions under which these three factors were optimised at a site would allow 'windows of opportunity for sowing' to be selected for desired species in terms of water availability, which in this region will be largely determined by soil water retention and climatic conditions.

Methods
Water characteristics of the replaced soils
Three rehabilitated sites with similar reconstructed duplex topsoils and sown with exotic pasture grasses 2.5, 5 and 16 years previously were selected for treatment plots. Three additional sets of treatment plots were also established on a stockpile of duplex topsoil supporting a 5-year-old pasture. On each treatment site, two sub-treatments were applied: grassed (undisturbed) and grass cut to ground level, created to reflect different seedbed conditions. Each sub-treatment was replicated three times. Altogether there were 27 treatment plots established

1 – 6 August 2010, Brisbane, Australia. Published on DVD.

and rain simulated. A field rainfall simulator (RFS) designed and developed at the Queensland Department of Primary Industries, Toowoomba, (Loch *et al*., 2001) was employed to apply simulated rain events on the treatment plots. Runoff and erosion data customarily produced by this type of experiment were recorded, together with soil moisture changes by depth (0-2.5, 2.5-5, 5-10 and 10-20 cm) over several days after the application of simulated rainfall of approximately 100 mm over a period of one hour. Plant available water was determined as the difference in water content (mm rainfall equivalent) between field capacity and permanent wilting point (-1.5MPa).

Germination characteristics of selected native species

A series of experiments was conducted in controlled temperature chambers at the University of Queensland on selected native species of trees (*Acacia holosericea, Acacia leiocalyx, Eucalyptus citriodora*), shrubs (*Lysiphyllum carronii*) and grasses (*Astrebla lappacea, A. pectinata, Dicanthium sericeum, Themeda triandra*) from central Queensland region, as well as the exotic pasture grass *Cenchrus ciliaris*. The following parameters were investigated in petri dishes under a range of water potentials from 0 to -1.5 MPa imposed by solutions of polyethylene glycol:

- *Imbibition*: to establish the rate and extent of water uptake by seeds.
- *Germination*: to determine the rate and completeness of germination.
- *Hydropedesis*: to determine the germinability of partly imbibed seeds that had been exposed to dry conditions for 1 to 5 days.
- *Radicle elongation*: to estimate the rate of radicle growth rate in germinating seeds.

However, only results from the first two experiments are reported in this paper.

Results

Moisture availability in surface soils

In this paper only results from rainfall simulation run on topsoil stockpile are discussed. Plant available water in each of the two uppermost soil layers (0-2.5 and 2.5-5.0 cm) varied between 3.5 and 4.5 mm after application of simulated rainfall (Figure 1). On the bare soil, the plant available water (above -1.5 MPa) in the 0-2.5 cm layer had been exhausted within two days after the simulated rainfall event. Most of the plant available water in the 2.5-5.0 cm layer had been lost in the first two days, but some remained until four days after rainfall. In the grassed treatment, the rate of water loss during the first day after simulated rainfall was similar to that on the bare plot, but the rate of loss slowed between 1 and 3 days and then accelerated in both the 0-2.5 and 2.5-5.0 cm layers so that plant available water was exhausted about four days after the rainfall application (Figure 1).

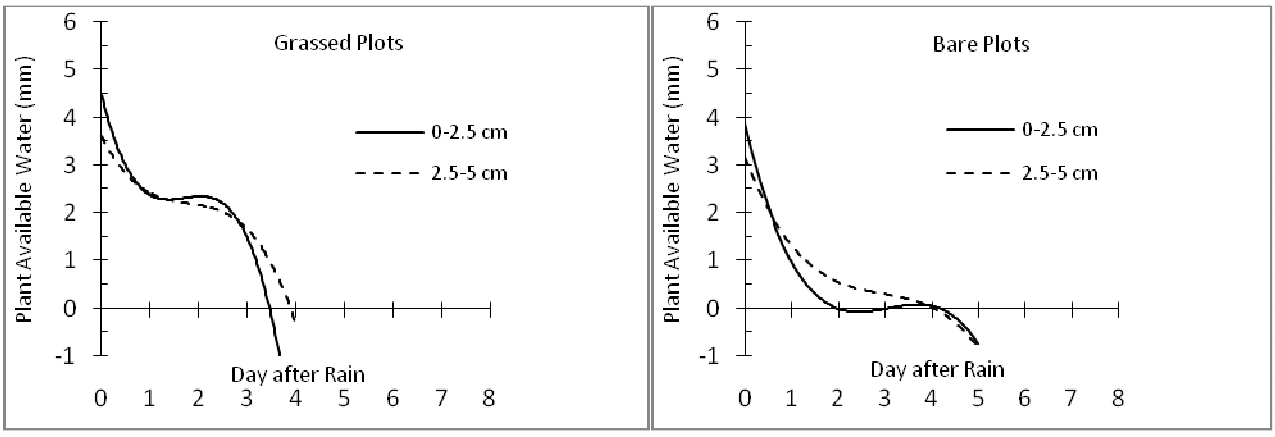

Figure 1. Moisture availability in the top 5 cm of stockpiled topsoil that had been under pasture for 5 years, showing the comparison between bare plots and grassed plots. Bare plots were prepared by removing the top 15 cm of the soil. Grassed plots were undisturbed.

Imbibition responses to water potential

The germination experiments showed that the process of germination in all species was delayed and inhibited at reduced osmotic potentials. For most species, it was possible to identify the three phases of germination as postulated by Bradford (1995). Phase I (imbibition) is associated with a relatively rapid increase in seed water content and the measurements were taken to determine any reduction in the rate of imbibition at the end of Phase I. A failure or substantial retardation of imbibition is likely to affect the eventual success of germination.

Phase II is a period during which seed water content changes slowly but important metabolic changes are occurring in the seed. The end of Phase II was taken to be the time at which germination first occurred or when the rate of imbibition increased again. The results of these interpolations for the species examined are set out in Table 1. The estimates of the duration of Phase I and the resulting rates of imbibition are approximate but non-dormant seeds of all species exposed to continuous saturation (~0 MPa) readily imbibed water and reached a water content of 45% or more within 12 hours. Two tree species (*E. citriodora* and *A. leiocalyx*) reached water contents of about 100% in that time, demonstrating the most rapid imbibition rates for the experiment.

Table 1. Summary of imbibition characteristics of nine tree, shrub and grass species at osmotic potentials of 0 MPa. Values are mean ± s.e. (P=0.05)

Species		Phase I			Phase II			Phase III
	Initial wc%	Dur. hr	Rate wc%/hr	Final wc%	Dur. hr	Rate wc%/hr	Final wc%	Begins hr
Tree								
Acacia holosericea	2.7±0.8	24	2.7±0.2	73±4.9	24	2.2±0.5	125±0.1	48
Acacia leiocalyx	7.6±0.5	24	6.4±0.3	162±6.7	24	0.6±0.3	178±1.5	48
Eucalyptus citriodora	9.7±0.7	12	6.8±0.3	91±23.4	36	0.3±0.4	101±3.6	48
Shrub								
Lysiphyllum carronii	10.5±0.6	24	4.5±0.7	118±2.9	48	0.1±0.1	153±5.6	72
Grass								
Astrebla lappacea	22.5±0.1	24	2.8±0.3	90±1.7	24	0.1±0.3	109±8.6	48
Astrebla pectinata	21.6±0.9	24	3.1±0.4	98±3.4	24	0.6±0.2	105±4.5	48
Cenchrus ciliaris	15.0±0.7	12	3.1±0.1	52±1.7	12	2.9±0.3	87±5.5	24
Dicanthium sericeum	15.0±0.7	12	2.5±0.1	45±0.8	12	0.1±0.4	46±4.1	24
Themeda triandra	13.7±0.5	12	2.4±0.3	42±1.3	>84	n.a.	n.a.	n.a.

Abbreviations:
wc%: seed water content per cent dry weight; Dur.: duration; n.a.: not applicable.

The commencement of Phase III can be taken as the time of detection of germination. It is clear that *Cenchrus ciliaris* and *Dicanthium sericeum* would be likely to commence germination well before the surface soils in the field study had reached the permanent wilting point. It is likely that a substantial portion of the seed population may have begun to germinate by this time. In contrast, the other species would have just commenced germination by the time the available water had been exhausted. In addition, the germination process in most species was retarded at reduced osmotic potentials (data not shown) so it would be less likely that successful germination would have occurred on bare soil by the time the available water had been exhausted.

Conclusion

This study shows that it may be possible to replace well established exotic pasture grasses such as *Cenchrus ciliaris* with native plant species in central Queensland. However, plant available soil water must be maintained for several days after a rain event if that is to happen. For seedling establishment under natural rainfall conditions, this means that several rain events must follow in quick succession over at least a week so the seedling roots can penetrate below the first 5 cm of soil. The most likely result is that without serious management intervention, *Cenchrus ciliaris* will become established sooner and more abundantly than the desired native species, reinforcing the dominance of this exotic species on mine rehabilitation sites.

References

Bradford, KJ (1995) Water relations in seed germination. In "Seed development and germination" (Eds J. Kigel and G. Galili), pp. 351-396. Marcel Dekker, Inc., New York.

Emmerton B, Elsol J (1998) "Selection of native species to develop natural ecosystems on open cut coal mines in the central Queensland region. Summary of methodology and overview of major findings of ACARP Research Project C4010." Land Reclamation Services Pty Limited, Emerald.

Loch RJ, Robotham BG, Zeller L, Masterman N, Orange DN, Bridge BJ, Sheridan GJ, Bourke JJ (2001) A multi-purpose rainfall simulator for field infiltration and erosion studies. *Australian Journal of Soil Research* **39**, 599-610.

Mulligan DR, Bell LC (1993) Strategies and techniques for the establishment of a self sustaining native ecosystem on mined land at the Curragh open-cut coal mine. A report to Curragh Queensland Mining Ltd. Brisbane, Department of Agriculture, the University of Queensland.

Roe PA, Mulligan DR, Bell LC (1996) Environmental management of coal mines in the Bowen Basin, central Queensland. In "Environmental management in the Australian minerals and energy industries. Principles and practices" (Ed. DR Mulligan) pp. 290-315. University of NSW Press, Sydney.

Walker, B, Kinzig A, Langridge J (1999) Plant attribute diversity, resilience, and ecosystem function: the nature and significance of dominant and minor species. *Ecosystems* **2**, 95-113.

Williams DA (2001). Risk assessments of Bowen Basin spoil rehabilitation. Brisbane, ACARP.